The Impact of Different Aircraft Categories on Emissions, Air Quality, and Human Health

Rick Nelen

TU Delft

The Impact of Different Aircraft Categories on Emissions, Air Quality, and Human Health

by

Rick Nelen

to obtain the degree of Master of Science
at the Delft University of Technology,
to be defended publicly on Wednesday 17 May 2023 at 13:00.

Student number:	4533186	
Project duration:	February 2022 – May 2023	
Thesis committee:	Dr. I.C. Dedoussi	Supervisor
	Prof. dr. D.G. Simons	Chair
	Dr. ir. T. Sinnige	Examiner

An electronic version of this thesis is available at http://repository.tudelft.nl/.

Cover image: https://wonderfulengineering.com

TU Delft

Acknowledgements

In front of you lies the result of a long and rewarding journey. With this MSc thesis, I complete my degree in Aerospace Engineering at Delft University of Technology. I have had an amazing time, and cannot express enough gratitude to all the people I have met, all the friends I have made, and all my family that supported me throughout these seven years. Like any good trip, it was not only about the destination, but also about the journey itself.

Over the past year, I have worked on a topic which is close to my heart: sustainability in aviation. I have often found myself concerned about the future of our planet and the health of its people, specifically when it comes to our own impact. Thus, when I found a thesis topic on the impact of aviation on air quality and human health, I wanted to deliver something I could be proud of. I hope that this work provides you with new insights and encourages you to consider the impact we have on the planet and humanity.

Throughout the course of my MSc thesis, I have received great feedback and help from my supervisor, Dr. Irene Dedoussi. I greatly appreciate her involvement and the time she took to listen to my questions, discuss new research, or to chat about anything and nothing. I would like to thank her here once again, as I would not have been able to deliver this thesis without her. I would also like to express my gratitude towards Prof. Dr. Dick Simons, the chair of my thesis committee. He helped me to explain my objectives and findings to the general public and I am thankful for his feedback at our milestone meetings.

Furthermore, I would like to thank the many people in the ANCE department for helping me out whenever I needed something, and for the general exchange of ideas. Specifically, I want to thank Flávio Quadros for all the help with the openAVEM model and sharing very useful papers with me. I am also thankful to Jurriaan van 't Hof for taking the time to explain how to work on the supercomputer, and for helping me out when needed.

I also want to acknowledge the data sources and infrastructure that were essential for this thesis. This work used the Dutch national e-infrastructure with the support of the SURF Cooperative using grant no. EINF-3842. Flight data was provided by Flightradar24 and the MERRA-2 wind data was taken from the Global Modeling and Assimilation Office at NASA Goddard Space Flight Center.

I could not have finished this thesis, let alone my degree, without the continuous support of my family and friends. From the moment I applied for the BSc Aerospace Engineering in Delft, until this very day, my family has always been there to support me. Whether we had serious conversations about the future during a bike ride, went out for dinner in Delft because I did not have the time to come home, or spent the much-needed quality time when I needed to wind down: thank you. Without this support, I might not have become the person I am today, and would certainly not have dared going to Australia and Slovenia for months; you have helped me grow as a person throughout my studies.

And finally, I want to thank all my friends and the people who have supported me during these seven years, no matter where I was. Sonia and Jack from Australia, my colleagues at Pipistrel in Slovenia: thank you for having me and making me feel at home away from home. To Floor, Daniël, Pepijn, Ruben, Maurizia, Nora, Paolo and Damian: thank you for making me feel at home in Delft. Greetje, Pascal, Claire, Wessel and Darcey; our adventure in China started off a sequence of trips which I'll never forget. Lars and Angela: many thanks for our friendships, even after all these years. To Hannah, Gerda, Cristina, Janaina, Merel, Nadine, Desiree, Praveen, Panos and Kevin: thank you for keeping me busy outside of uni and all the great times we have had. To all the people I shared a volleyball team with when I was a member at Punch; to all the aviation enthousiasts in Lambach; to my fantastic colleagues at SSL; to every great individual in my Eco-Runner team; to my fellow sustainability enthousiasts in GreenTeam AE: thank you for shaping my time here in Delft. Without you, it would never have been as amazing as it was.

Delft, May 2023

Contents

List of Figures

List of Tables

Nomenclature

Chemistry

BC	Black Carbon
CO_2	Carbon Dioxide
CO	Carbon Monoxide
H_2O	Water
HC	Hydrocarbon
HNO_3	Nitric Acid
NO_2	Nitrogen Dioxide
NO_x	Nitrogen Oxides
$nvPM_m$	Non-Volatile Particulate Matter (Mass)
$nvPM_N$	Non-Volatile Particulate Matter (Particle number)
nvPM	Non-Volatile Particulate Matter
O_3	Ozone
$PM_{2.5}$	Particulate matter with a mean diameter smaller than 2.5 µg
PM	Particulate Matter
SO_x	Sulfur Oxides
S	Sulfur

Other Abbreviations

ADS-B	Automatic Dependent Survaillance-Broadcast
AEDT	Aviation Environmental Design Tool
AOR	Advanced Open Rotor
BADA	Base of Aircraft Data
BWB	Blended Wing Body
CI	Confidence Interval
COPD	Chronic Obstructive Pulomnary Disease
CRF	Concentration Response Function
CTM	Chemistry-Transport Model
EI	Emission Index
FOA	First Order Approximation
FOX	Formation Oxidation
GEMM	Global Exposure Mortality Model
GEOS-Chem	Goddard Earth Observing System Atmospheric Chemistry
HSR	High-Speed Rail
ICAO	International Civil Aviation Organization
IEA	International Energy Agency
LRI	Lower Respiratory Infections
LTO	Landing and Take-Off
MDA8	8-hour Maximum Daily Average
MERRA-2	Modern-Era Retrospective Analysis for Research and Applications, version 2
NCD	Non-Communicable Diseases
openAVEM	Open Aviation Emissions Model
ppbv	parts per billion (volume)
pptv	parts per trillion (volume)
RPK	Revenue Passenger Kilometre
RR	Relative Risk
SAF	Sustainable Aviation Fuel
TIM	Time-In-Mode
UCX	Unified Tropospheric-Stratospheric Chemistry Extension
USD	U.S. Dollar
VSL	Value of Statistical Life
WHO	World Health Organization

Introduction

This MSc thesis was developed within the Aircraft Noise and Climate Effects department at the Faculty of Aerospace Engineering, TU Delft. The project ran from February 2022 to May 2023 under the supervision of Dr. Irene Dedoussi. It aims to provide insights in the contributions of aircraft to air quality degradation and subsequent health impacts. After an extensive literature review, simulations were performed to assess aviation emissions, the effects on atmospheric composition, and premature mortality.

Although previous studies have investigated impacts of individual aircraft categories on climate change, this is the first attempt to compare the effects of aircraft categories on air quality and aviation-attributable early deaths. Furthermore, this study discusses the implications on potential mitigation strategies using sustainable aviation alternatives. This may aid in future policy making regarding sustainable aviation, such that society can minimise its negative impact on air quality.

This thesis report is organised in two parts. First, the scientific paper is presented in part I. Then, part II provides the supporting information, which can be used to assess the results and conclusions in more detail.

Scientific Paper

The Impact of Different Aircraft Categories on Emissions, Air Quality, and Human Health

Rick Nelen*

Delft University of Technology, Delft, The Netherlands

Abstract

Previous studies have estimated that over 16,000 annual early deaths are induced by global aviation emissions. Combined with a growing industry, this calls for sustainable developments to reduce the negative impact on human health. However, the potential application of more sustainable technologies varies amongst aircraft size and range. Thus, an understanding of the impacts on air quality for different aircraft types and flight distances is required to estimate the impact mitigation potential of sustainable aviation alternatives. In this study, we compare the impact of aircraft size and flight distance on emissions intensity, associated changes in air quality, and aviation-attributable premature mortality to evaluate these potential mitigation options. Specifically, we use the openAVEM emissions inventory to estimate aircraft emissions and the GEOS-Chem atmospheric chemistry-transport model to evaluate their impacts on ground-level concentrations of ozone (O_3), nitrogen dioxide (NO_2), and fine particulate matter ($PM_{2.5}$) including black carbon (BC).
We estimate that aviation activities in 2019 were responsible for nearly 80,000 early deaths, of which 65% are found in Asia. We find that widebody aircraft are associated with 57% of aviation-attributable premature mortality, and that this type has a 66% higher impact per revenue passenger kilometre (RPK) than narrowbody aircraft. Furthermore, O_3 impacts are largest for long-haul flights, while intra-European flights yield 50% larger impacts per RPK than similar flights globally. We conclude that only 5% of all aviation-attributable premature mortality is associated with regional aircraft and that the 5% longest flights are responsible for almost half of the impact. Results of this work provide insights on the potential air quality impacts of the sustainable aviation mitigation options relevant for different aircraft categories and flight distances.

1. Introduction

In the wake of the COVID-19 pandemic, the aviation industry has proven to be capable of rapid recovery.[1] While this demonstrated resilience is received positively by the industry, it also means that aviation fuel burn is expected to increase in the coming decades, following trends and projections in past studies [1–4]. This poses threats to the climate and air quality, as both are impacted by aircraft emissions [5–11].

In a recent study, Grobler et al. [12] concluded that the societal cost of aviation's air quality impacts exceeds that of climate change. Yet, the global air quality effects of full flights have received less attention than climate impacts. Meanwhile, urbanisation and growing populations in developing countries, paired with an increase in flights in these regions, is expected to increase air quality issues in the coming decades [3, 13, 14].

Studies have found connections between aviation emissions and various types of air pollution that have been associated with negative impacts on hu-

*MSc Student, Flight Performance and Propulsion, Faculty of Aerospace Engineering, Delft University of Technology

[1] https://www.icao.int/Newsroom/Pages/Air-traffic-recovery-is-fastapproaching-prepandemic-levels.aspx. Last accessed on 19 December 2022.

man health [5–7, 9, 11, 12, 15–31]. These include gaseous species such as ozone (O_3) and nitrogen dioxide (NO_2), but also particulate matter (PM), in particular with a mean diameter smaller than 2.5 µm ($PM_{2.5}$). Recent studies have shown that the toxicity of $PM_{2.5}$ is not uniform and suggested to investigate the health impacts of black carbon (BC), a constituent of $PM_{2.5}$, separately from those of general $PM_{2.5}$ [32–34]. The air quality effects of aviation are mostly caused by aviation emissions of NO_x, sulfur oxides (SO_x) and PM [5, 28, 31, 35, 36].

Aviation NO_x emissions have several effects on air quality. First of all, there is the direct increase in NO_2 concentrations due to landing and take-off (LTO) emissions [24]. However, these effects are highly localised, such that studies using coarse global grids have not managed to capture these LTO impacts accurately [11].

Secondly, the formation of tropospheric O_3 due to aviation NO_x emissions degrades air quality on a large scale, provided that background atmospheric chemistry is not in the NO_x-saturated regime [37, 38]. Given the extended lifetimes of both NO_x and O_3 at cruise altitude, their impact is larger than at sea-level, and strongest at low latitudes [18, 36, 37, 39–41]. The O_3 also reacts with background NO_2, reducing overall NO_x levels on a global scale and yielding lower ground-level NO_2 concentrations in areas less impacted by LTO emissions [24, 28]. However, the reduction of NO_2 due to aviation SO_x emissions, as well as their positive impact on the abundance of active chlorine species, leads to a reduction of O_3 levels [31]. On a longer time scale, a similar effect is caused by methane depletion resulting from aviation NO_x emissions [31, 40].

Finally, NO_x emissions are responsible for the majority of secondary sulfate-ammonium-nitrate aerosol, which constitute up to 99% of aviation-attributable $PM_{2.5}$ [5]. Thus, the majority of aviation-induced air quality impacts are either directly or indirectly linked to NO_x emissions. Previous studies have found that the impact of cruise emissions on air quality exceeds that of LTO operations [5, 7, 12, 24, 25]. For $PM_{2.5}$, these effects are mostly driven by aviation NO_x and their impact on nitric acid (HNO_3), while the extended atmospheric lifetime of O_3 at cruise altitude enables large scale effects on air quality [9, 24].

Air quality degradation is associated with a multitude of adverse effects on human health, such that the World Health Organization (WHO) has sharpened their air quality guidelines on multiple occasions [42–44]. Elevated O_3 levels can increase the risk of premature mortality caused by both respiratory and cardiovascular diseases [45–48]. Previous studies were divided on whether this effect occurs at all ambient O_3 levels or not. Some studies in the early 2000s concluded that this effect was only significant above a threshold of 10 ppbv [49, 50]. More recent studies found (sometimes limited) evidence for a higher threshold at approximately 35 ppbv, while others concluded that a threshold could not be observed throughout the measured range of pollutant levels [46, 51–53].

With an estimated 4 to 9 million deaths in 2015 related to fine particulate matter, $PM_{2.5}$ is also recognised as a major contributor to global premature mortality [54, 55]. Despite improved air quality in developed countries relative to 1990, $PM_{2.5}$ remains relevant for health impact assessments [54, 56]. Long-term exposure can lead to a variety of respiratory and cardiovascular diseases, as well as lung cancer [43, 54–58]. These effects are present also at low ambient concentrations; studies agree that if a threshold is present, it would be in the order of 2 to 3 $\mu g\,m^{-3}$ [43, 55, 59–61].

As explained by Schraufnagel et al. [42], ultrafine particles have greater systemic toxicity than coarse particles as they can reach virtually all cells in the human body. Specifically, BC may accumulate in the lungs and lead to a variety of respiratory diseases due to toxic components attached to the particle's surface [32, 33, 42]. Several studies have looked into these health impacts and concluded that the sensitivity of the human body to BC and these associated toxins can be up to an order of magnitude greater than that towards $PM_{2.5}$ in general [32–34].

Although literature regarding the effects of aviation-attributable NO_2 on human health is scarce, recent studies have identified the potential harm of elevated NO_2 concentrations [11, 62]. Prolonged exposure is associated with an increased risk of cardiovascular diseases, as well as respiratory infections such as chronic obstructive pulmonary disease (COPD) [48, 63, 64]. Few studies identified a threshold concentration above which these effects were clearly visible [65, 66]. As the body of evidence grew, studies have also found NO_2-attributable health impacts at lower concentrations [34, 63, 65–67].

In an attempt to reduce the impact of aviation on climate change and air quality degradation, solutions are sought in various dimensions. From an operational perspective, for example, there may be a modal shift towards other forms of transportation like

the train. For short-haul flights, total travel times can be competitive with aviation, and regions with well-developed high-speed rail (HSR) tend to show a smaller contribution of short-haul flights to the total impact of aviation [68–70]. In the technical domain, more sustainable alternatives are being developed by industry and academic partners [71–73]. For example, advanced airframe technologies such as the blended wing body (BWB), advanced open rotor (AOR), or the Flying V promise to improve efficiency compared to regular tube and wing aircraft [71, 74, 75]. However, given the steady growth of the aviation industry, these solutions will not suffice to drastically reduce the industry's environmental impact [76].

Solutions can also be found in the propulsion system domain. For small, short-haul aircraft, electrification using batteries may be feasible, albeit at high cost and limited impact on the global fleet [77, 78]. For larger aircraft, hydrogen technology could be used. Although up-scaling is required to enable the use of hydrogen fuel cells on commercial aircraft, hydrogen can also be used in gas turbine engines for higher power ranges [78–80]. Finally, sustainable aviation fuel (SAF) can be used on most flights (with limited modifications to the fuel system) as a substitute for conventional jet fuel, potentially reducing the net climate and air quality impacts [78, 81–83]. Being implemented already in practice, it offers a more realistic alternative for the near future compared to hydrogen or battery technology [78, 84–86]. One of the drawbacks of using SAF or hydrogen in gas turbine engines, however, is that they do not fully eliminate the non-CO_2 climate and air quality impacts [80, 83]. Thus, it is expected that aviation will continue to impact human health for the foreseeable future [4].

Currently, governing bodies recognise the need for a more sustainable aviation industry and financial support for SAF production is available [81, 85]. Furthermore, inefficient technologies are discouraged through carbon taxing and the implementation of stricter standards [84, 87, 88]. However, more support is needed in the development of regulations and standards for novel technologies [73].

While the present regulations provide a generic framework for aircraft manufacturers, new standards for non-CO_2 emissions are not disruptive enough to counteract industry growth [81, 87, 89]. Therefore, air quality impacts of aviation continue to increase, while they are already associated with significant loss of life [7, 9, 25, 28]. Recent estimates vary from 16,000 (90% CI: 8,300 - 24,000) yearly early deaths by Eastham and Barrett [28] to 58,600 (95% CI: 31,400 - 98,100) by Quadros et al. [9]. Hence, understanding which aircraft categories contribute most to these mortalities is a first step towards more specific and effective policies aimed at reducing aviation-attributable premature mortality.

For climate impacts, variations amongst aircraft categories have been identified by Dahlmann et al. [90]. They found that very short flights have a negative impact on global warming due to a lack of contrail formation, small water vapour (H_2O) impact and methane (CH_4) destruction caused by NO_x emissions. With increasing flight distance, the impact on global warming becomes more positive, irrespective of the mean latitude [90]. Furthermore, they also concluded that the climate impact of aviation shows spatial variations, with flights showing larger specific impacts at high latitudes compared to routes in the tropics.

However, to the best of the author's knowledge, previous studies have not yet focused on the distinct contributions of individual aircraft categories on air quality impacts and the associated health effects. Since each technology for sustainable aviation is applicable to a different type of aircraft (both in terms of size and range), we first need to understand the impact of these aircraft categories before the mitigation potential can be assessed. Therefore, this study aims to provide insights into the impact of aircraft categories on air quality and human health through a consistent comparison of flight data and related emission estimates. By eliminating aviation emissions for particular aircraft categories, it shows the maximum relief that can be obtained regarding aviation-induced premature mortality upon the full transition of a particular industry segment towards sustainable aviation. As such, it provides a global perspective on the issue and indicates areas that require attention.

2. Methods

In order to establish the impact of aircraft categories on air quality and human health, a multi-step approach is required. First, we define the relevant aircraft categories and estimate their fuel burn, together with the emission indices of NO_x, SO_x, hydrocarbons (HC), carbon monoxide (CO) and non-volatile particulate matter (nvPM). Then, a chemistry-transport model (CTM) is employed to evaluate the effects on ground-level concentrations of pollutants. Combining this with data on population density, we then obtain the change in population-weighted concentration of the relevant species. Fi-

Table 2.1: Overview of the aircraft categories used in this study, combined with brief statements on the relevance and scope of the impact assessment.

Study	Categories	Relevance	Assessed	Notes
Aircraft size	Piston Business jet Turboprop Regional jet Narrowbody Widebody	Policy implications, comparison of emissions to literature.	All impacts	-
Distance [km]	< 750 750 - 1,500 1,500 - 2,500 2,500 - 4,000 4,000 - 8,000 > 8,000	Policy implications, comparison of emissions to literature.	All impacts	-
EU-flights	< 750 km within Europe	Potential impact of replacing flights with rail connections.	All impacts	Upper bound, the real potential is limited by rail infrastructure.
Short-haul	Turboprop Regional jet Narrowbody	Potential impact of replacing jet aircraft by turboprop aircraft.	All impacts	Wasiuk et al. [91] showed that the replacement of turbofan aircraft by turboprop counterparts may reduce aviation's NO_x emissions and associated O_3 impacts.
Medium-haul	Narrowbody Widebody	Potential of replacing widebody aircraft by narrowbody aircraft.	Emissions only	-
Aircraft age	Old narrowbody Old widebody New narrowbody New widebody	Potential impact of fleet renewal.	Emissions only	'Old': certified in 1999 or before; 'New': certified in 2000 or after.

nally, through the use of concentration response functions (CRFs), we estimate the resulting aviation-attributable mortality for each aircraft category.

2.1. Aircraft categories

In this study, two comparisons of global aviation-induced air quality impacts are provided: one based on the aircraft size and one on the flight distance. These categorisations can be translated to policy adjustments using clear boundaries and were thus deemed fit for this purpose.

Furthermore, four case studies are presented to further aid policy development: one in which intra-European flights shorter than 750 km are replaced by train connections; another two cases to study the impacts of aircraft size on short-haul and medium-haul routes; a last study to investigate the effects of fleet modernisation. All studies, together with the individual categories that are included, are presented in table 2.1. A detailed overview of the criteria used to compose the flight lists for each category can be found in section SI 1.2.

2.2. Aviation emissions

We use Automatic Dependent Surveillance-Broadcast (ADS-B) data from the year 2019 provided by FlightRadar24[2] to simulate the aviation activity. We select this year as it provides the most recent pre-pandemic data, offering the best estimate for current nominal flight operations. Furthermore,

[2] https://www.flightradar24.com. Last accessed on 7 December 2022.

we filter the flights based on the following selection criteria:

- The flight shall be operated by an aircraft type which is recognised as commercial or general aviation;[3]
- The flight shall have valid and non-identical origin and destination airport codes;[4]
- The flight distance shall not exceed 120% of the nominal operational range of the aircraft.[5]

These filters reduced the data set from 45.14 million flights to 42.21 million flights. 33.61 million commercially operated flights are present in the used data set, down from 33.64 million flights in the original flight data. Please see section SI 1.2 for more details.

To evaluate the emissions resulting from these flights, we use the Open Aviation Emissions Model (openAVEM), developed by Quadros et al. [92]. This model estimates the fuel burn based on a Time-In-Mode (TIM) approach during the LTO phase and the base of aircraft data (BADA[6]) performance model for the remainder of the flight.

Regarding the TIM method, past studies have used the 4-phase (take-off, climb, approach and taxi) method developed by the International Civil Aviation Organization (ICAO) [26, 87, 93–96]. However, a more detailed method was proposed by Stettler et al. [22] and used by Yim et al. [23] and Quadros et al. [92]. We select this 12-phase TIM method to estimate LTO fuel burn.

Furthermore, openAVEM also provides estimates for the emissions of NO_x (measured as NO_2 equivalent), CO and HC. These are estimated using engine specific emission indices (EIs) from the ICAO Engine Emissions Databank [89]. Emissions of nvPM are taken from engine measurements if available; otherwise, they are estimated using the First Order Approximation (FOA) 4 method [97]. If the engine type is not implemented in FOA4, a constant emission index of 30 mg kg^{-1} is assumed, in line with previous studies [7, 9, 20].

The emissions inventory is set up at a $0.5^\circ \times 0.625^\circ$ horizontal (latitude $\times$ longitude) resolution, and a vertical resolution based on the second version of the Modern-Era Retrospective Analysis for Research and Applications (MERRA-2; [98]), which is consistent with the atmospheric simulation grid.[7] In order to include seasonal effects, we divide the data in monthly sets and assume that they are uniformly distributed per month (as shown in figures S3 and S4). Throughout the year, the global average daily aviation fuel burn varies from -5.7% (in January) to +7.1% (in July) compared to the yearly average. This temporal trend agrees with results of previous studies [20, 92].

Besides the nominal results, we also provide emission estimates normalised towards revenue passenger kilometres (RPK) to identify trends in efficiency and personal impacts. To do so, a constant mass load factor of 70% is used, similar to the approach by Quadros et al. [92]. Section SI 5.3 shows the sensitivity of the results towards the load factor: the total change in emissions is limited to ±1% for a 10% change in load factor. This yields nearly proportional variations in emissions per RPK; +10% and -8% for a 10% decrease and increase in load factor, respectively.

2.3. Atmospheric modeling

To estimate the impact of the aviation emissions on air quality, we use the Goddard Earth Observing System Atmospheric Chemistry (GEOS-Chem) model version 13.3.3,[8] run on the Snellius supercomputer. This chemistry-transport model simulates transport and chemistry processes of species throughout the atmosphere and has been used extensively in literature [9, 28, 99–108]. Since aviation cruise emissions occur near the tropopause, the unified tropospheric-stratospheric chemistry extension (UCX) module by Eastham et al. [105] is employed to simulate stratospheric behaviour. The model is driven by meteorology from the MERRA-2 model [98].

We spin up the global model using all aviation emissions from openAVEM to adjust the atmospheric state to the settings and emissions used for our

[3] The recognised aircraft types are: 'piston', 'business jet', 'turboprop', 'regional jet', 'narrowbody' and 'widebody'. Military aircraft and helicopters are excluded.

[4] While this filter may unintentionally remove valid general aviation flights, openAVEM is not capable of handling flights with the same origin and destination airport.

[5] Please consult section SI 1.1 for a detailed explanation on the estimation method for the operational range.

[6] License available upon request via https://www.eurocontrol.int/model/bada. Last accessed on 7 December 2022.

[7] http://wiki.seas.harvard.edu/geos-chem/index.php/GEOS-Chem_vertical_grids. Last accessed on 8 December 2022.

[8] http://www.geos-chem.org. Last accessed on 24 June 2022.

study. This spin-up is performed on a coarse $4^\circ \times 5^\circ$ grid using atmospheric data from 1 January 2017 until 25 June 2018. In this study, a top-down perturbation approach is applied to minimise errors in our estimation due to non-linearities in the atmospheric chemistry model [109–111]. For each simulation, the openAVEM emissions without the selected category are used for an additional spin-up on a finer $2^\circ \times 2.5^\circ$ grid from 25 June 2018 until 1 January 2019. We then use the same aviation emissions and grid for the actual simulation covering the year 2019 through two 6-month runs. In total, 18 scenarios are studied (one of which is the baseline) at the cost of approximately 420,000 core hours on the supercomputer.

To analyse the impact of aviation emissions on air quality, we identify the change in ground-level concentration of O_3, NO_2, $PM_{2.5}$ and BC. To do so, we select the lowest of the 72 vertical pressure levels and take the yearly averaged concentrations per grid cell. For O_3, the large seasonal and diurnal variations require one or two additional steps [45, 112]. First, we determine the 8-hour maximum daily average (MDA8), a period of eight consecutive hours per day which shows the highest running mean O_3 levels. For specific health estimates (see section 2.4), peak season mean values are required. The peak season is defined as the six consecutive months with the highest running average O_3 concentration. We then take the mean of the MDA8 values throughout this period. However, as the aviation impact on O_3 concentrations shows a trend opposite to the background concentration of O_3, this peak season metric tends to show smaller impacts of aviation in regions with high anthropogenic activities [28]. For our main study, we thus use a metric based on yearly averaged MDA8 values [46].

2.4. Human health impact

In order to analyse the effects of aviation on human health, we use two metrics: additional population-weighted concentration and excess mortality. For the first metric, the aviation-attributable differences in ground-level concentrations are computed and, if applicable, multiplied by the global population density taken from LandScan.[9] Specifically, the concentrations are multiplied by the local grid cell population and divided by the global mean population (of populated grid cells only). After applying these modifications to both the baseline and case results, the difference is taken to obtain the additional population-weighted concentration for a specific aircraft category.

We recognise that using ambient concentrations as a proxy for exposure may yield significant overestimations of health impacts. For example, indoor O_3 levels can be smaller than 20% of the outdoor concentrations [112]. However, like past literature, we accept this caveat as there is no availability of data on indoor pollution levels which spans our scope of work.

The excess mortality due to aviation can be determined through the use of concentration response functions. These provide the relative risk (RR) of mortality due to a change in pollutant concentration relative to the baseline scenario. We use log-linear CRFs for NO_2, O_3 and BC, and a supralinear CRF for $PM_{2.5}$.

For the main study, the CRF proposed by Turner et al. [46] for respiratory mortality is used to estimate health impacts of O_3. The $PM_{2.5}$-attributable mortality is estimated using the CRF for non-communicable diseases (NCD) and lower respiratory infections (LRI) by Burnett et al. [55]. Furthermore, the all-cause premature mortalities due to elevated NO_2 concentrations are estimated using relative risk values established by Faustini et al. [67]. Finally, Hoek et al. [34] provided a CRF for all-cause mortality estimations related to BC. Additional CRFs and mortality endpoints are provided in section SI 4.3.

Most studies providing relative risk fractions for use in CRFs are based on single-pollutant models. We recognise that the pollutants used in this study are not independent and correlations between species have been observed using multi-pollutant models [43, 46, 48, 113]. However, high correlation between pollutants limits the ability to separate out the associations of mortality with the individual species and may contribute to the association of effects with the incorrect pollutant [48, 114]. Although such multi-pollutant models are an active area of research, they are not yet robust enough to be used with high confidence [32, 115]. We recognise that the use of single-pollutant CRFs implies risking to overestimate the combined health effects [116]. However, as a combined risk estimate of four pollutants is not available, this study uses the single-pollutant models to provide a maximum attainable health benefit.

[9] https://landscan.ornl.gov. Last accessed on 8 December 2022.

Finally, we find the total mortality for each case through the multiplication of the relative risk and baseline mortality, which is provided by the WHO [117]. Since this study investigates the effects of removing a particular aircraft category from operations, the baseline was defined as the case including all flights of 2019. Subtraction of the case-specific mortality from the baseline mortality thus yields the excess mortality caused by the aircraft category under investigation. Throughout this paper, we provide global mortality estimates rounded to hundreds, while we show the original results (as integers) in the provided figures. As for the aviation emissions, results are also normalised towards RPKs, passengers, and number of flights to identify sensitivities. Additionally, we analyse the sensitivity towards fuel burn and NO_x emissions.

2.5. Uncertainty

Although aviation fuel burn and associated emissions are estimated from an extensive data set, the openAVEM model yields approximately 10% lower fuel burn than the jet kerosene consumption statistics from the International Energy Agency (IEA) [92]. Several other aviation emission inventories provide estimates which are a few percent smaller than those of openAVEM. Overall, we expect the uncertainties in the fuel burn to be limited to a few percent, while those for NO_x, HC, and CO may be up to 10 percent compared to the Aviation Environmental Design Tool (AEDT) [92, 118]. However, comparisons to certification EIs showed an uncertainty of ±90% for HC and ±60% for CO in model estimates [22, 64]. For nvPM, large variations exist between engine models, as well as different emission estimation methods. Quadros et al. [92] showed that the use of a different method such as the Formation Oxidation (FOX) method (see Stettler et al. [35] for more details) can yield nvPM mass emission estimates up to 2.8 times as high as for the baseline model using the FOA4 method.

Although previous studies have validated the GEOS-Chem model for a wide variety of applications, including the estimation of aviation impacts on atmospheric composition, model errors are likely to affect the results [101–105, 108, 119–122]. This is particularly true for local effects near airports, which are expected to be missed on a global grid like ours [11, 23, 120, 123]. However, without systematic bias, their impact on our aggregate results is expected to be small; it is challenging to assess the true size of these errors [122].

A major source of uncertainty in this study is the health impact assessment through the concentration response functions. For the $PM_{2.5}$ CRF, we include the nominal results, as well as a 95% confidence interval considering a normal distribution in the theta parameter of the global exposure mortality model (GEMM) [55]. For other CRFs, we implement the confidence intervals as reported in the epidemiological literature [34, 46, 67]. For other uncertainties, such as those related to the baseline disease incidence rates or population density, we follow Anenberg et al. [124] and do not consider them.

3. Results and discussion

The aviation fuel burn and associated emissions as estimated by the openAVEM model are presented in section 3.1. A brief overview of aviation's impact on air quality is provided in section 3.2, after which section 3.3 discusses the estimated health impacts for different aircraft categories. We also present a discussion on the mitigation potential of various sustainable aviation alternatives and policy implications in sections 3.4 and 3.5, respectively. Finally, we discuss several limitations of this study in section 3.6.

3.1. Aviation fuel burn and emissions

The ADS-B data showed that a total of 42.2 million civil aviation flights were registered in 2019, of which 38.0 million were flown by commercial passenger aircraft. Although the aggregate flights are comparable to those in the scheduled data provided by Graver et al. [125], the current study is based on a larger contribution of widebody aircraft. As explained in section 2.2, a filtering process was applied to the flight data, yielding a slightly smaller, yet more consistent data set than used by Quadros et al. [92].

We find that the global civil aviation fuel burn in 2019 totalled 296 Tg, which is 1.6% higher than the total fuel burn estimate of Graver et al. [126], and 11% lower than the IEA's aviation fuel sales statistics.[10] The filtering process results in 0.3% lower fuel burn than estimated by Quadros et al. [92] using the same model for 2019. As mentioned by Quadros et al. [92], one of the reasons for the discrepancy with the IEA data is the exclusion of military flights from the current data set. Our global CO_2 emissions estimate of 934 Tg is equivalent to roughly 12% of all transportation related CO_2 emissions [127, 128].

[10] https://www.iea.org/reports/aviation. Last accessed on 8 February 2023.

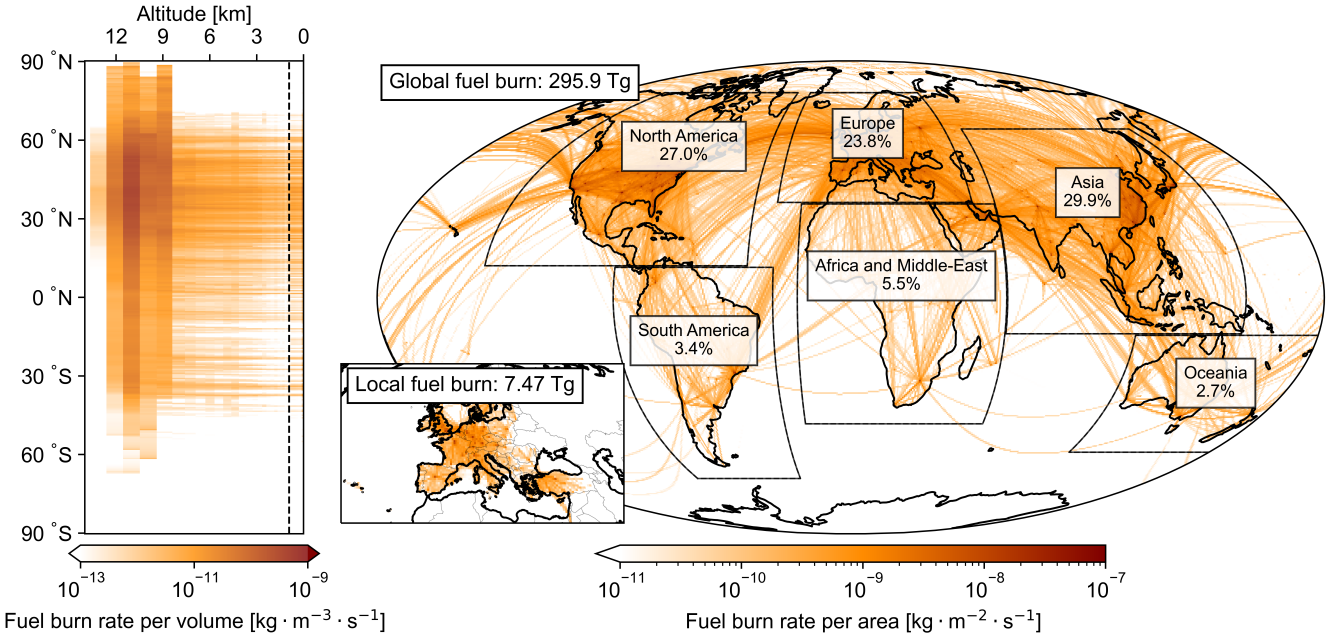

Figure 3.1: Average fuel burn rates in 2019 shown as the zonal average (left) and summed vertically (right). The percentages shown are the portion of the total fuel burn in 2019 that occurred within the bounded region. The inset shows the fuel burn for intra-European flights shorter than 750 km. The dashed line indicates the LTO threshold at 3,000 ft altitude.

3.1.1. Spatial distribution of fuel burn

The spatial distribution of fuel burn in 2019 is given in figure 3.1. The regions North America, Europe, and Asia combined contribute to 81% of the global aviation fuel burn. These regions were also identified as the major sources of emissions in previous studies [1, 7, 20, 126]. However, the division amongst these regions has changed, with Asia taking over as the region with the largest contribution to aviation emissions: we find that 30% of all emissions occurred in this region, versus 20% in 2006 [7].

Approximately 91% of the global aviation fuel burn is caused by the cruise phase (i.e. above 3000 ft altitude), which is in line with previous estimates [1, 7, 12]. The majority of fuel burn (74%) occurs at high altitudes, above flight level 270, which corresponds to cruise altitudes of jet aircraft. More details regarding the vertical distribution of the fuel burn are provided in section SI 2.4.

3.1.2. Emission indices

Table 3.1 provides an overview of the global aviation emissions estimated by the openAVEM model. 8.7% of all CO_2 and SO_x emissions (which are linearly related to the fuel burn) occur during the LTO phase. For most of the other emitted species, the LTO phase has an increased relative impact due to higher fleet-average emission indices during this part of the flight.

This holds especially for emissions of CO and HC, byproducts of incomplete combustion. The EI of CO for the LTO phase is close to those found by experiments for low engine settings, while that for HC is on the higher end of the observed range [64]. However, given the high levels of modeling uncertainty

Table 3.1: Global emissions and fleet-average emission indices and their division between LTO and cruise flight phases.

Species	Emissions	LTO / cruise [%]	EI [kg^{-1}]			Notes
			Full flight	LTO	Cruise	
CO_2	934 Tg	8.7 / 91.3	3.155 g	3.155 g	3.155 g	-
NO_x	4.61 Tg	8.2 / 91.8	15.58 g	14.58 g	15.68 g	As mass of NO_2
SO_x	178 Gg	8.7 / 91.3	0.600 g	0.600 g	0.600 g	As mass of S
CO	760 Gg	28.6 / 71.4	2.569 g	8.397 g	2.011 g	-
HC	40.9 Mg	39.9 / 60.1	138.1 mg	630.7 mg	91.00 mg	-
$nvPM_m$	9.65 Mg	21.7 / 78.3	32.60 mg	81.15 mg	27.95 mg	Particle mass
$nvPM_N$	$3.47 \cdot 10^{26}$	11.8 / 88.2	$1.17 \cdot 10^{15}$	$1.58 \cdot 10^{15}$	$1.13 \cdot 10^{15}$	Particle number

for CO and HC, the results are within the uncertainty ranges provided by previous studies [22, 64].

Similarly, mass-based $nvPM_m$ emission indices are also higher for the LTO phase due to high thrust settings during take-off, matching the experimental results of previous studies [94, 129–131]. Regarding cruise EIs, experiments using a chase aircraft suggest values in the order of 10 mg kg^{-1} [129]. As these experiments were conducted at reduced power settings, however, real operations are expected to yield higher values [35, 132]. More recently, emission indices used in aviation emission inventories ranged from 25 mg kg^{-1} to 40 mg kg^{-1} for full flight operations [5, 19, 20]. Compared to the 1992 fleet, the average $nvPM_m$ emission index has reduced from approximately 40 mg kg^{-1} to just under 28 mg kg^{-1}.

Emission indices based on particle number, $EI\text{-}nvPM_N$, agree with the range of $2 \cdot 10^{14}$ to $3 \cdot 10^{15}$ kg^{-1} as measured during the SULFUR flight campaigns [132]. The $nvPM_N$ emission index of $1.13 \cdot 10^{15}$ kg^{-1} is slightly smaller than the $1.2 \cdot 10^{15}$ kg^{-1} in 1992.

The emission index for NO_x, on the other hand, is lower during LTO operations than in other flight phases. In general, NO_x emission indices increase with increasing operating temperatures in the combustion chamber, matching high thrust settings [4, 64]. This suggests that in the overall LTO results, the effects of lower thrust settings during landing and taxiing dominate over those of increased thrust during take-off for these specific emissions.

Considering the global average, the emission index of NO_x has increased by roughly 10% compared to studies with older emission estimates [1]. The emission indices of HC and CO, on the other hand, are approximately 50% and 10% lower than previously estimated, respectively. This is in agreement with the increased efficiency of modern engines and their higher operating temperatures in the combustion chamber [4].

3.1.3. Effects of aircraft size

Figure 3.2 shows the contributions to the total fuel burn for various aircraft sizes and flight distances. For the former, similar results are found to those presented by recent studies: 52% of the fuel is burned by widebody aircraft, while another 42% is associated with narrowbody aircraft [4, 77, 92]. These aircraft types are the predominant source of fuel burn in all regions, with the fraction of total fuel burn attributable to these aircraft ranging from 85% in North America to 98% in Asia. Especially in the regions Oceania and Africa and the Middle-East, widebody aircraft are used profoundly, contributing to 63% and 72% of the regional fuel burn, respectively.

Turboprop aircraft are estimated to use 1.1% of all aviation fuel, which is in line with the decline in fuel burn for this aircraft type as discussed by Kim et al. [1]. Business jets, on the other hand, show a particularly high fuel burn within the North American region, accounting for 3.1% of the local fuel burn. In other regions, the contribution of business jets to all local fuel burn varies from 0.13% in Asia to 0.66% in Europe. A similar trend is visible for regional jets: 10% of all fuel burn over North America is associated with this type of aircraft, while other regional fractions vary from 0.75% in Asia to 4.2% in Europe. Hence, of all fuel burn associated with business jets and regional jets, 78% and 63% occurs over North America, respectively.

We find that narrowbody aircraft have the highest fuel efficiency (i.e. they show the smallest fuel burn per RPK) of the aircraft types investigated, and emit 103 g of CO_2 per RPK. Smaller aircraft are associated with the highest CO_2 intensity; business jets

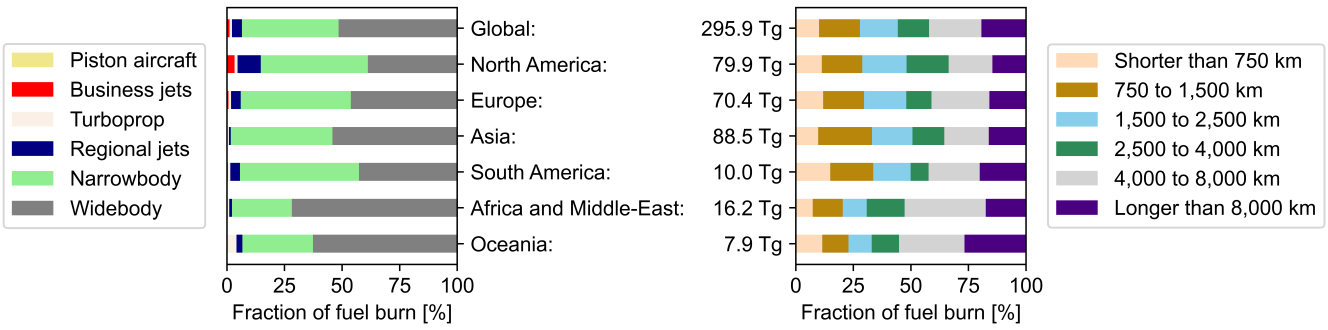

Figure 3.2: Division of global and regional fuel burn in 2019 for aircraft size (left) and flight distance (right). The central panel provides total fuel burn estimates per region. The results show the fuel burn directly above each region, which are bounded as shown in figure 3.1.

emit up to 569 g CO_2 per RPK. Comparing airliners, it is estimated that widebody aircraft emit approximately 24% more CO_2 per RPK than narrowbody aircraft. These figures are approximately 20% and 44% higher than the estimates of Graver et al. [125] for narrowbody and widebody CO_2 intensity, respectively. This is partially explained by the use of a lower load factor (we use 70% instead of 70-85% by Graver et al. [125]) and in agreement with our lower estimate of RPKs, especially for narrowbody aircraft [125, 126]. Furthermore, we assign all emissions to passengers, while Graver et al. [125] exclude cargo-related (≈ 5 - 35%) emissions. As these are more relevant on larger aircraft, our estimates deviate more for this aircraft category than for smaller aircraft.

Considering other emitted species, widebody aircraft emissions of NO_x per RPK are estimated to be 75% larger than those of narrowbody aircraft, while normalised emissions of HC, CO, and $nvPM_m$ are 9%, 43%, and 51% smaller, respectively. This is in agreement with a longer mean flight distance for widebody aircraft, yielding full flight emission indices which are closer to those for the cruise phase (as shown in table 3.1).

When the fuel burn efficiency of narrowbody aircraft is directly compared to that of widebody aircraft on shared medium-haul routes, the fuel burn of narrowbody aircraft is found to be 26% lower on an RPK basis than that of widebody jets. As this number is only slightly larger than the 24% difference in narrowbody and widebody aircraft fuel burn per RPK found for all global flights, we conclude that the bias caused by the route network in our main study is limited. The lower fuel efficiency of widebody aircraft may partially be explained by how they are operated in the network. The average flight distance of widebody aircraft on these shared routes is only 1,918 km, while it is 4,318 km when all widebody aircraft are considered. Since widebody aircraft are designed for longer flights, they are inherently heavier and used in a less optimal manner on short flights compared to narrowbody aircraft [133].

This effect is less significant for narrowbody aircraft on short routes. When these aircraft are compared to turboprop aircraft and regional jets on shared routes, it is evident that the higher capacity of the narrowbody jets yields 18% and 23% lower fuel burn per RPK, respectively. However, turboprop aircraft show lower NO_x emissions (up to 30% less than narrowbody aircraft) and may thus have a smaller impact on air quality. This confirms the findings of previous studies investigating the effects of replacing regional jets by turboprop aircraft, although the differences are estimated to be smaller in our study [91, 134].

3.1.4. Effects of flight distance

Globally, we find that long-haul flights (longer than 4,000 km) are responsible for 42% of all fuel burn, while constituting only 5.3% of all flights. Conversely, short-haul flights (shorter than 1,500 km) account for 28% of global fuel burn, while they make up 72% of all flights. The disproportionality of the fuel share is visualised in figure 3.3; it is slightly larger than that found for 2006 by Wilkerson et al. [20] and for 2018 by Graver et al. [126]. The latter estimated short-haul flights to be responsible for 32% of all fuel burn. We expect that the difference is mostly caused by a difference in fleet composition between the two studies: Graver et al. [126] used a data set with 23% fewer flights operated by widebody aircraft, while narrowbody aircraft were assigned to 5% more flights than in our study. As widebody aircraft are typically associated with longer flights than narrowbody aircraft, we expect that the smaller presence of widebody aircraft yields a larger contribution of short-haul flights to the overall fuel burn.

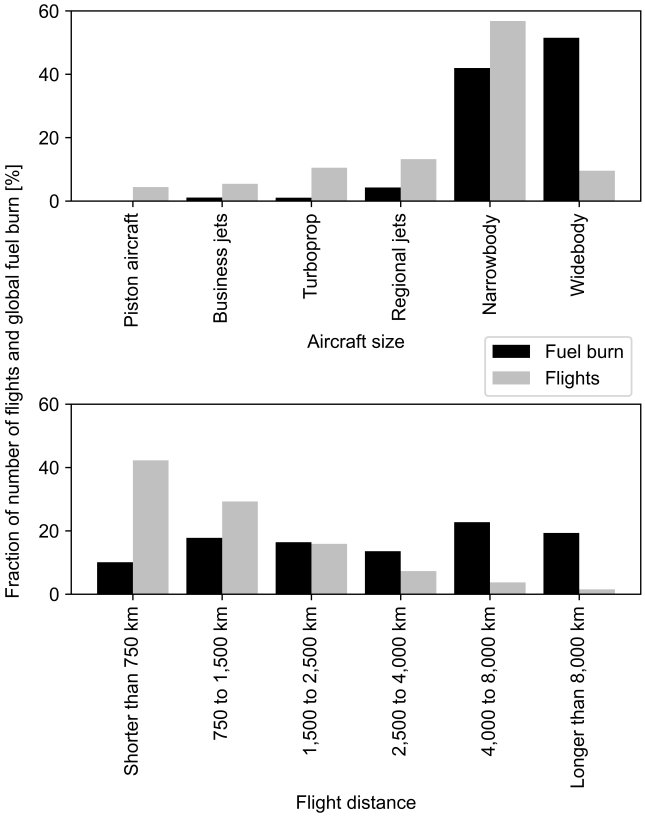

Figure 3.3: Relative contributions to global fuel burn and flight numbers for aircraft size (top) and flight distance (bottom).

The heavy use of widebody aircraft in Oceania and Africa and the Middle-East corresponds to an increased contribution to fuel burn of long-haul routes in these regions. In Oceania, this can be attributed to its remote location and need for long-haul flights to connect with other regions. For the African region, this trend is expected to be the result of a combination of two factors. First of all, there is limited inter-regional traffic and associated need for narrowbody aircraft [92, 126]. Secondly, the Gulf States in the Middle-East are home to several airlines performing primarily long-haul flights to connect regions such as Europe and Oceania.

Regarding CO_2 intensity, the observed trend (see section SI 5.2) matches the results obtained in literature [125, 126]. The emissions per RPK are highest on short routes, decreasing to a value of approximately 75 g of CO_2 per RPK for routes between 1,500 and 4,000 km, while they increase towards 90 g of CO_2 per RPK for long-haul flights.

Finally, intra-European flights shorter than 750 km are associated with 3% of global fuel burn, and 11% of fuel burned over Europe. The average fuel burn intensity of these flights is 37% higher than the average of all aviation, yielding 163 g CO_2 per RPK. This can be attributed to the short distances flown on routes included in this data set. On average, a single flight only transports 88 passengers for a distance of 446 km. When the results are compared to the global average for flights shorter than 750 km, however, a 3% lower carbon intensity is observed. This is in agreement with previous findings and expected to result from European airlines (especially low cost carriers) typically using more fuel efficient aircraft than the global fleet average [126, 135].

3.1.5. Effects of aircraft generation

In total, 4.9 million flights were simulated to compare the fuel burn and emissions of different generations aircraft. The number of flights performed by old model types (defined in subsection SI 1.2.4) was 3.2 times that of flights operated by new generation aircraft for narrowbody models and 1.8 times for widebody aircraft. Furthermore, within this data set, older generation aircraft are more frequently used on shorter flights. The average flight distance of aircraft certified before 2000 is 16% and 26% shorter than that for narrowbody and widebody aircraft certified in 2000 or later, respectively. This is in line with the increase in average aircraft size and range over time [136]. In order to make a fair comparison, we take the fuel burn normalised per RPK as the selected metric.

Comparing old and new generation narrowbody aircraft, we observe a 12% decrease in fuel burn per RPK. Furthermore, the emission indices of HC, CO, $nvPM_m$ and $nvPM_N$ also reduced by 9%, 10%, 70%, and 57%, respectively. Especially the reductions in nvPM emission indices shows the effects of increased efforts towards clean combustion technologies [87, 137]. However, the overall increase in fuel efficiency is accompanied by a 6% increase in the NO_x emission index. While the overall NO_x emissions per RPK are 6% smaller for new generation narrowbody aircraft compared to the older generation, the increased emission index is in line with the findings of Quadros et al. [4].

Widebody aircraft show a similar reduction in fuel burn between generations, with the newer aircraft burning 9% less fuel per RPK than aircraft certified before 2000. However, whereas most emission indices of new narrowbody aircraft were lower than those of older models, widebody aircraft show the opposite trend: only the HC emission index decreased by 28%. The emission indices of NO_x, CO, $nvPM_m$, and $nvPM_N$ increased by 11%, 10%, 44%, and 52%, respectively. Combined with the reduced fuel burn per RPK, this yields almost constant CO emissions per RPK between the two generations of aircraft, while total emissions of NO_x increased slightly (1%), HC emissions decreased (35%), and $nvPM_m$ and $nvPM_N$ emissions rose by 31% and 38%, respectively. While the changes in NO_x emissions agree well with the observations of Quadros et al. [4], the higher EI of nvPM is surprising, given the sharpened regulations of these emissions [87]. We realise that these results may be sensitive to the aircraft and engine types involved in the analysis, and that the limited availability of engine test data for selected engines may impact the estimations of nvPM emissions across generations of aircraft [129, 131]. Thus, other trends may be observed for aircraft types that deviate from those described in subsection SI 1.2.4.

3.2. Impact on air quality

As the impacts of aviation on air quality and human health show similar patterns, we only discuss general effects for all aviation in this section for the purpose of brevity. Air quality impacts of individual aircraft categories can be found in the supporting information (SI 6). Figure 3.4 shows that the impact of all aviation in 2019 on NO_2 ground-level concen-

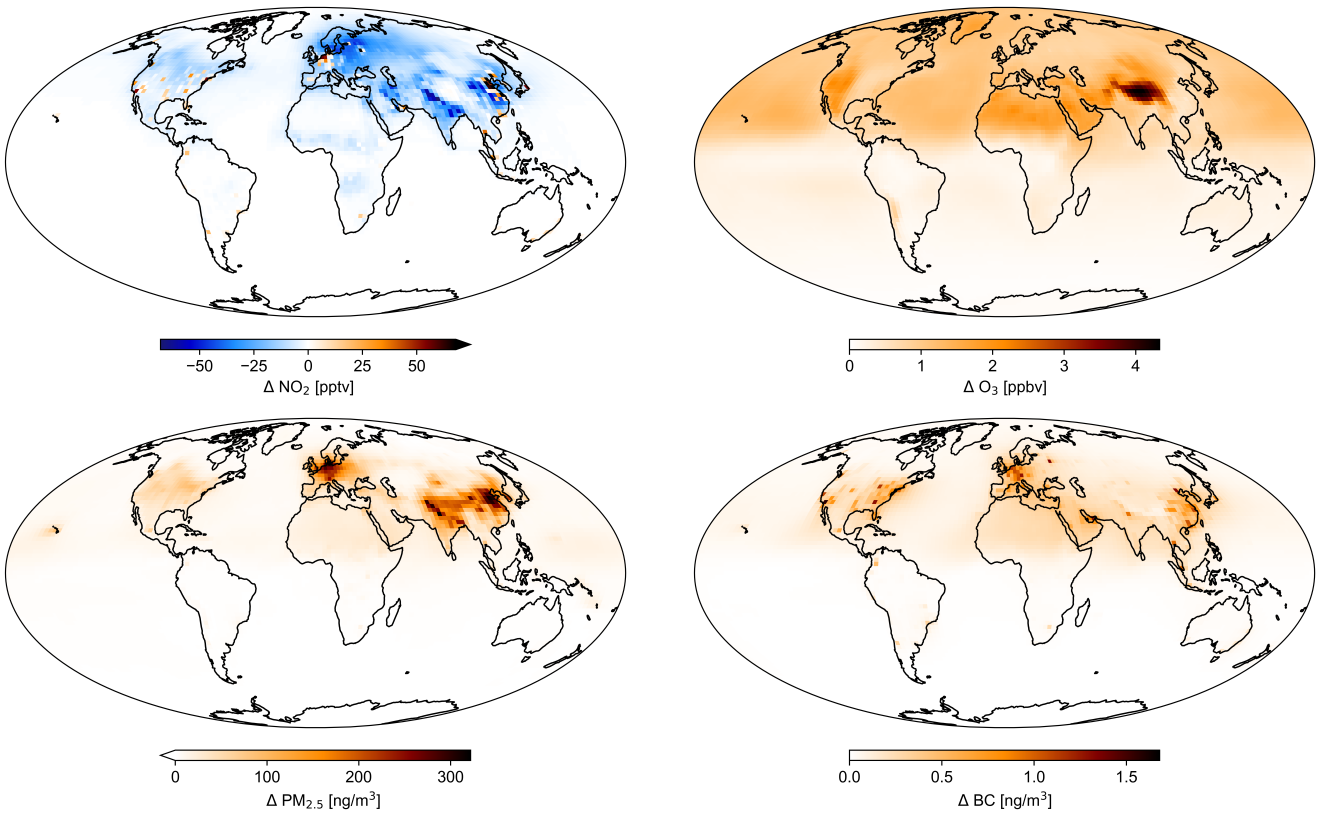

Figure 3.4: Global annual mean ground-level changes in NO_2 (top left), O_3 (top right), $PM_{2.5}$ (bottom left), and BC (bottom right) due to all aviation in 2019.

trations is negative in most regions, with the exception of grid cells near airports and large conglomerations. These findings agree with previous studies, which found that cruise emissions reduce ground-level NO_2, while LTO emissions increase local NO_2 concentrations [24, 28]. However, as NO_2 shows rather local behaviour, further grid refinement would be needed to fully capture the LTO effects [11, 138]. The population-weighted concentration shows that a large fraction of the impact is found in Asia, followed by Europe. Very limited effects are observed in the Southern Hemisphere, following the global distribution of aviation intensity.

For O_3, we find that aviation-attributable impacts on population-weighted concentrations show a temporal trend opposite to background O_3 levels, as was also established in literature [9, 24, 28]. Thus, peak season O_3 impacts are generally smaller than impacts averaged over the entire year. Our results show this effect particularly in North America and Europe, while areas with limited population (and thus other anthropogenic emissions) generally present a stronger impact during the peak season. While we present both peak season and annual concentration impacts in section SI 6.4, the discussion here focuses on annual average values in agreement with our main metric used to determine the additional premature mortality [46].

Regarding the total population-weighted concentration, the largest impact is found in Asia (up to almost 2 ppbv on average), with Europe being second and the Southern Hemisphere showing more limited impacts. This agrees with the larger aviation activity in the Northern Hemisphere (and limited cross-over of O_3 towards the Southern Hemisphere, as found previously in literature [38, 41]), as well as the high population density in especially Asia. Southbound eastward transport yields elevated O_3 levels in North Africa and Asia due to emissions in the Atlantic flight corridor, while zonal jet streams further increase O_3 levels in Western North America [5, 9, 41].

On a global scale, we estimate an increase of 0.8 ppbv in O_3 ground-level concentrations, which is consistent with results of previous studies considering the increase in aviation activity since these studies [7, 23, 24, 28]. Per unit of fuel burn, our estimated increase in population-weighted concentration of 2.71 pptv $(\text{Tg of fuel})^{-1}$ is significantly smaller than the 3.29 - 4.47 pptv $(\text{Tg of fuel})^{-1}$ estimated by Quadros et al. [9]. They used regional perturbations and a finer grid, which could result in higher sensitivities depending on the region. Our results are,

however, close to those found by Eastham and Barrett [28] (2.87 pptv (Tg of fuel)$^{-1}$). It is important to realise that these results are for short-term O_3 only; without longer simulations to estimate the long-term effects of methane depletion on O_3 levels, we are likely to overestimate the total effect [24].

Compared to O_3, the aviation-induced change in population-weighted concentration of $PM_{2.5}$ is more concentrated in Asia (especially near the Tibetan Plateau and the Beijing area) and Western Europe. The majority of $PM_{2.5}$ consists of secondary nitrate aerosols. These are formed when sufficient ammonia is available, i.e. when the gas ratio is higher than 1.[11] The peaks of $PM_{2.5}$ concentrations in our results are consistent with findings in previous studies and associated with high ammonia concentrations or major airports in Europe and Asia [5, 7]. Mean changes in ground-level concentrations are approximately 50% higher than estimated by Yim et al. [7], which is in line with the difference in aviation emissions relative to our study. Per unit of fuel burn, our estimate of 0.329 µg m^{-3} (Tg of fuel)$^{-1}$ is again smaller than that of Quadros et al. [9] (0.430 - 0.707 µg m^{-3} (Tg of fuel)$^{-1}$, depending on the region), but slightly larger than the increases found by Eastham and Barrett [28] (0.282 µg m^{-3} (Tg of fuel)$^{-1}$).

We find that 0.4% of all aviation-attributable population-weighted $PM_{2.5}$ is BC. This is double of that estimated by Koo et al. [25] and regional results vary from 0.3% in Asia to 2.9% in Oceania. Compared to general $PM_{2.5}$, the impacts of BC are more focused around large airports, confirming that these impacts are predominantly caused by LTO emissions. However, based on population-weighted concentration, the effects in different regions are less dispersed. This is most likely caused by the BC affecting mostly highly-populated areas around airports in each region, while further intra-regional transport is limited. Although Asia still shows the largest impacts, these are only a factor 90 larger than in Oceania (the region with the smallest impacts), compared to a factor of nearly 900 for generic $PM_{2.5}$.

3.3. Health impact

We estimate that approximately 80,000 (95% CI: 55,600 - 106,300) premature mortalities could be attributed to global aviation-related emissions in 2019. This is in the order of 20% to 50% of the total transport-related health impact found in previous studies for the period 2005 to 2015 [124]. The estimated number of premature mortality is also 33% higher than for shipping emissions in 2012, while total fuel burn is similar [141]. While this suggests a relatively high sensitivity of human health impact to aviation fuel burn (2 to 4 times higher than for transportation in general and 1.3 times higher than for shipping), we must note that, like for aviation emissions, the air quality impacts of road and shipping emissions are not fully understood yet [124, 128].

The increase of our mortality estimates relative to older studies is impacted by higher baseline mortality rates (22% higher than in 2005), as well as a 64% increase in global aviation fuel burn since 2005. Corrected for these changes, our results show a 156% larger impact than the estimates by Yim et al. [7] or Eastham and Barrett [28], but a 30% smaller impact than presented by Quadros et al. [9]. Besides variations in atmospheric background composition, the applied concentration response functions are expected to be the main source of the differences observed between ours and previous studies.

Figure 3.5 shows that almost 65% of the global early deaths are observed in Asia, specifically in India and China. Using the adjoint of the GEOS-Chem model, Koo et al. [25] found that this region contributed to 73% of global mortality associated with aviation-attributable changes in $PM_{2.5}$ concentrations. While our estimate of total early deaths associated with $PM_{2.5}$ in Asia is close to that of Koo et al. [25], we find larger impacts in North America (7% of the global total versus less than 3% estimated by Koo et al. [25]) and Europe (27% versus 17%). These variations are a combined effect of changes in global population and the use of a different aviation emissions model, as well as the application of different concentration response functions.

While large regional variations are observed in the contribution of different species, O_3 is estimated to be responsible for approximately 65% of global aviation-related mortality. This result was also obtained by Quadros et al. [9], while older studies found smaller (13-43%) relative impacts of O_3 [7, 28]. In Europe, 47% of premature mortality is associated with $PM_{2.5}$, while this number ranges from 10% to 19% for regions in the Southern Hemisphere.

Regions with high aviation activity show a lower contribution of BC to all $PM_{2.5}$ impacts. Several effects may explain this observation; first of all, these regions incur higher aviation NO_x emissions, which can lead to increased secondary aerosol formation.

[11] Please refer to e.g. Dennis et al. [139] and Zhang et al. [140] for more details about the gas ratio.

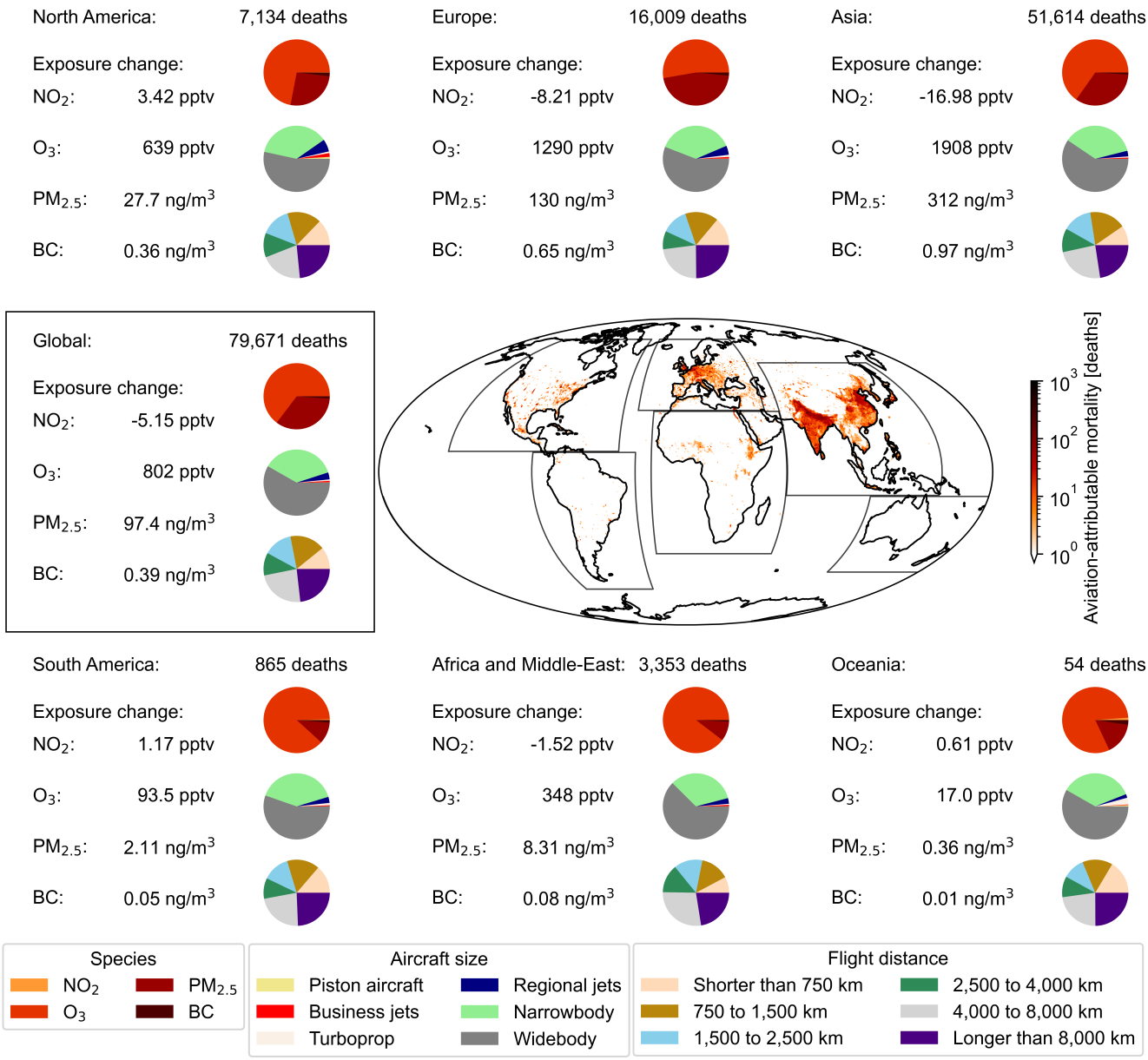

Figure 3.5: Global and regional aviation-attributable changes in population-weighted concentration of NO_2, O_3, $PM_{2.5}$, and BC, along with global and regional aviation-attributable premature mortality estimates and contributions of aircraft categories. The pie charts show, from top to bottom in each region, 1) the mortality associated with each species, 2) the impact of each aircraft size, and 3) the contribution of each flight distance to the regional aviation-attributable early deaths. The map shows the global distribution of all aviation-attributable premature mortality.

Secondly, these regions tend to have a higher population density in areas further away from airports, reducing the population-weighted effect of BC. As general $PM_{2.5}$ is dispersed more (and secondary aerosols can form at locations away from the emission source), the impact of $PM_{2.5}$ shows a smaller reduction away from the airports [7, 23].

The effect of aviation emissions on NO_2 related mortality is limited to within 2% of the total mortality in each region, with a global opposite effect of 0.02%. This is dominated by the expected abatement of 158 premature mortalities in Asia, while the Americas and Oceania show positive impacts on premature mortality caused by NO_2 concentration increases. We thus find very limited effects of NO_2 due to aviation, but recognise that the global $2° \times 2.5°$ grid is too coarse to capture local NO_2 effects. As discussed in previous studies, grid refinement may thus yield higher premature mortality impacts for aviation-attributable NO_2 [11, 138].

As mentioned in section 2.5, the concentration response functions are an important source of uncertainty in our impact assessment. For O_3 related premature mortality, nominal estimates vary from approximately 18,300 (using the CRF for respiratory mortality by Huangfu and Atkinson [48]) to almost

75,000 (applying the single-pollutant CRF by Di et al. [59]). The width of the 95% confidence intervals also varies amongst studies, up to 100% of the nominal values for the all-cause CRFs by Turner et al. [46] and Huangfu and Atkinson [48]. In general, mortality estimates using all-cause mortality as an end-point tend to yield higher impacts than those using respiratory infections only.

Alternative CRFs for $PM_{2.5}$ yield nominal mortality estimates between 12,000 (for all-cause mortality using the CRF by Krewski et al. [142]) and 57,000 (for the CRF by Beelen et al. [143]). Similar to the O_3 impacts, aviation-attributable premature mortality is estimated to be highest when all-cause mortality is considered as the health end-point. For NO_2 and BC, uncertainties are of similar magnitude relative to the nominal values; more details are provided in section SI 6.4.

3.3.1. Impact of aircraft size

We find that widebody aircraft operations are responsible for approximately 57% of global aviation-attributable premature mortality. Figure 3.6 shows that about two thirds of this impact is associated with O_3 increases. Although some regional variation exists, figure 3.5 indicates that this aircraft category is associated with the majority of impacts in each region investigated in this study. Narrowbody aircraft contribute 32% (in Africa and the Middle-East) to 39% (in South America) towards all aviation-related early deaths. However, their impact on premature mortality related to increases in BC concentrations exceeds that of widebody aircraft and is approximately 70% of all global BC impact. This agrees with the stronger effect of LTO operations on BC versus the pathways of NO_x to $PM_{2.5}$.

All other aircraft categories affect less than 5% of global premature mortalities (see figure 3.6), but large variations between regions are observed. For example, business jets and regional jets show significantly higher impacts in North America and Europe than in other regions, mostly due to increases in $PM_{2.5}$ concentrations. Turboprop aircraft, on the other hand, are more profound in Oceania and their impacts exceed those of regional jets in this region. Globally, however, turboprop aircraft are associated with less early deaths than either business jets or regional jets, mostly due to their limited impact on BC and O_3.

Figure 3.7 shows that the estimated aviation-attributable excess mortality normalised per RPK is 4 to 6 times larger for business jets and piston aircraft than for narrowbody aircraft, respectively. The sensitivity of air quality impacts and resulting excess mortality towards aviation emissions varies significanlty amongst these categories. For business jets, the same amount of fuel burn yields only 0.7 times as many early deaths as for narrowbody aircraft, while piston aircraft show a sensitivity which is 3.6 times as high as for narrowbody aircraft. Health impacts of widebody aircraft are 66% larger than those of narrowbody aircraft when normalised per RPK. However, after correcting for the increased fuel burn per RPK and higher NO_x emission index, the sensitivity of aviation-attributable premature mortality towards NO_x emissions of widebody aircraft is 24%

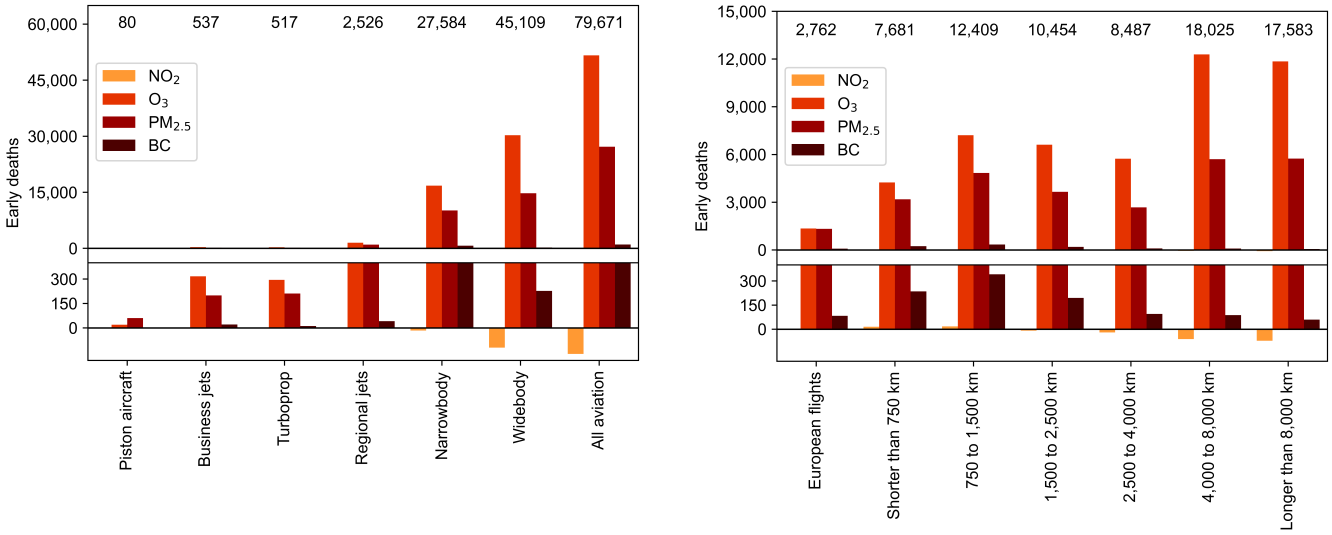

Figure 3.6: Global aviation-attributable mortality for each aircraft size, as well as all aviation (left) and for each flight distance, as well as intra-European flights shorter than 750 km (right). The impacts due to NO_2 and BC, as well as small aircraft, are shown in zoomed plots at the bottom.

smaller than for narrowbody aircraft. When a single flight is taken into account, widebody operations show an impact which is one to two orders of magnitude larger than those of other aircraft types, while a single passenger has the smallest impact on turboprop flights. For more details, please refer to section SI 7.3.

Finally, we estimate the sensitivity of aviation-attributable health impacts due to aircraft types on shared short-haul routes. The results indicate that turboprop aircraft, regional jets and narrowbody aircraft all show a higher fuel burn per RPK on these routes than the global fleet-average. However, the impact on aviation-attributable mortality is small especially for turboprop aircraft, showing approximately 14 times fewer early deaths per RPK than the global fleet-average. We noted significant noise in the GEOS-Chem results and thus have low confidence in these results. A further discussion on these results can be found in section SI 7.1, along with the zonal mean plots showing the atmospheric impacts in subsection SI 6.3.4.

3.3.2. Impact of flight distance

Figure 3.6 shows that the division of mortality impacts amongst different flight distance groups is more uniform than for aircraft size. However, small regional variations are visible in figure 3.5, and the groups of long-haul flights tend to show larger impacts than those of short-haul flights, contributing to almost half of the global aviation-related mortality. Figure 3.6 indicates especially large effects on O_3-related mortality for these flights, whereas $PM_{2.5}$ is relatively more important for mortality caused by shorter flights.

The relative impact on premature mortality of O_3 compared to $PM_{2.5}$ increases with flight distance. In most regions, O_3 is the main contributor to aviation-attributable early deaths. However, in Europe, mortality associated with short-haul flights is mostly caused by $PM_{2.5}$. Simultaneously, the portion of $PM_{2.5}$-attributable premature mortality that is caused by BC decreases globally with flight distance. While short-haul flights show an increase in premature mortality due to aviation-attributable elevated NO_2 levels, this effect is opposite for long-haul flights, following previous observations [7, 11, 24, 31].

While aviation-attributable mortality per RPK reduces with increasing flight distance for both NO_2 and BC, it generally shows a minimum for medium-haul flights for O_3 and $PM_{2.5}$. The overall effect follows that of O_3 and $PM_{2.5}$, as can be seen in the right panel of figure 3.7. This trend is similar to the one observed for CO_2 intensity in subsection 3.1.4.

A similar trend is observed for the sensitivity of mortality towards fuel burn, although the sensitivity for O_3 tends to be minimal for short- to medium-haul flights. From the perspective of a single passenger or flight, section SI 7.3 shows that short-haul flights incur the smallest negative impact on human health, with monotonically increasing aviation-attributable mortality rates for longer flights.

Furthermore, we estimate that globally, 2,800 excess premature mortalities are caused by intra-

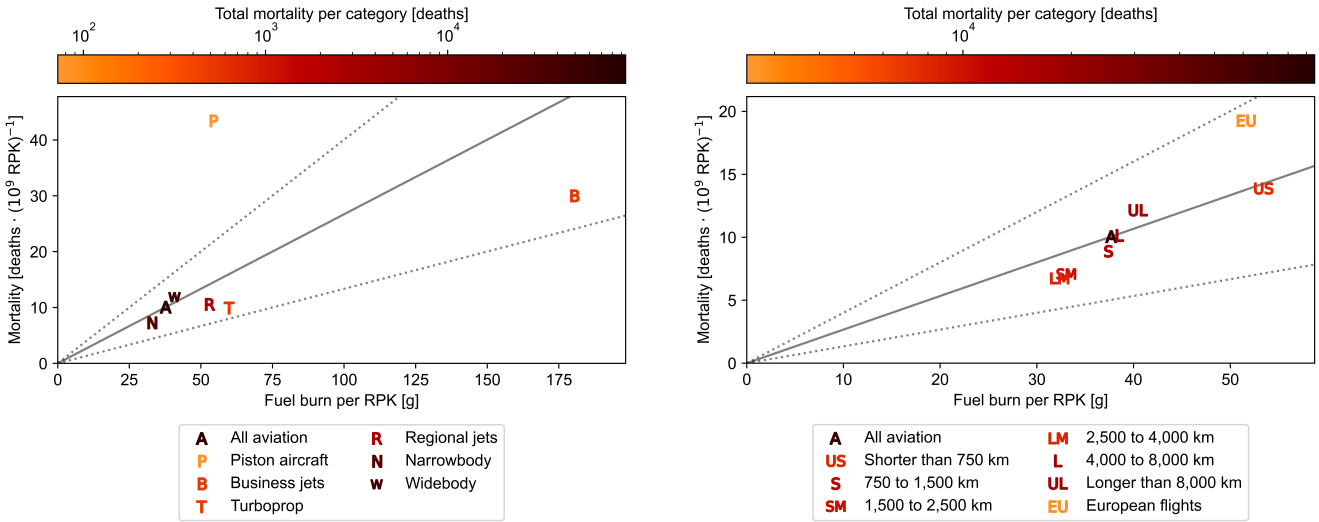

Figure 3.7: Sensitivity of aviation-attributable mortality rates per RPK to fuel burn vs fuel burn per RPK in 2019 per aircraft size (left) and flight distance (right). The colour of the markers indicates the total mortality attributed to each aircraft category. The grey line shows the sensitivity for all aviation, with the dashed lines representing a 50% increase or decrease in sensitivity.

European flights shorter than 750 km. This corresponds to 3.5% of all premature mortalities associated with aviation. Of these excess mortalities, 49% is incurred in Europe, while 44% affects the Asian population. Specifically, Asia is the receptor to 55% of O_3 and 35% of $PM_{2.5}$ impacts. Previous studies found that approximately 54% of $PM_{2.5}$ related premature mortality due to aviation emissions in Europe is found in Asia [9, 25]. Our results show a larger local impact in Europe, which is likely to result from the fact that we considered short-haul flights only. Within Europe, we also find that 8% of all $PM_{2.5}$ related mortalities are linked to BC, which is higher than for any other aircraft category included in this study.

Considering global mortality, these European flights constitute 36% of all impacts associated with flights shorter than 750 km globally. For any normalised metric, the impact of this selection of flights is larger than the global average for ultra short-haul flights. Per RPK, the intra-European flights show a 50% higher impact on mortality, while the normalised fuel burn is 3% lower, indicating an above-average sensitivity of the atmosphere towards the associated aircraft emissions. For more details, we refer to section SI 7.3.

3.4. Mitigation potential of sustainable alternatives

As discussed in the introduction, a variety of options exist to reduce future impacts of aviation on climate change and air quality. Before presenting a range of potential technological solutions, we briefly discuss the estimated effect of replacing old aircraft with newer generation models. Fleet renewal has shown to be an efficient method to reduce aviation carbon intensity, with fuel efficiency increasing over time [76]. However, as discussed in subsection 3.1.5, increased NO_x emission indices limit expectations for the associated air quality impact benefits. On the routes that we investigated (representing 12% of all flights and 15% of NO_x emissions in 2019), fleet renewal could reduce overall NO_x emissions by 3%. Extrapolating these results towards all global flights shows that the total effect of fleet renewal on NO_x emissions might be in the order of 1%. Combined with the decrease in fuel burn as mentioned in subsection 3.1.5, fleet renewal can have a positive impact on climate change mitigation efforts. However, further research is needed to quantify the impacts on air quality and human health.

Of the technological solutions, many are focused on alternative propulsion systems [71, 72, 75, 78–85]. Table 3.2 provides an overview of these technologies and their mortality mitigation potential. It also shows the potential of replacing all intra-European flights shorter than 750 km by train. We provide an upper bound of this mitigation potential, as not all routes included in this analysis are easy to replace in practice [68, 144]. In addition, this upper bound assumes that trains run on 100% renewable energy. While a large fraction of the European rail network is electrified, approximately 20% of rail traffic is powered by diesel engines.[12] Furthermore, the energy mix for electric trains also varies between countries and may rely on fossil fuels at least in the short term.[13] Thus, the overall impact of this strategy is expected to be less than 3.5% in terms of mitigated global early deaths. However, as seen in figure 3.7, the sensitivity of premature mortality to these flights is higher than the global average. In combination with the relatively well-organised rail network, Europe has the potential to mitigate the negative impacts of aviation with relatively limited effort compared to other regions.[12]

Given the limited energy density of battery packs, we assume that battery technology is only applied to small aircraft, up to regional jets [77, 145]. For these aircraft types, 73% of all flights are shorter than 750 km. Thus, by assuming the use of batteries on all flights operated by these aircraft, including those longer than 750 km, we overestimate the potential effect of the implementation of this technology. Table 3.2 shows that the implementation of battery technology can yield a global reduction of 4.6% in aviation-attributable premature mortality, but in practice this effect is expected to be smaller. In Europe, roughly 30% of the current energy mix is produced using renewable sources, while the global average is half of this figure [146, 147]. The remainder comes mostly from conventional power plants, contributing to air pollution; flying electric on energy produced by these plants would shift rather than mitigate the impacts of air quality degradation [122, 146].

Hydrogen fuel cells provide a clean and relatively lightweight alternative for small aircraft, although its application is mainly limited by the output power

[12] https://alternative-fuels-observatory.ec.europa.eu/transport-mode/rail. Last accessed on 5 May 2023.
[13] https://nachhaltigkeit.deutschebahn.com/en/measures/ice. Last accessed on 5 May 2023.

Table 3.2: Overview of sustainable aviation alternatives and their mitigation potential regarding aviation-induced premature mortality. The percentage shown denotes the percentage of all mortality that can potentially be prevented through the application of each technology.

Technology	Replaced aircraft	Mitigated mortality (95% CI)	[%]	Notes
Train	< 750 km in Europe	2,800 (2,000 - 3,700)	3.5	Assuming all flights can be replaced by train and aviation emissions are reduced to zero
Batteries	Piston; business jet; turboprop; regional jet	3,700 (2,600 - 4,900)	4.6	27% of these flights are longer than 750 km, the expected range for this technology, yielding an overestimation of the effects
Hydrogen Fuel Cell	Piston; business jet; turboprop	1,100 (800 - 1,500)	1.4	84% of these flights are shorter than 750 km; this technology will mainly be used on short-haul flights
Hydrogen Combustion Turbofan	< 4,000 km	22,000 (15,500 - 29,500)	27.7	Assuming 50% NO_x reductions and a linear relationship between NO_x emissions and air quality related premature mortality
	< 8,000 km	30,800 (21,800 - 41,500)	38.7	
SAF	> 8,000 km	60 (48 - 71)	0.1	Assuming no change in NO_x and SO_x emissions but a 100% reduction of BC impacts
	All	1,000 (800 - 1,200)	1.3	

(and associated cooling requirements) [78, 84]. Based on recent developments in industry and the expected technological improvements in the near future, we assume that hydrogen fuel cells can be used for all aircraft types up to turboprops [78]. We estimate that this technology can provide a reduction in aviation-attributable early deaths of approximately 1.4%. Here, we implicitly assume that the hydrogen is generated from 100% renewable energy sources. Although the potential for hydrogen production in Europe is expected to meet future demands, currently there is no significant hydrogen production based on renewable sources [148].

The implementation of hydrogen-powered turbofans could yield a significant reduction of aviation-related premature mortality, as this technology may also be applicable to larger aircraft and longer flights [78, 79, 145]. Uncertainties exist on the range of hydrogen-powered aircraft, so we provide two scenarios: one in which all flights up to 4,000 km burn hydrogen instead of traditional jet fuel, and one in which flights up to 8,000 km do so. In our analysis, we assume a 50% reduction in NO_x emissions resulting from the adoption of hydrogen as a fuel, which is in line with ICAOs NO_x reduction targets and expected technological advancements [80, 87, 149]. For these scenarios, we assume a linear relationship between NO_x emissions and the total mortality; previous studies showed that NO_x emissions are responsible for both O_3 enhancement and 72% of aviation-attributable $PM_{2.5}$ increases, as well as 93% of population exposure to $PM_{2.5}$ [25, 31]. We do not consider the impacts due to the absence of SO_x emissions. As is shown in table 3.2, the use of hydrogen could potentially mitigate up to 39% of all aviation-attributable premature mortalities under the aforementioned assumptions. We stress, however, that this estimate assumes that global NO_x emissions are cut by 50%; our estimate is likely an upper bound of the mitigation potential.

Finally, another option which may aid in the reduction of aviation-related climate and air quality impacts is to replace conventional jet fuel with SAF. Depending on its constituents, the impact of SAF usage on aircraft emissions may vary, yielding uncertainties in estimations of its impact on air quality [84, 150]. In our analysis, we assume that the fuel has a similar composition to regular kerosene, such that the impacts of emissions on O_3 and secondary $PM_{2.5}$ does not change. Instead, we assume that BC concentrations are no longer affected when SAF is used and estimate the mortality effects as a 100% reduction in aviation-attributable BC impacts [84]. When SAF is considered only for flights longer than 8,000 km (assuming that ultra long-haul flights are the most likely field of ap-

plication for SAF), our analysis shows that 60 early deaths may be prevented. In case SAF were used on all flights, the mitigated premature mortality is estimated at approximately 1,000, i.e. 1.3% of all aviation-attributable impact. Thus, from a global air quality perspective, we expect SAF to have limited benefits over conventional aviation fuel. On a regional scale around airports, however, reduced BC concentrations may yield larger health benefits, given the localised impacts of BC [23]. Such impacts may be larger than what we are able to capture using our global grid. Furthermore, SAF also provides certain climate benefits, since its lifetime CO_2 emissions are expected to be lower than those of regular fuel; estimates range from 20% to 90% reductions, depending on the methods used to produce SAF [78, 81, 145, 151].

In conclusion, we expect that the early death mitigation potential of electric-powered aircraft (including hydrogen fuel cells) is limited to approximately 5% of all aviation impacts. Although this is more than what may be expected of SAF (without reductions in NO_x or SO_x emissions), more substantial changes require technologies that can be applied to large aircraft, such as turbofan engines running on hydrogen. These may reduce aviation-attributable mortality by approximately 39% and thus prevent a further rise in air quality impacts over the next decade. A key factor going forward is whether sufficient green hydrogen (and SAF) will be available in time, and for a price which can compete with conventional fuel [81, 84, 145]. In line with the conclusions of Arter et al. [11] on LTO related air quality impacts, we conclude that NO_x reductions may help to mitigate the total aviation-attributable health impacts. However, one should also consider the climate impacts, which tend to increase when engines are designed for lower NO_x emissions [152, 153].

3.5. Monetised impacts

Our results show that the impact of business jets, normalised for either RPKs or number of passengers, is several factors higher than that of commercial transport aircraft. However, compared to commercial aviation, the total impact is limited. In order to allow a comparison of impacts per passenger for single flights, we provide an impact assessment based on flight distance. Figure 3.8 shows the monetised air quality externality of a single passenger trip based on the flight distance. We use a 2015-based global value of statistical life (VSL) of USD 3.81 million, similar to Grobler et al. [12]. This yields an average air quality externality of USD 73.53 per flight for all aviation, while the monetised impacts increase rapidly for long-haul flights. As shown in figure 3.8, the average value associated with the air quality impacts of ultra long-haul flights is over 18 times larger than that of ultra short-haul flights.

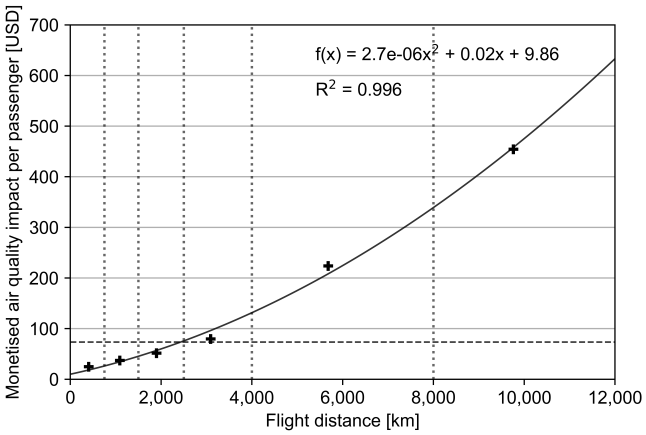

Figure 3.8: Estimated price increment needed to account for the air quality externality of various flight distances. A uniform VSL value of USD 3.81 million is assumed globally, based on Grobler et al. [12]. The plot shows a 2 degrees of freedom least squared interpolation of the averaged values (+) per flight distance bin (enclosed by vertical dotted lines). The horizontal dashed line shows the average monetised air quality impact per passenger for all aviation.

3.6. Limitations

The purpose of this study is to provide a general understanding of how aircraft size and flight distance relate to air quality impacts. In our analysis, we take a practical approach to ease policy implementation. This means that we take the actually observed flights of 2019 and in doing so, we introduce a bias towards results from regions with high aviation activity. It also means that individual aircraft categories are less fit for a direct comparison, as they are not evenly spread across regions and are thus affected by the non-uniform atmospheric chemistry processes. Our results thus provide insights in the current state of aviation-related impacts, but cannot be generalised when emission patterns are altered.

In this study, we use a global $2° \times 2.5°$ grid for the atmospheric simulations as a compromise between the required level of detail to be captured and the computational resources available. This means that local effects are likely underestimated compared to other studies that use regional grids of $0.5° \times 0.625°$ or smaller [120]. We expect that as a consequence, especially BC and NO_2 impacts are underestimated relative to the general $PM_{2.5}$ and O_3 impacts [123]. Another consequence of our grid choice is that the gas ratio cannot be computed with high confidence,

therefore further limiting the certainty of the regional variations in $PM_{2.5}$ sensitivity towards aviation NO_x emissions.

For some study cases, the investigated aviation emissions have such limited effect on the tropospheric composition that the results are impacted by numerical noise. This is especially true for $PM_{2.5}$, as was previously observed by Lee et al. [24] as well. Therefore, we have little confidence in a direct comparison between the turboprop and regional aircraft operations on short-haul routes. For such scenarios, in which only a small fraction of all aviation emissions are to be investigated, we suggest that a fictional scenario is used instead, in which the emissions are increased to prevent this issue.

Furthermore, we do not consider feedback mechanisms which are an integral part of the non-linear atmosphere. In reality, a change in aviation emissions would affect the atmospheric composition. This may cause changes in meteorology (e.g. lightning, which is a source of NO_x of similar magnitude as aviation [154]) and the effect of other emissions (such as shipping emissions) [30]. By not accounting for this feedback, we may underestimate the impact of the changes in our emission scenarios. Cameron et al. [30] found global mean surface perturbations of O_3 to be up to 35% higher when the atmospheric feedback was included in the model, although these variations were smaller than the observed seasonal variations within each model. For $PM_{2.5}$, they found effects including feedback to be up to 4 times larger than those without atmospheric feedback. However, they warned that these differences could partially be explained by the specific feedback mechanisms applied by the models. We also stress that our results are applicable only to present day atmospheric conditions and are thus not fit for predicting future impacts of sustainable aviation. If the aim is to estimate such impacts, one would need to use future scenarios for both aviation emissions and the state of the atmosphere [155].

Finally, we assume that the health effects of the individual pollutants can be combined to obtain the aggregate impact of the air quality degradation on human health. However, the species under investigation are closely interlinked, and by artificially decoupling the effects of NO_2, $PM_{2.5}$ and O_3, we expect to overestimate the total impact. As there are currently no CRFs available which are applicable to all four species used in this study, we choose to accept this error. Since we aim to provide an overview of maximum attainable mitigation, this approach provides conservative results.

4. Conclusions

Using a multidisciplinary approach, we find that almost 80,000 early deaths in 2019 can be associated with aviation emissions. While this figure is 5 times as high as the 16,000 annual early deaths estimated by Yim et al. [7] and Eastham and Barrett [28], our estimate of the health impact is based on a 22% increase in baseline mortality rate and 64% increase in aviation fuel burn since past studies. Correcting for these differences, our estimate is 2.6 times as high as that of Yim et al. [7] and Eastham and Barrett [28], but 30% lower than the impact found by Quadros et al. [9]. We also estimate that almost 65% of the global aviation-attributable premature mortality is related to O_3. Furthermore, 65% of the global impact is incurred in Asia, mainly driven by the high population density in this region, as well as the impacts due to emissions over Europe and North America.

Furthermore, we estimate the contribution of flights towards all aviation emissions, air quality impacts, and aviation-related premature mortality based on aircraft size and flight distance. Widebody aircraft are associated with 52% of global fuel burn and 57% of global aviation-attributable early deaths. Normalised per RPK, their fuel burn is 24% higher than for narrowbody aircraft, while the impact on human health is 66% larger. Furthermore, regional variations are observed, with a larger contribution of regional jets and business jets in North America than elsewhere. Overall, the effects of smaller aircraft are small when compared to those of commercial airliners, contributing to less than 5% of the total impact.

However, the flights associated with these aircraft are most likely to be replaced in the quest for a more sustainable aviation sector. We stress that, while the current focus on these aircraft types is understandable, technologies need to be scaled up towards applications on narrowbody aircraft to mitigate more than 5% of all aviation-related health impacts. Based on this study, hydrogen-powered turbofan technology may provide the largest relief regarding aviation-attributable premature mortality. These results are largely driven by assumed reductions in NO_x emissions, indicating that the implementation of low-NO_x technologies could have a larger impact than the development of electric aviation. Similarly, the expected mortality mitigation through the usage of SAF is limited to approximately

1% if NO_x and SO_x emissions remain the same as for conventional jet fuel.

We also find that the total fuel burn is rather evenly spread out across various flight distance bins, but that 42% of the global fuel burn and 49% of aviation NO_x emissions is caused by only 5.3% of the flights which operate on long-haul routes. These flights are also associated with almost half of the global mortality, which is especially O_3 related. Very limited regional variations are observed, except for a stronger impact of longer flights in Africa and the Middle-East.

Overall, however, the results show rather high consistency, allowing a uniform approach in mortality abatement strategies. We find that monetisation of the impacts yields progressively higher needs for offsetting for longer flights, with ultra long-haul flights being associated with more than 18 times higher impacts on mortality per flight than ultra short-haul flights.

In agreement with Quadros et al. [9], we find large inter-regional effects of emissions, such that the removal of intra-European flights yields almost as many averted early deaths in Asia as in Europe. These flights also have a 50% larger impact per RPK than similar flights globally. Furthermore, the contribution of individual species varies per flight distance, with BC impacts being mostly relevant on short flights and the ratio of O_3 to $PM_{2.5}$ impacts increasing with flight distance. For NO_2, a positive impact is found for short flights, but reductions are observed for long flights. We recognise the caveat that our grid level is too coarse to capture all LTO impacts and therefore is likely to underestimate the concentration increases near airports or conglomerations in general.

With this study, we provide insights into the impact of aircraft size and flight distance on aviation emissions, air quality, and human health. The trends that were discussed in this paper can be used for developing general policies regarding the future of aviation. However, we also see added value in technology-specific impact assessment, in which the aviation emissions are tailored to fit the expected emissions pattern of a certain technology. For example, emissions of selected aircraft can be adjusted for the introduction of hydrogen fuel cells or SAF into part of the global fleet. Future studies may provide more detailed insights into the effectiveness of such measures.

Furthermore, our findings suggest that the penalty of using a coarse grid in the Southern Hemisphere for the atmospheric chemistry-transport model is limited, and more accurate results may be obtained through the usage of a nested grid model focusing on the regions North America, Europe, and Asia, where the majority of air quality impacts are found. Finally, research efforts into multi-pollutant concentration response functions could reduce the uncertainty in health impact assessments and would contribute to a more accurate understanding of the real impact of aviation on air quality and human health.

References

[1] B. Y. Kim, G. G. Fleming, J. J. Lee, I. A. Waitz, J. P. Clarke, S. Balasubramanian, A. Malwitz, K. Klima, M. Locke, C. A. Holsclaw, L. Q. Maurice, and M. L. Gupta. System for assessing Aviation's Global Emissions (SAGE), Part 1: Model description and inventory results. *Transportation Research Part D: Transport and Environment*, 12:325–346, 2007. ISSN 13619209. DOI: 10.1016/j.trd.2007.03.007.

[2] D. S. Lee, D. W. Fahey, P. M. Forster, P. J. Newton, R. C. Wit, L. L. Lim, B. Owen, and R. Sausen. Aviation and global climate change in the 21st century. *Atmospheric Environment*, 43:3520–3537, July 2009. ISSN 13522310. DOI: 10.1016/j.atmosenv.2009.04.024.

[3] B. Owen, D. S. Lee, and L. Lim. Flying into the Future: Aviation Emissions Scenarios to 2050. *Environmental Science and Technology*, 44:2255–2260, April 2010. ISSN 0013936X. DOI: 10.1021/es902530z.

[4] F. D. Quadros, M. Snellen, and I. C. Dedoussi. Recent and Projected Trends in Global Civil Aviation Fleet Average NO_x Emissions Indices. In *AIAA SCITECH 2022 Forum*. American Institute of Aeronautics and Astronautics (AIAA), January 2022. DOI: 10.2514/6.2022-2051.

[5] S. R. Barrett, R. E. Britter, and I. A. Waitz. Global Mortality Attributable to Aircraft Cruise Emissions. *Environmental Science and Technology*, 44:7736–7742, October 2010. ISSN 0013936X. DOI: 10.1021/es101325r.

[6] C. S. Dorbian, P. J. Wolfe, and I. A. Waitz. Estimating the climate and air quality benefits of aviation fuel and emissions reductions. *Atmospheric Environment*, 45:2750–2759, May 2011. ISSN 13522310. DOI: 10.1016/j.atmosenv.2011.02.025.

[7] S. H. Yim, G. L. Lee, I. H. Lee, F. Allroggen, A. Ashok, F. Caiazzo, S. D. Eastham, R. Malina, and S. R. Barrett. Global, regional and local health impacts of civil aviation emissions. *Environmental Research Letters*, 10, March 2015. ISSN 17489326. DOI: 10.1088/1748-9326/10/3/034001.

[8] G. P. Brasseur, M. Gupta, B. E. Anderson, S. Balasubramanian, S. Barrett, D. Duda, G. Fleming, P. M. Forster, J. Fuglestvedt, A. Gettelman, R. N. Halthore, S. D. Jacob, M. Z. Jacobson, A. Khodayari, K. N. Liou, M. T. Lund, R. C. Miake-Lye, P. Minnis, S. Olsen, J. E. Penner, R. Prinn, U. Schumann, H. B. Selkirk, A. Sokolov, N. Unger, P. Wolfe, H. W. Wong, D. W. Wuebbles, B. Yi, P. Yang, and C. Zhou. Impact of Aviation on Climate: FAA's Aviation Climate Change Research Initiative (ACCRI) Phase II. *Bulletin of the American Meteorological Society*, 97:561–583, April 2016. ISSN 00030007. DOI: 10.1175/BAMS-D-13-00089.1.

[9] F. D. Quadros, M. Snellen, and I. C. Dedoussi. Regional sensitivities of air quality and human health impacts to aviation emissions. *Environmental Research Letters*, 15, October 2020. ISSN 17489326. DOI: 10.1088/1748-9326/abb2c5.

[10] D. S. Lee, D. W. Fahey, A. Skowron, M. R. Allen, U. Burkhardt, Q. Chen, S. J. Doherty, S. Freeman, P. M. Forster, J. Fuglestvedt, A. Gettelman, R. R. D. León, L. L. Lim, M. T. Lund, R. J. Millar, B. Owen, J. E. Penner, G. Pitari, M. J. Prather, R. Sausen, and L. J. Wilcox. The contribution of global aviation to anthropogenic climate forcing for 2000 to 2018. *Atmospheric Environment*, 244, July 2021. ISSN 18732844. DOI: 10.1016/j.atmosenv.2020.117834.

[11] C. A. Arter, J. J. Buonocore, C. Moniruzzaman, D. Yang, J. Huang, and S. Arunachalam. Air quality and health-related impacts of traditional and alternate jet fuels from airport aircraft operations in the U.S. *Environment International*, 158, January 2022. ISSN 18736750. DOI: 10.1016/j.envint.2021.106958.

[12] C. Grobler, P. J. Wolfe, K. Dasadhikari, I. C. Dedoussi, F. Allroggen, R. L. Speth, S. D. Eastham, A. Agarwal, M. D. Staples, J. Sabnis, and S. R. Barrett. Marginal climate and air quality costs of aviation emissions. *Environmental Research Letters*, 14, 2019. ISSN 17489326. DOI: 10.1088/1748-9326/ab4942.

[13] G. Chen, X. Li, X. Liu, Y. Chen, X. Liang, J. Leng, X. Xu, W. Liao, Y. Qiu, Q. Wu, and K. Huang. Global projections of future urban land expansion under shared socioeconomic pathways. *Nature Communications*, 11, December 2020. ISSN 20411723. DOI: 10.1038/s41467-020-14386-x.

[14] V. Gaigbe-Togbe, L. Bassarsky, D. Gu, T. Spoorenberg, and L. Zeifman. World Population Prospects 2022: Summary of Results. Technical Report 3, United Nations Department of Economic and Social Affairs, Population Division, 2022.

[15] A. Unal, Y. Hu, M. E. Chang, M. T. Odman, and A. G. Russell. Airport related emissions and impacts on air quality: Application to the Atlanta International Airport. *Atmospheric Environment*, 39:5787–5798, October 2005. ISSN 13522310. DOI: 10.1016/j.atmosenv.2005.05.051.

[16] J. Wormhoudt, S. C. Herndon, P. E. Yelvington, R. C. Miake-Lye, and C. Wey. Nitrogen Oxide (NO/NO_2/HONO) Emissions Measurements in Aircraft Exhausts. *Journal of Propulsion and Power*, 23:906–911, 2007. ISSN 15333876. DOI: 10.2514/1.23461.

[17] D. C. Carslaw, K. Ropkins, D. Laxen, S. Moorcroft, B. Marner, and M. L. Williams. Near-Field Commercial Aircraft Contribution to Nitrogen Oxides by Engine, Aircraft Type, and Airline by Individual Plume Sampling. *Environmental Science and Technology*, 42:1871–1876, March 2008. ISSN 0013936X. DOI: 10.1021/es071926a.

[18] M. O. Köhler, G. Rädel, O. Dessens, K. P. Shine, H. L. Rogers, O. Wild, and J. A. Pyle. Impact of perturbations to nitrogen oxide emissions from global aviation. *Journal of Geophysical Research Atmospheres*, 113, June 2008. ISSN 01480227. DOI: 10.1029/2007JD009140.

[19] D. S. Lee, G. Pitari, V. Grewe, K. Gierens, J. E. Penner, A. Petzold, M. J. Prather, U. Schumann, A. Bais, T. Berntsen, D. Iachetti, L. L. Lim, and R. Sausen. Transport impacts on atmosphere and climate: Aviation. *Atmospheric Environment*, 44:4678–4734, December 2010. ISSN 13522310. DOI: 10.1016/j.atmosenv.2009.06.005.

[20] J. T. Wilkerson, M. Z. Jacobson, A. Malwitz, S. Balasubramanian, R. Wayson, G. Fleming, A. D. Naiman, and S. K. Lele. Analysis of emission data from global commercial aviation: 2004 and 2006. *Atmospheric Chemistry and Physics*, 10:6391–6408, 2010. ISSN 16807316. DOI: 10.5194/acp-10-6391-2010.

[21] M. Givoni and P. Rietveld. The environmental implications of airlines' choice of aircraft size. *Journal of Air Transport Management*, 16:159–167, May 2010. ISSN 09696997. DOI: 10.1016/j.jairtraman.2009.07.010.

[22] M. E. Stettler, S. Eastham, and S. R. Barrett. Air quality and public health impacts of UK airports. Part I: Emissions. *Atmospheric Environment*, 45:5415–5424, October 2011. ISSN 1352-2310. DOI: 10.1016/j.atmosenv.2011.07.012.

[23] S. H. Yim, M. E. Stettler, and S. R. Barrett. Air quality and public health impacts of UK airports. Part II: Impacts and policy assessment. *Atmospheric Environment*, 67:184–192, March 2013. ISSN 13522310. DOI: 10.1016/j.atmosenv.2012.10.017.

[24] H. Lee, S. C. Olsen, D. J. Wuebbles, and D. Youn. Impacts of aircraft emissions on the air quality near the ground. *Atmospheric Chemistry and Physics*, 13:5505–5522, 2013. ISSN 16807316. DOI: 10.5194/acp-13-5505-2013.

[25] J. Koo, Q. Wang, D. K. Henze, I. A. Waitz, and S. R. Barrett. Spatial sensitivities of human health risk to intercontinental and high-altitude pollution. *Atmospheric Environment*, 71:140–147, June 2013. ISSN 13522310. DOI: 10.1016/j.atmosenv.2013.01.025.

[26] A. Ashok, I. C. Dedoussi, S. H. Yim, H. Balakrishnan, and S. R. Barrett. Quantifying the air quality-CO_2 trade-off potential for airports. *Atmospheric Environment*, 99:546–555, December 2014. ISSN 1352-2310. DOI: 10.1016/J.ATMOSENV.2014.10.024.

[27] M. Masiol and R. M. Harrison. Quantification of air quality impacts of London Heathrow Airport (UK) from 2005 to 2012. *Atmospheric Environment*, 116:308–319, September 2015. ISSN 18732844. DOI: 10.1016/j.atmosenv.2015.06.048.

[28] S. D. Eastham and S. R. Barrett. Aviation-attributable ozone as a driver for changes in mortality related to air quality and skin cancer. *Atmospheric Environment*, 144:17–23, November 2016. ISSN 1352-2310. DOI: 10.1016/J.ATMOSENV.2016.08.040.

[29] M. C. Woody, H. W. Wong, J. J. West, and S. Arunachalam. Multiscale predictions of aviation-attributable $PM_{2.5}$ for U.S. airports modeled using CMAQ with plume-in-grid and an aircraft-specific 1-D emission model. *Atmospheric Environment*, 147:384–394, December 2016. ISSN 18732844. DOI: 10.1016/j.atmosenv.2016.10.016.

[30] M. A. Cameron, M. Z. Jacobson, S. R. Barrett, H. Bian, C. C. Chen, S. D. Eastham, A. Gettelman, A. Khodayari, Q. Liang, H. B. Selkirk, N. Unger, D. J. Wuebbles, and X. Yue. An intercomparative study of the effects of aircraft emissions on surface air quality. *Journal of Geophysical Research*, 122:8325–8344, 2017. ISSN 21562202. DOI: 10.1002/2016JD025594.

[31] P. Prashanth, S. D. Eastham, R. L. Speth, and S. R. H. Barrett. Aerosol formation pathways from aviation emissions. *Environmental Research Communications*, 4:021002, February 2022. DOI: 10.1088/2515-7620/ac5229.

[32] N. A. Janssen, G. Hoek, M. Simic-Lawson, P. Fischer, L. van Bree, H. T. Brink, M. Keuken, R. W. Atkinson, H. R. Anderson, B. Brunekreef, and F. R. Cassee. Black Carbon as an Additional Indicator of the Adverse Health Effects of Airborne Particles Compared with PM_{10} and $PM_{2.5}$. *Environmental Health Perspectives*, 119:1691–1699, 2011. ISSN 15529924. DOI: 10.1289/ehp.1003369.

[33] N. A. Janssen, M. E. Gerlofs-Nijland, T. Lanki, R. S. Salonen, F. Cassee, G. Hoek, P. Fischer, B. Brunekreef, and M. Krzyzanowski. Health effects of black carbon. Technical report, World Health Organization, 2012.

[34] G. Hoek, R. M. Krishnan, R. Beelen, A. Peters, B. Ostro, B. Brunekreef, and J. D. Kaufman. Long-term air pollution exposure and cardio-respiratory mortality: A review. *Environmental Health: A Global Access Science Source*, 12, 2013. ISSN 1476069X. DOI: 10.1186/1476-069X-12-43.

[35] M. E. Stettler, A. M. Boies, A. Petzold, and S. R. Barrett. Global Civil Aviation Black Carbon Emissions. *Environmental Science and Technology*, 47:10397–10404, September 2013. ISSN 0013936X. DOI: 10.1021/es401356v.

[36] M. O. Köhler, G. Rädel, K. P. Shine, H. L. Rogers, and J. A. Pyle. Latitudinal variation of the effect of aviation NO_x emissions on atmospheric ozone and methane and related climate metrics. *Atmospheric Environment*, 64:1–9, 2013. ISSN 13522310. DOI: 10.1016/j.atmosenv.2012.09.013.

[37] L. Jaegleh, D. J. Jacob, W. H. Brune, and P. O. Wennberg. Chemistry of HO_x radicals in the upper troposphere. *Atmospheric Environment*, 35:469–489, 2001. DOI: 10.1016/S1352-2310(00)00376-9.

[38] O. A. Søvde, S. Matthes, A. Skowron, D. Iachetti, L. Lim, B. Owen, Øivind Hodnebrog, G. D. Genova, G. Pitari, D. S. Lee, G. Myhre, and I. S. Isaksen. Aircraft emission mitigation by changing route altitude: A multi-model estimate of aircraft NO_x emission impact on O_3 photochemistry. *Atmospheric Environment*, 95:468–479, 2014. ISSN 18732844. DOI: 10.1016/j.atmosenv.2014.06.049.

[39] K. Dahlmann, V. Grewe, M. Ponater, and S. Matthes. Quantifying the contributions of individual NO_x sources to the trend in ozone radiative forcing. *Atmospheric Environment*, 45:2860–2868, June 2011. ISSN 13522310. DOI: 10.1016/j.atmosenv.2011.02.071.

[40] J. H. Seinfeld and S. N. Pandis. *Atmospheric Chemistry and Physics: From Air Pollution to Climate Change*. John Wiley & Sons, Inc., Hoboken, New Jersey, 3rd edition, 2016. ISBN 9781119221173.

[41] J. Maruhashi, V. Grewe, C. Frömming, P. Jöckel, and I. C. Dedoussi. Transport patterns of global aviation NO_x and their short-term O_3 radiative forcing - a machine

learning approach. *Atmospheric Chemistry and Physics*, 22:14253–14282, November 2022. ISSN 16807324. DOI: 10.5194/acp-22-14253-2022.

[42] D. E. Schraufnagel, J. R. Balmes, C. T. Cowl, S. D. Matteis, S. H. Jung, K. Mortimer, R. Perez-Padilla, M. B. Rice, H. Riojas-Rodriguez, A. Sood, G. D. Thurston, T. To, A. Vanker, and D. J. Wuebbles. Air Pollution and Noncommunicable Diseases: A Review by the Forum of International Respiratory Societies' Environmental Committee, Part 1: The Damaging Effects of Air Pollution. *Chest*, 155:409–416, February 2019. ISSN 19313543. DOI: 10.1016/j.chest.2018.10.042.

[43] J. Chen and G. Hoek. Long-term exposure to PM and all-cause and cause-specific mortality: A systematic review and meta-analysis. *Environment International*, 143, October 2020. ISSN 18736750. DOI: 10.1016/j.envint.2020.105974.

[44] WHO. WHO global air quality guidelines. Particulate matter ($PM_{2.5}$ and PM_{10}), ozone, nitrogen dioxide, sulfur dioxide and carbon monoxide. Technical report, World Health Organization, 2021.

[45] M. Jerrett, R. T. Burnett, C. A. Pope, K. Ito, G. Thurston, D. Krewski, Y. Shi, E. Calle, and M. Thun. Long-Term Ozone Exposure and Mortality. *The New England Journal of Medicine*, 360:1085–1095, March 2009.

[46] M. C. Turner, M. Jerrett, C. A. Pope, D. Krewski, S. M. Gapstur, W. R. Diver, B. S. Beckerman, J. D. Marshall, J. Su, D. L. Crouse, and R. T. Burnett. Long-Term Ozone Exposure and Mortality in a Large Prospective Study. *American journal of respiratory and critical care medicine*, 193:1134–1142, May 2016. ISSN 15354970. DOI: 10.1164/rccm.201508-1633OC.

[47] G. Pizzino, N. Irrera, M. Cucinotta, G. Pallio, F. Mannino, V. Arcoraci, F. Squadrito, D. Altavilla, and A. Bitto. Oxidative Stress: Harms and Benefits for Human Health. *Oxidative Medicine and Cellular Longevity*, 2017, 2017. ISSN 19420994. DOI: 10.1155/2017/8416763.

[48] P. Huangfu and R. Atkinson. Long-term exposure to NO_2 and O_3 and all-cause and respiratory mortality: A systematic review and meta-analysis. *Environment International*, 144, November 2020. ISSN 18736750. DOI: 10.1016/j.envint.2020.105998.

[49] S. Y. Kim, J. T. Lee, Y. C. Hong, K. J. Ahn, and H. Kim. Determining the threshold effect of ozone on daily mortality: An analysis of ozone and mortality in Seoul, Korea, 1995-1999. *Environmental Research*, 94:113–119, 2004. ISSN 00139351. DOI: 10.1016/j.envres.2003.09.006.

[50] M. L. Bell, R. D. Peng, and F. Dominici. The exposure-response curve for ozone and risk of mortality and the adequacy of current ozone regulations. *Environmental Health Perspectives*, 114:532–536, April 2006. ISSN 00916765. DOI: 10.1289/ehp.8816.

[51] R. W. Atkinson, D. Yu, B. G. Armstrong, S. Pattenden, P. Wilkinson, R. M. Doherty, M. R. Heal, and H. R. Anderson. Concentration-response function for ozone and daily mortality: Results from five urban and five rural U.K. populations. *Environmental Health Perspectives*, 120:1411–1417, October 2012. ISSN 00916765. DOI: 10.1289/ehp.1104108.

[52] World Health Organization: Regional Office for Europe. Health risks of air pollution in Europe – HRAPIE project, Recommendations for concentration–response functions for cost–benefit analysis of particulate matter, ozone and nitrogen dioxide, 2013. URL http://www.euro.who.int/pubrequest.

[53] S. Bae, Y. H. Lim, S. Kashima, T. Yorifuji, Y. Honda, H. Kim, and Y. C. Hong. Non-linear concentration-response relationships between ambient ozone and daily mortality. *PLoS ONE*, 10, June 2015. ISSN 19326203. DOI: 10.1371/journal.pone.0129423.

[54] A. J. Cohen, M. Brauer, R. Burnett, H. R. Anderson, J. Frostad, K. Estep, K. Balakrishnan, B. Brunekreef, L. Dandona, R. Dandona, V. Feigin, G. Freedman, B. Hubbell, A. Jobling, H. Kan, L. Knibbs, Y. Liu, R. Martin, L. Morawska, C. A. Pope, H. Shin, K. Straif, G. Shaddick, M. Thomas, R. van Dingenen, A. van Donkelaar, T. Vos, C. J. Murray, and M. H. Forouzanfar. Estimates and 25-year trends of the global burden of disease attributable to ambient air pollution: an analysis of data from the Global Burden of Diseases Study 2015. *The Lancet*, 389:1907–1918, May 2017. ISSN 1474547X. DOI: 10.1016/S0140-6736(17)30505-6.

[55] R. Burnett, H. Chen, M. Szyszkowicz, N. Fann, B. Hubbell, C. A. Pope, J. S. Apte, M. Brauer, A. Cohen, S. Weichenthal, J. Coggins, Q. Di, B. Brunekreef, J. Frostad, S. S. Lim, H. Kan, K. D. Walker, G. D. Thurston, R. B. Hayes, C. C. Lim, M. C. Turner, M. Jerrett, D. Krewski, S. M. Gapstur, W. R. Diver, B. Ostro, D. Goldberg, D. L. Crouse, R. V. Martin, P. Peters, L. Pinault, M. Tjepkema, A. V. Donkelaar, P. J. Villeneuve, A. B. Miller, P. Yin, M. Zhou, L. Wang, N. A. Janssen, M. Marra, R. W. Atkinson, H. Tsang, T. Q. Thach, J. B. Cannon, R. T. Allen, J. E. Hart, F. Laden, G. Cesaroni, F. Forastiere, G. Weinmayr, A. Jaensch, G. Nagel, H. Concin, and J. V. Spadaro. Global estimates of mortality associated with long-term exposure to outdoor fine particulate matter. In *Proceedings of the National Academy of Sciences of the United States of America*, volume 115, pages 9592–9597. National Academy of Sciences, September 2018. DOI: 10.1073/pnas.1803222115.

[56] A. Juginović, M. Vuković, I. Aranza, and V. Biloš. Health impacts of air pollution exposure from 1990 to 2019 in 43 European countries. *Scientific Reports*, 11, December 2021. ISSN 20452322. DOI: 10.1038/s41598-021-01802-5.

[57] C. A. Pope, R. T. Burnett, M. C. Turner, A. Cohen, D. Krewski, M. Jerrett, S. M. Gapstur, and M. J. Thun. Lung Cancer and Cardiovascular Disease Mortality Associated with Ambient Air Pollution and Cigarette Smoke: Shape of the Exposure-Response Relationships. *Environmental Health Perspectives*, 119:1616–1621, November 2011. ISSN 00916765. DOI: 10.1289/ehp.1103639.

[58] C. Swanton, W. Hill, E. Lim, C. Lee, C. Weeden, M. Augustine, K. Chen, F. Kuan, F. Marongiu, F. Rodrigues, H. Cha, T. Jacks, M. Luchtenborg, I. Malanchi, J. Downward, C. Carlsten, A. Hackshaw, K. Litchfield, J. DeGregori, and M. Jamal-Hanjani. Mechanism of action

and an actionable inflammatory axis for air pollution induced non-small cell lung cancer: Towards molecular cancer prevention. In *Annals of Oncology*, volume 33, Via Ginevra 4, 6900 Lugano, September 2022. ESMO.

[59] Q. Di, Y. Wang, A. Zanobetti, Y. Wang, P. Koutrakis, C. Choirat, F. Dominici, and J. D. Schwartz. Air pollution and mortality in the medicare population. *New England Journal of Medicine*, 376:2513–2522, June 2017. ISSN 0028-4793. DOI: 10.1056/nejmoa1702747.

[60] J. Lelieveld. Estimating pollution-attributable mortality at the regional and global scales: Challenges in uncertainty estimation and causal inference. *European Heart Journal*, 40:1597–1599, May 2019. ISSN 15229645. DOI: 10.1093/eurheartj/ehz200.

[61] A. Vodonos, Y. A. Awad, and J. Schwartz. The concentration-response between long-term $PM_{2.5}$ exposure and mortality; A meta-regression approach. *Environmental Research*, 166:677–689, October 2018. ISSN 10960953. DOI: 10.1016/j.envres.2018.06.021.

[62] P. Achakulwisut, M. Brauer, P. Hystad, and S. C. Anenberg. Global, national, and urban burdens of paediatric asthma incidence attributable to ambient NO_2 pollution: estimates from global datasets. *The Lancet Planetary Health*, 3:e166–e178, April 2019. ISSN 25425196. DOI: 10.1016/S2542-5196(19)30046-4.

[63] U. Latza, S. Gerdes, and X. Baur. Effects of nitrogen dioxide on human health: Systematic review of experimental and epidemiological studies conducted between 2002 and 2006. *International Journal of Hygiene and Environmental Health*, 212:271–287, May 2009. ISSN 14384639. DOI: 10.1016/j.ijheh.2008.06.003.

[64] M. T. Timko, W. B. Knighton, S. C. Herndon, E. C. Wood, T. B. Onasch, M. J. Northway, J. T. Jayne, M. R. Canagaratna, and R. C. Lye. Gas Turbine Engine Emissions—Part I: Volatile Organic Compounds and Nitrogen Oxides. *Journal of Engineering for Gas Turbines and Power*, 132:1–14, 2010. ISSN 15288919. DOI: 10.1115/1.4000131.

[65] Øyvind Næss, P. Nafstad, G. Aamodt, B. Claussen, and P. Rosland. Relation between concentration of air pollution and cause-specific mortality: Four-year exposures to nitrogen dioxide and particulate matter pollutants in 470 neighborhoods in Oslo, Norway. *American Journal of Epidemiology*, 165:435–443, February 2007. ISSN 00029262. DOI: 10.1093/aje/kwk016.

[66] Y. J. Oak, R. J. Park, J.-T. Lee, and G. Byun. Future air quality and premature mortality in Korea. *Science of The Total Environment*, 865:161134, 3 2023. ISSN 00489697. DOI: 10.1016/j.scitotenv.2022.161134.

[67] A. Faustini, R. Rapp, and F. Forastiere. Nitrogen dioxide and mortality: Review and meta-analysis of long-term studies. *European Respiratory Journal*, 44:744–753, September 2014. ISSN 13993003. DOI: 10.1183/09031936.00114713.

[68] N. Avogadro, M. Cattaneo, S. Paleari, and R. Redondi. Replacing short-medium haul intra-European flights with high-speed rail: Impact on CO_2 emissions and regional accessibility. *Transport Policy*, 114:25–39, December 2021. ISSN 1879310X. DOI: 10.1016/j.tranpol.2021.08.014.

[69] W. Liao, Y. Fan, C. Wang, and Z. Wang. Emissions from intercity aviation: An international comparison. *Transportation Research Part D: Transport and Environment*, 95, June 2021. ISSN 13619209. DOI: 10.1016/j.trd.2021.102818.

[70] A. Filippone, N. Bojdo, S. Mehta, and B. Parkes. Using the OpenSky ADS-B Data to Estimate Aircraft Emissions. *Engineering Proceedings*, 13, 2022. ISSN 26734591. DOI: 10.3390/engproc2021013011.

[71] F. Faggiano, R. Vos, M. Baan, and R. V. Dijk. Aerodynamic Design of a Flying V Aircraft. In *17th AIAA Aviation Technology, Integration, and Operations Conference, 2017*. American Institute of Aeronautics and Astronautics Inc, AIAA, 2017. ISBN 9781624105081. DOI: 10.2514/6.2017-3589.

[72] H. D. Kim, A. T. Perry, and P. J. Ansell. A Review of Distributed Electric Propulsion Concepts for Air Vehicle Technology. In *2018 AIAA/IEEE Electric Aircraft Technologies Symposium, EATS 2018*. Institute of Electrical and Electronics Engineers Inc., November 2018. ISBN 9781624105722. DOI: 10.2514/6.2018-4998.

[73] B. J. Brelje and J. R. Martins. Electric, hybrid, and turboelectric fixed-wing aircraft: A review of concepts, models, and design approaches. *Progress in Aerospace Sciences*, 104:1–19, January 2019. ISSN 0376-0421. DOI: 10.1016/J.PAEROSCI.2018.06.004.

[74] H. Nakamura, Y. Kajikawa, and S. Suzuki. Multi-level perspectives with technology readiness measures for aviation innovation. *Sustainability Science*, 8:87–101, January 2013. ISSN 18624065. DOI: 10.1007/s11625-012-0187-z.

[75] Z. Lyu and J. R. Martins. Aerodynamic Design Optimization Studies of a Blended-Wing-Body Aircraft. *Journal of Aircraft*, 51:1604–1617, September 2014. ISSN 15333868. DOI: 10.2514/1.C032491.

[76] D. Rutherford and M. Zeinali. Efficiency Trends for New Commercial Jet Aircraft, 1960 to 2008. Technical report, The International Council on Clean Transportation, 2009. URL https://theicct.org/publication/efficiency-trends-for-new-commercial-jet-aircraft-1960-to-2008/.

[77] A. H. Epstein and S. M. O'Flarity. Considerations for Reducing Aviation's CO_2 with Aircraft Electric Propulsion. *Journal of Propulsion and Power*, 35:572–582, 2019. ISSN 15333876. DOI: 10.2514/1.B37015.

[78] A. Bauen, N. Bitossi, L. German, A. Harris, and K. Leow. Sustainable aviation fuels: Status, challenges and prospects of drop-in liquid fuels, hydrogen and electrification in aviation. *Johnson Matthey Technology Review*, 64:263–278, July 2020. ISSN 20565135. DOI: 10.1595/205651320x15816756012040.

[79] D. Verstraete. On the energy efficiency of hydrogen-fuelled transport aircraft. *International Journal of Hydrogen Energy*, 40:7388–7394, June 2015. ISSN 03603199. DOI: 10.1016/j.ijhydene.2015.04.055.

[80] IATA. Fact sheet 7: Liquid hydrogen as a potential low-carbon fuel for aviation. Technical report, International Air Transport Association, August 2019.

[81] J. Bosch, S. D. Jong, R. Hoefnagels, and R. Slade. Aviation biofuels: strategically important, technically achievable, tough to deliver. Technical report, Imperial Collage London - Grantham Institute, November 2017.

[82] A. Goldmann, W. Sauter, M. Oettinger, T. Kluge, U. Schröder, J. R. Seume, J. Friedrichs, and F. Dinkelacker. A Study on Electrofuels in Aviation. *Energies*, 11, February 2018. ISSN 19961073. DOI: 10.3390/en11020392.

[83] R. H. Moore, K. L. Thornhill, B. Weinzierl, D. Sauer, E. D'ascoli, J. Kim, M. Lichtenstern, M. Scheibe, B. Beaton, J. Beyersdorf, J. Barrick, D. Bulzan, C. A. Corr, E. Crosbie, T. Jurkat, R. Martin, D. Riddick, M. Shook, G. Slover, C. Voigt, R. White, E. Winstead, R. Yasky, L. D. Ziemba, A. Brown, H. Schlager, and B. E. Anderson. Biofuel blending reduces particle emissions from aircraft engines at cruise conditions. *Nature*, 543: 411–415, March 2017. DOI: 10.1038/nature21420.

[84] K. Dahal, S. Brynolf, C. Xisto, J. Hansson, M. Grahn, T. Grönstedt, and M. Lehtveer. Techno-economic review of alternative fuels and propulsion systems for the aviation sector. *Renewable and Sustainable Energy Reviews*, 151:111564, November 2021. ISSN 1364-0321. DOI: 10.1016/J.RSER.2021.111564.

[85] IATA. Sustainable Aviation Fuels: Fact sheet. Technical report, International Air Transport Association, May 2019.

[86] IATA. Fact Sheet 2 - Sustainable Aviation Fuel: Technical Certification. Technical report, International Air Transport Association, 2020.

[87] T. Rindlisbacher and S. D. Jacob. On Board a Sustainable Future: ICAO Environmental Report 2016. Technical report, International Civil Aviation Organisation, 2016. URL https://www.icao.int/environmental-protection/documents/ICAO%20Environmental%20Report%202016.pdf.

[88] B. Lin and X. Li. The effect of carbon tax on per capita CO_2 emissions. *Energy Policy*, 39:5137–5146, September 2011. ISSN 03014215. DOI: 10.1016/j.enpol.2011.05.050.

[89] W. Hoermann. Introduction to the ICAO Engine Emissions Databank. Technical report, European Union Aviation Safety Agency, 2021.

[90] K. Dahlmann, V. Grewe, S. Matthes, and H. Yamashita. Climate assessment of single flights: Deduction of route specific equivalent CO_2 emissions. *International Journal of Sustainable Transportation*, September 2021. ISSN 15568334. DOI: 10.1080/15568318.2021.1979136.

[91] D. K. Wasiuk, M. A. Khan, D. E. Shallcross, R. G. Derwent, and M. H. Lowenberg. A mitigation strategy for commercial aviation impact on NO_x-related O_3 change. *Journal of Geophysical Research*, 121: 8730–8740, 2016. ISSN 21562202. DOI: 10.1002/2016JD025051.

[92] F. D. A. Quadros, M. Snellen, J. Sun, and I. C. Dedoussi. Global Civil Aviation Emissions Estimates for 2017–2020 Using ADS-B Data. *Journal of Aircraft*, pages 1–11, May 2022. ISSN 1533-3868. DOI: 10.2514/1.C036763.

[93] J. Patterson, G. J. Noel, D. A. Senzig, C. J. Roof, and G. G. Fleming. Analysis of departure and arrival profiles using real-time aircraft data. *Journal of Aircraft*, 46:1094–1103, 2009. ISSN 15333868. DOI: 10.2514/1.42432.

[94] M. Mazaheri, G. R. Johnson, and L. Morawska. An inventory of particle and gaseous emissions from large aircraft thrust engine operations at an airport. *Atmospheric Environment*, 45:3500–3507, June 2011. ISSN 1352-2310. DOI: 10.1016/J.ATMOSENV.2010.12.012.

[95] A. Filippone and N. Bojdo. Statistical model for gas turbine engines exhaust emissions. *Transportation Research Part D: Transport and Environment*, 59:451–463, March 2018. ISSN 13619209. DOI: 10.1016/j.trd.2018.01.019.

[96] B. Wang, J. Li, C. Li, and D. Wu. A Method for Computing Flight Operation Fuel Burn and Emissions Based on ADS-B Trajectories. *Journal of Aeronautics, Astronautics and Aviation*, 52:183–196, June 2020. ISSN 19907710. DOI: 10.6125/JoAAA.202006_52(2).05.

[97] *ICAO DOC 9889: Airport Air Quality Manual*. ICAO, Montréal, Quebec, Canada, 2nd edition, 2020. DOC 9889.

[98] R. Gelaro, W. McCarty, M. J. Suárez, R. Todling, A. Molod, L. Takacs, C. A. Randles, A. Darmenov, M. G. Bosilovich, R. Reichle, K. Wargan, L. Coy, R. Cullather, C. Draper, S. Akella, V. Buchard, A. Conaty, A. M. da Silva, W. Gu, G. K. Kim, R. Koster, R. Lucchesi, D. Merkova, J. E. Nielsen, G. Partyka, S. Pawson, W. Putman, M. Rienecker, S. D. Schubert, M. Sienkiewicz, and B. Zhao. The Modern-Era Retrospective Analysis for Research and Applications, Version 2 (MERRA-2). *Journal of Climate*, 30:5419–5454, July 2017. ISSN 08948755. DOI: 10.1175/JCLI-D-16-0758.1.

[99] X. Liu, K. Chance, C. E. Sioris, T. P. Kurosu, R. J. Spurr, R. V. Martin, T. M. Fu, J. A. Logan, D. J. Jacob, P. I. Palmer, M. J. Newchurch, I. A. Megretskaia, and R. B. Chatfield. First directly retrieved global distribution of tropospheric column ozone from GOME: Comparison with the GEOS-CHEM model. *Journal of Geophysical Research Atmospheres*, 111, January 2006. ISSN 01480227. DOI: 10.1029/2005JD006564.

[100] A. P. Protonotariou, M. Tombrou, C. Giannakopoulos, E. Kostopoulou, and P. L. Sager. Study of CO surface pollution in Europe based on observations and nested-grid applications of GEOS-CHEM global chemical transport model. *Tellus, Series B: Chemical and Physical Meteorology*, 62:209–227, September 2010. ISSN 02806509. DOI: 10.1111/j.1600-0889.2010.00462.x.

[101] B. Ford and C. L. Heald. Aerosol loading in the Southeastern United States: Reconciling surface and satellite observations. *Atmospheric Chemistry and Physics*, 13: 9269–9283, 2013. ISSN 16807316. DOI: 10.5194/acp-13-9269-2013.

[102] A. P. Protonotariou, E. Bossioli, M. Tombrou, N. Mihalopoulos, G. Biskos, J. Kalogiros, G. Kouvarakis, and V. Amiridis. Air Pollution in Eastern Mediterranean: Nested-Grid GEOS-CHEM Model Results and Airborne Observations. In C. G. Helmis and P. T. Nastos, editors, *Advances in Meteorology, Climatology and Atmospheric Physics*, pages 1203–1209, Berlin, Heidelberg, 2013. Springer Berlin Heidelberg. ISBN 978-3-642-29172-2.

[103] J. Lin, A. van Donkelaar, J. Xin, H. Che, and Y. Wang. Clear-sky aerosol optical depth over East China estimated from visibility measurements and chemical transport modeling. *Atmospheric Environment*, 95:258–267, 2014. ISSN 18732844. DOI: 10.1016/j.atmosenv.2014.06.044.

[104] E. A. Marais, D. J. Jacob, K. Wecht, C. Lerot, L. Zhang, K. Yu, T. P. Kurosu, K. Chance, and B. Sauvage. Anthropogenic emissions in Nigeria and implications for atmospheric ozone pollution: A view from space. *Atmospheric Environment*, 99:32–40, December 2014. ISSN 18732844. DOI: 10.1016/j.atmosenv.2014.09.055.

[105] S. D. Eastham, D. K. Weisenstein, and S. R. Barrett. Development and evaluation of the unified tropospheric-stratospheric chemistry extension (UCX) for the global chemistry-transport model GEOS-Chem. *Atmospheric Environment*, 89:52–63, June 2014. ISSN 13522310. DOI: 10.1016/j.atmosenv.2014.02.001.

[106] Y. Y. Yan, J. T. Lin, Y. Kuang, D. Yang, and L. Zhang. Tropospheric carbon monoxide over the Pacific during HIPPO: two-way coupled simulation of GEOS-Chem and its multiple nested models. *Atmospheric Chemistry and Physics*, 14:12649–12663, December 2014. ISSN 16807324. DOI: 10.5194/acp-14-12649-2014.

[107] S. D. Eastham, M. S. Long, C. A. Keller, E. Lundgren, R. M. Yantosca, J. Zhuang, C. Li, C. J. Lee, M. Yannetti, B. M. Auer, T. L. Clune, J. Kouatchou, W. M. Putman, M. A. Thompson, A. L. Trayanov, A. M. Molod, R. V. Martin, and D. J. Jacob. GEOS-Chem High Performance (GCHP v11-02c): A next-generation implementation of the GEOS-Chem chemical transport model for massively parallel applications. *Geoscientific Model Development*, 11:2941–2953, July 2018. ISSN 19919603. DOI: 10.5194/gmd-11-2941-2018.

[108] L. Hu, C. A. Keller, M. S. Long, T. Sherwen, B. Auer, A. D. Silva, J. E. Nielsen, S. Pawson, M. A. Thompson, A. L. Trayanov, K. R. Travis, S. K. Grange, M. J. Evans, and D. J. Jacob. Global simulation of tropospheric chemistry at 12.5 km resolution: performance and evaluation of the GEOS-Chem chemical module (v10-1) within the NASA GEOS Earth system model (GEOS-5 ESM). *Geoscientific Model Development*, 11:4603–4620, November 2018. ISSN 19919603. DOI: 10.5194/gmd-11-4603-2018.

[109] A. Clappier, C. A. Belis, D. Pernigotti, and P. Thunis. Source apportionment and sensitivity analysis: Two methodologies with two different purposes. *Geoscientific Model Development*, 10:4245–4256, November 2017. ISSN 19919603. DOI: 10.5194/gmd-10-4245-2017.

[110] M. Mertens, V. Grewe, V. S. Rieger, and P. Jöckel. Revisiting the contribution of land transport and shipping emissions to tropospheric ozone. *Atmospheric Chemistry and Physics*, 18:5567–5588, April 2018. ISSN 16807324. DOI: 10.5194/acp-18-5567-2018.

[111] V. Grewe, S. Matthes, and K. Dahlmann. The contribution of aviation NO_x emissions to climate change: are we ignoring methodological flaws? *Environmental Research Letters*, 14, December 2019. ISSN 17489326. DOI: 10.1088/1748-9326/ab5dd7.

[112] J. J. Zhang, Y. Wei, and Z. Fang. Ozone Pollution: A Major Health Hazard Worldwide. *Frontiers in Immunology*, 10, 2019. ISSN 16643224. DOI: 10.3389/fimmu.2019.02518.

[113] D. Nuvolone, D. Petri, and F. Voller. The effects of ozone on human health. *Environmental Science and Pollution Research*, 25:8074–8088, March 2018. ISSN 16147499. DOI: 10.1007/s11356-017-9239-3.

[114] S. Vedal and J. D. Kaufman. What does multi-pollutant air pollution research mean? *American Journal of Respiratory and Critical Care Medicine*, 183:3–4, January 2011. ISSN 1073449X. DOI: 10.1164/rccm.201011-1881ED.

[115] A multi-pollutant model: a method suitable for studying complex relationships in environmental epidemiology. *Air Quality, Atmosphere and Health*, 13:645–657, June 2020. ISSN 18739326. DOI: 10.1007/s11869-020-00829-3.

[116] H. Walton, P. Wilkinson, G. Shaddick, D. Jarvis, A. Hansell, J. Stedman, M. Holland, and D. Lee. Summary of COMEAP recommendations for quantification of health effects associated with air pollutants, October 2020. URL https://www.gov.uk/government/publications/air-pollutants-quantification-of-associated-health-effects.

[117] Global Health Estimates 2019: Deaths by Cause, Age, Sex, by Country and by Region, 2000-2019. Technical report, World Health Organization, Geneva, 2020.

[118] C. Lee, T. Thrasher, E. Boeker, R. Downs, S. Gorshkov, A. Hansen, S. Hwang, J. Koopmann, A. Malwitz, G. Noel, C. Reherman, M. A. Shumway, G. B. Solan, Y. Tosa, A. Wilson, A. Zubrow, J. DiPardo, M. Majeed, J. Bernal, A. Biederman, E. Dinges, D. Rickel, M. Yaworski, D. Senzig, C. Hall, S. Augustine, and R. Foley. Aviation Environmental Design Tool (AEDT) Technical Manual: Version 3b. Technical report, U.S. Department of Transportation. Volpe National Transportation Systems Center, September 2019. URL https://aedt.faa.gov/.

[119] J. T. Lin and M. B. McElroy. Impacts of boundary layer mixing on pollutant vertical profiles in the lower troposphere: Implications to satellite remote sensing. *Atmospheric Environment*, 44:1726–1739, May 2010. ISSN 13522310. DOI: 10.1016/j.atmosenv.2010.02.009.

[120] J. Zhuang, D. J. Jacob, and S. D. Eastham. The importance of vertical resolution in the free troposphere for modeling intercontinental plumes. *Atmospheric Chemistry and Physics*, 18:6039–6055, May 2018. ISSN 16807324. DOI: 10.5194/acp-18-6039-2018.

[121] L. Bindle, R. V. Martin, M. J. Cooper, E. W. Lundgren, S. D. Eastham, B. M. Auer, T. L. Clune, H. Weng, J. Lin, L. T. Murray, J. Meng, C. A. Keller, W. M. Putman, S. Pawson, and D. J. Jacob. Grid-stretching capability for the GEOS-Chem 13.0.0 atmospheric chemistry model. *Geoscientific Model Development*, 14:5977–5997, October 2021. ISSN 19919603. DOI: 10.5194/gmd-14-5977-2021.

[122] K. Vohra, A. Vodonos, J. Schwartz, E. A. Marais, M. P. Sulprizio, and L. J. Mickley. Global mortality from outdoor fine particle pollution generated by fossil fuel combustion: Results from GEOS-Chem. *Environmental Research*, 195, April 2021. ISSN 10960953. DOI: 10.1016/j.envres.2021.110754.

[123] S. Arunachalam, B. Wang, N. Davis, B. H. Baek, and J. I. Levy. Effect of chemistry-transport model scale and resolution on population exposure to $PM_{2.5}$ from aircraft emissions during landing and takeoff. *Atmospheric Environment*, 45:3294–3300, June 2011. ISSN 13522310. DOI: 10.1016/j.atmosenv.2011.03.029.

[124] S. C. Anenberg, J. Miller, D. K. Henze, R. Minjares, and P. Achakulwisut. The global burden of transportation tailpipe emissions on air pollution-related mortality in 2010 and 2015. *Environmental Research Letters*, 14, September 2019. ISSN 17489326. DOI: 10.1088/1748-9326/ab35fc.

[125] B. Graver, D. Rutherford, and S. Zheng. CO_2 emissions from commercial aviation: 2013, 2018, and 2019. Technical report, International Council on Clean Transportation, October 2020.

[126] B. Graver, K. Zhang, and D. Rutherford. CO_2 emissions from commercial aviation, 2018. Technical report, International Council on Clean Transportation, September 2019.

[127] International Energy Agency. Transport. Online, September 2022. URL https://www.iea.org/reports/transport. Retrieved 28 April 2023.

[128] United Nations Environmental Programme. The Closing Window - Climate crisis calls for rapid transformation of societies, 2022. URL https://www.unep.org/emissions-gap-report-2022.

[129] A. Petzold, A. Döpelheuer, C. A. Brock, and F. Schröder. In situ observations and model calculations of black carbon emission by aircraft at cruise altitude. *Journal of Geophysical Research: Atmospheres*, 104:22171–22181, September 1999. ISSN 01480227. DOI: 10.1029/1999JD900460.

[130] M. T. Timko, W. B. Knighton, S. C. Herndon, E. C. Wood, T. B. Onasch, M. J. Northway, J. T. Jayne, M. R. Canagaratna, and R. C. Lye. Gas Turbine Engine Emissions—Part II: Chemical Properties of Particulate Matter. *Journal of Engineering for Gas Turbines and Power*, 132:1–15, 2010. ISSN 15288919. DOI: 10.1115/1.4000132.

[131] A. Agarwal, R. L. Speth, T. M. Fritz, S. D. Jacob, T. Rindlisbacher, R. Iovinelli, B. Owen, R. C. Miake-Lye, J. S. Sabnis, and S. R. Barrett. SCOPE11 Method for Estimating Aircraft Black Carbon Mass and Particle Number Emissions. *Environmental Science and Technology*, 53:1364–1373, February 2019. ISSN 15205851. DOI: 10.1021/acs.est.8b04060.

[132] U. Schumann, F. Arnold, R. Busen, J. Curtius, B. Kärcher, A. Kiendler, A. Petzold, H. Schlager, F. Schröder, and K. H. Wohlfrom. Influence of fuel sulfur on the composition of aircraft exhaust plumes: The experiments SULFUR 1-7. *Journal of Geophysical Research: Atmospheres*, 107:AAC 2–1 – AAC 2–27, November 2002. ISSN 01480227. DOI: 10.1029/2001JD000813.

[133] G. K. Kenway, R. Henderson, J. E. Hicken, N. B. Kuntawala, D. W. Zingg, J. R. Martins, and R. G. McKeand. Reducing aviation's environmental impact through large aircraft for short ranges. American Institute of Aeronautics and Astronautics Inc., 2010. ISBN 9781600867392. DOI: 10.2514/6.2010-1015.

[134] F. Nicolosi, S. Corcione, V. Trifari, and A. D. Marco. Design and optimization of a large turboprop aircraft. *Aerospace*, 8, May 2021. ISSN 22264310. DOI: 10.3390/aerospace8050132.

[135] B. Graver, D. Rutherford, T. Johnson, A. Murphy, A. Kharina, and A. Smorodin. Transatlantic Airline Fuel Efficiency Ranking, 2017. White paper, September 2018. URL https://theicct.org/publication/transatlantic-airline-fuel-efficiency-ranking-2017/.

[136] A. Bejan, J. D. Charles, and S. Lorente. The evolution of airplanes. *Journal of Applied Physics*, 116, July 2014. ISSN 10897550. DOI: 10.1063/1.4886855.

[137] B. Owen, J. G. Anet, N. Bertier, S. Christie, M. Cremaschi, S. Dellaert, J. Edebeli, U. Janicke, J. Kuenen, L. Lim, and E. Terrenoire. Review: Particulate Matter Emissions from Aircraft. *Atmosphere*, 13:1230, August 2022. ISSN 2073-4433. DOI: 10.3390/atmos13081230. URL https://www.mdpi.com/2073-4433/13/8/1230.

[138] A. Mohegh, D. Goldberg, P. Achakulwisut, and S. C. Anenberg. Sensitivity of estimated NO_2-attributable pediatric asthma incidence to grid resolution and urbanicity. *Environmental Research Letters*, 16, 2020. ISSN 17489326. DOI: 10.1088/1748-9326/abce25.

[139] R. L. Dennis, P. V. Bhave, and R. W. Pinder. Observable indicators of the sensitivity of $PM_{2.5}$ nitrate to emission reductions - Part II: Sensitivity to errors in total ammonia and total nitrate of the CMAQ-predicted non-linear effect of SO_2 emission reductions. *Atmospheric Environment*, 42:1287–1300, 2008. ISSN 13522310. DOI: 10.1016/j.atmosenv.2007.10.036.

[140] Y. Zhang, X.-Y. Wen, K. Wang, K. Vijayaraghavan, and M. Z. Jacobson. Probing into regional O_3 and particulate matter pollution in the United States: 2. An examination of formation mechanisms through a process analysis technique and sensitivity study. *Journal of Geophysical Research*, 114, November 2009. ISSN 0148-0227. DOI: 10.1029/2009jd011900.

[141] J. J. Corbett, J. J. Winebrake, E. H. Green, P. Kasibhatla, V. Eyring, and A. Lauer. Mortality from ship emissions: A global assessment. *Environmental Science and Technology*, 41:8512–8518, December 2007. ISSN 0013936X. DOI: 10.1021/es071686z.

[142] D. Krewski, M. Jerrett, R. T. Burnett, R. Ma, E. Hughes, Y. Shi, M. C. Turner, C. A. P. III, G. Thurston, E. E. Calle, and M. J. Thun. Extended follow-up and spatial analysis of the american cancer society study linking particulate air pollution and mortality, May 2009. URL https://www.researchgate.net/publication/26690365.

[143] R. Beelen, O. Raaschou-Nielsen, M. Stafoggia, Z. J. Andersen, G. Weinmayr, B. Hoffmann, K. Wolf, E. Samoli, P. Fischer, M. Nieuwenhuijsen, P. Vineis, W. W. Xun, K. Katsouyanni, K. Dimakopoulou, A. Oudin, B. Forsberg, L. Modig, A. S. Havulinna, T. Lanki, A. Turunen, B. Oftedal, W. Nystad, P. Nafstad, U. D. Faire, N. L. Pedersen, C. G. Östenson, L. Fratiglioni, J. Penell, M. Korek, G. Pershagen, K. T. Eriksen, K. Overvad, T. Ellermann, M. Eeftens, P. H. Peeters, K. Meliefste, M. Wang, B. Bueno-De-Mesquita, D. Sugiri, U. Krämer, J. Heinrich, K. D. Hoogh, T. Key, A. Peters, R. Hampel, H. Concin, G. Nagel, A. Ineichen, E. Schaffner, N. Probst-Hensch, N. Künzli, C. Schindler, T. Schikowski, M. Adam, H. Phuleria, A. Vilier, F. Clavel-Chapelon, C. Declercq, S. Grioni, V. Krogh, M. Y. Tsai, F. Ricceri, C. Sacerdote, C. Galassi, E. Migliore, A. Ranzi, G. Cesaroni, C. Badaloni, F. Forastiere, I. Tamayo, P. Amiano, M. Dorronsoro, M. Katsoulis, A. Trichopoulou, B. Brunekreef, and G. Hoek. Effects of long-term exposure to air pollution on natural-cause mortality: An analysis of 22 European cohorts within the multicentre ESCAPE project. *The Lancet*, 383:785–795, 2014. ISSN 1474547X. DOI: 10.1016/S0140-6736(13)62158-3.

[144] V. Reiter, A. Voltes-Dorta, and P. Suau-Sanchez. The substitution of short-haul flights with rail services in German air travel markets: A quantitative analysis. *Case Studies on Transport Policy*, 10:2025–2043, December 2022. ISSN 22136258. DOI: 10.1016/j.cstp.2022.09.001.

[145] International Energy Agency. Aviation. Online, September 2022. URL https://www.iea.org/reports/aviation. Retrieved 23 April 2023.

[146] R. C. Pietzcker, S. Osorio, and R. Rodrigues. Tightening EU ETS targets in line with the European Green Deal: Impacts on the decarbonization of the EU power sector. *Applied Energy*, 293, July 2021. ISSN 03062619. DOI: 10.1016/j.apenergy.2021.116914.

[147] P. J. Megia, A. J. Vizcaino, J. A. Calles, and A. Carrero. Hydrogen Production Technologies: From Fossil Fuels toward Renewable Sources. A Mini Review. *Energy and Fuels*, 35:16403–16415, October 2021. ISSN 15205029. DOI: 10.1021/acs.energyfuels.1c02501.

[148] G. Kakoulaki, I. Kougias, N. Taylor, F. Dolci, J. Moya, and A. Jäger-Waldau. Green hydrogen in Europe – A regional assessment: Substituting existing production with electrolysis powered by renewables. *Energy Conversion and Management*, 228, January 2021. ISSN 01968904. DOI: 10.1016/j.enconman.2020.113649.

[149] P. Agarwal, X. Sun, P. Q. Gauthier, and V. Sethi. Injector design space exploration for an ultra-low NO_x hydrogen micromix combustion system. volume 3. American Society of Mechanical Engineers (ASME), 2019. ISBN 9780791858608. DOI: 10.1115/GT2019-90833.

[150] A. M. Starik, A. M. Savel'ev, O. N. Favorskii, and N. S. Titova. Analysis of emission characteristics of gas turbine engines with some alternative fuels. *International Journal of Green Energy*, 15:161–168, February 2018. ISSN 15435083. DOI: 10.1080/15435075.2017.1324790.

[151] ICAO. Sustainable aviation fuels guide, December 2018.

[152] S. Freeman, D. S. Lee, L. L. Lim, A. Skowron, and R. R. D. León. Trading off Aircraft Fuel Burn and NO_x Emissions for Optimal Climate Policy. *Environmental Science and Technology*, 52:2498–2505, March 2018. ISSN 15205851. DOI: 10.1021/acs.est.7b05719.

[153] A. Skowron, D. S. Lee, R. R. D. León, L. L. Lim, and B. Owen. Greater fuel efficiency is potentially preferable to reducing NO_x emissions for aviation's climate impacts. *Nature Communications*, 12, December 2021. ISSN 20411723. DOI: 10.1038/s41467-020-20771-3.

[154] B. Koffi, S. Szopa, A. Cozic, D. Hauglustaine, and P. V. Velthoven. Present and future impact of aircraft, road traffic and shipping emissions on global tropospheric ozone. *Atmospheric Chemistry and Physics*, 10:11681–11705, 2010. ISSN 16807316. DOI: 10.5194/acp-10-11681-2010.

[155] I. C. Dedoussi. Implications of future atmospheric composition in decision-making for sustainable aviation. *Environmental Research Letters*, 16, March 2021. ISSN 17489326. DOI: 10.1088/1748-9326/abe74d.

II

Supporting Information

SI 1. Processing the flight lists

This chapter provides more details about the methodology used to obtain the flight lists which were used as input for the openAVEM model. First, a general filtering process was used to obtain a consistent and more reliable data set out of the raw ADS-B data. This process is described in section SI 1.1. Then, the input flight lists for individual studies were obtained through additional filtering as discussed in section SI 1.2.

SI 1.1. Generic filters applied to the flight lists

Three filters were applied to the flight lists before performing any analysis in openAVEM. First, a filter was used on the aircraft classes. Then, invalid airport entries were removed. Finally, flights which exceeded the range of the aircraft were removed.

In order to provide a consistent analysis which still captured the majority of flights, it was decided to exclude cargo and military aircraft from the data set. Flights for which the aircraft class was unknown were also removed; including these flights may incorrectly alter the results per aircraft category. It was deemed preferable to use a slightly smaller, yet more accurate data set instead. It was recognised that by applying this filter, it is most likely that the general aviation segment is underrepresented in the adjusted data set.

Furthermore, flights with an invalid departure or arrival airport were removed as well. In this context, a combination of departure and arrival airports was considered invalid if the ICAO code of either airport was non-existing or if the departure and arrival airport codes were identical. It was recognised that, by removing flights with the same origin and destination, some general aviation flights are likely ignored. However, openAVEM is unable to correctly predict the emissions of such flights. While openAVEM has the option to remove these flights internally, this function was extracted outside the model to provide a more transparent filtering process.

Finally, the flight data from FlightRadar24 was screened for abnormalities and it was discovered that several flights of general aviation aircraft were entered as having a distance which exceeded the maximum range of the aircraft. It was thus clear that these data points were incorrect (as the flights would be impossible from a physical perspective) and needed to be removed. In order to filter the flights, the following approach was used: first, the range of each aircraft type was extracted from the data; then a margin on top of this range was selected and finally all longer flights were removed.

Given that the anomalies were mostly observed in general aviation aircraft, while the entries for airliners were largely according to what could be expected based on their maximum range, a division was made between airliners and other aircraft. Here, airliners were defined as all aircraft corresponding to the classes ‘regional jet’, ‘narrowbody’ or ‘widebody’. For the airliners, the maximum range was set to the 99.95th percentile of all the flights for the respective aircraft type in the database. Upon inspection of the resulting range, this value was deemed appropriate; smaller values resulted in an underestimation of the range for popular aircraft such as the Boeing 737 and Airbus A320 families, while larger values left some outliers undetected. For other aircraft, however, and in particular for general aviation aircraft, setting the maximum range at this percentile would overestimate the range. Therefore, for these aircraft, the range was set to the 95th percentile of all flight entries. Again, the variation of the expected range was analysed for multiple settings; smaller ranges were concluded to exclude too many flights, while a larger range was deemed infeasible for several aircraft types.

As it was recognised that the provided range was aimed to approximate the actual range of aircraft, and that in certain conditions (such as delivery flights, all-business flights and private jets) the flight distance can be larger than the default range, a margin was added to the found range. Flight entries were only removed when they had a great circle distance larger than the approximated range plus the margin. A brief sensitivity analysis was performed on this margin, yielding the results as shown in table S1. Please note that the total data set included 45,138,953 flights in 2019. Of these, 33,644,311 were flown by aircraft considered airliners as discussed previously. In table S1, the percentage of airliner flights removed relates to the total number of airliner flights (i.e. 33.64 million flights).

Table S1: Sensitivity of flight list to margin on aircraft ranges. Percentages in parentheses for 10% and 30% entries show the deviation relative to the 20% baseline.

Margin	Flights removed	[%]	Airliner flights removed	[%]
10%	346,999 (+46.8%)	0.769	5,186 (+69.3%)	0.0154
20%	236,336	0.524	3,064	0.0091
30%	167,613 (-29.1%)	0.371	2,330 (-24.0%)	0.0069

As may be expected, the number of removed flights reduces once the margin is increased, as flights with a larger distance are then also included in the valid entries. Based on the results from table S1, a margin of 20% was chosen. A smaller margin caused a clear increase in airliner flights being removed, which was not preferred. On the other hand, selecting a larger margin had a limited effect in reducing the number of airliner flights to be removed, while it did allow for more invalid general aviation flights to remain in the data set.

Based on these criteria, 2,926,511 flights were removed from the original data set using all three filters. This means that, after filtering, 42,212,442 flights remained. A summary is provided in table S2.

Table S2: Overview of flights affected by the filtering process.

	Number of flights	[%]	Airliner flights	[%]
Original dataset	45,138,953	100.0	33,644,311	100.0
Removed due to aircraft class	1,458,582	3.231	0	0.000
Removed due to invalid airports	1,231,593	2.728	34,643	0.103
Removed due to invalid range	236,336	0.524	3,064	0.009
Remaining flights	42,212,442	93.52	33,606,604	99.89

SI 1.2. Flight data per aircraft category

This section contains information on the methods applied to categorise global flights, as well as on the resulting flight data sets. First, the flight data for the main studies, i.e. the aircraft size and flight distance, are provided in subsections SI 1.2.1 and SI 1.2.2, respectively. These are then followed by the case studies in subsections SI 1.2.3 to SI 1.2.5. When data refers to revenue passenger kilometres, the number of RPKs per aircraft-origin-destination triplet was obtained through equation (SI 1.1):

$$RPK = n \cdot pax \cdot d \tag{SI 1.1}$$

Here, n is the number of flights that the aircraft type performed on this route, pax is the average number of passengers on board of this aircraft, and d is the Great Circle Distance (GCD). This value was used, instead of the actual flown distance, as it yields the results independent of operational procedures.

SI 1.2.1. Aircraft size

To distinguish the impacts of various aircraft sizes, separate flight lists were created for each aircraft size. To do so, a supplementary file from the openAVEM model was used. This file contained the aircraft class allocations for each of the aircraft type codes that were included in the model. For the present analysis, the following aircraft classes were used for unique categories: piston, business, turboprop, regional jet, narrowbody, and widebody. Then, for each of these, the flights with aircraft type codes corresponding to that particular class were selected and saved in a separate flight list. The division of flights over the various categories for the year 2019 is presented in table S3, along with trip details.

Table S3: Trip details per category for flights of various aircraft sizes in 2019. The percentage of flights relates to all global flights after filtering as discussed in section SI 1.1.

					Mean value per flight	
Aircraft size	Flights	Flights [%]	Pax [10^6]	RPKs [10^9]	Pax	Distance [km]
Piston	1,864,044	4.42	10	2	6	178
Business jets	2,304,317	5.46	17	18	7	995
Turboprop	4,437,477	10.51	140	52	31	356
Regional jets	5,585,107	13.23	295	239	53	788
Narrowbody	23,983,460	56.82	2,790	3,795	116	1,342
Widebody	4,038,037	9.57	840	3,747	208	4,318

Table S3 shows that the majority of passenger flights were performed using narrowbody aircraft. Furthermore, approximately 90.1% of the flights logged by FlightRadar24 in 2019 were operated by airliners. The remainder of the flights were mostly for personal use, either in piston aircraft or business jets.

SI 1.2.2. Flight distance

Splitting the flight list based on flight distance was a straightforward procedure. Since the distance for each flight was provided in the flight list, this value could be compared to the bounds of the distance categories directly. While the distance provided in the flight list was the Great Circle Distance and not the actual flown distance (or an estimate thereof), it was decided to use the GCD for reproduction purposes; if one prefers to use a different correction for flight path inefficiencies than that provided in openAVEM, the given flight lists can still be used. Given any ascending sequence of bounds for the categories, the following logic was used:

- For the first category, i.e. the shortest flights, select those flights shorter than the first bound;
- For the last category, i.e. the longest flights, select those flights longer than the last bound;
- For any interval between two subsequent bounds, select those flights longer than the lower bound but shorter than the upper bound.

For this study, six bins for flight distance were selected: ultra short-haul (i.e. shorter than 750 km), short-haul (750 to 1,500 km), short and long medium-haul (1,500 to 2,500 and 2,500 to 4,000 km, respectively), long-haul (4,000 to 8,000 km) and ultra long-haul (over 8,000 km). This categorisation allows for comparisons with other studies and clear policy implications [1–3].

Table S4: Trip details per category for various flight distances in 2019. The percentage of flights relates to all global flights after filtering as discussed in section SI 1.1.

					Mean value per flight	
Flight distance	Flights	Flights [%]	Pax [10^6]	RPKs [10^9]	Pax	Distance [km]
Under 750 km	17,850,105	42.29	1,192	561	67	405
750 to 1,500 km	12,354,790	29.27	1,282	1,409	104	1,090
1,500 to 2,500 km	6,707,531	15.89	771	1,472	115	1,899
2,500 to 4,000 km	3,076,388	7.29	401	1,246	131	3,091
4,000 to 8,000 km	1,574,276	3.73	302	1,748	192	5,681
Over 8,000 km	649,352	1.54	144	1,418	222	9,761

To filter the length of the flown routes, a module from the openAVEM model was used. This module takes the latitude and longitude of both the origin and destination airports and computes the distance between these two points. The latitudes and longitudes were retrieved from airport objects, which in turn were created with the openAVEM module `load_airports()` [4].

SI 1.2.3. Aircraft size per route

In this section, it is explained how various aircraft types are compared on the same routes. This reduces the size of the data set considerably, but aims to eliminate non-uniform effects of emissions for different locations by comparing routes on which all compared aircraft types operate. To do so, the initial flight lists are reduced based on the following criteria:

1. The flight distance shall be at least 500 km;
2. Routes need to be operated by all of the aircraft types under investigation;
3. For each aircraft-route combination, at least 5 flights per month must take place.

Two comparisons were made: one between turboprops, regional jets and narrowbody aircraft on short-haul flights, and one between narrowbody and widebody aircraft on medium-haul routes. Table S5 shows data related to the flights for the short-haul comparison, while the flight data used in the medium-haul comparison can be found in table S6.

Table S5: Trip details per category for various aircraft sizes on shared short-haul routes in 2019. The percentage of flights relates to all global flights after filtering as discussed in section SI 1.1.

					Mean value per flight	
Aircraft size	Flights	Flights [%]	Pax [10^6]	RPKs [10^9]	Pax	Distance [km]
Turboprop	71,632	0.17	3	2	45	677
Regional jets	94,788	0.22	6	4	64	670
Narrowbody	226,739	0.54	26	18	113	689

Table S6: Trip details per category for various aircraft sizes on shared medium-haul routes in 2019. The percentage of flights relates to all global flights after filtering as discussed in section SI 1.1.

					Mean value per flight	
Aircraft size	Flights	Flights [%]	Pax [10^6]	RPKs [10^9]	Pax	Distance [km]
Narrowbody	4,251,175	10.07	509	817	120	1,589
Widebody	1,625,477	3.85	329	633	202	1,918

Clearly, the data sets in table S6 are an order of magnitude larger than those in table S5, providing a higher level of confidence regarding the applicability of these results.

SI 1.2.4. Aircraft age per route

Another case study involved the comparison between old and new generation aircraft. The age of the aircraft was based on the certification date, assuming that minimal technology improvements are obtained throughout the lifetime of the aircraft. It was decided to use the year 2000 as the cut-off date to distinguish between these categories. Furthermore, a seat requirement was set to the aircraft to minimise the impact of aircraft size. This filter was set to 170 to 200 seats for narrowbody aircraft, and 280 to 320 seats for widebody aircraft. These ranges allowed for the inclusion of the most popular narrowbody and widebody aircraft types, while keeping the variation in seat numbers within sample sets to a minimum. The resulting set of aircraft matching these requirements is shown in table S7.

Table S7: Aircraft types included for each simulation related to aircraft certification periods.

Year of certification	Narrowbody aircraft		Widebody aircraft	
1999 or before	A321	B722	A306	A333
	B738	B752	B772	B773
	T204			
2000 or later	A21N	B38M	A339	A359
	B39M	B739	B77L	B789

In tables S8 and S9, the number of flights performed by these aircraft is shown for narrowbody and widebody aircraft, respectively. They also provide the contribution of each set to the total set of flights and several other details.

Table S8: Trip details per category for various aircraft certification periods for narrowbody aircraft in 2019. The percentage of flights relates to all global flights after filtering as discussed in section SI 1.1.

					Mean value per flight	
Year of certification	Flights	Flights [%]	Pax [10^6]	RPKs [10^9]	Pax	Distance [km]
1999 or before	3,190,251	7.56	398	585	125	1,463
2000 or later	1,007,821	2.39	131	223	130	1,704

Table S9: Trip details per category for various aircraft certification periods for widebody aircraft in 2019. The percentage of flights relates to all global flights after filtering as discussed in section SI 1.1.

					Mean value per flight	
Year of certification	Flights	Flights [%]	Pax [10^6]	RPKs [10^9]	Pax	Distance [km]
1999 or before	470,291	1.11	98	278	208	2,829
2000 or later	263,290	0.62	53	204	202	3,833

SI 1.2.5. Intra-European flights shorter than 750 km

For this particular case study, only a selection of the global flights was considered, as it was focused on aviation that could be replaced by European rail connections. The following criteria were used to obtain the selection:

1. The flight distance shall be less than 750 km;
2. Both the origin and destination of the flight is located within Europe, based on the ICAO code reference system as given in figure S1;
3. Only flights of commercial aircraft shall be included, i.e. flights of turboprop, regional jet, narrowbody, or widebody aircraft.

The International Civil Aviation Organization (ICAO) has allocated unique 4-letter codes to airports around the world.[1] These are systematically ordered, where the first letter denotes a specific region or country, the second letter a smaller region, until the combination of all four letters provides a unique code for one airport. In this case study, the first letter of the ICAO codes was used to identify which airports were located in Europe. As can be seen in figure S1, some countries such as the USA, Canada and Australia have their own prefix, while other letters are reserved for larger regions consisting of multiple countries.

[1] https://en.wikipedia.org/wiki/File:ICAO_FirstLetter.svg. Last accessed on 18 July 2022

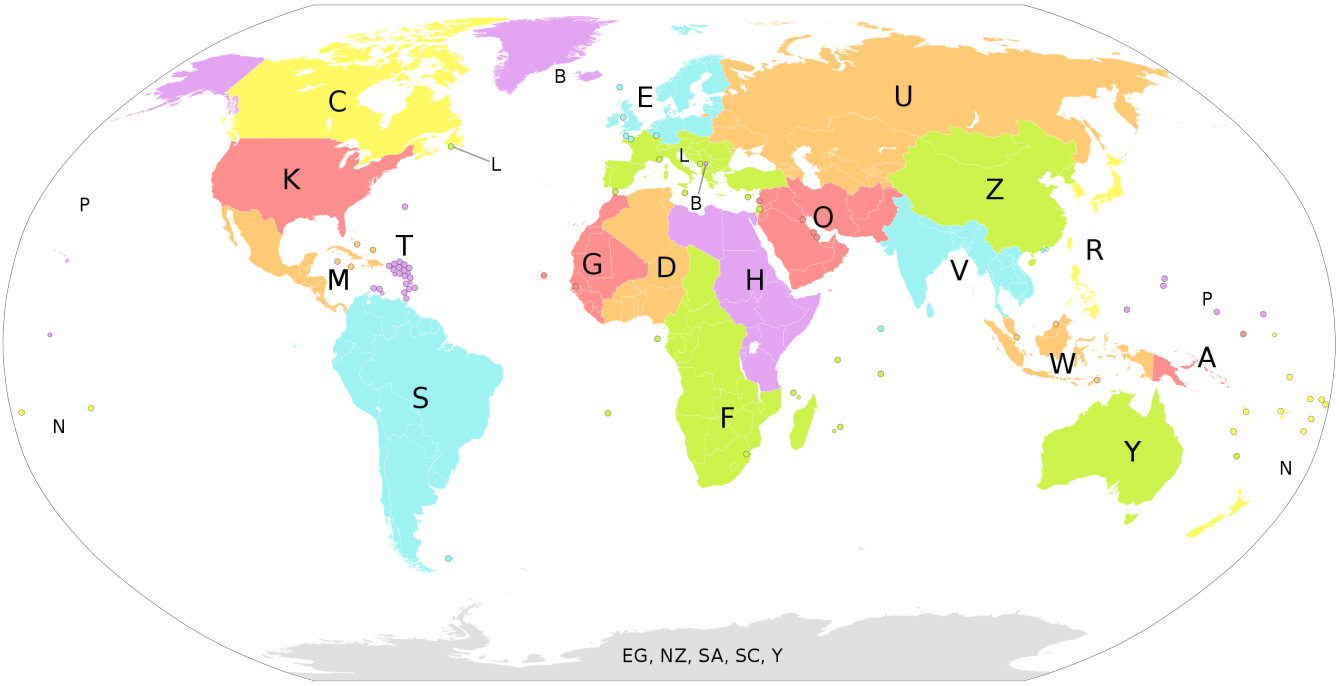

Figure S1: First letter of ICAO code per region. Taken from https://en.wikipedia.org/wiki/File:ICAO_FirstLetter.svg on 18 July 2022

For this case study, European airports were defined as those located in the regions starting with the letters 'E' (for Northern Europe), 'L' (for Southern Europe), or 'BK' (for Kosovo). Note that other combinations starting with the letter 'B', which indicate airports in Greenland and Iceland, were not included. As these countries do not have a dedicated railway system, it would be unrealistic to expect that flights within these countries could be replaced by trains. Furthermore, the remote location means that there are no flights between these countries and continental Europe that comply with the first criterion on flight distance. While the UN provides a different definition of Europe, in which Turkey is excluded but Russia and Ukraine are included,[2] it was decided to use the ICAO airport codes for consistency.

For simplicity, no further limitations were set on the availability of rail travel between two airports in this set. This means that the actual total number of flights which could be replaced by rail is lower than those included in this data set. However, this approach was deemed more consistent than excluding individual airport pairs. Extensive research would be required to create a complete, yet concise set of routes for which rail transport is a feasible alternative. Using this method, it is clear that no realistic figure can be given on the amount of emissions that could be avoided when these flights are replaced by train rides. However, it allows to obtain an upper limit of what is achievable and can therefore put policies of this kind in perspective. Details of this set of flights can be found in table S10.

Table S10: Trip details for intra-European flights in 2019. The percentage of flights relates to all global flights after filtering as discussed in section SI 1.1.

				Mean value per flight	
Flights	Flights [%]	Pax [10^6]	RPKs [10^9]	Pax	Distance [km]
3,513,784	8.32	309	145	88	446

[2] https://unstats.un.org/unsd/methodology/m49/. Last accessed on 26 July 2022

SI 2. The openAVEM model

The Open Aviation Emissions model was developed by Flávio Quadros at the Aircraft Noise and Climate Effects section of the Faculty of Aerospace Engineering at Delft University of Technology, in the Netherlands [4]. It is a Python package that calculates the fuel burn and atmospheric emissions of NO_x, HC, CO and nvPM from a list of flights. This chapter provides a brief overview of relevant settings for this study. For more details, please refer to the original paper on this model [4].

SI 2.1. Data sources

The openAVEM package is available under an Apache v2.0 OSS licence and can be downloaded from GitHub[1]. The version used as the basis for this study was updated last on 15 March 2022. Furthermore, table S11 provides an overview of the external data on which the model relies.

Table S11: Sources for input data of openAVEM.

Data	Author	Reference
List of flights	FlightRadar24	[2]
Aircraft performance model	EUROCONTROL	[3]
Airport data	OurAirports	[4]
Engine properties	ICAO	[5]
Payload mass fractions	IATA	[5]
Aircraft ICAO type codes	ICAO	[6]
Meteorology data	MERRA2	[7]

Please note that in order to use the BADA aircraft performance model provided by EUROCONTROL, one must first obtain a licence for the BADA 3 model.

SI 2.2. Emission indices and model settings

For CO_2, H_2O and SO_x, constant emission indices were used. These values were the same as those used by Quadros et al. [4] and are given in table S12. For other species, the emission indices were based on engine models and varied between aircraft and engine types. However, typical values from literature are provided in table S12 to provide an indication. Note that individual engines may show values well beyond the provided range, depending on the used technologies.

Table S12: Emission indices for the combustion process of kerosene. Mean values and ranges for full flight based on multiple studies.

Species	EI [g kg^{-1}]	(range)	Source
CO_2	3,155		[4]
H_2O	1,237		[4]
NO_x	14	(12-17)	[6]
BC	0.035	(0.011-0.093)	[7]
SO_x	0.6		[4]
CO	3	(2-3)	[6]
HC	0.4	(0.1-0.6)	[6]

[1] https://github.com/flavioquadros/openavem. Last accessed on 24 November 2022.
[2] https://www.flightradar24.com/. Last accessed on 23 November 2022.
[3] https://www.eurocontrol.int/model/bada. Last accessed on 23 November 2022.
[4] https://ourairports.com. Last accessed on 23 November 2022.
[5] https://www.iata.org/economics/. Last accessed on 23 November 2022.
[6] https://www.icao.int/publications/DOC8643/Pages/Search.aspx. Last accessed on 23 November 2022.
[7] https://disc.gsfc.nasa.gov/datasets?page=1&subject=Atmospheric%20Winds&project=MERRA-2&temporalResolution=3%20hours. Lasr accessed on 8 December 2022.

In this study, the same model settings were used as those initially described by Quadros et al. [4]. These were mostly the default options given in the openAVEM model, with the exception of those reported in table S13.

Table S13: Adjusted model settings for openAVEM simulations.

Setting	Used value	Reason
`ignore_missing_airports`	True	Disregard flights that occur between airports not covered by the airport database. Otherwise the simulation would exit with an error.
`apt_closed`	True	Use airports which were labeled as closed in the database. The flight data was considered more accurate than the information on the operating status of the airport.
`reverse_rand_occurence`	True	A random number generator is used to determine whether reverse thrust is applied during landing. This setting was also used by Quadros et al. [4].
`yyyymm`	'2019MM'	The payload mass fraction is specified for each month 'MM' to be more precise than using a single fraction for the entire year.
`sstep_cr`	50 NM	The horizontal resolution during cruise was increased from 125 NM to 50 NM for improved accuracy of emission locations.
`wind`	'fixed-field'	An input file containing data on wind direction and magnitude is used to model the wind.
`grid_vertical`	'GC72'	72 vertical levels are used to lump the emissions, instead of the original 33, to improve accuracy of emission locations.
`verify_flightfuel`	1.0	A warning is triggered if the fuel burn exceeds the difference between the maximum and minimum operating weight of the aircraft. By default, this warning was not triggered.

SI 2.3. Verification of the model

The results of the openAVEM model were verified against those obtained by Quadros et al. [4]. The spatial distribution of emissions (shown for fuel burn in figure S2) showed no deviation from the original study.

However, minor deviations were observed in the total global emission estimates resulting from the simulation. The present study showed a 0.11% lower fuel burn and emission rate for those species which have a constant emission index (i.e. CO_2, H_2O and SO_x). As shown in table S14, the largest differences occur in the emission estimates of CO and HC.

Table S14: Comparison of emitted species for the year 2019 between the current study and Quadros et al. [4].

Species	Study by Quadros et al. [4]	This study	Difference [%]
Fuel, Tg	297	297	- 0.11
CO_2, Tg	937	936	- 0.11
H_2O, Tg	367	367	- 0.11
NO_x, Tg	4.62	4.62	- 0.01
SO_x, Gg	178	178	- 0.11
CO, Gg	814	805	- 1.08
HC, Gg	42.6	41.9	- 1.61
$nvPM_m$, Gg	9.68	9.68	0.00
$nvPM_N$, 10^{26}	3.47	3.48	0.26

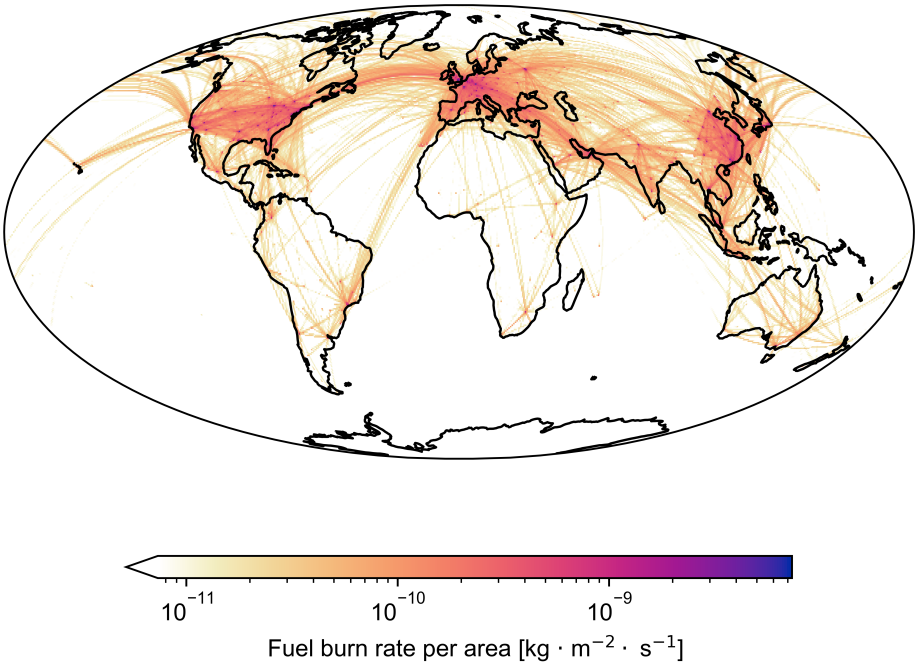

Figure S2: Global distribution of aviation fuel burn rater per area, averaged for 2019. Results obtained through openAVEM, using the methodology described in Quadros et al. [4].

Upon consultation with the author of the original study, it was concluded that the deviations were the result of a change in the input data for airports and engine emission indices, as well as the use of a random number generator to determine whether reverse thrust was used during landing. The first update can affect emissions through a change in taxiing time at specific airports, or through the omission of particular airports from the database. The second change can affect the non-linear emission indices of engines and thus the total emissions of species that are not directly proportional to fuel burn. Unfortunately, the older versions of the input data as used by Quadros et al. [4] were not available to test these hypotheses.

Finally, the randomly activated reverse thrust was used in the original study. Therefore, not using this option would yield a larger deviation compared to the current results. Although the total number of thrust reverse being activated is expected to be in close proximity with the original study, deviations may occur as the impact of one aircraft's thrust reverser may be different to that of another aircraft's. Nevertheless, given the rather small deviations in results, it was concluded that the model was sufficiently accurate to be used in the present study.

SI 2.4. Distribution of global aviation fuel burn per month and altitude bin

The temporal variation of aviation fuel burn results from the differences in monthly flight data used as input for the openAVEM model. It is assumed that the emissions are uniformly distributed within each month. The deviations in monthly emissions relative to the annual mean of the same category are shown in figures S3 and S4 for aircraft size and flight distance, respectively.

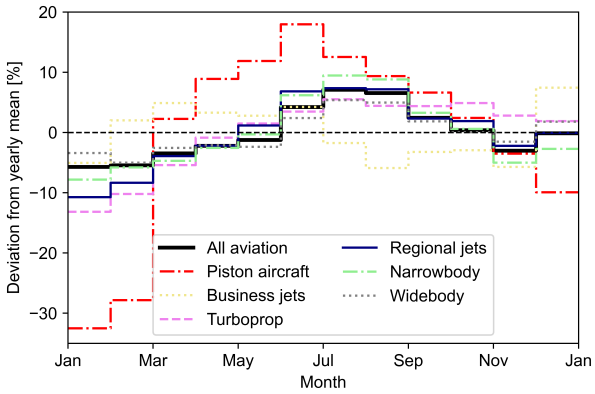

Figure S3: Monthly deviation in daily global fuel burn relative to the annual mean for various aircraft sizes in 2019.

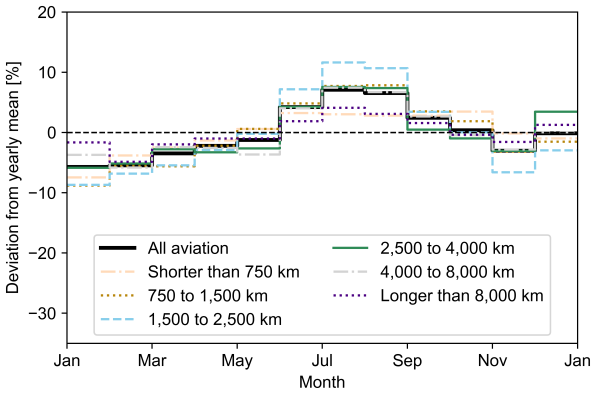

Figure S4: Monthly deviation in daily global fuel burn relative to the annual mean for various flight distances in 2019.

The vertical distribution of aviation emissions is shown for the different aircraft sizes in figures S5 and S6. Please note the difference in scale on the x-axis; emissions of narrowbody and widebody aircraft are one to two orders of magnitude larger than for other aircraft sizes. While a clear altitude band is visible showing the cruise emissions, it must be noted that these figures may not fully represent the actual vertical distribution of emissions. The openAVEM model lumps all cruise emissions of a particular aircraft type into one altitude bin which shows the largest contribution to all fuel burn for that aircraft. Thus, the presence of outliers or a widely spread distribution of emissions versus altitude is ignored through this process. Still, the results provide a rough indication of typical operations of the different aircraft types, showing higher cruise altitudes for business jets and lower for turboprop aircraft.

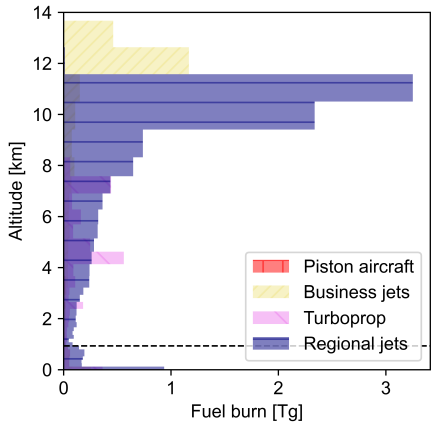

Figure S5: Vertical distribution of global fuel burn for piston aircraft, business jets, turboprop aircraft and regional jets. The dashed line shows the border between LTO and cruise operations.

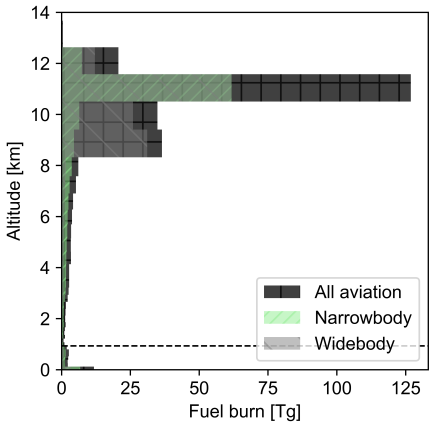

Figure S6: Vertical distribution of global fuel burn for all aviation, narrowbody aircraft and widebody aircraft. The dashed line shows the border between LTO and cruise operations.

SI 3. Atmospheric simulations

For this study, the Goddard Earth Observing System Atmospheric Chemistry (GEOS-Chem) model was used to evaluate the atmospheric impact of changes in aviation emissions. It is a 3D chemical transport model based on meteorological observations by the Goddard Earth Observing System (GEOS) of NASA's Global Modeling Assimilation Office (GMAO)[1] and has been applied widely in previous studies [8–14]. This chapter provides a brief overview of the settings used for the simulations, as well as the differences between annual and peak season values for O_3 concentrations.

SI 3.1. The GEOS-Chem model

The GEOS-Chem model used in this study is the GEOS-Chem Classic (GCC) v13.3.3, using a rectilinear grid with a horizontal resolution of 2° × 2.5°. GCC provides two options for the vertical resolution: 47 or 72 layers, using a terrain following hybrid sigma-pressure level definition as given in equation (SI 3.1).[2]

$$\sigma = \frac{p - p_t}{p_s - p_t} \tag{SI 3.1}$$

Here, p_s denotes the pressure at the surface, while p_t is the pressure at the top of the modeling domain. In GCC, this corresponds to 0.01 hPa at either resolution. For any vertical coordinate, the local pressure p then yields the sigma coordinate at that altitude. In our study, we opt to use 72 vertical levels, as well as the Unified Tropospheric-Stratospheric Chemistry Extension (UCX) module, in order to capture effects of aviation cruise emissions more accurately [10, 15]. The atmospheric model is run with the default time step of 10 minutes for transport related processes and 20 minutes for chemistry processes and emissions.[3]

For the non-aviation emissions, the inventories provided with GEOS-Chem v13.3.3 were used, as shown in table S15. The main inventories are identical to those used by Quadros et al. [15]. Please note that the interaction between aviation and shipping emissions may yield secondary effects when aviation emissions are removed. In our simulations, we do not separate the primary and secondary effects, such that the use of an alternative shipping emissions inventory (as opposed to CEDS), may result in different effect quantification.

Table S15: Non-aviation emission inventories and emission modules selected for the GEOS-Chem simulations.

Inventory / module	Type of emissions
CEDS (v2)	Anthropogenic
GEIA	Natural sources of NH_3, 1990 only
TZOMPASOSA	Fuel emissions, 2010 only
XIAO	C_3H_8 emissions, 1985 only
LIANG_BROMOCARB	Bromocarbon emissions, 2000 only
ORDONEZ_IODOCARB	Iodocarbon emissions, 2000 only
GFED4	Biomass burning
PARANOX	Ship plume model
	Lightning NO_x
DEAD	Dust (offline)
	Sea salt (offline)
MEGAN	Biogenic (offline)
SOILNOX	Soil NO_x emissions (offline)
AeroCom	Volcanic

[1] http://www.geos-chem.org. Last accessed on 24 June 2022.
[2] https://wiki.seas.harvard.edu/geos-chem/index.php/GEOS-Chem_vertical_grids. Last accessed on 24 March 2023.
[3] http://wiki.seas.harvard.edu/geos-chem/index.php/The_input.geos_file. Last accessed on 8 September 2022.

SI 3.2. Ozone peak season

For some CRFs (discussed further in chapter SI 4), the mean peak season concentration is selected as a metric to measure O_3 exposure. This peak season was identified in each grid cell by computing the means of 6-month consecutive periods and selecting the highest value and the corresponding period. In order to compute the 6-month periods spanning multiple calendar years, the results were cycled: instead of requiring additional data from December 2018, the results of December 2019 were used along with those of January 2019 until May 2019, for example. Similarly, the first months of 2019 were used to replace data from early 2020. The resulting two central months of this peak season are shown for each grid cell in figure S7.

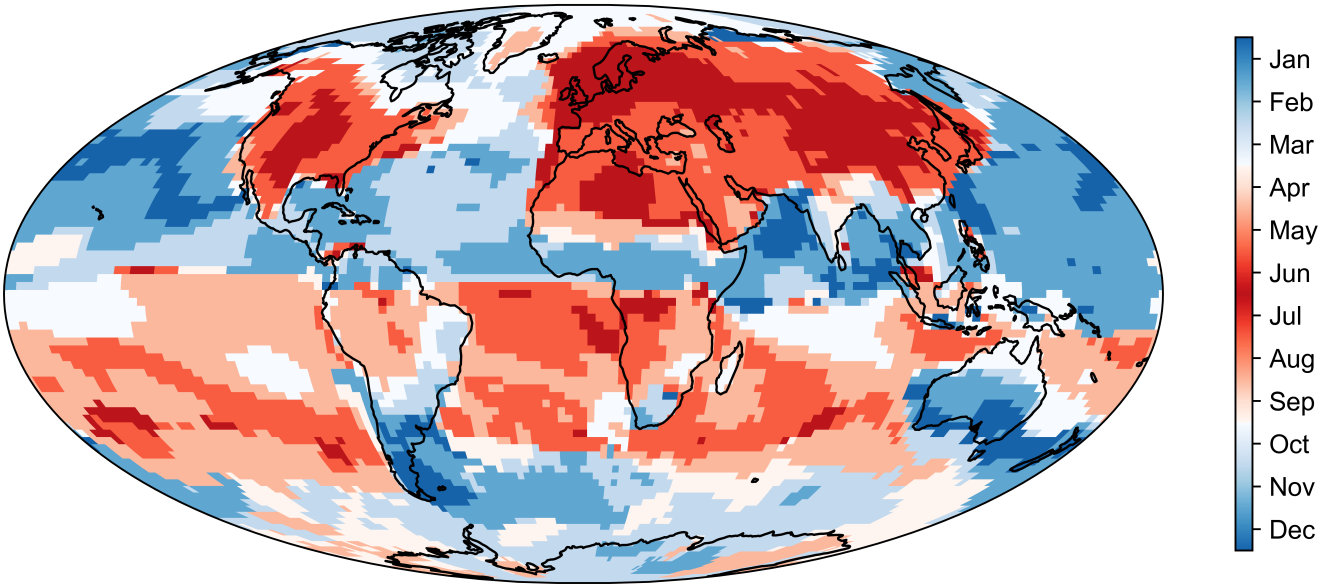

Figure S7: Central months of the 6-month peak season for ground-level O_3 concentrations in each 2° × 2.5° grid cell.

The difference in ground-level O_3 concentrations between the peak season and annual mean for the baseline scenario can be found in figure S8.

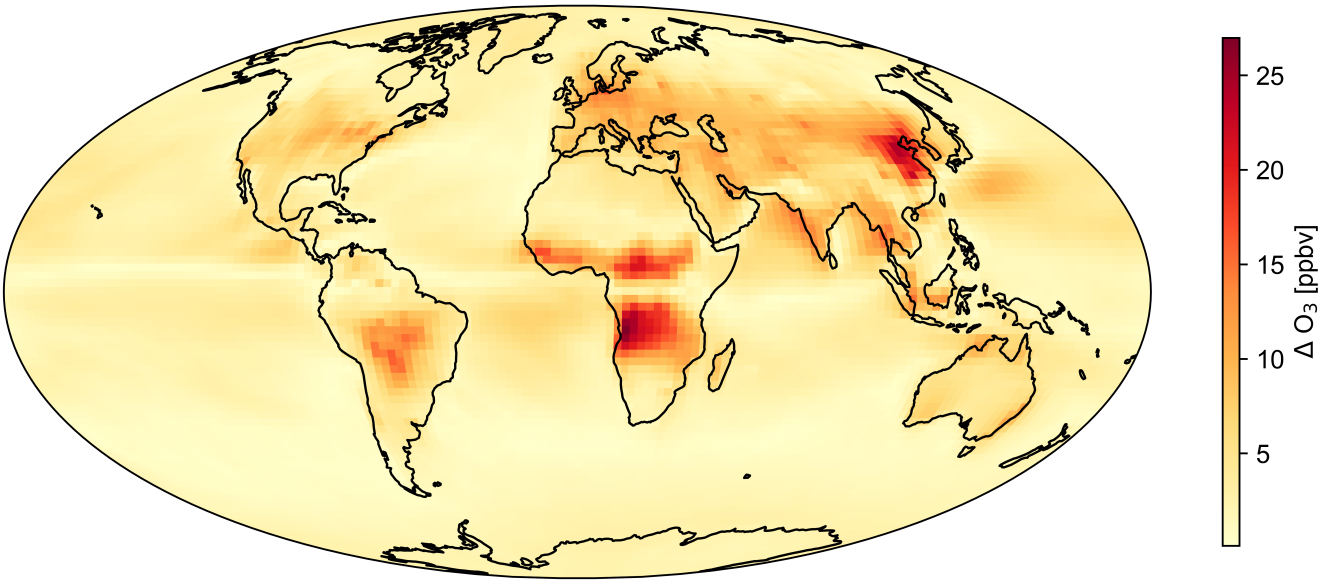

Figure S8: Difference between 6-month peak season average ground-level MDA8 O_3 concentrations and the yearly average.

SI 4. Estimation of health impacts

This chapter provides additional information and methods that were used to estimate the health impact of aviation. First of all, section SI 4.1 provides information on general global mortality estimates, independent of aviation. Furthermore, additional information related to the concentration response functions is provided in sections SI 4.2 to SI 4.4.

SI 4.1. Baseline mortality

To estimate the baseline mortality rates, LandScan population data[1] was combined with incidence rates from the Global Health Estimates (GHE) of 2019 for the population over 30 years of age [16]. figure S9 shows the global population density for 2019 on a 0.5° × 0.625° grid.

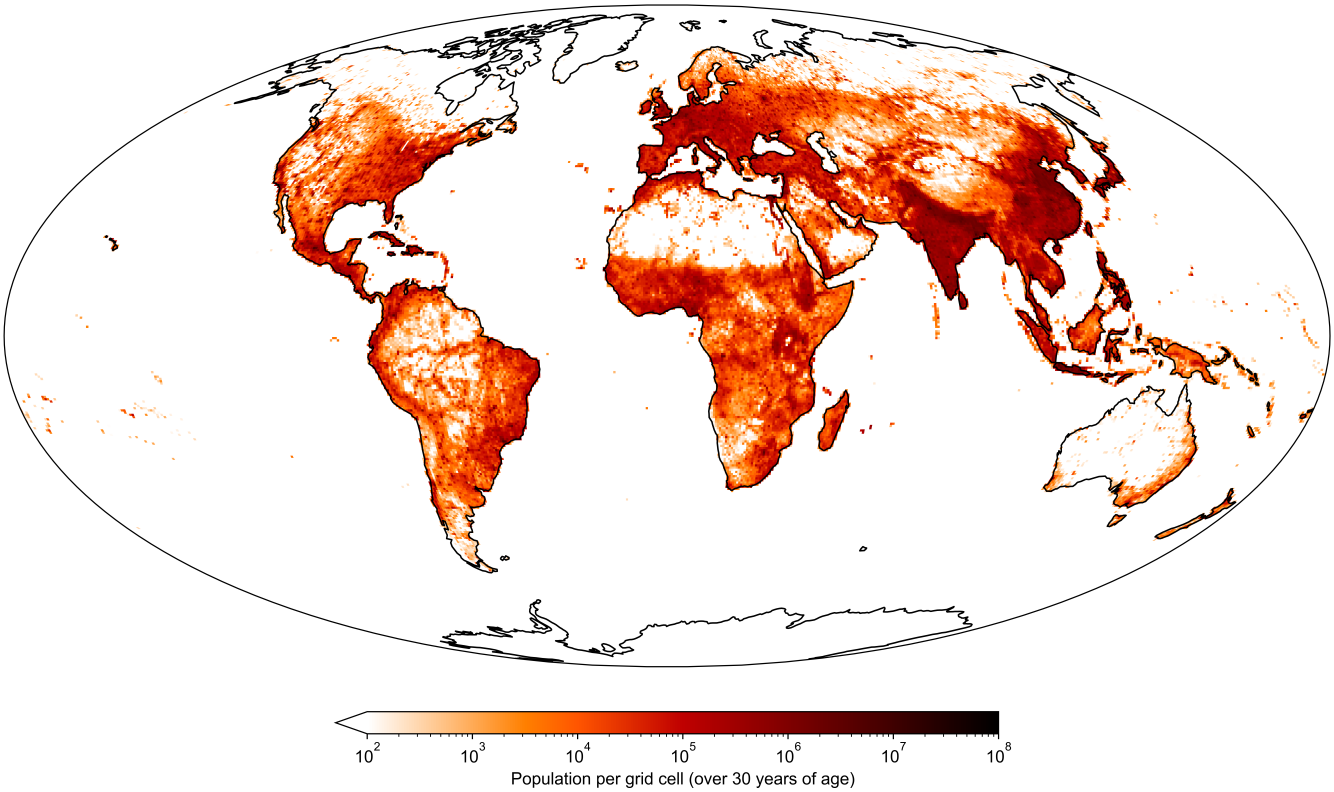

Figure S9: Global population density for people over 30 years of age according to LandScan population data on a 0.5° × 0.625° grid.

The GHE2019 data contains baseline mortality rates per country. Given the uneven population density between regions, these mortality rates were normalised per 1,000 inhabitants. The resulting incidence rates were then allocated to all populated grid cells, yielding the relative baseline mortality per country as shown in figure S10. Multiplying these incidence rates by the local population yielded the total non-accidental baseline mortality rates in figure S11.

[1] https://landscan.ornl.gov. Last accessed on 8 December 2022.

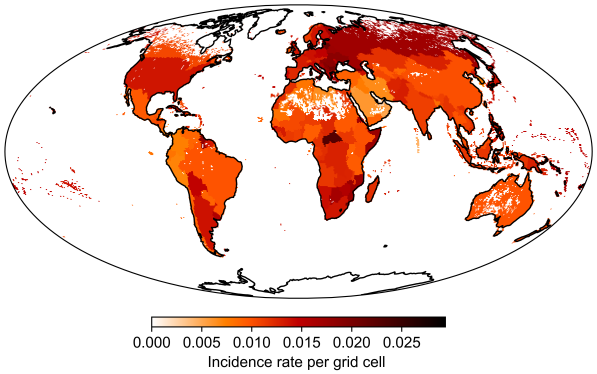

Figure S10: Relative baseline mortality per country in 2019, according to the Global Health Estimates [16].

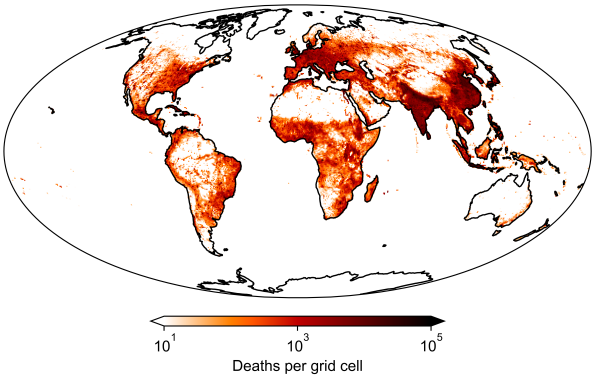

Figure S11: Total estimated non-accidental global baseline mortality in 2019 on a 0.5° × 0.625° grid.

SI 4.2. Implementation of concentration response functions

Except for the CRF used to estimate $PM_{2.5}$ impacts in the main study (for which the parameters are described in more detail in Burnett et al. [17]), the CRFs used in this study all adhere to the log-linear relationship provided in equation (SI 4.1) (adjusted from the hazard ratio as defined by Goodkind et al. [18]).

$$ER = 1 - e^{-\gamma(c_1 - c_0)} \tag{SI 4.1}$$

Here, ER stands for excess risk, which is the fraction of the baseline risk that is superimposed through the shift of the pollution concentration to a higher level. Furthermore, c_1 and c_0 are the higher and lower pollutant concentration levels, respectively. Finally, γ is defined through equation (SI 4.2) [18].

$$\gamma = \frac{\ln RR}{\Delta c} \tag{SI 4.2}$$

Finally, RR is the relative risk caused by an increase in concentration Δc, usually obtained through large-scale cohort studies. In combination with the baseline mortality (obtained as discussed in section SI 4.1), this yields the following formulation of aviation-attributable premature mortality:

$$M_{\text{aviation}} = I_{>30} \cdot P_{>30} \cdot ER \tag{SI 4.3}$$

Here, $I_{>30}$ is the baseline incidence rate based on the population older than 30 years and $P_{>30}$ is the population over 30 years of age.

SI 4.3. Alternative concentration response functions

This section provides the relative risk factors, as used in equation (SI 4.2), as well as the 95% confidence intervals of these estimates for a variety of concentration response functions used in literature. Where applicable, the threshold level is provided, below which no health impacts are assumed. The relative risk factor is based on a concentration change Δc as given in the last column of each table. In case one source provided both single- and multi-pollutant model results, * indicates the multi-pollutant result. In table S17, the O_3 metrics can be interpreted as follows: for daily concentrations, either the daily average (24h), 8-hour maximum daily average (MDA8), or 1-hour maximum daily average (MDA1) is used. 'Annual' metrics refer to yearly averaged values of these metrics, while 'season' metrics only consider the 6-month O_3 peak season.

Table S16: A collection of concentration response functions to estimate health impacts due to changes in NO_2 concentrations.

CRF		Relative risk		Concentration range	
Reference	End-point	Nominal	95% CI	Threshold	Δ $[NO_2]$[2]
Faustini et al. [19]	**Respiratory**	**1.024**	**(1.017 - 1.032)**	-	**10** $\mu g\,m^{-3}$
Faustini et al. [19]	Cardiovascular	1.133	(1.088 - 1.180)	-	10 $\mu g\,m^{-3}$
Faustini et al. [19]	All-cause	1.041	(1.019 - 1.064)	-	10 $\mu g\,m^{-3}$
Hoek et al. [20]	All-cause	1.055	(1.031 - 1.080)	-	10 $\mu g\,m^{-3}$
Turner et al. [21]	Circulatory	1.08	(1.06 - 1.09)	-	10 ppbv
Turner et al. [21]	All-cause	1.04	(1.03 - 1.06)	-	10 ppbv
Huangfu and Atkinson [22]	Respiratory	1.03	(1.01 - 1.05)	-	10 $\mu g\,m^{-3}$
Huangfu and Atkinson [22]	All-cause	1.02	(1.01 - 1.04)	-	10 $\mu g\,m^{-3}$
Beelen et al. [23]	All-cause	1.01	(0.99 - 1.04)	-	10 $\mu g\,m^{-3}$
Beelen et al. [23]*	All-cause	1.01	(0.97 - 1.05)	-	10 $\mu g\,m^{-3}$

Table S17: A collection of concentration response functions to estimate health impacts due to changes in O_3 concentrations.

	CRF		Relative risk		Concentration range	
Reference	End-point	O_3 metric	Nominal	95% CI	Threshold	Δ $[O_3]$[3]
Turner et al. [21]	**Respiratory**	**MDA8 annual**	**1.12**	**(1.08 - 1.16)**	-	**10** ppbv
Turner et al. [21]	Respiratory	MDA8 annual	1.17	(1.11 - 1.22)	35 ppbv	10 ppbv
Jerrett et al. [24]	Respiratory	MDA1 season	1.027	(1.007 - 1.046)	-	10 ppbv
Jerrett et al. [24]*	Respiratory	MDA1 season	1.040	(1.013 - 1.067)	-	10 ppbv
Huangfu and Atkinson [22]	Respiratory	MDA8 season	1.02	(0.99 - 1.05)	-	10 $\mu g\,m^{-3}$
Huangfu and Atkinson [22]	All-cause	MDA8 season	1.01	(1.00 - 1.02)	-	10 $\mu g\,m^{-3}$
Di et al. [25]	All-cause	24h season	1.023	(1.022 - 1.024)	-	10 ppbv
Di et al. [25]*	All-cause	24h season	1.011	(1.010 - 1.012)	-	10 ppbv
Turner et al. [21]	All-cause	MDA8 annual	1.02	(1.01 - 1.04)	-	10 ppbv

Table S18: A collection of concentration response functions to estimate health impacts due to changes in $PM_{2.5}$ concentrations.

CRF		Relative risk		Concentration range	
Reference	End-point	Nominal	95% CI	Threshold	Δ [BC]
Burnett et al. [17]	**NCD + LRI**	**n.a.**	**(n.a.)**	2.4 $\mu g\,m^{-3}$	**n.a.**
Chen and Hoek [26]	All-cause	1.08	(1.06 - 1.09)	-	10 $\mu g\,m^{-3}$
Hoek et al. [20]	Cardiovascular	1.106	(1.054 - 1.160)	-	10 $\mu g\,m^{-3}$
Hoek et al. [20]	All-cause	1.062	(1.041 - 1.084)	-	10 $\mu g\,m^{-3}$
Jerrett et al. [24]	Cardiovascular	1.150	(1.111 - 1.191)	-	10 $\mu g\,m^{-3}$
Jerrett et al. [24]*	Cardiovascular	1.206	(1.150 - 1.264)	-	10 $\mu g\,m^{-3}$
Krewski et al. [27]	Cardio-pulmonary	1.09	(1.06 - 1.12)	-	10 $\mu g\,m^{-3}$
Krewski et al. [27]	All-cause	1.03	(1.01 - 1.05)	-	10 $\mu g\,m^{-3}$
Di et al. [25]	All-cause	1.084	(1.081 - 1.086)	-	10 $\mu g\,m^{-3}$
Di et al. [25]*	All-cause	1.073	(1.071 - 1.075)	-	10 $\mu g\,m^{-3}$
Janssen et al. [28]	All-cause	1.007	(1.004 - 1.009)	-	1 $\mu g\,m^{-3}$
Vodonos et al. [29]	All-cause	1.0103	(1.0097 - 1.0111)	-	1 $\mu g\,m^{-3}$
Beelen et al. [23]	All-cause	1.07	(1.02 - 1.13)	-	5 $\mu g\,m^{-3}$

[2]A conversion factor 1.88 $\mu g/m^3$/ppbv is used [22].
[3]A conversion factor 1.96 $\mu g/m^3$/ppbv is used [22].

Table S19: A collection of concentration response functions to estimate health impacts due to changes in BC concentrations.

CRF		Relative risk		Concentration range	
Reference	End-point	Nominal	95% CI	Threshold	Δ [BC]
Hoek et al. [20]	**All-cause**	**1.061**	**(1.049 - 1.073)**	-	**1** $\mu g\,m^{-3}$
Janssen et al. [28]	All-cause	1.06	(1.04 - 1.09)	-	1 $\mu g\,m^{-3}$

SI 4.4. Visualisations of concentration response functions

This section provides a visualisation of the implementation of the concentration response functions mentioned in section SI 4.3 to ease comparison between results. Where needed, concentrations in $\mu g^3\,m^{-1}$ were converted to ppbv by dividing the concentrations by a factor 1.88 for NO_2 and 1.96 for O_3.

SI 4.4.1. Concentration response functions for NO_2

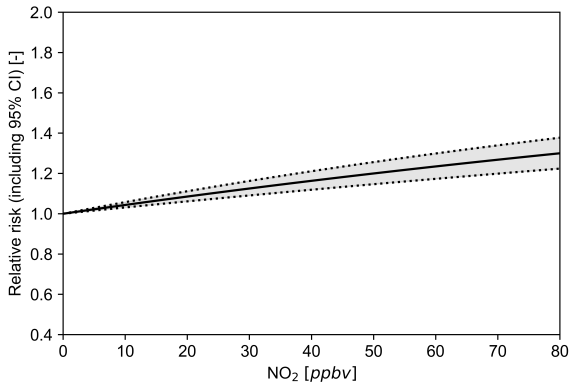

Figure S12: Concentration Response Function showing the relative risk of mortality due to respiratory diseases; proposed by Faustini et al. [19]. The shaded area shows the 95% confidence interval.

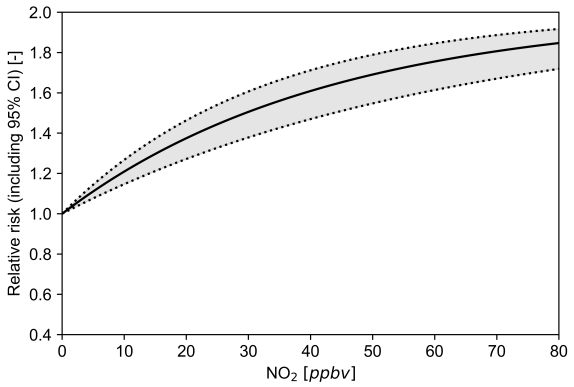

Figure S13: Concentration Response Function showing the relative risk of mortality due to cardiovascular diseases; proposed by Faustini et al. [19]. The shaded area shows the 95% confidence interval.

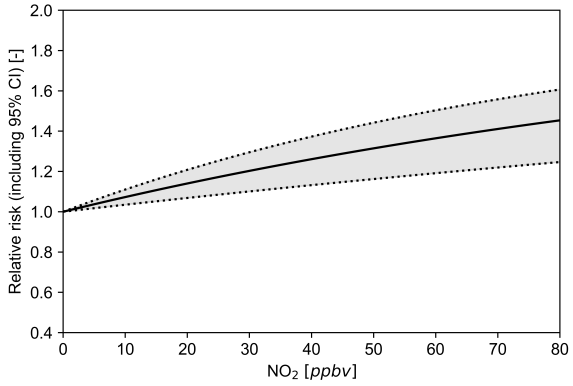

Figure S14: Concentration Response Function showing the relative risk of all-cause mortality; proposed by Faustini et al. [19]. The shaded area shows the 95% confidence interval.

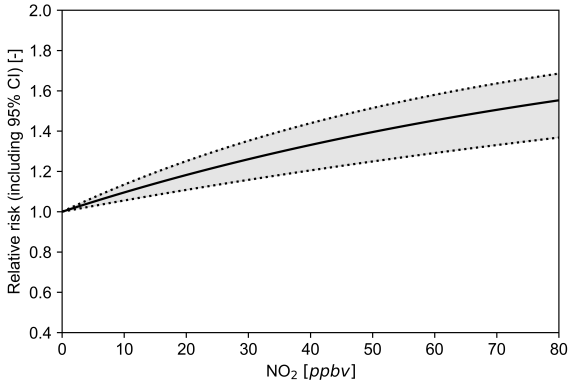

Figure S15: Concentration Response Function showing the relative risk of all-cause mortality; proposed by Hoek et al. [20]. The shaded area shows the 95% confidence interval.

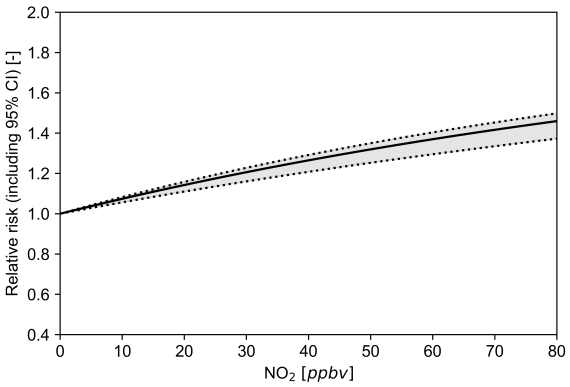

Figure S16: Concentration Response Function showing the relative risk of mortality due to circulatory diseases; proposed by Turner et al. [21]. The shaded area shows the 95% confidence interval.

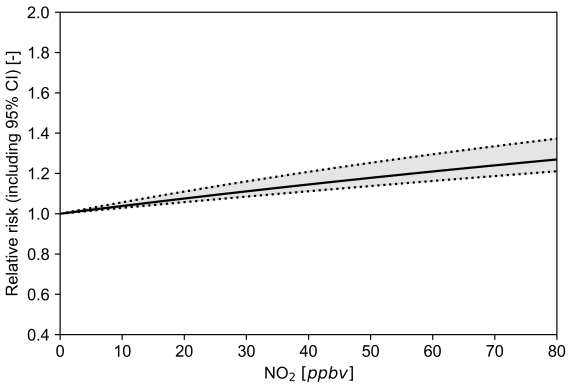

Figure S17: Concentration Response Function showing the relative risk of all-cause mortality; proposed by Turner et al. [21]. The shaded area shows the 95% confidence interval.

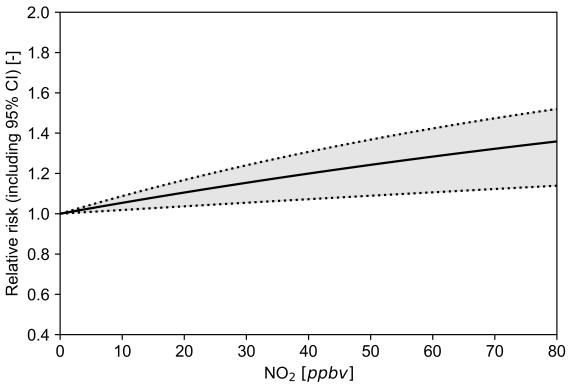

Figure S18: Concentration Response Function showing the relative risk of mortality due to respiratory diseases; proposed by Huangfu and Atkinson [22]. The shaded area shows the 95% confidence interval.

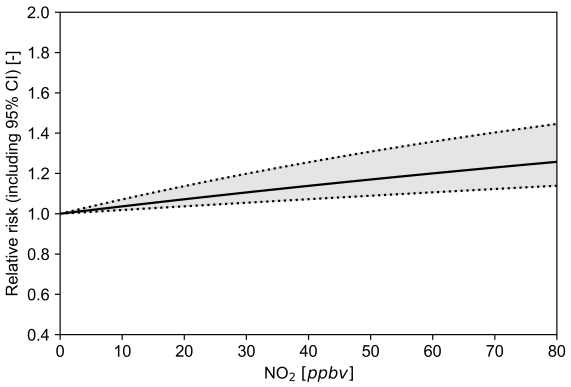

Figure S19: Concentration Response Function showing the relative risk of all-cause mortality; proposed by Huangfu and Atkinson [22]. The shaded area shows the 95% confidence interval.

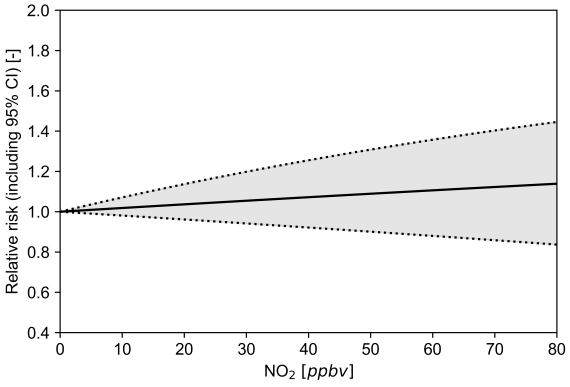

Figure S20: Concentration Response Function showing the relative risk of all-cause mortality; proposed by Beelen et al. [23]. The shaded area shows the 95% confidence interval.

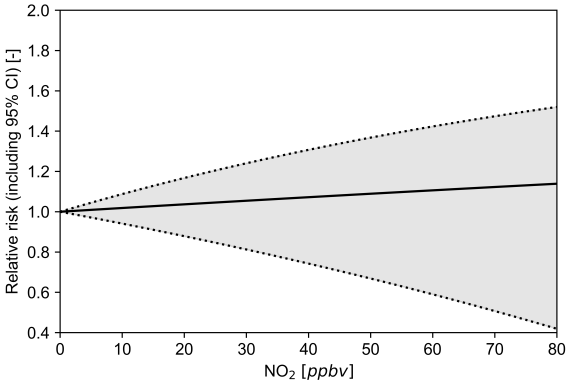

Figure S21: Concentration Response Function showing the relative risk of all-cause mortality; proposed by Beelen et al. [23], using a multi-pollutant model. The shaded area shows the 95% confidence interval.

SI 4.4.2. Concentration response functions for O_3

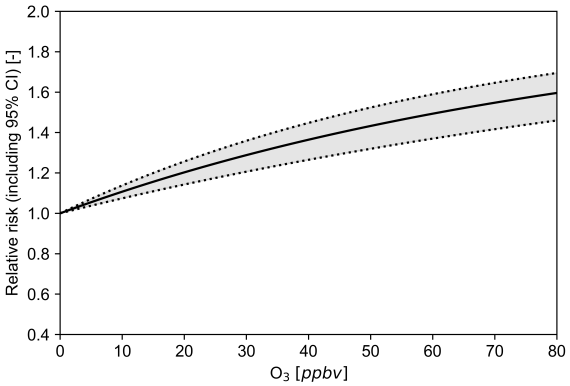

Figure S22: Concentration Response Function showing the relative risk of mortality due to respiratory diseases; proposed by Turner et al. [21]. The shaded area shows the 95% confidence interval.

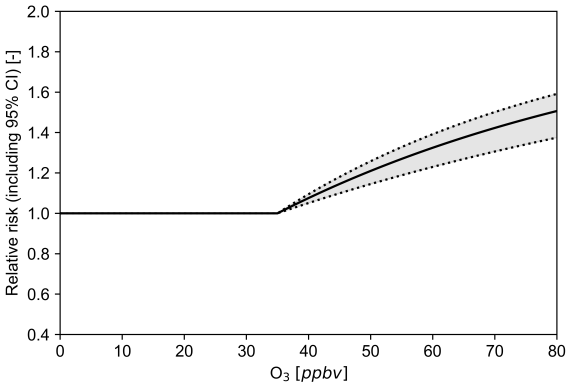

Figure S23: Concentration Response Function showing the relative risk of mortality due to respiratory diseases; proposed by Turner et al. [21], using a threshold model. The shaded area shows the 95% confidence interval.

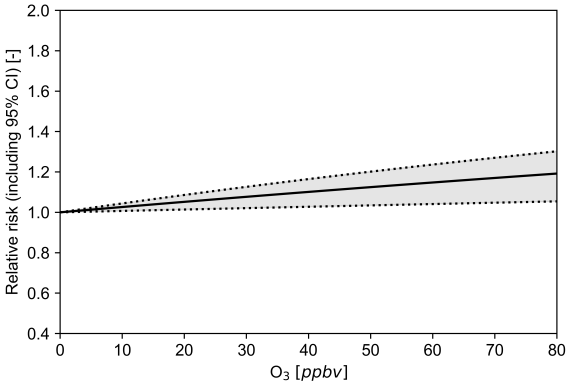

Figure S24: Concentration Response Function showing the relative risk of mortality due to respiratory diseases; proposed by Jerrett et al. [24]. The shaded area shows the 95% confidence interval.

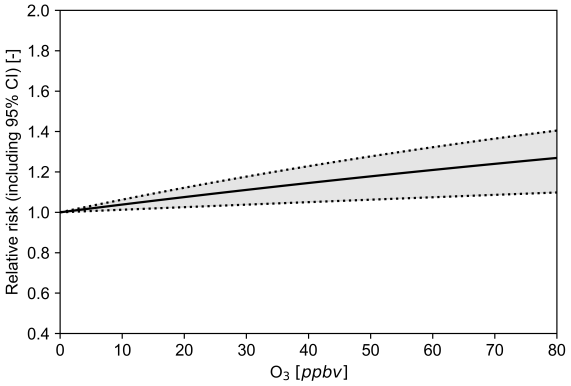

Figure S25: Concentration Response Function showing the relative risk of mortality due to respiratory diseases; proposed by Jerrett et al. [24], using a multi-pollutant model. The shaded area shows the 95% confidence interval.

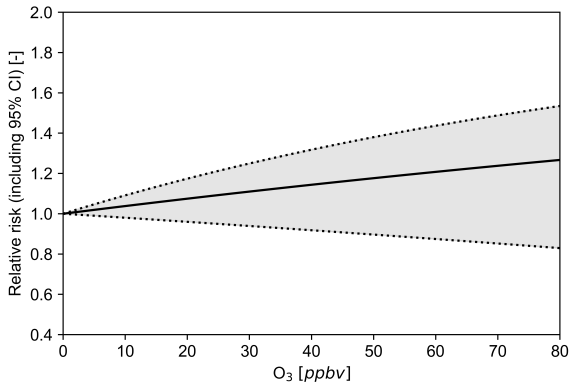

Figure S26: Concentration Response Function showing the relative risk of mortality due to respiratory diseases; proposed by Huangfu and Atkinson [22]. The shaded area shows the 95% confidence interval.

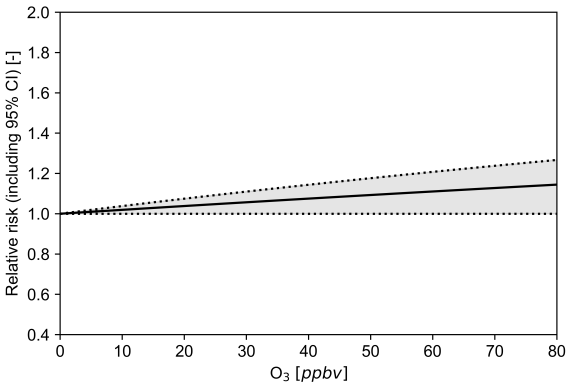

Figure S27: Concentration Response Function showing the relative risk of all-cause mortality; proposed by Huangfu and Atkinson [22]. The shaded area shows the 95% confidence interval.

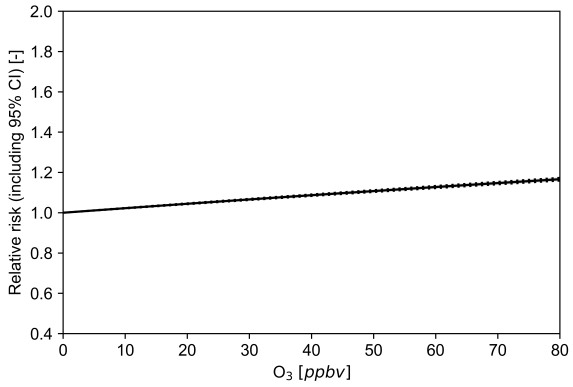

Figure S28: Concentration Response Function showing the relative risk of all-cause mortality; proposed by Di et al. [25]. The shaded area shows the 95% confidence interval.

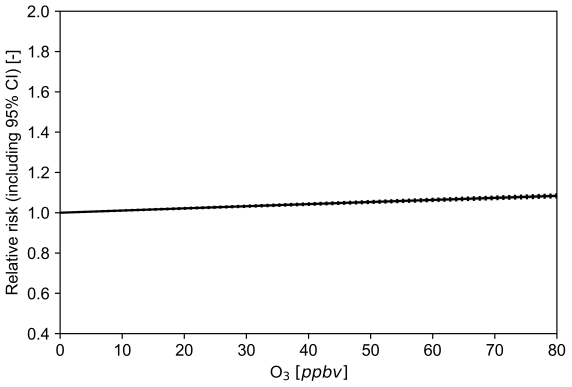

Figure S29: Concentration Response Function showing the relative risk of all-cause mortality; proposed by Di et al. [25], using a multi-pollutant model. The shaded area shows the 95% confidence interval.

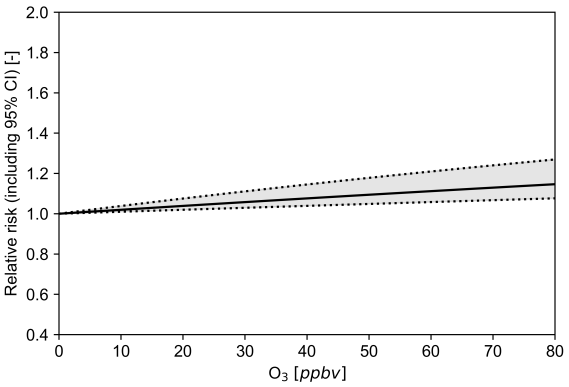

Figure S30: Concentration Response Function showing the relative risk of all-cause mortality; proposed by Turner et al. [21]. The shaded area shows the 95% confidence interval.

SI 4.4.3. Concentration response functions for $PM_{2.5}$

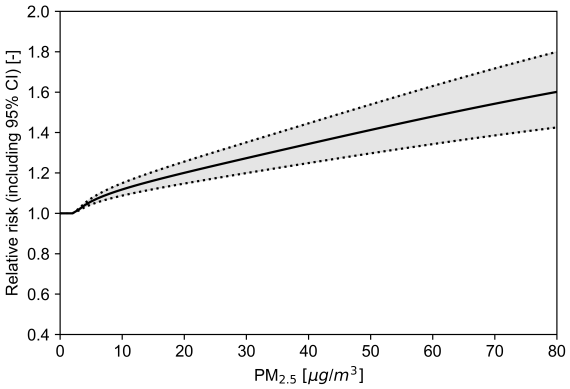

Figure S31: CRF for $PM_{2.5}$ showing the relative risk of mortality due to Non-Communicable Diseases and Lower Respiratory Infections; proposed by Burnett et al. [17]. The shaded area shows the 95% confidence interval.

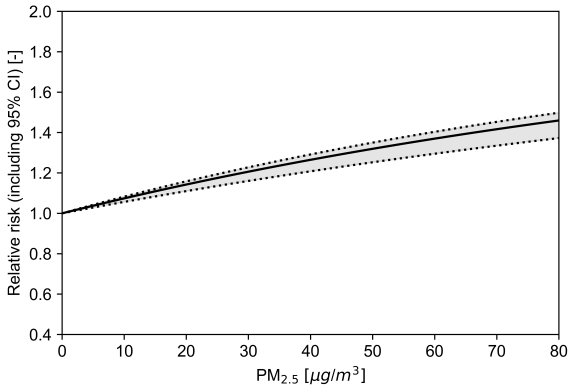

Figure S32: CRF for $PM_{2.5}$ showing the relative risk of all-cause mortality; proposed by Chen and Hoek [26]. The shaded area shows the 95% confidence interval.

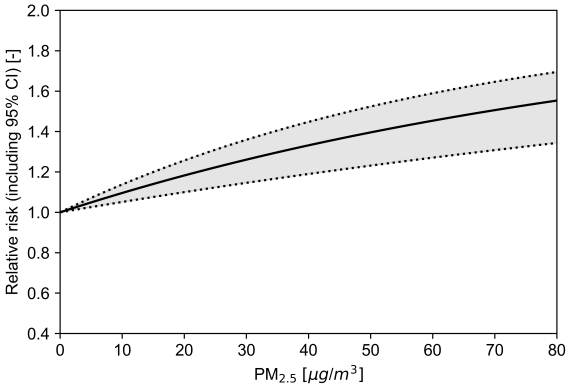

Figure S33: CRF for $PM_{2.5}$ showing the relative risk of mortality due to cardiovascular diseases; proposed by Hoek et al. [20]. The shaded area shows the 95% confidence interval.

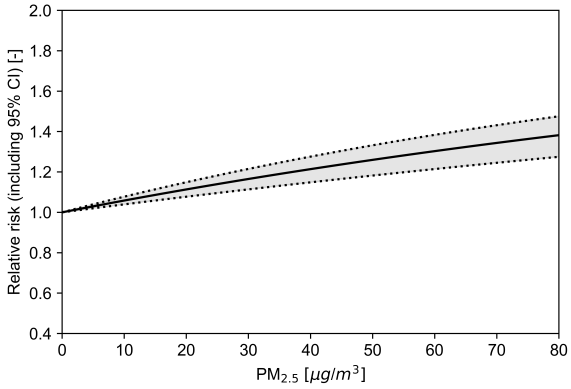

Figure S34: CRF for $PM_{2.5}$ showing the relative risk of all-cause mortality; proposed by Hoek et al. [20]. The shaded area shows the 95% confidence interval.

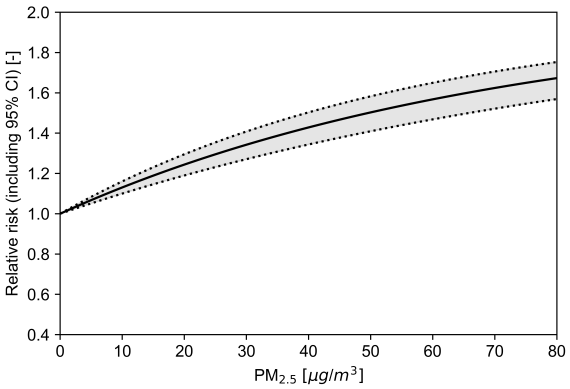

Figure S35: CRF for $PM_{2.5}$ showing the relative risk of mortality due to cardiovascular diseases; proposed by Jerrett et al. [24]. The shaded area shows the 95% confidence interval.

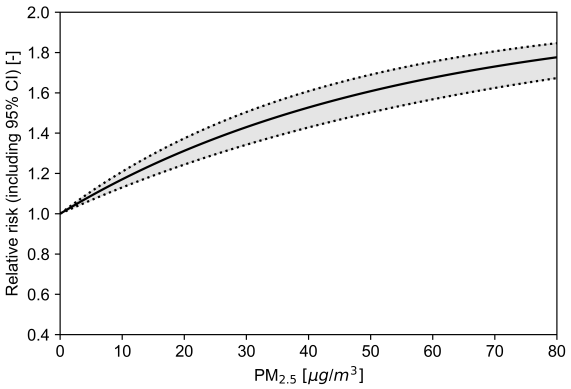

Figure S36: CRF for $PM_{2.5}$ showing the relative risk of mortality due to cardiovascular diseases; proposed by Jerrett et al. [24], using a multi-pollutant model. The shaded area shows the 95% confidence interval.

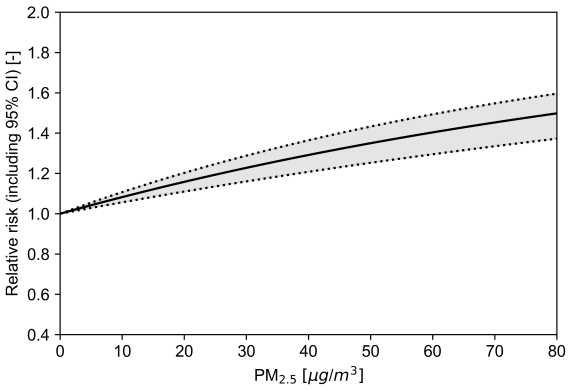

Figure S37: CRF for $PM_{2.5}$ showing the relative risk of mortality due to cardiopulmonary diseases; proposed by Krewski et al. [27]. The shaded area shows the 95% confidence interval.

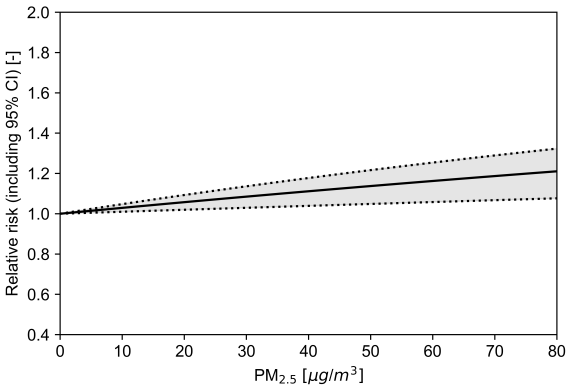

Figure S38: CRF for $PM_{2.5}$ showing the relative risk of all-cause mortality; proposed by Krewski et al. [27]. The shaded area shows the 95% confidence interval.

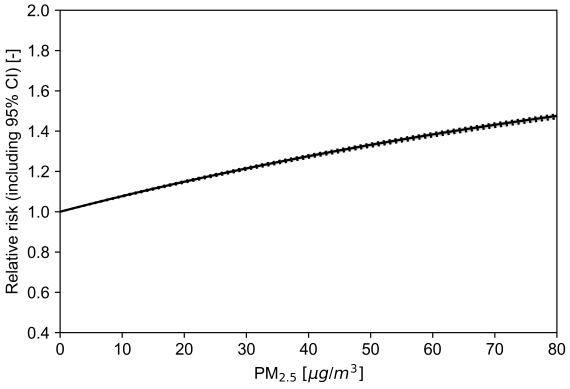

Figure S39: CRF for $PM_{2.5}$ showing the relative risk of all-cause mortality; proposed by Di et al. [25]. The shaded area shows the 95% confidence interval.

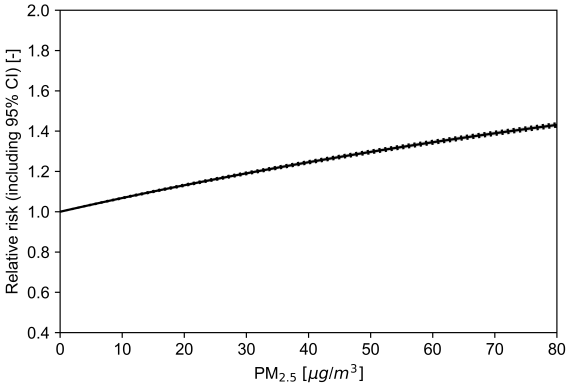

Figure S40: CRF for $PM_{2.5}$ showing the relative risk of all-cause mortality; proposed by Di et al. [25], using a multi-pollutant model. The shaded area shows the 95% confidence interval.

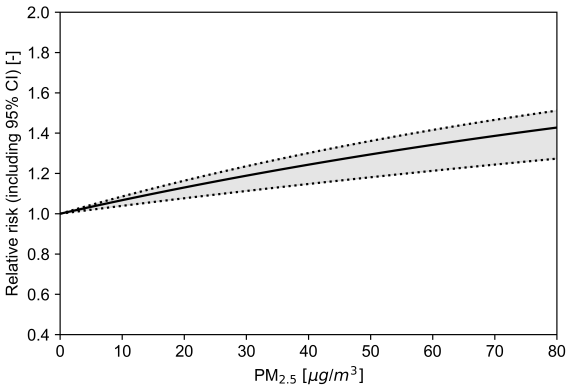

Figure S41: CRF for $PM_{2.5}$ showing the relative risk of all-cause mortality; proposed by Janssen et al. [28]. The shaded area shows the 95% confidence interval.

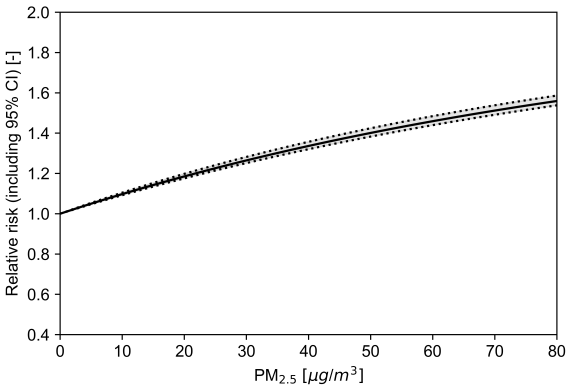

Figure S42: CRF for $PM_{2.5}$ showing the relative risk of all-cause mortality; proposed by Vodonos et al. [29]. The shaded area shows the 95% confidence interval.

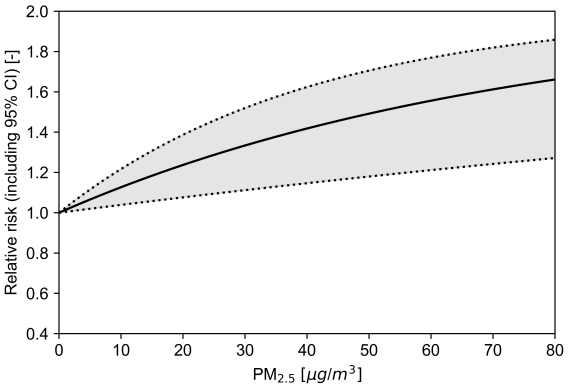

Figure S43: CRF for $PM_{2.5}$ showing the relative risk of all-cause mortality; proposed by Beelen et al. [23]. The shaded area shows the 95% confidence interval.

SI 4.4.4. Concentration response functions for BC

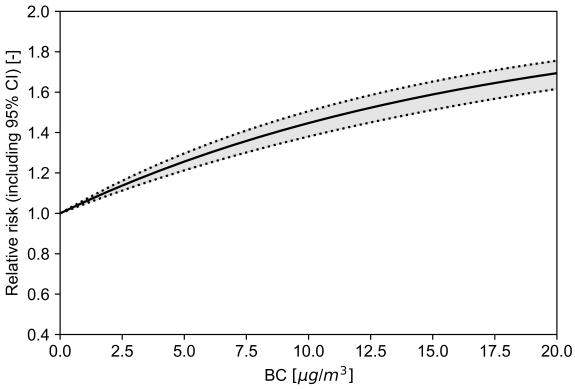

Figure S44: CRF for BC showing the relative risk of all-cause mortality; proposed by Hoek et al. [20]. The shaded area shows the 95% confidence interval.

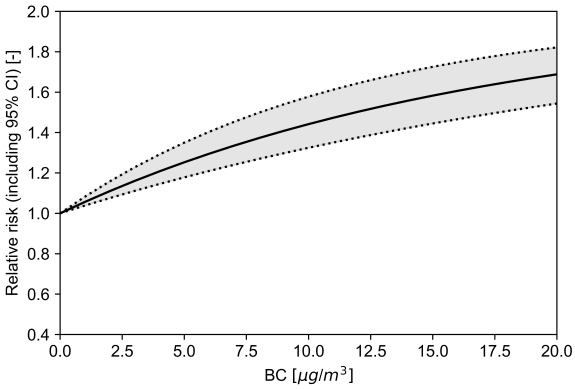

Figure S45: CRF for BC showing the relative risk of all-cause mortality; proposed by Janssen et al. [28]. The shaded area shows the 95% confidence interval.

SI 5. openAVEM results

This chapter provides additional detailed emission estimates supporting the findings in the main paper. In section SI 5.1, the emission estimates by openAVEM are provided for all relevant aircraft categories, both in absolute terms and as a percentage of all aviation emissions. A comparison of normalised emissions per RPK or passenger can be found in section SI 5.2. Finally, a sensitivity analysis on the effect of passenger load factor assumption is provided in section SI 5.3.

SI 5.1. Global emission estimates

Tables S20 to S33 show the number of flights, estimated fuel burn and associated emission estimates for each scenario used in this study.

Table S20: Number of flights and emissions for all flights in 2019.

Flights	Fuel [Tg]	NO_x [Gg]	CO [Gg]	HC [Gg]	nvPM [Mg]	nvPM [#]
42,212,442	295.90	4,610.81	760.06	40.88	9.65	3.47e26

Table S21: Total number of flights and emissions per category for various aircraft sizes.

Aircraft size	Flights	Fuel [Tg]	NO_x [Gg]	CO [Gg]	HC [Gg]	nvPM [Gg]	nvPM [#]
Piston	1,864,044	0.10	0.32	1,158	1.65	0.01	1.52e22
Business jets	2,304,317	3.25	32.33	32.29	4.89	0.18	3.98e24
Turboprop	4,437,477	3.12	30.37	19.21	3.68	0.11	1.82e23
Regional jets	5,585,107	12.65	141.25	49.98	2.71	0.32	9.17e24
Narrowbody	23,983,460	124.29	1,615.57	348.16	14.70	6.10	2.17e26
Widebody	4,038,037	152.49	2,790.97	194.59	13.24	2.92	1.17e26

Table S22: Relative number of flights and emissions per category for various aircraft sizes, as a percentage of all flights.

Aircraft size	Flights [%]	Fuel [%]	NO_x [%]	CO [%]	HC [%]	nvPM [%]	nvPM [% #]
Piston	4.4	0.03	0.01	15.24	4.05	0.14	0.01
Business jets	5.5	1.10	0.70	4.25	11.95	1.85	1.13
Turboprop	10.5	1.05	0.66	2.53	9.00	1.18	0.05
Regional jets	13.2	4.27	3.06	6.58	6.64	3.29	2.68
Narrowbody	56.8	42.00	35.04	45.81	35.97	63.22	60.32
Widebody	9.6	51.53	60.53	25.60	32.39	30.32	35.81

Table S23: Total number of flights and emissions per category for various flight distances.

Flight distance	Flights	Fuel [Tg]	NO_x [Gg]	CO [Gg]	HC [Gg]	nvPM [Gg]	nvPM [#]
Under 750 km	17,850,105	29.92	418.11	238.20	12.78	1.72	3.98e25
750 to 1,500 km	12,354,790	52.63	719.77	176.25	9.42	2.42	7.92e25
1,500 to 2,500 km	6,707,531	48.55	655.07	123.15	6.00	1.90	7.31e25
2,500 to 4,000 km	3,076,388	40.23	564.73	79.79	3.82	1.24	5.29e25
4,000 to 8,000 km	1,574,276	67.29	1,152.95	85.09	5.33	1.29	5.42e25
Over 8,000 km	649,352	57.28	1,100.17	57.58	3.53	1.09	4.79e25

Table S24: Relative number of flights and emissions per category for various flight distances, as a percentage of all flights.

Flight distance	Flights [%]	Fuel [%]	NO_x [%]	CO [%]	HC [%]	nvPM [%]	nvPM [% #]
Under 750 km	42.3	10.11	9.07	31.34	31.26	17.81	11.12
750 to 1,500 km	29.3	17.79	15.61	23.19	23.05	25.05	21.90
1,500 to 2,500 km	15.9	16.41	14.21	16.20	14.68	19.67	20.32
2,500 to 4,000 km	7.3	13.60	12.25	10.50	9.34	12.81	14.49
4,000 to 8,000 km	3.7	22.74	25.01	11.20	13.05	13.41	15.61
Over 8,000 km	1.5	19.36	23.86	7.58	8.63	11.25	13.80

Table S25: Total number of flights and emissions per aircraft size on shared short-haul routes.

Aircraft size	Flights	Fuel [Tg]	NO_x [Gg]	CO [Gg]	HC [Mg]	nvPM [Mg]	nvPM [#]
Turboprop	71,632	0.11	0.85	0.65	185.15	3.60	4.18e21
Regional jets	94,788	0.21	2.44	1.02	71.65	8.17	1.51e23
Narrowbody	226,739	0.72	9.88	2.65	124.74	41.56	1.20e24

Table S26: Total number of flights and emissions per aircraft size on shared medium-haul routes.

Aircraft size	Flights	Fuel [Tg]	NO_x [Gg]	CO [Gg]	HC [Gg]	nvPM [Gg]	nvPM [#]
Narrowbody	4,251,175	25.96	341.72	67.28	2.78	1.25	4.62e25
Widebody	1,625,477	27.24	492.82	48.75	3.55	0.54	1.82e25

Table S27: Relative number of flights and emissions per aircraft size on shared short-haul routes, as a percentage of all flights and emissions in this set.

Aircraft size	Flights [%]	Fuel [%]	NO_x [%]	CO [%]	HC [%]	nvPM [%]	nvPM [% #]
Turboprop	18.2	10.30	6.43	15.13	48.53	6.75	0.31
Regional jets	24.1	20.58	18.56	23.53	18.78	15.32	11.16
Narrowbody	57.7	69.12	75.01	61.34	32.69	77.94	88.53

Table S28: Relative number of flights and emissions per aircraft size on shared medium-haul routes, as a percentage of all flights and emissions in this set.

Aircraft size	Flights [%]	Fuel [%]	NO_x [%]	CO [%]	HC [%]	nvPM [%]	nvPM [% #]
Narrowbody	72.3	48.80	40.95	57.98	43.90	69.80	71.73
Widebody	27.7	51.20	59.05	42.02	56.10	30.20	28.27

Table S29: Total number of flights and emissions per aircraft age category on shared narrowbody routes.

Year of certification	Flights	Fuel [Tg]	NO_x [Gg]	CO [Gg]	HC [Gg]	nvPM [Mg]	nvPM [#]
1999 or before	3,190,251	19.38	263.76	50.50	2.15	854.66	2.99e25
2000 or later	1,007,831	6.54	94.64	15.35	0.66	85.92	4.36e24

Table S30: Total number of flights and emissions per aircraft age category on shared widebody routes.

Year of certification	Flights	Fuel [Tg]	NO_x [Gg]	CO [Gg]	HC [Gg]	nvPM [Mg]	nvPM [#]
1999 or before	470,291	11.04	200.73	13.50	0.74	174.51	8.33e24
2000 or later	263,290	7.36	148.52	9.87	0.36	167.93	8.44e24

Table S31: Relative number of flights and emissions per aircraft age category on shared narrowbody routes, as a percentage of all narrowbody flights and emissions on these routes.

Year of certification	Flights [%]	Fuel [%]	NO_x [%]	CO [%]	HC [%]	nvPM [%]	nvPM [% #]
1999 or before	76.0	74.76	73.59	76.69	76.48	90.87	87.26
2000 or later	24.0	25.24	26.41	23.31	23.52	9.13	12.74

Table S32: Relative number of flights and emissions per aircraft age category on shared widebody routes, as a percentage of all widebody flights and emissions on these routes.

Year of certification	Flights [%]	Fuel [%]	NO_x [%]	CO [%]	HC [%]	nvPM [%]	nvPM [% #]
1999 or before	64.1	59.99	57.47	57.75	67.69	50.96	49.68
2000 or later	35.9	40.01	42.53	42.25	32.31	49.04	50.32

Table S33: Number of flights and emissions of intra-European flights shorter than 750 km.

Flights	Fuel [Tg]	NO_x [Gg]	CO [Gg]	HC [Gg]	nvPM [Mg]	nvPM [#]
3,513,784	7.47	105.32	31.67	2.42	460.82	1.07e25

SI 5.2. Normalised emissions

In this section, the normalised emission estimates for each aircraft category in this study are shown. The darkly shaded bars indicate emissions per RPK, whereas the lightly shaded bars show the emissions per passenger. Please note the different scales between the left and right parts of the plots.

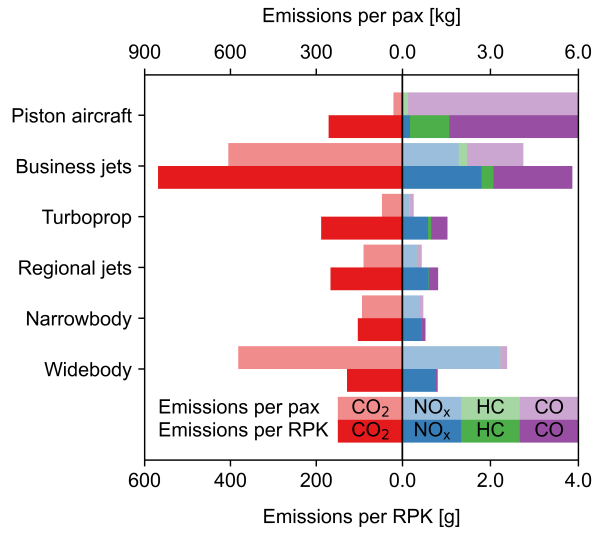

Figure S46: Emissions of CO_2, NO_x, HC and CO per passenger (top) and per RPK (bottom). Comparison between aircraft sizes.

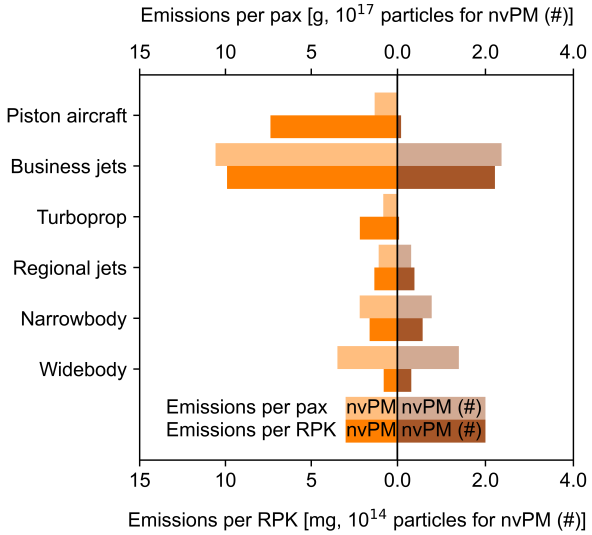

Figure S47: Emissions of BC (left: mass; right: particle number) per passenger (top) and per RPK (bottom). Comparison between aircraft sizes.

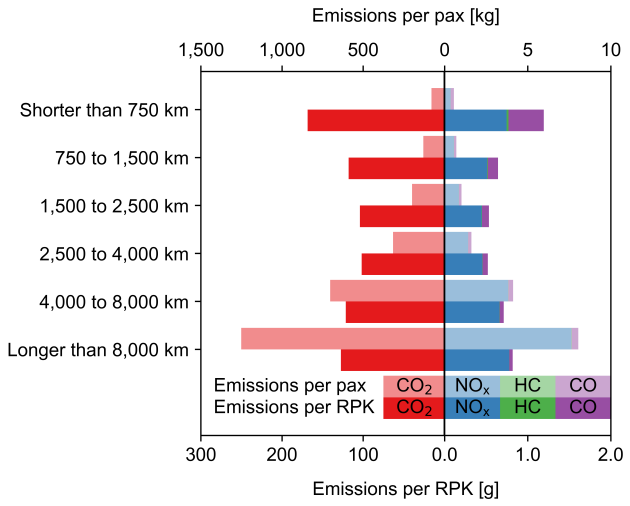

Figure S48: Emissions of CO_2, NO_x, HC and CO per passenger (top) and per RPK (bottom). Comparison between flight distances.

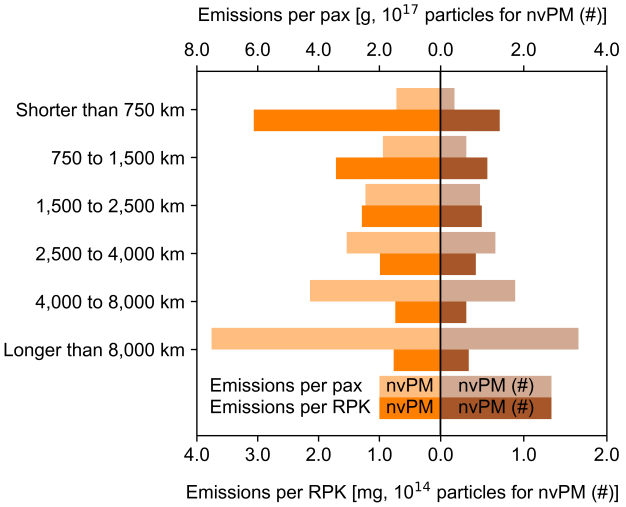

Figure S49: Emissions of BC (left: mass; right: particle number) per passenger (top) and per RPK (bottom). Comparison between flight distances.

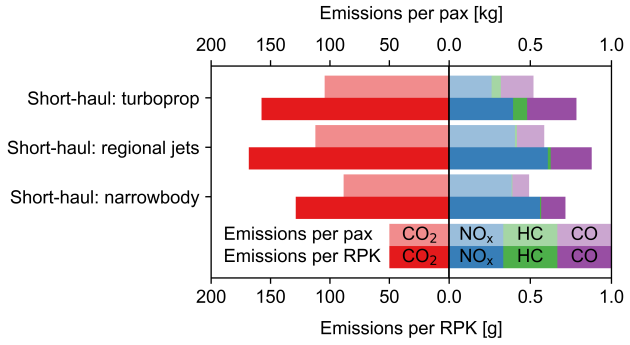

Figure S50: Emissions of CO_2, NO_x, HC and CO per passenger (top) and per RPK (bottom). Comparison between aircraft sizes on short-haul routes.

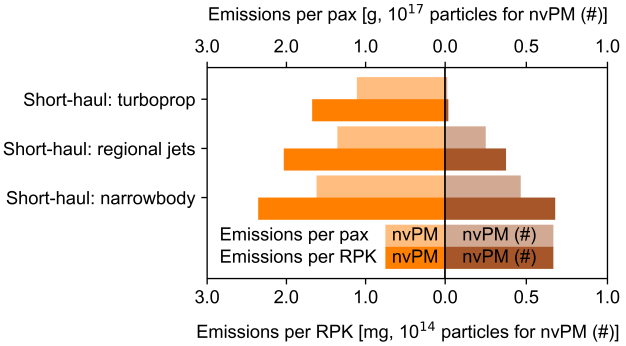

Figure S51: Emissions of BC (left: mass; right: particle number) per passenger (top) and per RPK (bottom). Comparison between aircraft sizes on short-haul routes.

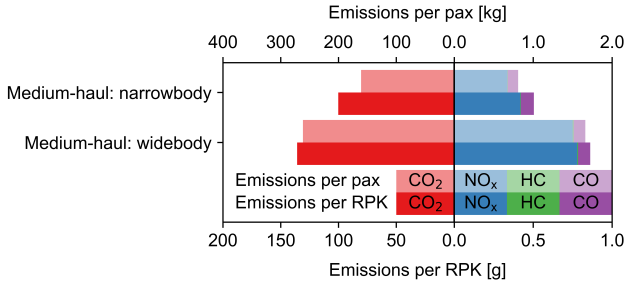

Figure S52: Emissions of CO_2, NO_x, HC and CO per passenger (top) and per RPK (bottom). Comparison between aircraft sizes on medium-haul routes.

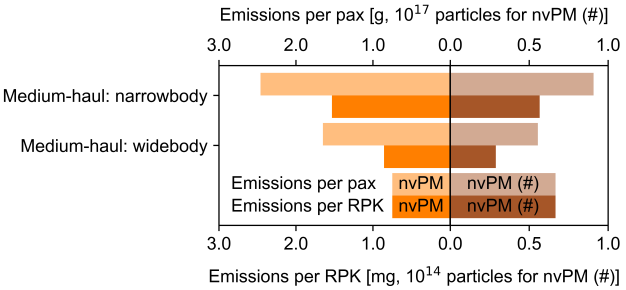

Figure S53: Emissions of BC (left: mass; right: particle number) per passenger (top) and per RPK (bottom). Comparison between aircraft sizes on medium-haul routes.

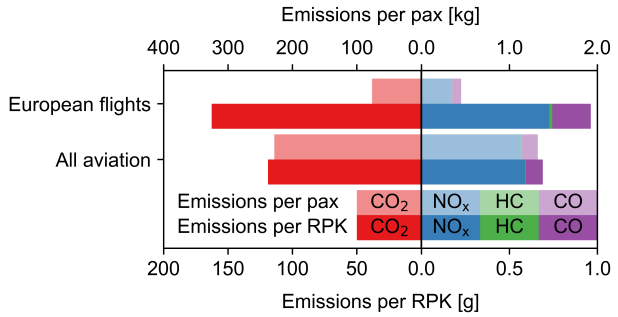

Figure S54: Emissions of CO_2, NO_x, HC and CO per passenger (top) and per RPK (bottom). Comparison between intra-European flights shorter than 750 km and the global average.

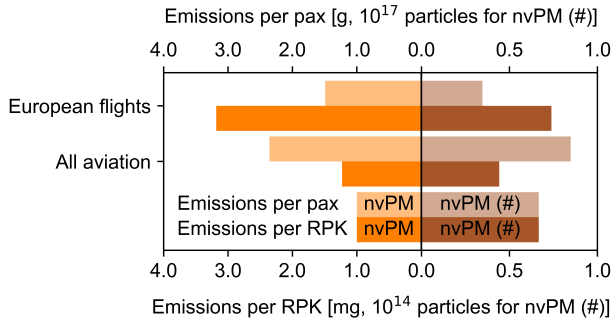

Figure S55: Emissions of BC (left: mass; right: particle number) per passenger (top) and per RPK (bottom). Comparison between intra-European flights shorter than 750 km and the global average.

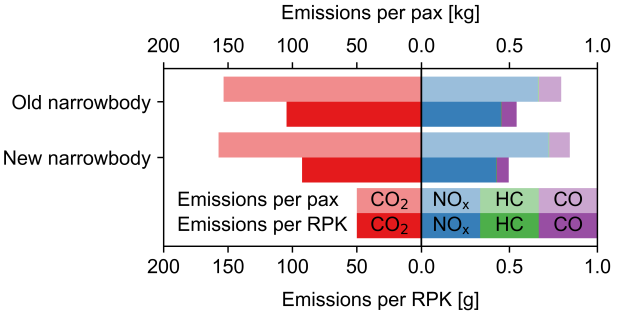

Figure S56: Emissions of CO_2, NO_x, HC and CO per passenger (top) and per RPK (bottom). Comparison between narrowbody aircraft initially certified before and after 1 January 2000.

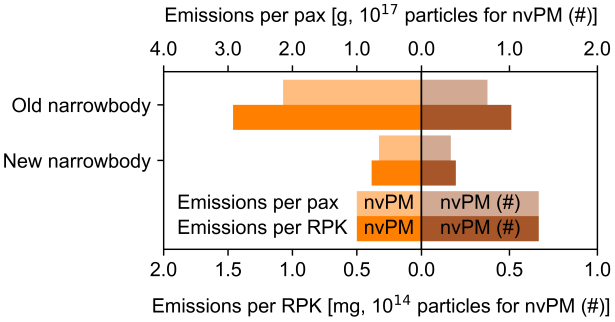

Figure S57: Emissions of BC (left: mass; right: particle number) per passenger (top) and per RPK (bottom). Comparison between narrowbody aircraft initially certified before and after 1 January 2000.

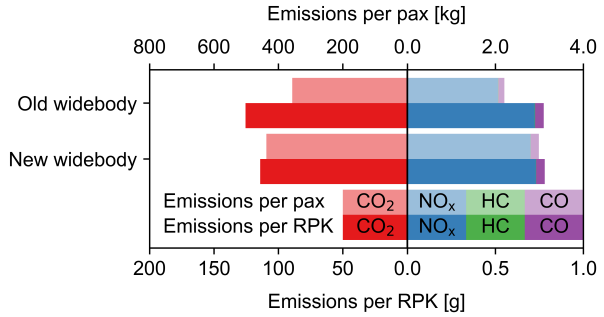

Figure S58: Emissions of CO_2, NO_x, HC and CO per passenger (top) and per RPK (bottom). Comparison between widebody aircraft initially certified before and after 1 January 2000.

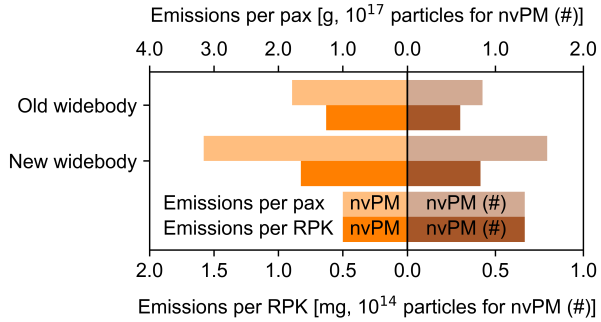

Figure S59: Emissions of BC (left: mass; right: particle number) per passenger (top) and per RPK (bottom). Comparison between widebody aircraft initially certified before and after 1 January 2000.

SI 5.3. Sensitivity towards load factor

Tables S34 to S41 show the sensitivity of the fuel burn and NO_x emission estimates towards a 10% change in passenger load factor with respect to the baseline of a 70% load factor. The results show a nearly proportional response, with the effects on NO_x emissions per RPK being smaller than on fuel burn. This means that the absolute emission estimates vary more with changed load factors than the fuel burn. This

can indicate higher thrust settings at higher load factors, thus yielding higher NO_x emission indices, and vice versa for lower thrust settings at reduced load factors.

Table S34: Sensitivity of fuel burn and NO_x emissions per RPK towards a 10% decrease (Low) or increase (High) in passenger load factor (LF) for all aviation.

Δ Fuel burn / RPK [%]		Δ NO_x emissions / RPK [%]	
Low LF	High LF	Low LF	High LF
10.02	-8.20	9.33	-7.63

Table S35: Sensitivity of fuel burn and NO_x emissions per RPK towards a 10% decrease (Low) or increase (High) in passenger load factor (LF) for various aircraft sizes.

	Δ Fuel burn / RPK [%]		Δ NO_x emissions / RPK [%]	
Aircraft size	Low LF	High LF	Low LF	High LF
Piston	10.74	-8.76	10.50	-8.56
Business jets	10.83	-8.85	10.66	-8.71
Turboprop	10.41	-8.50	9.91	-8.06
Regional jets	10.08	-8.23	9.56	-7.80
Narrowbody	9.87	-8.06	9.15	-7.45
Widebody	10.12	-8.30	9.40	-7.71

Table S36: Sensitivity of fuel burn and NO_x emissions per RPK towards a 10% decrease (Low) or increase (High) in passenger load factor (LF) for various flight distances.

	Δ Fuel burn / RPK [%]		Δ NO_x emissions / RPK [%]	
Flight distance	Low LF	High LF	Low LF	High LF
Under 750 km	10.05	-8.20	9.49	-7.71
750 to 1,500 km	9.90	-8.08	9.23	-7.51
1,500 to 2,500 km	9.90	-8.09	9.17	-7.48
2,500 to 4,000 km	9.93	-8.11	9.16	-7.47
4,000 to 8,000 km	10.05	-8.23	9.24	-7.56
Over 8,000 km	10.27	-8.44	9.60	-7.92

Table S37: Sensitivity of fuel burn and NO_x emissions per RPK towards a 10% decrease (Low) or increase (High) in passenger load factor (LF) per aircraft size on shared short-haul routes.

	Δ Fuel burn / RPK [%]		Δ NO_x emissions / RPK [%]	
Aircraft size	Low LF	High LF	Low LF	High LF
Turboprop	10.37	-8.48	9.87	-8.04
Regional jets	10.02	-8.18	9.45	-7.69
Narrowbody	9.86	-8.04	9.22	-7.49

Table S38: Sensitivity of fuel burn and NO_x emissions per RPK towards a 10% decrease (Low) or increase (High) in passenger load factor (LF) per aircraft size on shared medium-haul routes.

	Δ Fuel burn / RPK [%]		Δ NO_x emissions / RPK [%]	
Aircraft size	Low LF	High LF	Low LF	High LF
Narrowbody	9.86	-8.06	9.12	-7.44
Widebody	10.00	-8.18	9.29	-7.58

Table S39: Sensitivity of fuel burn and NO_x emissions per RPK towards a 10% decrease (Low) or increase (High) in passenger load factor (LF) per aircraft age category on shared narrowbody routes.

	Δ Fuel burn / RPK [%]		Δ NO_x emissions / RPK [%]	
Year of certification	Low LF	High LF	Low LF	High LF
1999 or before	9.89	-8.08	9.17	-7.49
2000 or later	9.89	-8.08	9.12	-7.43

Table S40: Sensitivity of fuel burn and NO_x emissions per RPK towards a 10% decrease (Low) or increase (High) in passenger load factor (LF) per aircraft age category on shared widebody routes.

	Δ Fuel burn / RPK [%]		Δ NO_x emissions / RPK [%]	
Year of certification	Low LF	High LF	Low LF	High LF
1999 or before	10.07	-8.26	9.30	-7.63
2000 or later	9.98	-8.15	9.09	-7.40

Table S41: Sensitivity of fuel burn and NO_x emissions per RPK towards a 10% decrease (Low) or increase (High) in passenger load factor (LF) for intra-European flights shorter than 750 km.

Δ Fuel burn / RPK [%]		Δ NO_x emissions / RPK [%]	
Low LF	High LF	Low LF	High LF
10.02	-8.17	9.46	-7.69

SI 6. GEOS-Chem results

This chapter provides more detailed results for the air quality impacts of the aircraft categories used in the main study. First, section SI 6.1 presents a general discussion on the impact of aircraft categories on air quality. Then, supporting data is presented in the subsequent sections. In section SI 6.2, temporal trends are visualised for both background concentrations and aviation-related impacts for the main categories. In section SI 6.3, the yearly averaged concentration changes are visualised for all simulations, while details regarding population-weighted concentrations (and various related metrics) are provided in section SI 6.4.

SI 6.1. Air quality impacts per aircraft category

This section discusses the air quality impacts of various aircraft categories. First, the impacts of aircraft size are evaluated in subsection SI 6.1.1. Then, subsection SI 6.1.2 discusses the impacts of flight distance.

SI 6.1.1. Effects of aircraft size on air quality impacts

Our results show that the global aviation-attributable changes to population-weighted ground-level concentrations of NO_2 are predominantly negative, but that smaller aircraft have a positive impact. In South America and Oceania, however, such positive impacts are observed for all aircraft sizes (see section SI 6.3 for more details). Global results are largely driven by the negative contribution of widebody aircraft in Asia, while the impact of small aircraft is negligible, with the exception of business jets in North America. The effects on O_3 concentrations are more diffused and positive in all regions, with the largest impact found in Asia. Globally, we find that over 90% of the increase in O_3 levels is associated with narrowbody and widebody emissions.

In figure S60, the impacts of small aircraft are amplified by the normalisation with respect to RPKs. The absolute impact per RPK is smallest for narrowbody aircraft, both for NO_2 and O_3, while widebody aircraft have the largest absolute impacts of all commercial aircraft types. This remains when the results are analysed per passenger, with business jets and widebody aircraft both yielding O_3 impacts which are an order of magnitude larger than for other aircraft types. Turboprop and piston aircraft, on the other hand, show limited impact in all regions except Oceania.

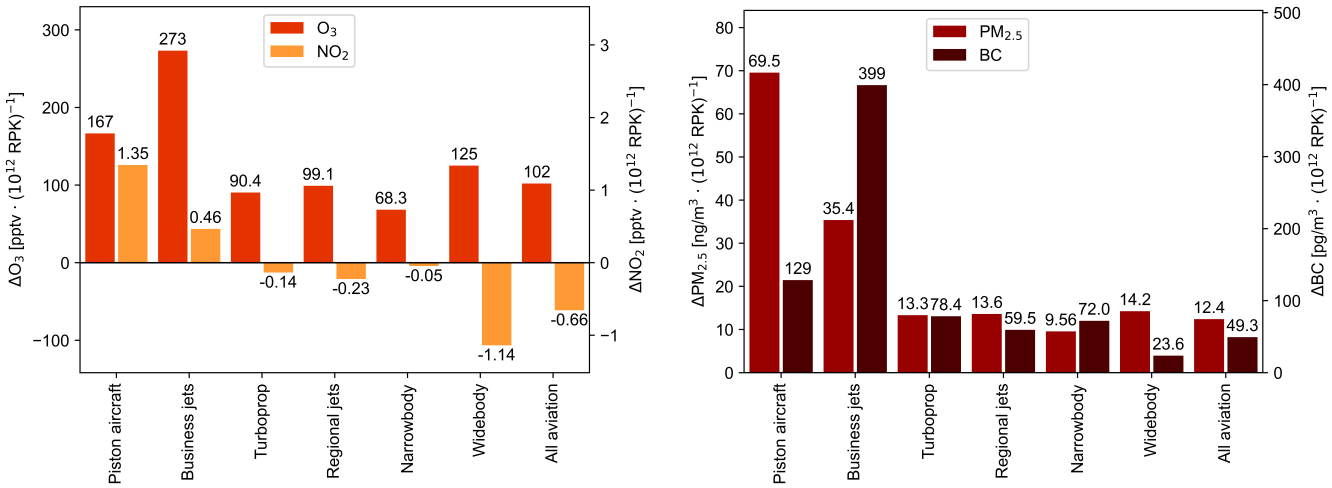

Figure S60: Aviation-attributable population-weighted concentration change in O_3 and NO_2 (left) and $PM_{2.5}$ and BC (right) per 10^{12} RPK for each aircraft size.

For both NO_2 and O_3, the sensitivity towards NO_x emissions is largest for piston aircraft in all regions. Generally, the sensitivity towards emissions of turboprop and narrowbody aircraft is limited when compared to other aircraft types, but large regional variations exist. The sensitivity of ground-level O_3 and NO_2 concentrations towards aviation NO_x emissions is largest in Asia, while it is most limited in North America and Oceania.

In most regions, aviation-attributable changes in $PM_{2.5}$ concentrations follow the trends of O_3 impacts, such that globally around 55% of all additional population-weighted $PM_{2.5}$ is associated with widebody aircraft. In the Americas, however, narrowbody aircraft show a larger relative impact compared to their effects on O_3. This aircraft type is also associated with the majority (≈ 70%) of global aviation-induced BC exposure. Especially in North America, business and regional jets are also strongly associated with increased BC concentrations. Figure S60 shows that globally, business jets have the largest impact on BC concentrations when normalised per RPK, while widebody aircraft have the smallest effect. For $PM_{2.5}$, the normalised impacts of piston aircraft are approximately twice as large as those of business jets, with other aircraft types showing an impact which is five to seven times smaller.

Globally, the impact on population-weighted concentration of $PM_{2.5}$ per passenger is smallest for turboprop aircraft. In general, both business jets and widebody aircraft show a larger impact than other aircraft types. This also holds for the impact on exposure to BC, but narrowbody aircraft show similar impacts as widebody aircraft. However, both impacts on $PM_{2.5}$ and BC show large regional variations, which are also affected by cross-regional transportation (and in case of $PM_{2.5}$, the formation of secondary aerosols).

Scaled for regional aviation NO_x emissions, the sensitivity of $PM_{2.5}$ is largest in Asia and Europe, while the effects are most limited in Oceania. In various regions, the sensitivity to emissions by piston aircraft is two orders of magnitude larger than for other aircraft types; globally, a factor 20 difference is observed.

The results from the case studies are presented in figure S61. On shared short-haul routes, the absolute impact of regional jets is largest when results are normalised per RPK. It is also the only aircraft type that shows a reduction in ground-level NO_2 concentrations due to aviation.

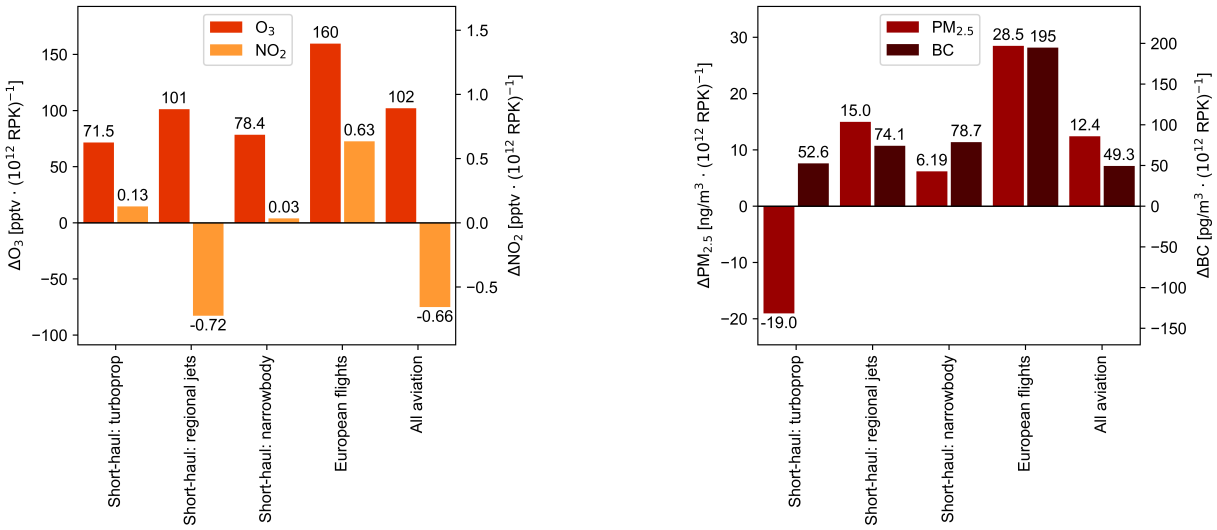

Figure S61: Aviation-attributable population-weighted concentration change in O_3 and NO_2 (left) and $PM_{2.5}$ and BC (right) per 10^{12} RPK for short-haul flights.

Figure S61 shows that the impact of turboprop aircraft is smaller than that of regional jets or narrowbody aircraft when they are compared on similar routes. Compared to the global fleet average, these relatively short routes yield higher BC impacts for all aircraft types shown in figure S61, while only regional jets exceed the average impact on $PM_{2.5}$.

Finally, some discrepancies are noticed when the summed impacts of the individual aircraft categories are compared to the impact of all aviation, showing signs of non-linear atmospheric responses. Especially the effects on NO_2 concentrations seem difficult to capture, with regional overestimations of 15% in North America and underestimations of 18% in Europe when the summed results of smaller data sets are compared to those of all aviation. For other species, we find weaker, but consistent underestimation of results. For O_3, the summed effects are underestimated by approximately 5%, rather consistently amongst regions. While the results for BC match to within 0.1% for all regions, $PM_{2.5}$ is mostly underestimated from summed datasets in regions with high aviation activity. In the Northern Hemisphere, the underestimations

vary from 1.8% in North America to 3.5% in Europe, while discrepancies in the Southern Hemisphere stay within 1%.

SI 6.1.2. Effects of flight distance on air quality impacts

The impacts of aviation emissions on ground-level NO_2 as shown in figure S62 follow the expected trends: cruise emissions reduce ground-level NO_2 concentrations, while LTO operations yield local increases [30–33]. Since the LTO phase becomes less relevant as the flight distance increases, the overall impact turns more negative for longer flights. This trend is visible both in absolute exposure changes as well as results normalised per RPK. The normalised effects on ground-level O_3 concentrations are minimum for medium-haul flights, while figure S62 shows larger impacts for both short and long-haul flights. This is in line with general fuel efficiency trends observed in previous studies [1, 2]. Most impacts are found in Europe and Asia, with very limited effects observed in the Southern Hemisphere.

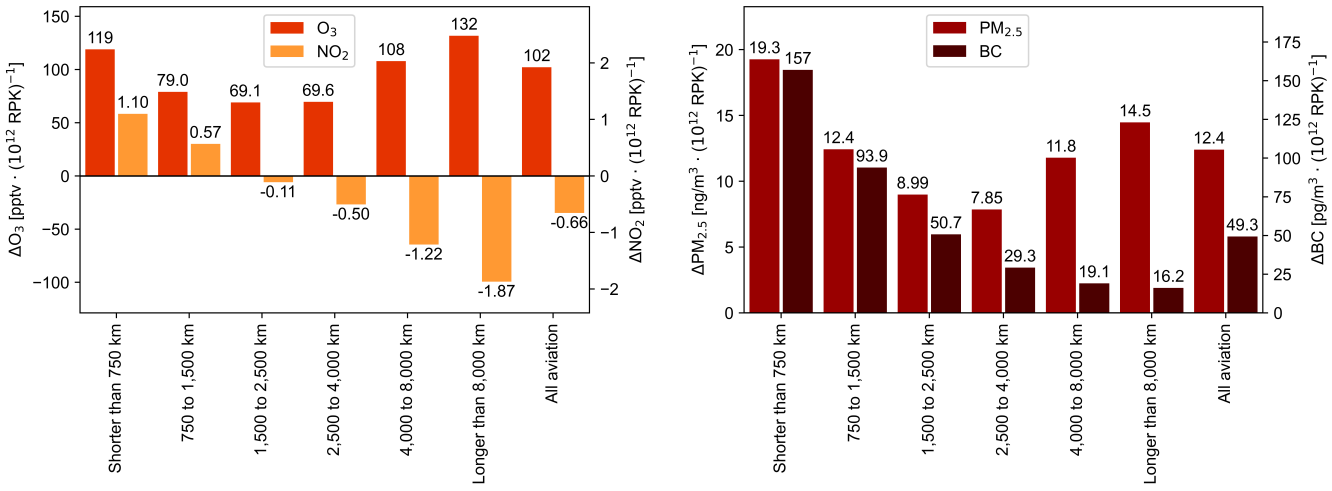

Figure S62: Aviation-attributable population-weighted concentration change in O_3 and NO_2 (left) and $PM_{2.5}$ and BC (right) per 10^{12} RPK for each flight distance.

As shown in figure S61, intra-European flights shorter than 750 km affect ground-level O_3 concentrations up to 57% more than the global average when compared on a per RPK basis. Compared to global flights shorter than 750 km (see figure S62), these European flights show a 34% larger impact on O_3 levels, but a 43% smaller effect on NO_2 concentrations.

After scaling for regional NO_x emissions, the observed trends remain: short flights generally increase NO_2 concentrations the most, while long-haul yields the strongest reduction in ground-level NO_2. Sensitivities within regions vary based on the flight distance, but the accumulated effect sensitivity is smallest in North America (showing a positive impact) and largest in Asia (yielding a negative effect). Although population-weighted concentration of O_3 tends to be slightly more sensitive towards long-haul flight NO_x emissions, large inter-regional heterogeneity in the sensitivity was observed.

The aviation-attributable increases in ground-level $PM_{2.5}$ of long-haul flights (over 4,000 km) account for almost half of the total observed impacts. However, when results are normalised per RPK, figure S62 shows that the trend follows the O_3 impacts previously shown in the left panel of figure S62. For BC, this is not the case: normalised concentration changes due to ultra short-haul flights are up to an order of magnitude larger than for ultra long-haul flights. This agrees with the smaller number of LTO operations performed by aircraft flying long distances, as was shown in section SI 5.1.

Globally, the sensitivity of ground-level $PM_{2.5}$ towards aviation NO_x emissions is smaller for long-haul flights compared to shorter flights. However, when regional results are considered, the regions in the Northern Hemisphere show the smallest impact for medium-haul flights, indicating that separating regional impacts affects the interpretation of results. For BC, this is not the case: a monotonic decrease in sensitivity is found for increasing flight distance, with a small exception for Africa and the Middle-East. This might be an artefact of the modeling method: a large number of ultra long-haul flights take off or land in this region,

but only limited full-flight emissions occur within the boundaries of this region, as these flights are usually operated by Gulf State airlines flying to Europe or Asia. Thus, part of the NO_x emissions related to these flights are not accounted for, yielding larger impacts after normalisation with respect to these emissions.

Short-haul intra-European flights, however, show a significantly larger impact per RPK than the global average for both BC and $PM_{2.5}$ in general. Figure S61 shows a 48% higher impact on general $PM_{2.5}$ and a 24% larger effect on BC concentrations for intra-European flights compared to global flights shorter than 750 km (as shown in figure S62).

We find that aggregating the results from the individual flight distance categories yields larger discrepancies towards the effect of all aviation than doing so for the different aircraft sizes. For NO_2, global impacts are underestimated by almost 20%, while large regional variations exist (from 28% underestimation in Europe to 23% overestimation in North America). For O_3 and $PM_{2.5}$, we also observe larger underestimations for combined results based on flight distance than for those based on aircraft size. For BC, however, no significant bias seems to be present, with only minimal (< 0.1%) negative (in North America and Europe) or positive deviations (in all other regions).

SI 6.2. Temporal evolution of global species concentrations

This section shows the temporal patterns of ground-level concentration changes due to individual aircraft categories for all evaluated pollutants. Atmospheric background levels (denoted as 'baseline') are also shown to provide a perspective on the relative impact of aviation.

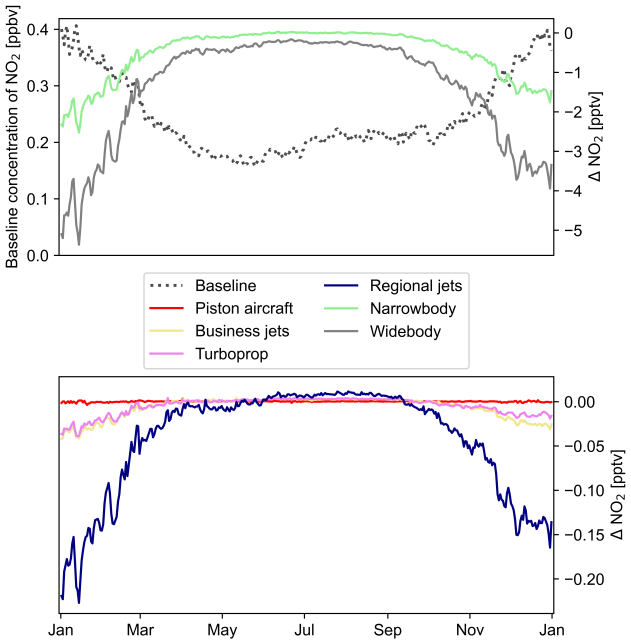

Figure S63: Global population-weighted aviation-attributable concentration change of NO_2 per aircraft size. The dashed line shows the baseline population-weighted NO_2 concentration.

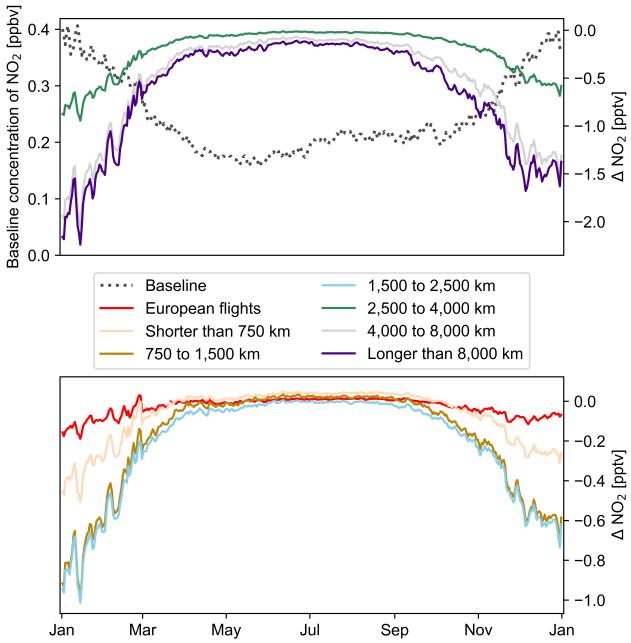

Figure S64: Global population-weighted aviation-attributable concentration change of NO_2 per flight distance. The dashed line shows the baseline population-weighted NO_2 concentration.

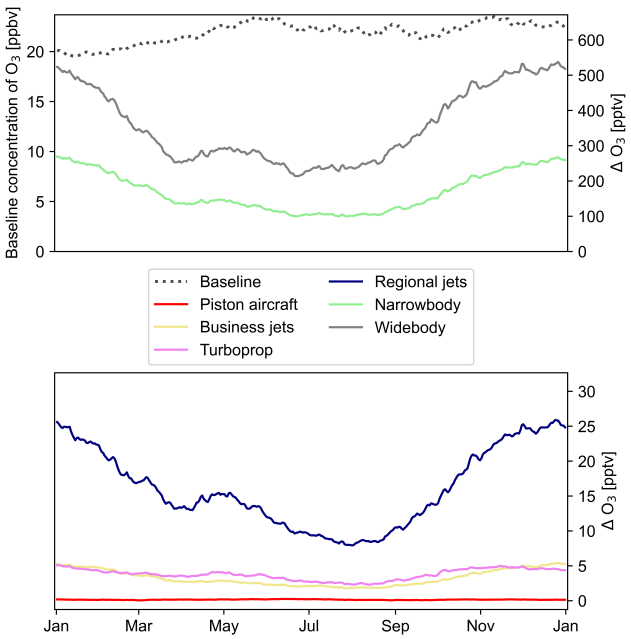

Figure S65: Global population-weighted aviation-attributable concentration change of O_3 per aircraft size. The dashed line shows the baseline population-weighted O_3 concentration.

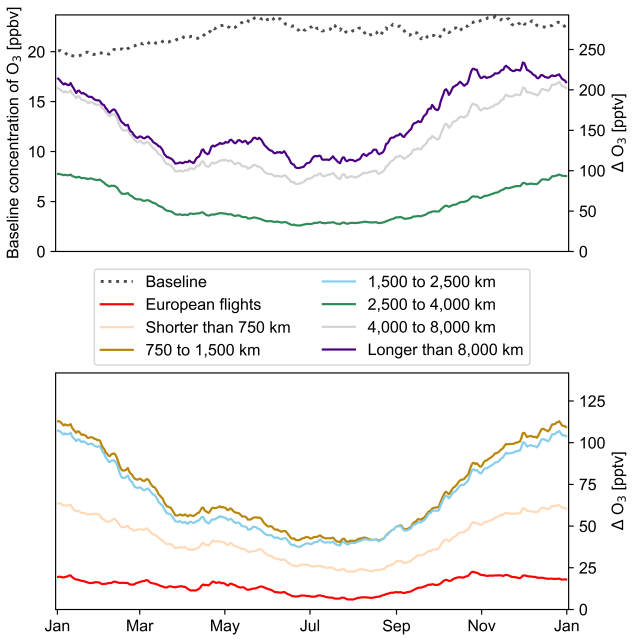

Figure S66: Global population-weighted aviation-attributable concentration change of O_3 per flight distance. The dashed line shows the baseline population-weighted O_3 concentration.

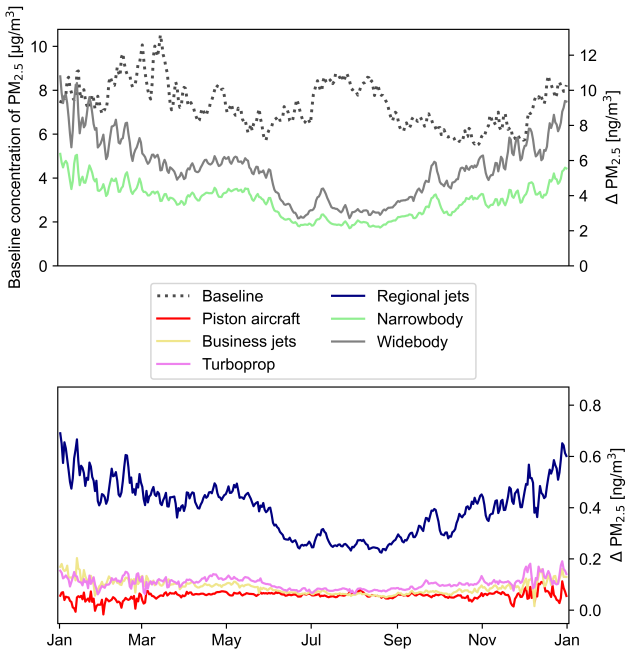

Figure S67: Global population-weighted aviation-attributable concentration change of $PM_{2.5}$ per aircraft size. The dashed line shows the baseline population-weighted $PM_{2.5}$ concentration.

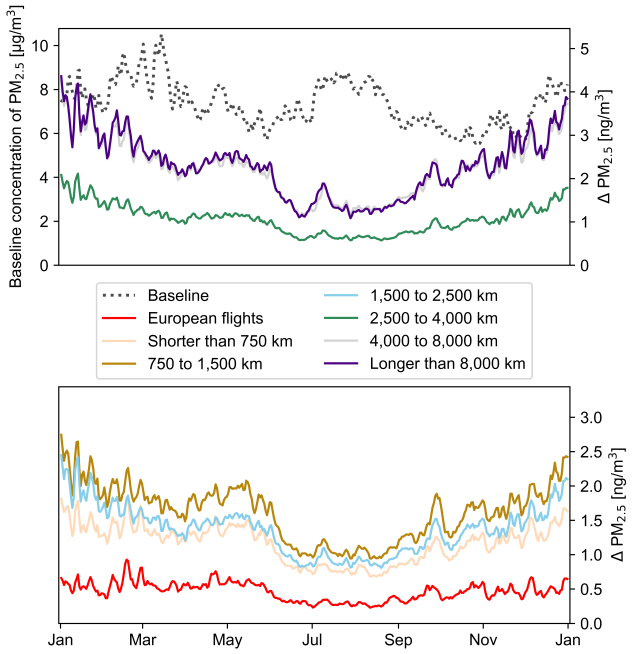

Figure S68: Global population-weighted aviation-attributable concentration change of $PM_{2.5}$ per flight distance. The dashed line shows the baseline population-weighted $PM_{2.5}$ concentration.

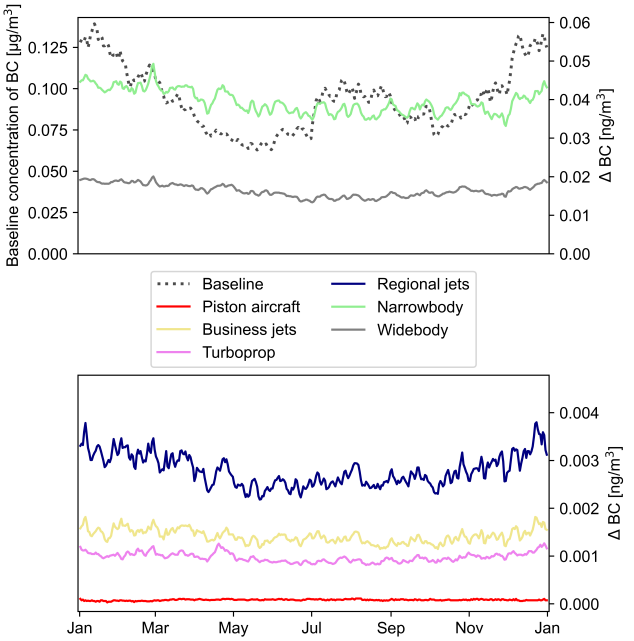

Figure S69: Global population-weighted aviation-attributable concentration change of BC per aircraft size. The dashed line shows the baseline population-weighted BC concentration.

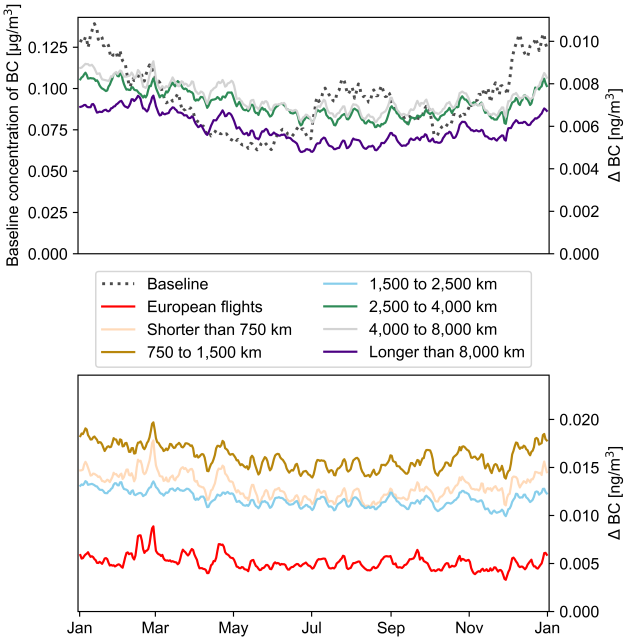

Figure S70: Global population-weighted aviation-attributable concentration change of BC per flight distance. The dashed line shows the baseline population-weighted BC concentration.

SI 6.3. Yearly averaged air quality impacts

This section provides the yearly averaged zonal mean and ground-level concentration changes of pollutants for each of the aircraft categories, with the total aviation impact shown first in subsection SI 6.3.1. Please note that colour scales differ between species and aircraft categories.

SI 6.3.1. All aviation

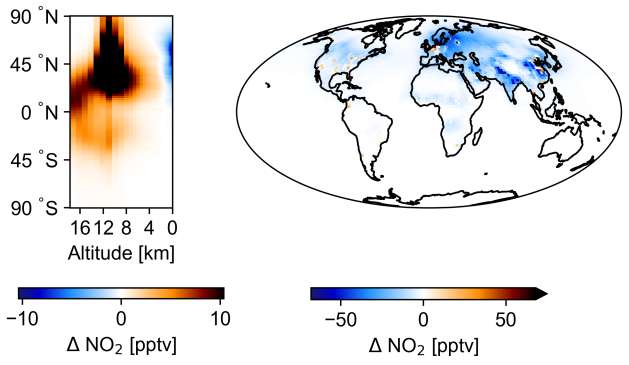

Figure S71: Yearly averaged changes in NO_2 concentrations due to all aviation, visualised through the change in zonal mean concentration (left) and ground-level concentration (right).

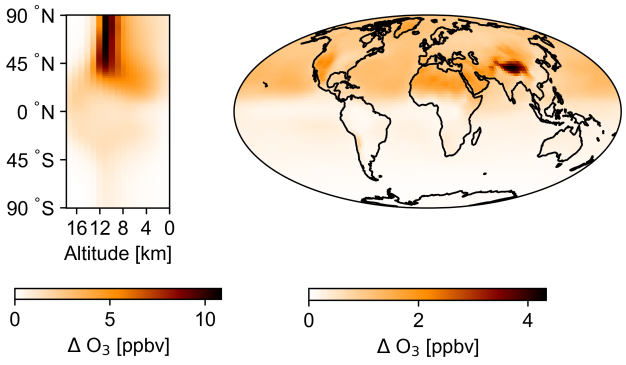

Figure S72: Yearly averaged changes in O_3 concentrations due to all aviation, visualised through the change in zonal mean concentration (left) and ground-level concentration (right).

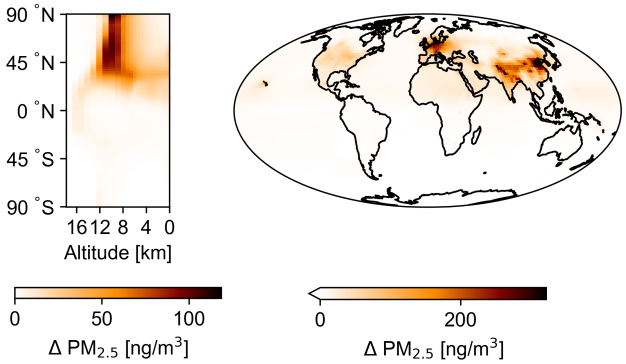

Figure S73: Yearly averaged changes in $PM_{2.5}$ concentrations due to all aviation, visualised through the change in zonal mean concentration (left) and ground-level concentration (right).

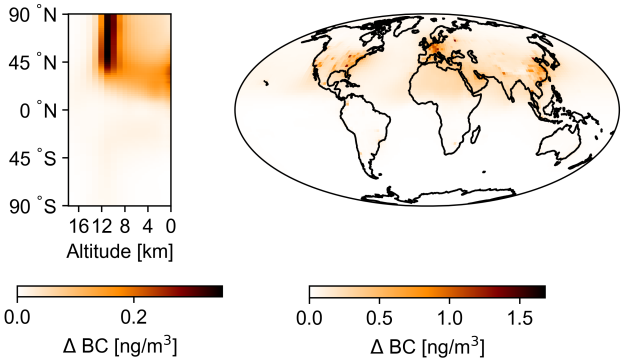

Figure S74: Yearly averaged changes in BC concentrations due to all aviation, visualised through the change in zonal mean concentration (left) and ground-level concentration (right).

SI 6.3.2. Comparison per aircraft size

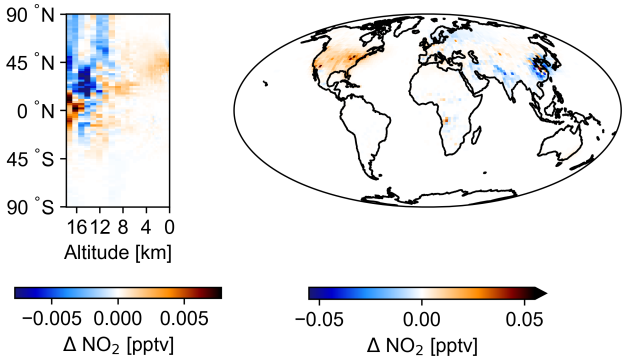

Figure S75: Yearly averaged changes in NO_2 concentrations due to piston aircraft, visualised through the change in zonal mean concentration (left) and ground-level concentration (right).

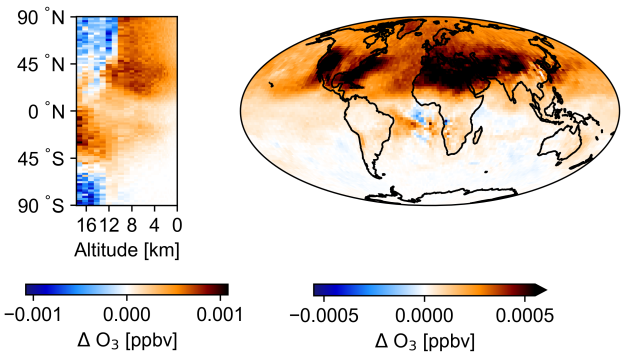

Figure S76: Yearly averaged changes in O_3 concentrations due to piston aircraft, visualised through the change in zonal mean concentration (left) and ground-level concentration (right).

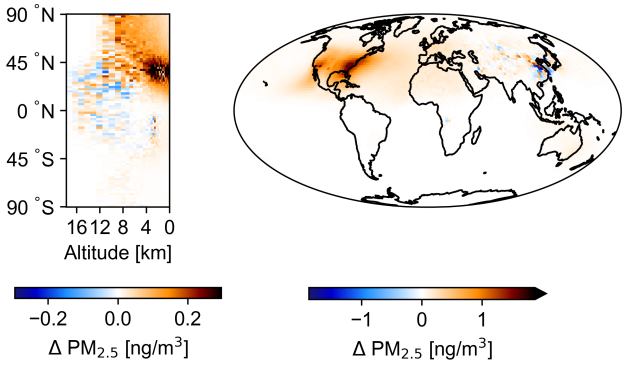

Figure S77: Yearly averaged changes in $PM_{2.5}$ concentrations due to piston aircraft, visualised through the change in zonal mean concentration (left) and ground-level concentration (right).

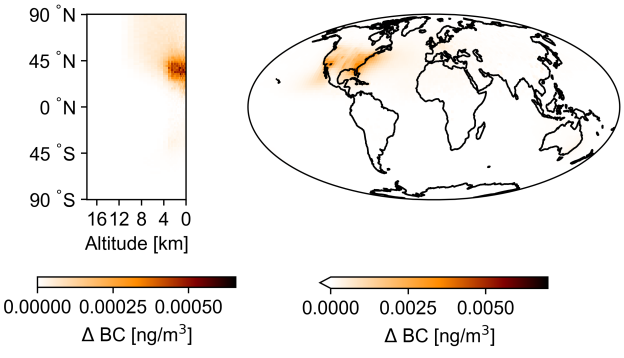

Figure S78: Yearly averaged changes in BC concentrations due to piston aircraft, visualised through the change in zonal mean concentration (left) and ground-level concentration (right).

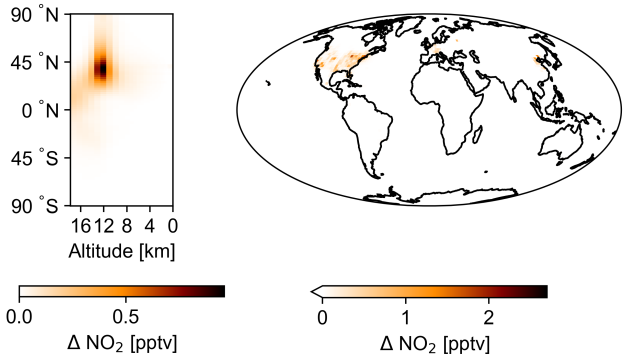

Figure S79: Yearly averaged changes in NO_2 concentrations due to business jets, visualised through the change in zonal mean concentration (left) and ground-level concentration (right).

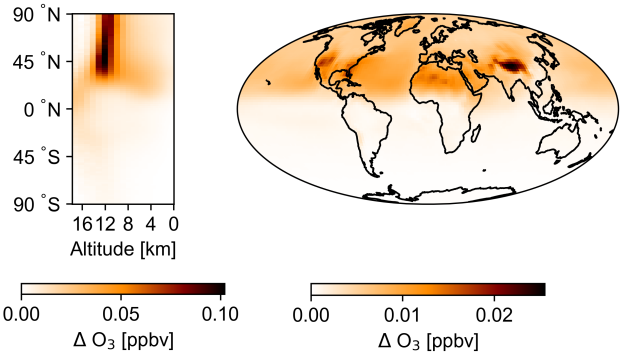

Figure S80: Yearly averaged changes in O_3 concentrations due to business jets, visualised through the change in zonal mean concentration (left) and ground-level concentration (right).

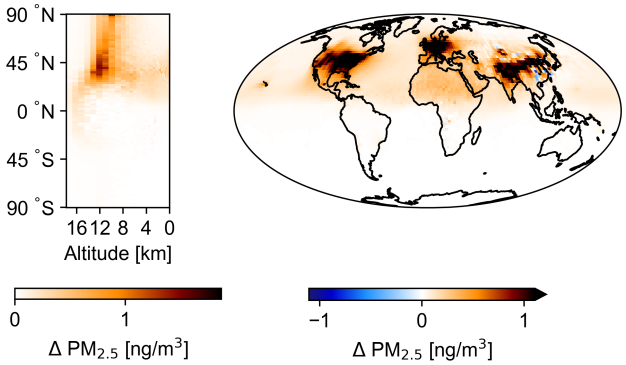

Figure S81: Yearly averaged changes in $PM_{2.5}$ concentrations due to business jets, visualised through the change in zonal mean concentration (left) and ground-level concentration (right).

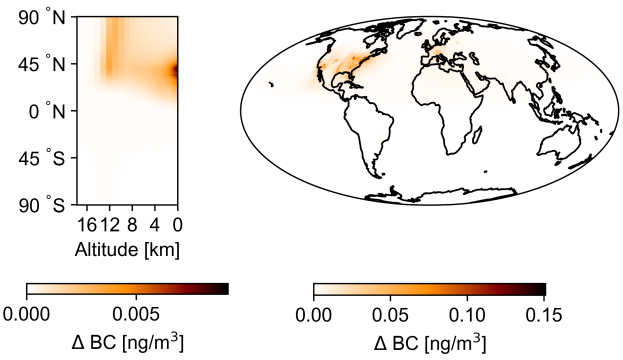

Figure S82: Yearly averaged changes in BC concentrations due to business jets, visualised through the change in zonal mean concentration (left) and ground-level concentration (right).

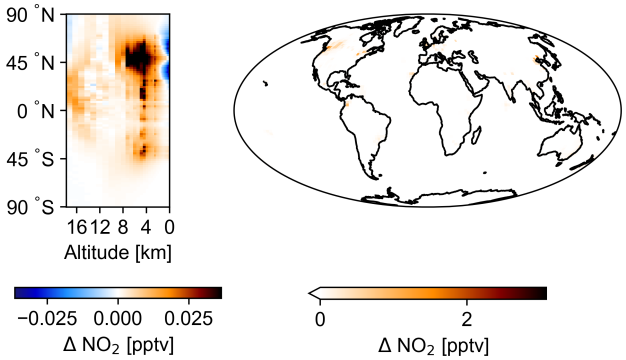

Figure S83: Yearly averaged changes in NO_2 concentrations due to turboprop aircraft, visualised through the change in zonal mean concentration (left) and ground-level concentration (right).

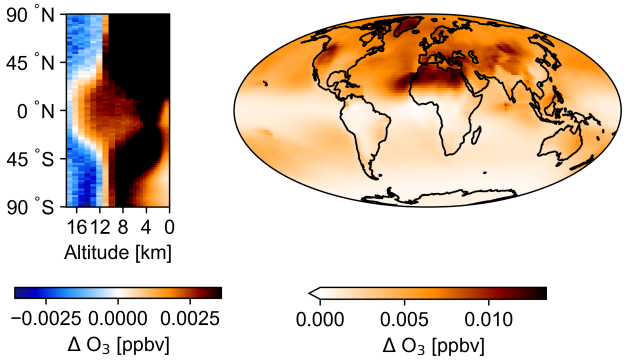

Figure S84: Yearly averaged changes in O_3 concentrations due to turboprop aircraft, visualised through the change in zonal mean concentration (left) and ground-level concentration (right).

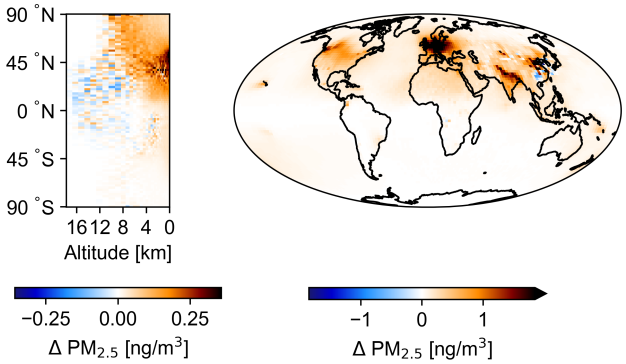

Figure S85: Yearly averaged changes in $PM_{2.5}$ concentrations due to turboprop aircraft, visualised through the change in zonal mean concentration (left) and ground-level concentration (right).

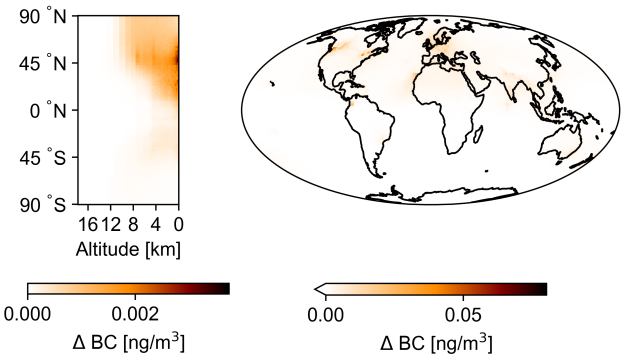

Figure S86: Yearly averaged changes in BC concentrations due to turboprop aircraft, visualised through the change in zonal mean concentration (left) and ground-level concentration (right).

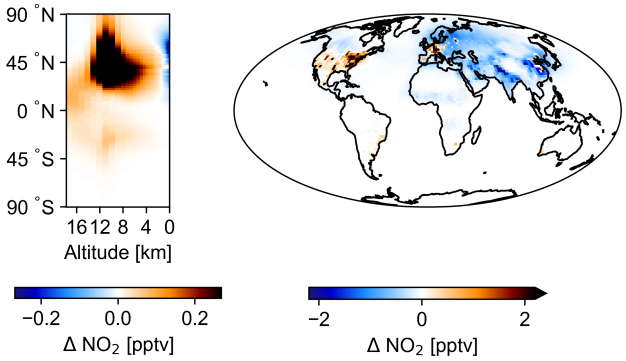

Figure S87: Yearly averaged changes in NO_2 concentrations due to regional jets, visualised through the change in zonal mean concentration (left) and ground-level concentration (right).

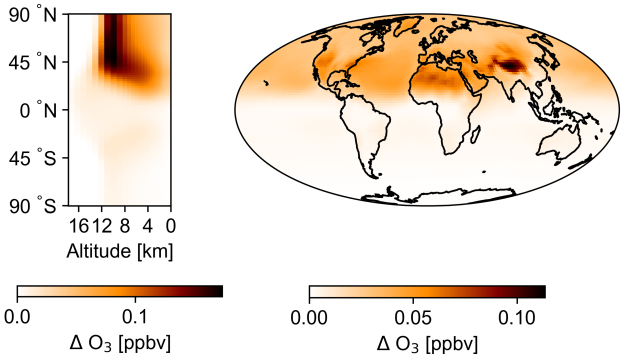

Figure S88: Yearly averaged changes in O_3 concentrations due to regional jets, visualised through the change in zonal mean concentration (left) and ground-level concentration (right).

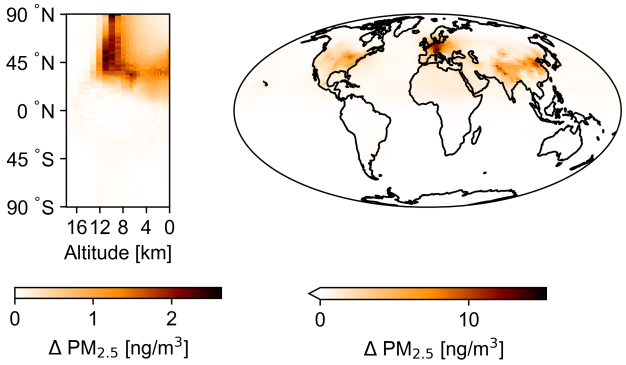

Figure S89: Yearly averaged changes in $PM_{2.5}$ concentrations due to regional jets, visualised through the change in zonal mean concentration (left) and ground-level concentration (right).

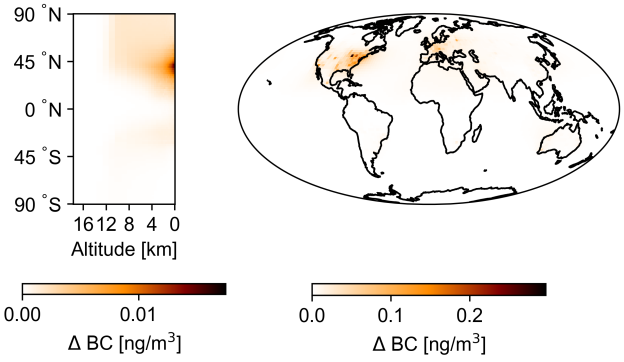

Figure S90: Yearly averaged changes in BC concentrations due to regional jets, visualised through the change in zonal mean concentration (left) and ground-level concentration (right).

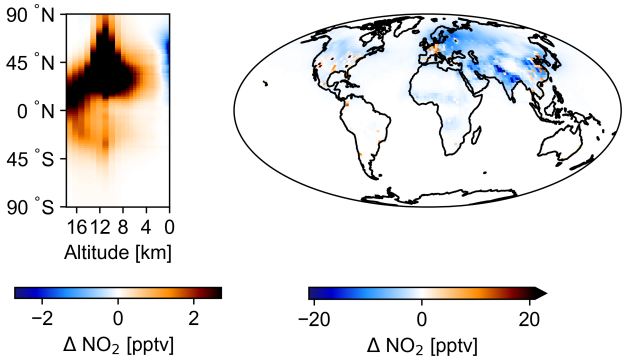

Figure S91: Yearly averaged changes in NO_2 concentrations due to narrowbody aircraft, visualised through the change in zonal mean concentration (left) and ground-level concentration (right).

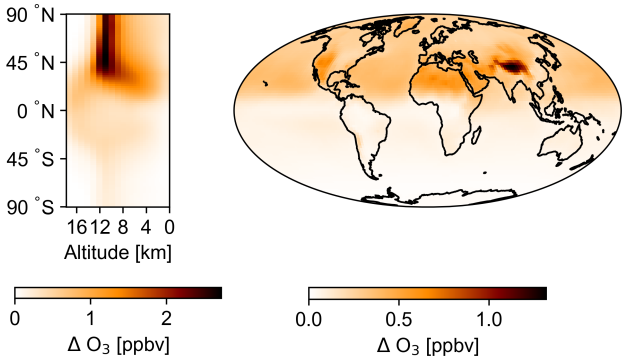

Figure S92: Yearly averaged changes in O_3 concentrations due to narrowbody aircraft, visualised through the change in zonal mean concentration (left) and ground-level concentration (right).

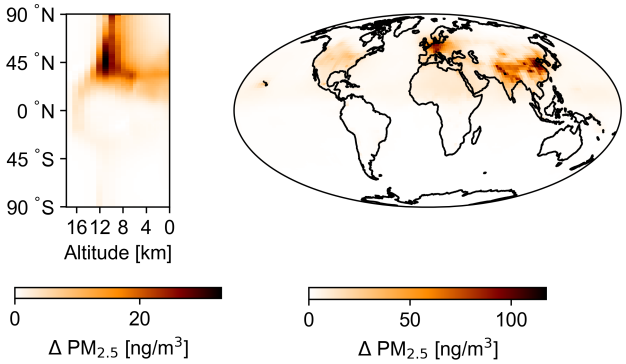

Figure S93: Yearly averaged changes in $PM_{2.5}$ concentrations due to narrowbody aircraft, visualised through the change in zonal mean concentration (left) and ground-level concentration (right).

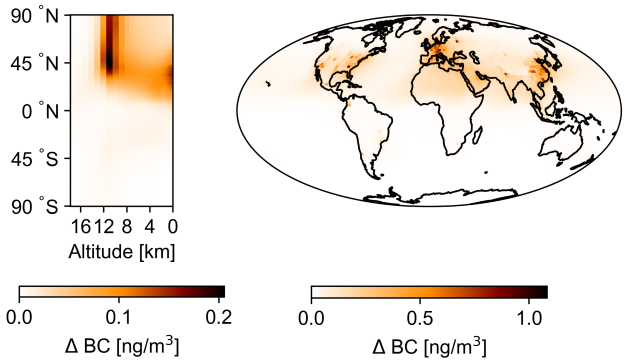

Figure S94: Yearly averaged changes in BC concentrations due to narrowbody aircraft, visualised through the change in zonal mean concentration (left) and ground-level concentration (right).

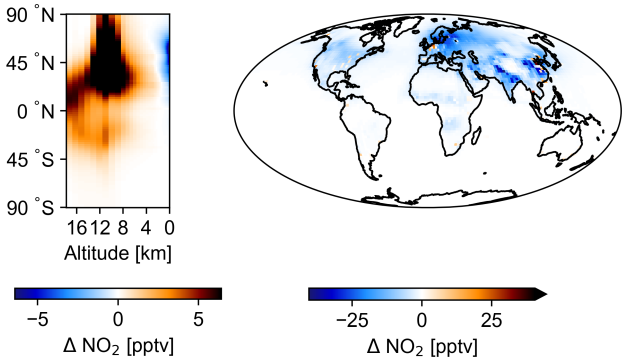

Figure S95: Yearly averaged changes in NO_2 concentrations due to widebody aircraft, visualised through the change in zonal mean concentration (left) and ground-level concentration (right).

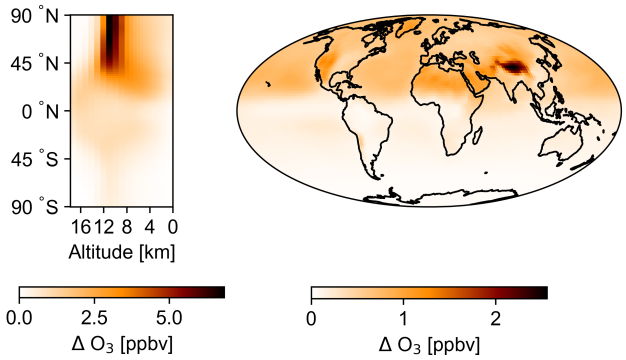

Figure S96: Yearly averaged changes in O_3 concentrations due to widebody aircraft, visualised through the change in zonal mean concentration (left) and ground-level concentration (right).

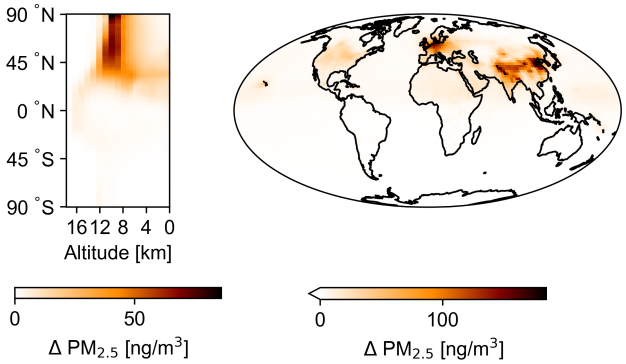

Figure S97: Yearly averaged changes in $PM_{2.5}$ concentrations due to widebody aircraft, visualised through the change in zonal mean concentration (left) and ground-level concentration (right).

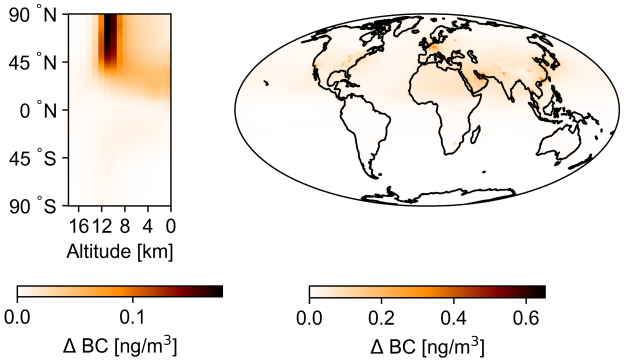

Figure S98: Yearly averaged changes in BC concentrations due to widebody aircraft, visualised through the change in zonal mean concentration (left) and ground-level concentration (right).

SI 6.3.3. Comparison per flight distance

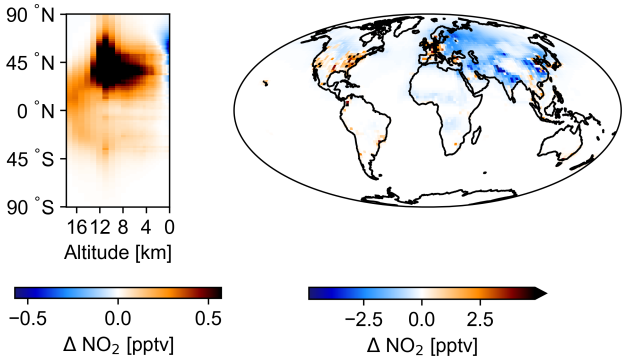

Figure S99: Yearly averaged changes in NO_2 concentrations due to flights shorter than 750 km, visualised through the change in zonal mean concentration (left) and ground-level concentration (right).

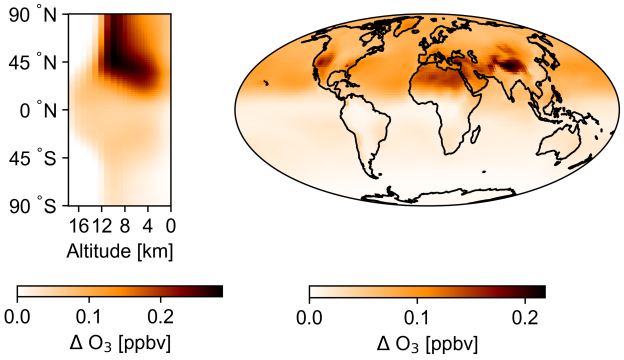

Figure S100: Yearly averaged changes in O_3 concentrations due to flights shorter than 750 km, visualised through the change in zonal mean concentration (left) and ground-level concentration (right).

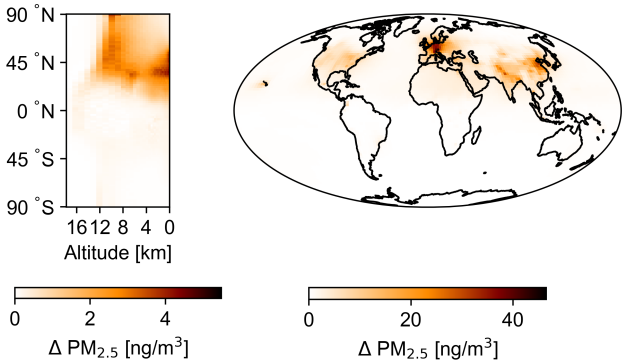

Figure S101: Yearly averaged changes in $PM_{2.5}$ concentrations due to flights shorter than 750 km, visualised through the change in zonal mean concentration (left) and ground-level concentration (right).

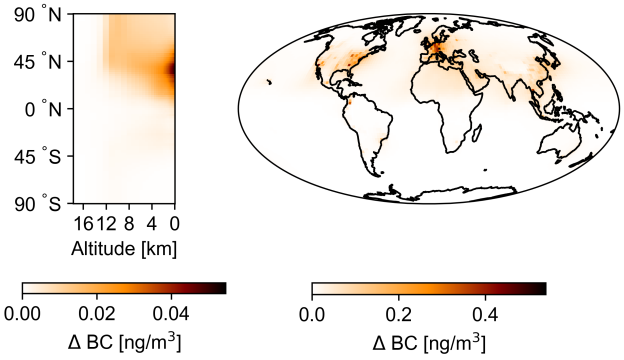

Figure S102: Yearly averaged changes in BC concentrations due to flights shorter than 750 km, visualised through the change in zonal mean concentration (left) and ground-level concentration (right).

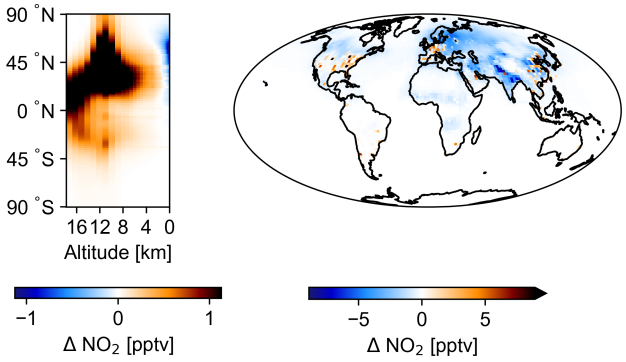

Figure S103: Yearly averaged changes in NO_2 concentrations due to flights of 750 to 1,500 km, visualised through the change in zonal mean concentration (left) and ground-level concentration (right).

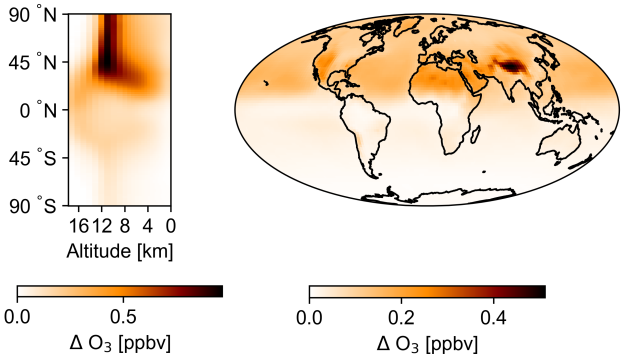

Figure S104: Yearly averaged changes in O_3 concentrations due to flights of 750 to 1,500 km, visualised through the change in zonal mean concentration (left) and ground-level concentration (right).

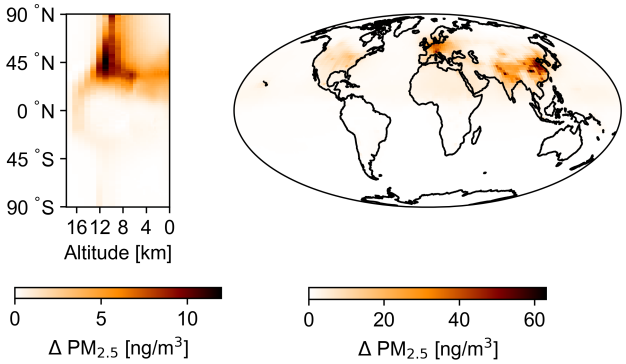

Figure S105: Yearly averaged changes in $PM_{2.5}$ concentrations due to flights of 750 to 1,500 km, visualised through the change in zonal mean concentration (left) and ground-level concentration (right).

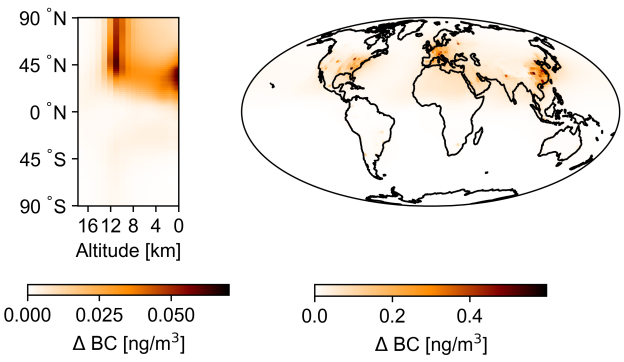

Figure S106: Yearly averaged changes in BC concentrations due to flights of 750 to 1,500 km, visualised through the change in zonal mean concentration (left) and ground-level concentration (right).

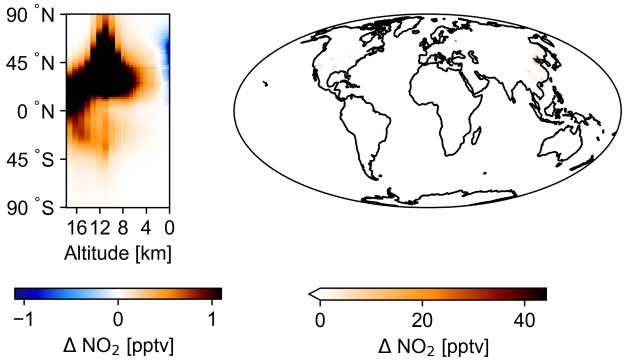

Figure S107: Yearly averaged changes in NO_2 concentrations due to flights of 1,500 to 2,500 km, visualised through the change in zonal mean concentration (left) and ground-level concentration (right).

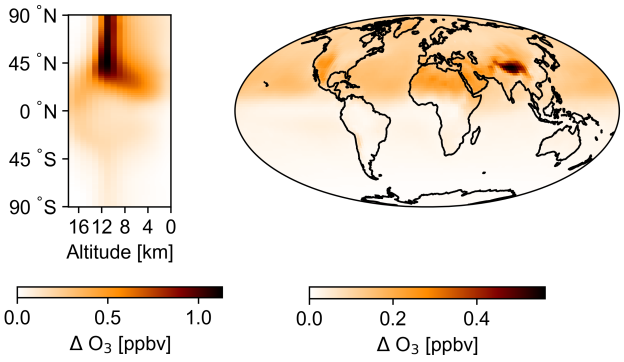

Figure S108: Yearly averaged changes in O_3 concentrations due to flights of 1,500 to 2,500 km, visualised through the change in zonal mean concentration (left) and ground-level concentration (right).

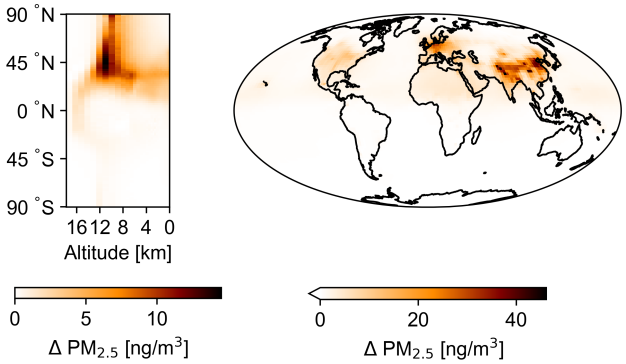

Figure S109: Yearly averaged changes in $PM_{2.5}$ concentrations due to flights of 1,500 to 2,500 km, visualised through the change in zonal mean concentration (left) and ground-level concentration (right).

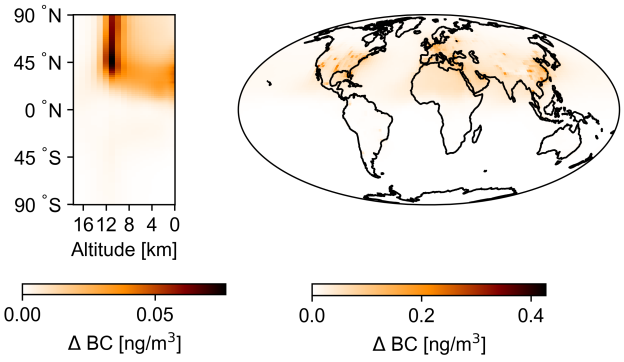

Figure S110: Yearly averaged changes in BC concentrations due to flights of 1,500 to 2,500 km, visualised through the change in zonal mean concentration (left) and ground-level concentration (right).

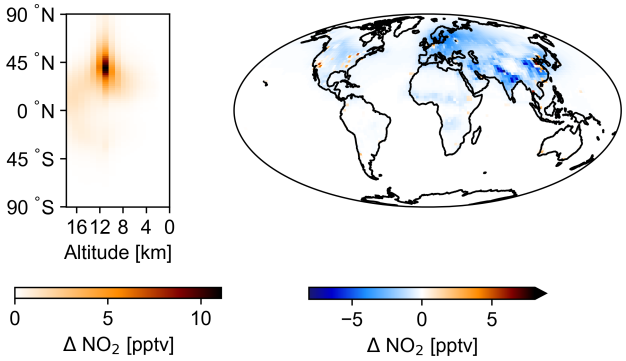

Figure S111: Yearly averaged changes in NO_2 concentrations due to flights of 2,500 to 4,000 km, visualised through the change in zonal mean concentration (left) and ground-level concentration (right).

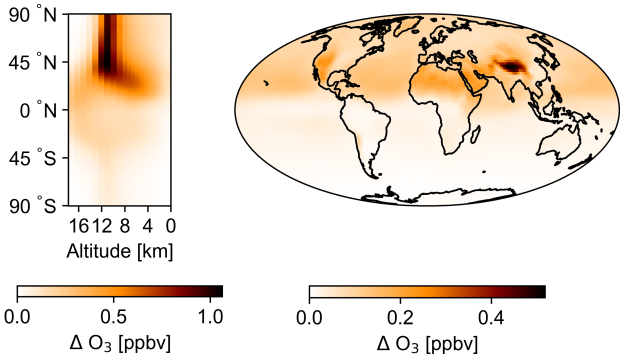

Figure S112: Yearly averaged changes in O_3 concentrations due to flights of 2,500 to 4,000 km, visualised through the change in zonal mean concentration (left) and ground-level concentration (right).

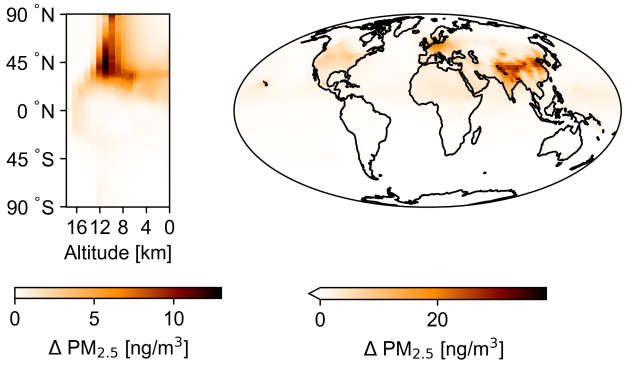

Figure S113: Yearly averaged changes in $PM_{2.5}$ concentrations due to flights of 2,500 to 4,000 km, visualised through the change in zonal mean concentration (left) and ground-level concentration (right).

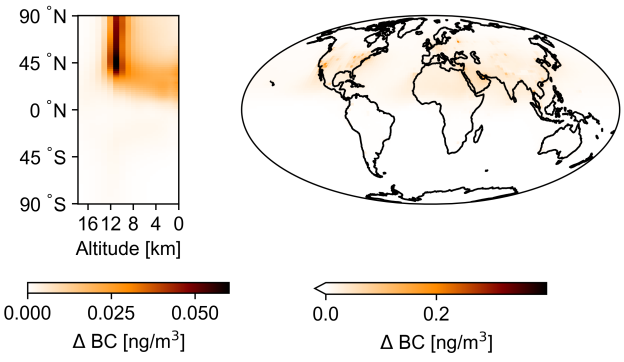

Figure S114: Yearly averaged changes in BC concentrations due to flights of 2,500 to 4,000 km, visualised through the change in zonal mean concentration (left) and ground-level concentration (right).

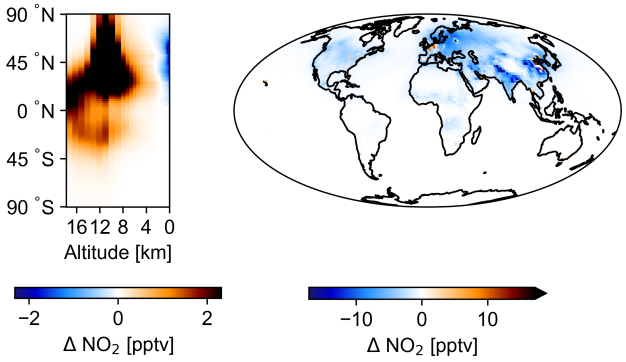

Figure S115: Yearly averaged changes in NO_2 concentrations due to flights of 4,000 to 8,000 km, visualised through the change in zonal mean concentration (left) and ground-level concentration (right).

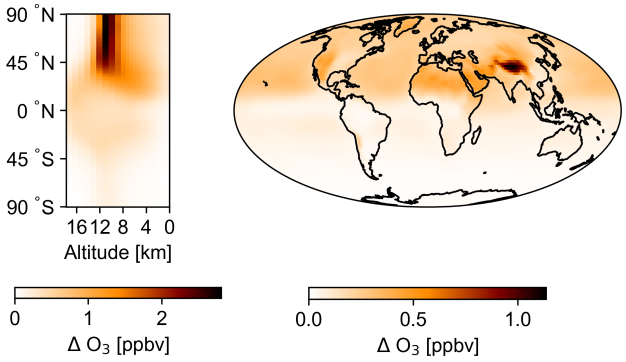

Figure S116: Yearly averaged changes in O_3 concentrations due to flights of 4,000 to 8,000 km, visualised through the change in zonal mean concentration (left) and ground-level concentration (right).

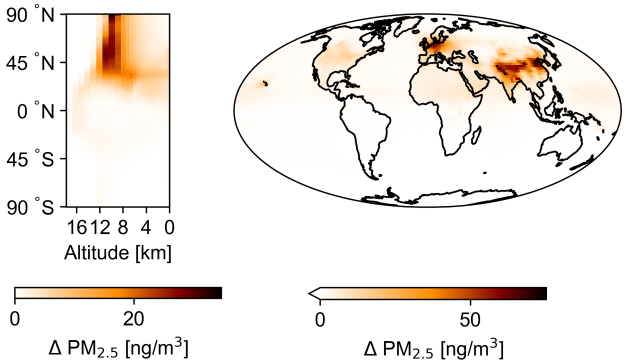

Figure S117: Yearly averaged changes in $PM_{2.5}$ concentrations due to flights of 4,000 to 8,000 km, visualised through the change in zonal mean concentration (left) and ground-level concentration (right).

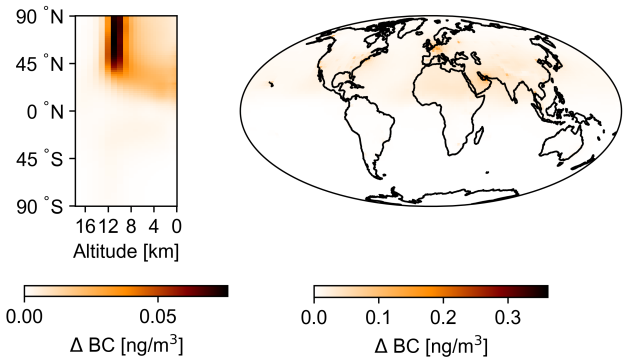

Figure S118: Yearly averaged changes in BC concentrations due to flights of 4,000 to 8,000 km, visualised through the change in zonal mean concentration (left) and ground-level concentration (right).

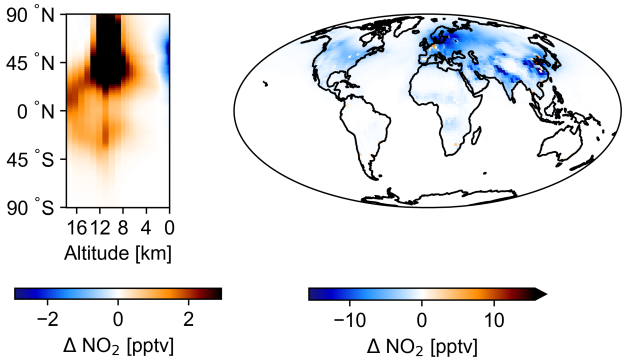

Figure S119: Yearly averaged changes in NO_2 concentrations due to flights longer than 8,000 km, visualised through the change in zonal mean concentration (left) and ground-level concentration (right).

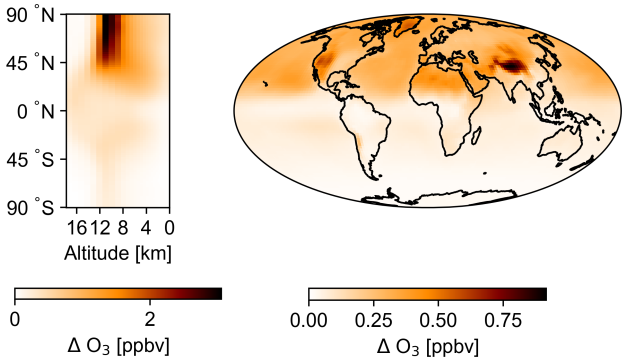

Figure S120: Yearly averaged changes in O_3 concentrations due to flights longer than 8,000 km, visualised through the change in zonal mean concentration (left) and ground-level concentration (right).

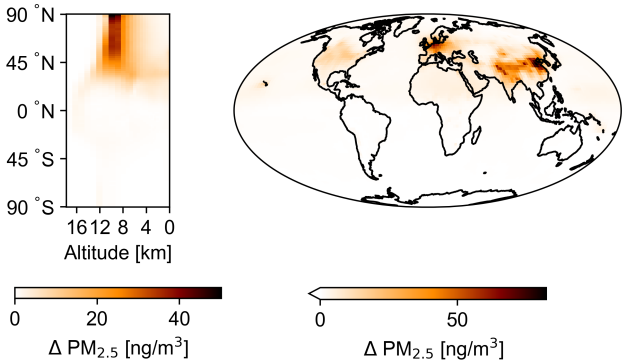

Figure S121: Yearly averaged changes in $PM_{2.5}$ concentrations due to flights longer than 8,000 km, visualised through the change in zonal mean concentration (left) and ground-level concentration (right).

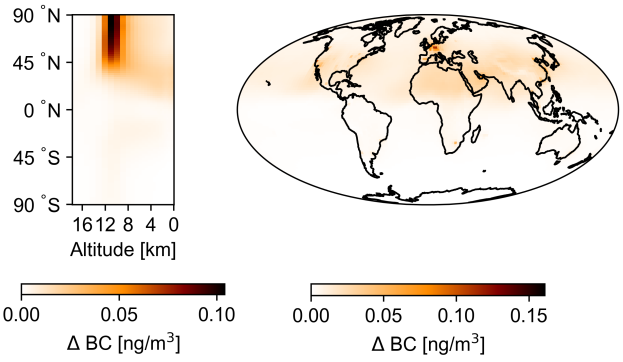

Figure S122: Yearly averaged changes in BC concentrations due to flights longer than 8,000 km, visualised through the change in zonal mean concentration (left) and ground-level concentration (right).

SI 6.3.4. Comparison of aircraft size on shared short-haul routes

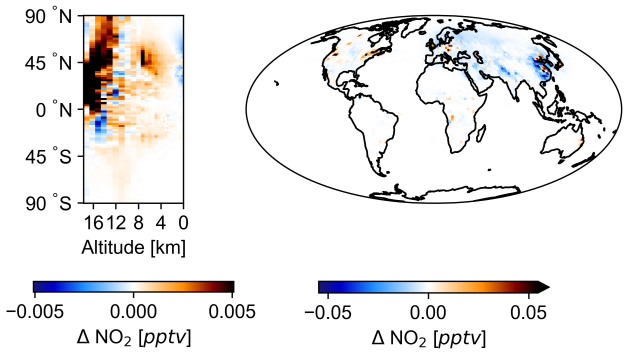

Figure S123: Yearly averaged changes in NO_2 concentrations due to turboprop aircraft on shared short-haul routes, visualised through the change in zonal mean concentration (left) and ground-level concentration (right).

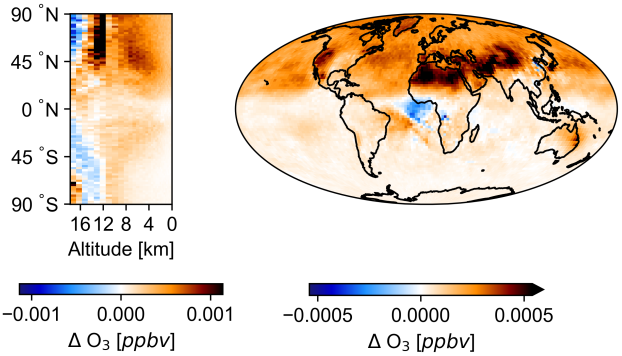

Figure S124: Yearly averaged changes in O_3 concentrations due to turboprop aircraft on shared short-haul routes, visualised through the change in zonal mean concentration (left) and ground-level concentration (right).

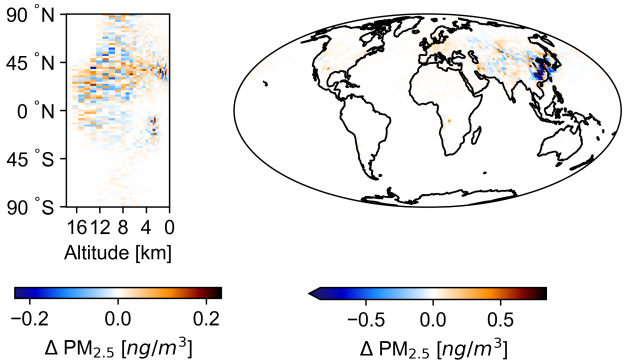

Figure S125: Yearly averaged changes in $PM_{2.5}$ concentrations due to turboprop aircraft on shared short-haul routes, visualised through the change in zonal mean concentration (left) and ground-level concentration (right).

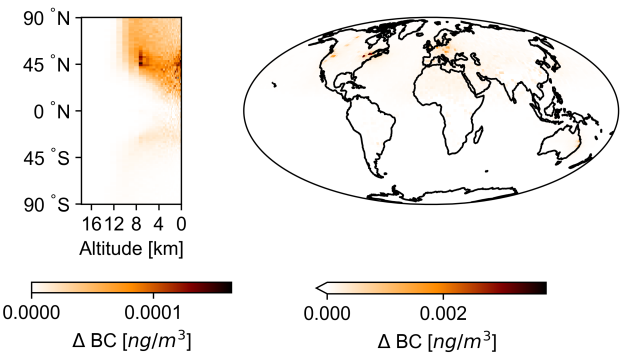

Figure S126: Yearly averaged changes in BC concentrations due to turboprop aircraft on shared short-haul routes, visualised through the change in zonal mean concentration (left) and ground-level concentration (right).

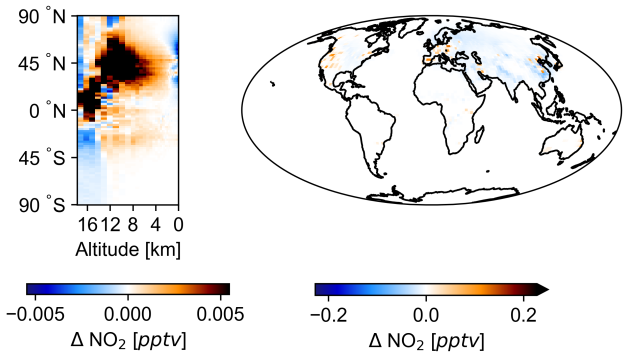

Figure S127: Yearly averaged changes in NO_2 concentrations due to regional jets on shared short-haul routes, visualised through the change in zonal mean concentration (left) and ground-level concentration (right).

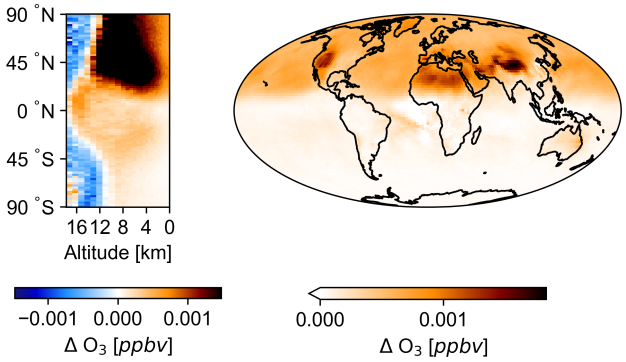

Figure S128: Yearly averaged changes in O_3 concentrations due to regional jets on shared short-haul routes, visualised through the change in zonal mean concentration (left) and ground-level concentration (right).

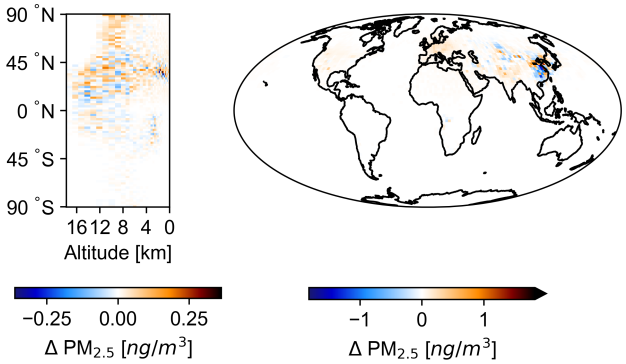

Figure S129: Yearly averaged changes in $PM_{2.5}$ concentrations due to regional jets on shared short-haul routes, visualised through the change in zonal mean concentration (left) and ground-level concentration (right).

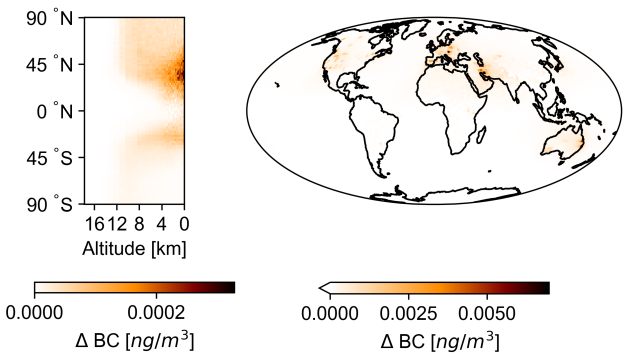

Figure S130: Yearly averaged changes in BC concentrations due to regional jets on shared short-haul routes, visualised through the change in zonal mean concentration (left) and ground-level concentration (right).

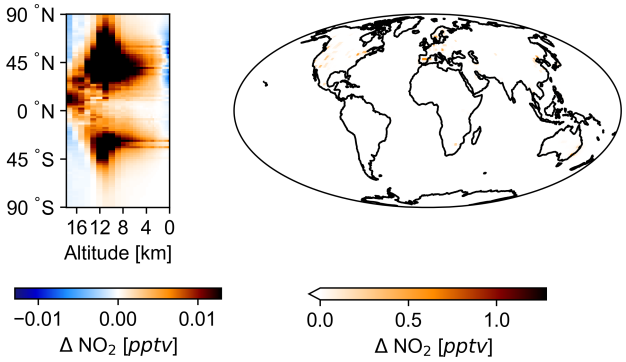

Figure S131: Yearly averaged changes in NO_2 concentrations due to narrowbody aircraft on shared short-haul routes, visualised through the change in zonal mean concentration (left) and ground-level concentration (right).

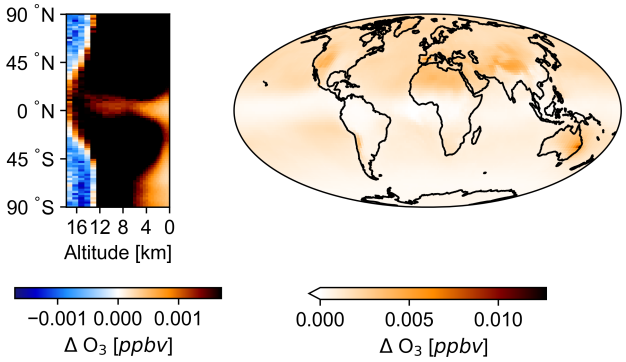

Figure S132: Yearly averaged changes in O_3 concentrations due to narrowbody aircraft on shared short-haul routes, visualised through the change in zonal mean concentration (left) and ground-level concentration (right).

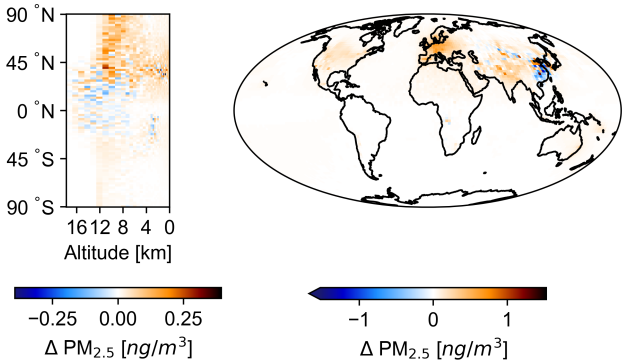

Figure S133: Yearly averaged changes in $PM_{2.5}$ concentrations due to narrowbody aircraft on shared short-haul routes, visualised through the change in zonal mean concentration (left) and ground-level concentration (right).

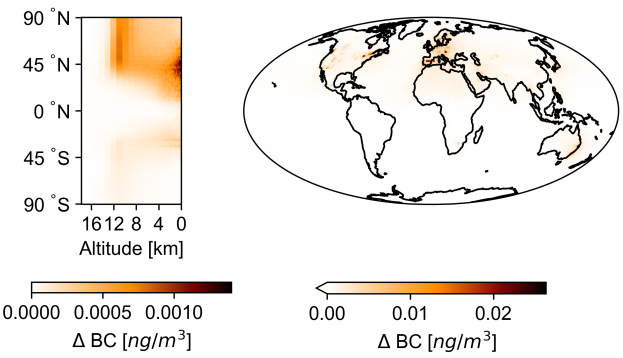

Figure S134: Yearly averaged changes in BC concentrations due to narrowbody aircraft on shared short-haul routes, visualised through the change in zonal mean concentration (left) and ground-level concentration (right).

SI 6.3.5. Intra-European flights

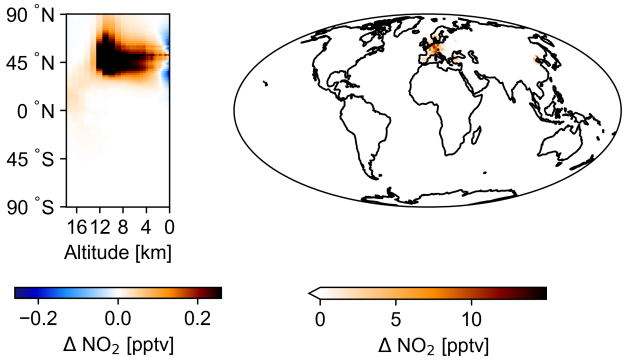

Figure S135: Yearly averaged changes in NO_2 concentrations due to intra-European flights shorter than 750 km, visualised through the change in zonal mean concentration (left) and ground-level concentration (right).

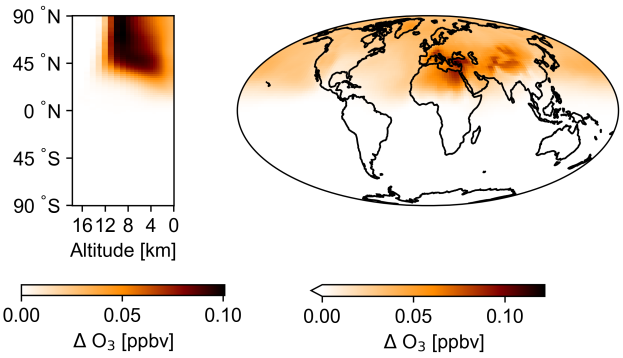

Figure S136: Yearly averaged changes in O_3 concentrations due to intra-European flights shorter than 750 km, visualised through the change in zonal mean concentration (left) and ground-level concentration (right).

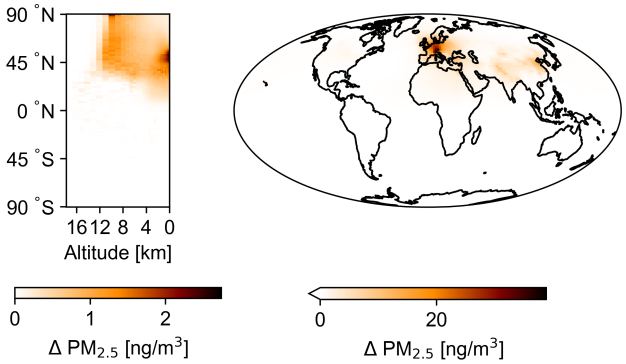

Figure S137: Yearly averaged changes in $PM_{2.5}$ concentrations due to intra-European flights shorter than 750 km, visualised through the change in zonal mean concentration (left) and ground-level concentration (right).

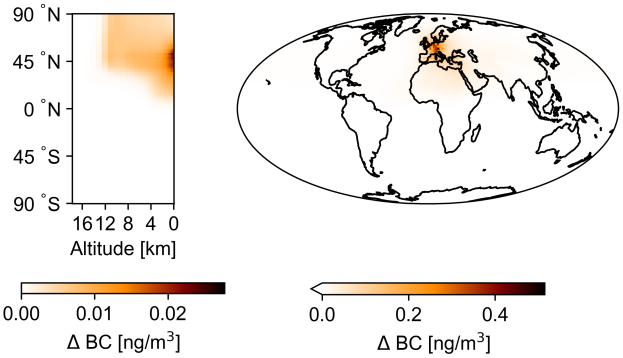

Figure S138: Yearly averaged changes in BC concentrations due to intra-European flights shorter than 750 km, visualised through the change in zonal mean concentration (left) and ground-level concentration (right).

SI 6.4. Regional population-weighted concentration changes

This section provides the annual average change in population-weighted concentrations of NO_2, O_3, $PM_{2.5}$ and BC caused by aviation. In subsections SI 6.4.2 to SI 6.4.8, the regional population-weighted concentrations due to aviation impacts are provided for different metrics. These differ from the observed ground-level concentration changes as presented in section SI 6.3 as the population density is taken into account. As there are also variations within regions, the maps in subsection SI 6.4.1 provide some insight in the general spread for all aviation impacts. Furthermore, subsection SI 6.4.1 also provides a brief explanation on the differences between annual and peak season metrics for O_3.

SI 6.4.1. Global distribution for all aviation

As shown in section SI 6.2, the impact of aviation follows a yearly pattern which is opposite to the background concentration of O_3. Thus, the impact of aviation in populated areas is usually lower during the 'peak season', in which background levels are highest. In the main study, the annual average values are thus used. However, some CRFs rely on the use of peak-season impacts. Figure S139 shows how this peak-season effect relates to the annually averaged population-weighted concentrations.

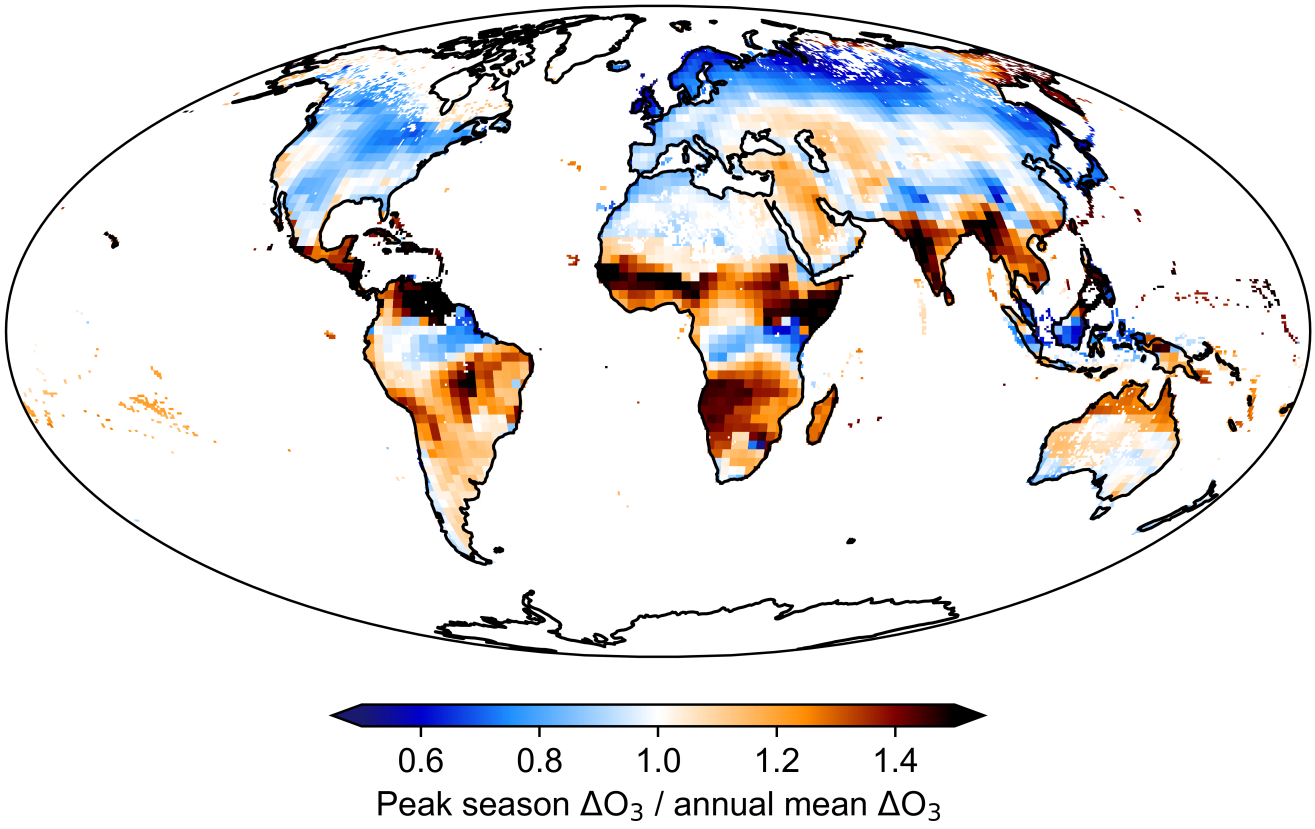

Figure S139: Map showing the relative impact using the O_3 peak season metric versus the annual mean metric for population-weighted O_3 concentrations due to all aviation.

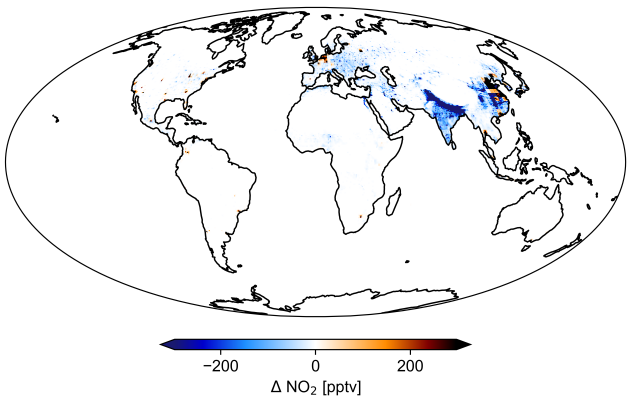

Figure S140: Distribution of annual mean changes in population-weighted concentrations of NO_2 due to aviation.

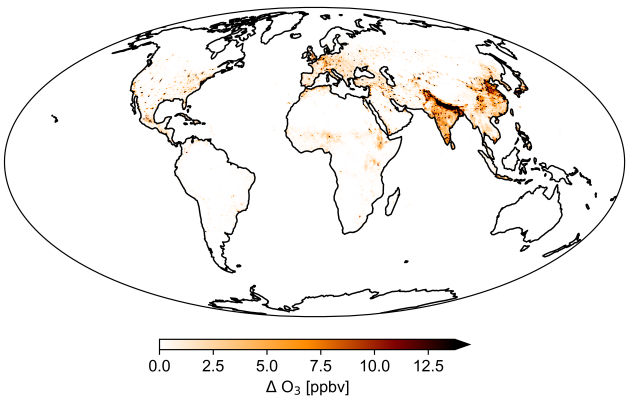

Figure S141: Distribution of peak season mean changes in population-weighted concentrations of O_3 due to aviation.

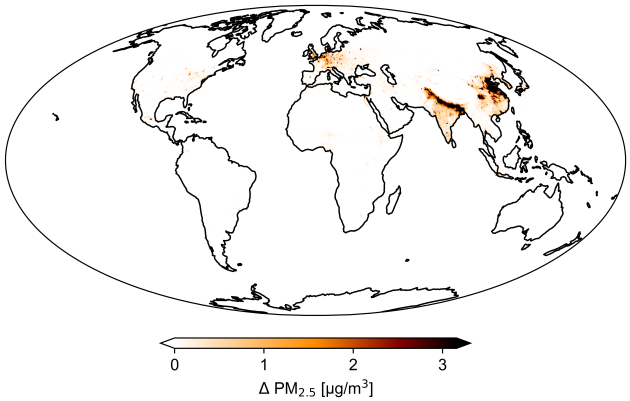

Figure S142: Distribution of annual mean changes in population-weighted concentrations of $PM_{2.5}$ due to aviation.

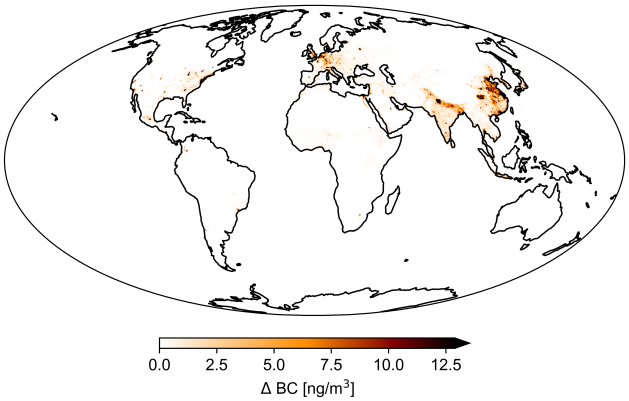

Figure S143: Distribution of peak season mean changes in population-weighted concentrations of BC due to aviation.

SI 6.4.2. Nominal estimates of air quality impacts

Table S42: NO_2 concentration change in pptv.

Aircraft category	Global	N.A.	EU.	AS.	S.A.	AF. + M.E.	OC.
All aviation	-5.151	3.416	-8.206	-16.980	1.171	-1.523	0.612
Piston aircraft	0.002	0.010	0.002	0.004	0.000	-0.000	0.000
Business jets	0.008	0.400	0.008	-0.172	0.006	-0.013	0.002
Turboprop	-0.007	0.067	0.011	-0.080	0.029	-0.005	0.019
Regional jets	-0.054	1.266	0.192	-0.967	0.049	-0.061	0.006
Narrowbody	-0.176	2.964	0.584	-2.260	0.797	-0.568	0.233
Widebody	-4.265	-0.775	-7.558	-12.053	0.304	-0.731	0.354
Shorter than 750 km	0.616	2.017	2.044	0.167	0.499	-0.022	0.139
750 to 1,500 km	0.799	1.403	0.554	2.388	0.266	-0.109	0.092
1,500 to 2,500 km	-0.163	0.967	-0.564	-0.660	0.186	-0.222	0.052
2,500 to 4,000 km	-0.628	0.918	-1.435	-2.116	0.055	-0.143	0.061
4,000 to 8,000 km	-2.124	-0.433	-1.812	-7.183	0.084	-0.315	0.160
Longer than 8,000 km	-2.653	-0.662	-4.694	-7.456	0.105	-0.494	0.111

Table S43: O_3 annual mean concentration change in pptv.

Aircraft category	Global	N.A.	EU.	AS.	S.A.	AF. + M.E.	OC.
All aviation	801.7	638.6	1,290.3	1,907.9	93.5	347.5	17.0
Piston aircraft	0.3	0.3	0.6	0.7	0.0	0.1	0.0
Business jets	4.9	6.6	8.3	10.1	0.4	2.1	0.0
Turboprop	4.7	3.5	10.3	10.0	0.9	1.4	0.4
Regional jets	23.7	25.9	46.0	49.2	2.2	8.9	0.3
Narrowbody	259.3	209.9	417.1	618.2	34.3	107.2	5.7
Widebody	468.5	359.8	743.9	1,121.1	54.3	211.3	10.5
Shorter than 750 km	66.7	54.8	123.7	151.0	10.5	23.5	2.1
750 to 1,500 km	111.3	88.8	172.1	272.8	13.3	43.9	2.4
1,500 to 2,500 km	101.7	83.7	153.6	246.3	12.1	44.6	1.8
2,500 to 4,000 km	86.8	70.6	116.3	214.5	10.0	44.4	1.7
4,000 to 8,000 km	188.7	136.4	289.7	456.3	22.3	91.8	4.1
Longer than 8,000 km	186.7	155.0	337.6	422.1	23.5	74.5	4.6

Table S44: O_3 peak season concentration change in pptv.

Aircraft category	Global	N.A.	EU.	AS.	S.A.	AF. + M.E.	OC.
All aviation	820.4	647.5	1,202.5	1,990.2	107.1	397.5	17.8
Piston aircraft	0.4	0.4	0.8	0.8	0.0	0.1	0.0
Business jets	5.1	8.0	7.7	10.4	0.5	2.5	0.0
Turboprop	4.7	3.5	11.0	9.4	1.0	1.5	0.4
Regional jets	24.3	29.9	44.5	49.7	2.5	10.3	0.3
Narrowbody	270.5	219.6	401.8	654.9	39.3	124.3	6.0
Widebody	480.9	358.5	689.8	1,178.7	62.2	241.6	11.0
Shorter than 750 km	69.2	60.2	127.0	155.1	11.6	26.3	2.4
750 to 1,500 km	117.7	93.6	163.6	296.4	15.4	50.6	2.5
1,500 to 2,500 km	106.5	87.1	143.9	263.9	14.1	52.2	2.0
2,500 to 4,000 km	88.3	73.3	98.0	223.9	12.1	51.1	1.8
4,000 to 8,000 km	194.8	135.0	272.1	481.3	25.6	105.2	4.3
Longer than 8,000 km	194.4	157.1	329.3	448.7	26.0	85.9	4.7

Table S45: $PM_{2.5}$ concentration change in $ng\,m^{-3}$.

Aircraft category	Global	N.A.	EU.	AS.	S.A.	AF. + M.E.	OC.
All aviation	97.40	27.67	129.83	312.12	2.11	8.31	0.36
Piston aircraft	0.13	0.52	0.22	0.11	0.01	0.02	0.01
Business jets	0.64	0.69	1.06	1.62	0.01	0.08	0.00
Turboprop	0.69	0.29	1.40	1.87	0.04	0.07	0.02
Regional jets	3.25	2.24	6.03	8.68	0.10	0.31	0.01
Narrowbody	36.29	10.66	49.37	115.39	1.11	3.10	0.15
Widebody	53.37	12.75	67.16	174.73	0.84	4.65	0.18
Shorter than 750 km	10.80	4.42	19.19	30.97	0.54	0.87	0.09
750 to 1,500 km	17.50	5.00	21.08	57.58	0.40	1.30	0.06
1,500 to 2,500 km	13.23	4.08	15.90	43.13	0.30	1.25	0.03
2,500 to 4,000 km	9.79	3.23	10.60	32.31	0.18	1.13	0.03
4,000 to 8,000 km	20.62	4.87	27.69	66.26	0.34	2.09	0.07
Longer than 8,000 km	20.52	5.26	28.09	65.83	0.35	1.53	0.07

Table S46: BC concentration change in pg m^{-3}.

Aircraft category	Global	N.A.	EU.	AS.	S.A.	AF. + M.E.	OC.
All aviation	387.5	357.2	650.5	970.6	45.3	79.4	10.6
Piston aircraft	0.2	1.3	0.3	0.1	0.0	0.0	0.0
Business jets	7.2	28.8	14.1	5.3	0.5	1.0	0.1
Turboprop	4.1	3.9	9.8	8.1	1.0	0.7	0.7
Regional jets	14.2	49.7	33.2	10.8	1.7	1.7	0.6
Narrowbody	273.4	216.4	467.6	705.1	35.3	47.7	6.2
Widebody	88.4	57.0	125.5	240.9	6.8	28.3	3.0
Shorter than 750 km	88.0	96.9	193.9	184.1	18.9	13.8	3.7
750 to 1,500 km	132.3	91.9	189.9	376.4	11.4	18.3	2.7
1,500 to 2,500 km	74.7	71.5	116.9	191.9	6.6	14.9	1.1
2,500 to 4,000 km	36.5	50.8	47.4	87.2	2.8	11.4	0.9
4,000 to 8,000 km	33.3	28.2	62.5	76.0	3.1	13.2	1.4
Longer than 8,000 km	22.9	17.8	39.8	55.6	2.6	7.9	1.0

SI 6.4.3. Air quality impacts normalised per RPK

Table S47: NO_2 concentration change in ppbv $\cdot (1 \cdot 10^{15}$ RPK$)^{-1}$.

Aircraft category	Global	N.A.	EU.	AS.	S.A.	AF. + M.E.	OC.
All aviation	-0.656	0.435	-1.045	-2.162	0.149	-0.194	0.078
Piston aircraft	1.345	5.246	1.138	2.255	0.065	-0.021	0.155
Business jets	0.465	22.196	0.453	-9.543	0.349	-0.749	0.093
Turboprop	-0.136	1.285	0.216	-1.530	0.555	-0.101	0.368
Regional jets	-0.225	5.295	0.802	-4.042	0.206	-0.254	0.024
Narrowbody	-0.046	0.781	0.154	-0.595	0.210	-0.150	0.061
Widebody	-1.138	-0.207	-2.017	-3.217	0.081	-0.195	0.095
Shorter than 750 km	1.099	3.598	3.647	0.297	0.891	-0.038	0.249
750 to 1,500 km	0.567	0.996	0.393	1.695	0.189	-0.078	0.065
1,500 to 2,500 km	-0.111	0.657	-0.383	-0.448	0.127	-0.151	0.036
2,500 to 4,000 km	-0.504	0.737	-1.151	-1.698	0.044	-0.115	0.049
4,000 to 8,000 km	-1.215	-0.248	-1.037	-4.109	0.048	-0.180	0.092
Longer than 8,000 km	-1.871	-0.467	-3.311	-5.259	0.074	-0.349	0.078

Table S48: O_3 annual mean concentration change in ppbv $\cdot (1 \cdot 10^{15}$ RPK$)^{-1}$.

Aircraft category	Global	N.A.	EU.	AS.	S.A.	AF. + M.E.	OC.
All aviation	102.1	81.3	164.3	242.9	11.9	44.3	2.2
Piston aircraft	166.6	169.2	325.1	360.9	17.1	49.9	3.9
Business jets	273.2	369.2	460.0	560.7	22.7	119.2	2.5
Turboprop	90.4	66.2	197.4	192.7	17.9	26.6	7.5
Regional jets	99.1	108.3	192.2	205.8	9.3	37.1	1.2
Narrowbody	68.3	55.3	109.9	162.9	9.0	28.2	1.5
Widebody	125.0	96.0	198.5	299.2	14.5	56.4	2.8
Shorter than 750 km	118.9	97.8	220.6	269.5	18.8	41.9	3.8
750 to 1,500 km	79.0	63.0	122.2	193.7	9.4	31.2	1.7
1,500 to 2,500 km	69.1	56.9	104.4	167.3	8.2	30.3	1.2
2,500 to 4,000 km	69.6	56.7	93.3	172.1	8.0	35.6	1.4
4,000 to 8,000 km	107.9	78.0	165.7	261.0	12.8	52.5	2.4
Longer than 8,000 km	131.7	109.3	238.2	297.8	16.5	52.6	3.2

Table S49: O_3 peak season concentration change in ppbv $\cdot (1 \cdot 10^{15}$ RPK$)^{-1}$.

Aircraft category	Global	N.A.	EU.	AS.	S.A.	AF. + M.E.	OC.
All aviation	104.5	82.5	153.1	253.4	13.6	50.6	2.3
Piston aircraft	202.7	205.5	414.0	430.5	16.7	62.1	4.1
Business jets	285.8	442.5	426.7	576.8	27.6	140.0	2.7
Turboprop	90.1	67.0	211.7	181.2	19.1	28.5	8.5
Regional jets	101.8	125.0	185.9	207.7	10.3	43.0	1.1
Narrowbody	71.3	57.9	105.9	172.6	10.4	32.7	1.6
Widebody	128.4	95.7	184.1	314.6	16.6	64.5	2.9
Shorter than 750 km	123.5	107.4	226.6	276.6	20.7	47.0	4.3
750 to 1,500 km	83.5	66.5	116.2	210.4	11.0	35.9	1.8
1,500 to 2,500 km	72.4	59.2	97.8	179.3	9.6	35.5	1.3
2,500 to 4,000 km	70.8	58.8	78.6	179.6	9.7	41.0	1.5
4,000 to 8,000 km	111.5	77.2	155.7	275.3	14.6	60.2	2.4
Longer than 8,000 km	137.2	110.8	232.3	316.5	18.3	60.6	3.3

Table S50: $PM_{2.5}$ concentration change in µg m^{-3} $\cdot (1 \cdot 10^{15}$ RPK$)^{-1}$.

Aircraft category	Global	N.A.	EU.	AS.	S.A.	AF. + M.E.	OC.
All aviation	12.40	3.52	16.53	39.75	0.27	1.06	0.05
Piston aircraft	69.54	281.38	117.42	60.91	3.28	10.64	4.77
Business jets	35.39	38.18	58.77	90.25	0.79	4.34	0.08
Turboprop	13.34	5.66	26.94	35.93	0.80	1.28	0.32
Regional jets	13.61	9.37	25.22	36.28	0.41	1.30	0.03
Narrowbody	9.56	2.81	13.01	30.40	0.29	0.82	0.04
Widebody	14.24	3.40	17.93	46.64	0.22	1.24	0.05
Shorter than 750 km	19.26	7.89	34.24	55.26	0.96	1.55	0.16
750 to 1,500 km	12.43	3.55	14.97	40.88	0.28	0.92	0.04
1,500 to 2,500 km	8.99	2.77	10.80	29.30	0.20	0.85	0.02
2,500 to 4,000 km	7.85	2.59	8.50	25.92	0.14	0.90	0.03
4,000 to 8,000 km	11.79	2.79	15.84	37.91	0.20	1.19	0.04
Longer than 8,000 km	14.47	3.71	19.82	46.44	0.25	1.08	0.05

Table S51: BC concentration change in µg m^{-3} $\cdot (1 \cdot 10^{18}$ RPK$)^{-1}$.

Aircraft category	Global	N.A.	EU.	AS.	S.A.	AF. + M.E.	OC.
All aviation	49.3	45.5	82.8	123.6	5.8	10.1	1.4
Piston aircraft	128.5	691.2	174.5	50.9	5.0	7.2	15.6
Business jets	399.3	1,599.7	782.4	297.1	28.2	54.1	5.2
Turboprop	78.4	74.9	188.8	156.1	19.7	13.4	12.7
Regional jets	59.5	207.8	138.6	45.2	7.2	7.1	2.6
Narrowbody	72.0	57.0	123.2	185.8	9.3	12.6	1.6
Widebody	23.6	15.2	33.5	64.3	1.8	7.6	0.8
Shorter than 750 km	157.0	172.8	346.0	328.5	33.7	24.7	6.6
750 to 1,500 km	93.9	65.3	134.8	267.2	8.1	13.0	1.9
1,500 to 2,500 km	50.7	48.6	79.5	130.4	4.5	10.1	0.7
2,500 to 4,000 km	29.3	40.7	38.0	70.0	2.3	9.1	0.7
4,000 to 8,000 km	19.1	16.1	35.7	43.5	1.7	7.6	0.8
Longer than 8,000 km	16.2	12.5	28.1	39.2	1.8	5.6	0.7

SI 6.4.4. Air quality impacts normalised per passenger

Table S52: NO_2 concentration change in ppbv · $(1 \cdot 10^{12}$ pax$)^{-1}$.

Aircraft category	Global	N.A.	EU.	AS.	S.A.	AF. + M.E.	OC.
All aviation	-1.259	0.835	-2.005	-4.149	0.286	-0.372	0.150
Piston aircraft	0.240	0.935	0.203	0.402	0.012	-0.004	0.028
Business jets	0.496	23.704	0.484	-10.192	0.373	-0.800	0.099
Turboprop	-0.051	0.480	0.081	-0.571	0.207	-0.038	0.137
Regional jets	-0.182	4.287	0.649	-3.273	0.166	-0.205	0.019
Narrowbody	-0.063	1.062	0.209	-0.810	0.285	-0.203	0.084
Widebody	-5.078	-0.923	-8.997	-14.349	0.361	-0.871	0.422
Shorter than 750 km	0.517	1.692	1.715	0.140	0.419	-0.018	0.117
750 to 1,500 km	0.624	1.095	0.432	1.863	0.207	-0.085	0.072
1,500 to 2,500 km	-0.211	1.254	-0.731	-0.856	0.242	-0.288	0.068
2,500 to 4,000 km	-1.565	2.287	-3.574	-5.271	0.136	-0.357	0.152
4,000 to 8,000 km	-7.035	-1.434	-5.999	-23.786	0.278	-1.044	0.530
Longer than 8,000 km	-18.375	-4.585	-32.515	-51.644	0.728	-3.422	0.766

Table S53: O_3 annual mean concentration change in ppbv · $(1 \cdot 10^{12}$ pax$)^{-1}$.

Aircraft category	Global	N.A.	EU.	AS.	S.A.	AF. + M.E.	OC.
All aviation	195.9	156.0	315.3	466.2	22.8	84.9	4.2
Piston aircraft	29.7	30.2	58.0	64.3	3.0	8.9	0.7
Business jets	291.8	394.3	491.3	598.8	24.3	127.3	2.7
Turboprop	33.7	24.7	73.7	71.9	6.7	9.9	2.8
Regional jets	80.2	87.7	155.6	166.7	7.5	30.1	1.0
Narrowbody	92.9	75.2	149.5	221.6	12.3	38.4	2.0
Widebody	557.7	428.4	885.6	1,334.7	64.6	251.6	12.5
Shorter than 750 km	55.9	46.0	103.7	126.7	8.8	19.7	1.8
750 to 1,500 km	86.8	69.2	134.3	212.9	10.4	34.3	1.9
1,500 to 2,500 km	131.9	108.6	199.3	319.5	15.6	57.8	2.4
2,500 to 4,000 km	216.1	175.9	289.6	534.2	24.9	110.6	4.3
4,000 to 8,000 km	624.7	451.6	959.1	1,510.9	73.8	303.9	13.7
Longer than 8,000 km	1,293.1	1,073.4	2,338.6	2,924.1	162.5	516.2	31.7

Table S54: O_3 peak season concentration change in ppbv · $(1 \cdot 10^{12}$ pax$)^{-1}$.

Aircraft category	Global	N.A.	EU.	AS.	S.A.	AF. + M.E.	OC.
All aviation	200.5	158.2	293.8	486.3	26.2	97.1	4.4
Piston aircraft	36.1	36.6	73.8	76.8	3.0	11.1	0.7
Business jets	305.2	472.6	455.6	615.9	29.5	149.5	2.8
Turboprop	33.6	25.0	79.0	67.6	7.1	10.6	3.2
Regional jets	82.4	101.2	150.5	168.2	8.4	34.8	0.9
Narrowbody	97.0	78.7	144.0	234.7	14.1	44.5	2.2
Widebody	572.5	426.8	821.1	1,403.2	74.0	287.6	13.0
Shorter than 750 km	58.1	50.5	106.6	130.1	9.7	22.1	2.0
750 to 1,500 km	91.8	73.0	127.7	231.3	12.0	39.5	2.0
1,500 to 2,500 km	138.2	112.9	186.7	342.3	18.3	67.7	2.5
2,500 to 4,000 km	219.8	182.7	244.0	557.7	30.1	127.2	4.6
4,000 to 8,000 km	645.2	446.9	901.0	1,593.7	84.7	348.2	14.1
Longer than 8,000 km	1,346.8	1,088.0	2,280.7	3,108.2	179.8	594.9	32.4

Table S55: $PM_{2.5}$ concentration change in $\mu g\,m^{-3} \cdot (1 \cdot 10^{12}\ \text{pax})^{-1}$.

Aircraft category	Global	N.A.	EU.	AS.	S.A.	AF. + M.E.	OC.
All aviation	23.80	6.76	31.73	76.27	0.52	2.03	0.09
Piston aircraft	12.40	50.17	20.93	10.86	0.59	1.90	0.85
Business jets	37.80	40.77	62.77	96.38	0.85	4.64	0.08
Turboprop	4.98	2.11	10.06	13.41	0.30	0.48	0.12
Regional jets	11.02	7.59	20.42	29.38	0.33	1.05	0.02
Narrowbody	13.01	3.82	17.69	41.36	0.40	1.11	0.05
Widebody	63.53	15.18	79.95	208.00	1.00	5.53	0.21
Shorter than 750 km	9.06	3.71	16.10	25.99	0.45	0.73	0.07
750 to 1,500 km	13.66	3.90	16.45	44.92	0.31	1.02	0.05
1,500 to 2,500 km	17.17	5.29	20.63	55.95	0.39	1.62	0.05
2,500 to 4,000 km	24.38	8.06	26.40	80.47	0.44	2.81	0.09
4,000 to 8,000 km	68.26	16.12	91.68	219.42	1.14	6.92	0.25
Longer than 8,000 km	142.11	36.43	194.60	455.97	2.46	10.58	0.49

Table S56: BC concentration change in $\mu g\,m^{-3} \cdot (1 \cdot 10^{15}\ \text{pax})^{-1}$.

Aircraft category	Global	N.A.	EU.	AS.	S.A.	AF. + M.E.	OC.
All aviation	94.7	87.3	158.9	237.2	11.1	19.4	2.6
Piston aircraft	22.9	123.2	31.1	9.1	0.9	1.3	2.8
Business jets	426.4	1,708.4	835.6	317.3	30.1	57.7	5.5
Turboprop	29.3	27.9	70.5	58.2	7.3	5.0	4.7
Regional jets	48.2	168.2	112.2	36.6	5.8	5.8	2.1
Narrowbody	98.0	77.6	167.6	252.7	12.7	17.1	2.2
Widebody	105.2	67.9	149.4	286.8	8.0	33.7	3.6
Shorter than 750 km	73.8	81.3	162.7	154.5	15.8	11.6	3.1
750 to 1,500 km	103.2	71.7	148.2	293.6	8.9	14.3	2.1
1,500 to 2,500 km	96.9	92.7	151.7	248.9	8.5	19.3	1.4
2,500 to 4,000 km	90.8	126.5	118.0	217.3	7.1	28.4	2.2
4,000 to 8,000 km	110.4	93.5	206.8	251.6	10.1	43.8	4.5
Longer than 8,000 km	158.6	123.1	275.7	385.4	17.9	54.7	6.6

SI 6.4.5. Air quality impacts per unit fuel burn

Table S57: NO_2 concentration change in $\text{ppbv} \cdot (1 \cdot 10^{14}\ \text{kg fuel})^{-1}$.

Aircraft category	Global	N.A.	EU.	AS.	S.A.	AF. + M.E.	OC.
All aviation	-1.741	1.154	-2.773	-5.738	0.396	-0.515	0.207
Piston aircraft	2.480	9.669	2.097	4.156	0.120	-0.039	0.286
Business jets	0.258	12.310	0.252	-5.293	0.193	-0.416	0.051
Turboprop	-0.227	2.148	0.361	-2.556	0.927	-0.170	0.615
Regional jets	-0.425	10.009	1.516	-7.642	0.389	-0.480	0.045
Narrowbody	-0.142	2.385	0.470	-1.818	0.641	-0.457	0.187
Widebody	-2.797	-0.508	-4.956	-7.904	0.199	-0.480	0.232
Shorter than 750 km	2.059	6.739	6.831	0.557	1.668	-0.072	0.466
750 to 1,500 km	1.519	2.667	1.053	4.538	0.505	-0.207	0.175
1,500 to 2,500 km	-0.336	1.991	-1.161	-1.359	0.384	-0.457	0.108
2,500 to 4,000 km	-1.562	2.282	-3.566	-5.260	0.135	-0.356	0.152
4,000 to 8,000 km	-3.157	-0.644	-2.693	-10.676	0.125	-0.469	0.238
Longer than 8,000 km	-4.631	-1.156	-8.196	-13.017	0.183	-0.863	0.193

Table S58: O_3 annual mean concentration change in ppbv $\cdot (1 \cdot 10^{14}$ kg fuel$)^{-1}$.

Aircraft category	Global	N.A.	EU.	AS.	S.A.	AF. + M.E.	OC.
All aviation	270.9	215.8	436.0	644.8	31.6	117.5	5.8
Piston aircraft	307.0	311.9	599.3	665.3	31.5	91.9	7.1
Business jets	151.5	204.8	255.1	311.0	12.6	66.1	1.4
Turboprop	151.0	110.7	329.9	322.1	29.9	44.4	12.5
Regional jets	187.3	204.7	363.4	389.1	17.5	70.2	2.2
Narrowbody	208.6	168.9	335.6	497.4	27.6	86.2	4.5
Widebody	307.2	236.0	487.8	735.2	35.6	138.6	6.9
Shorter than 750 km	222.8	183.2	413.2	504.7	35.2	78.5	7.0
750 to 1,500 km	211.5	168.7	327.1	518.5	25.2	83.5	4.6
1,500 to 2,500 km	209.4	172.4	316.4	507.3	24.8	91.8	3.8
2,500 to 4,000 km	215.7	175.5	289.0	533.1	24.8	110.4	4.3
4,000 to 8,000 km	280.4	202.7	430.5	678.1	33.1	136.4	6.2
Longer than 8,000 km	325.9	270.6	589.5	737.0	41.0	130.1	8.0

Table S59: O_3 peak season concentration change in ppbv $\cdot (1 \cdot 10^{14}$ kg fuel$)^{-1}$.

Aircraft category	Global	N.A.	EU.	AS.	S.A.	AF. + M.E.	OC.
All aviation	277.3	218.8	406.4	672.6	36.2	134.3	6.0
Piston aircraft	373.6	378.8	763.1	793.5	30.9	114.4	7.6
Business jets	158.5	245.4	236.6	319.9	15.3	77.6	1.5
Turboprop	150.5	112.0	353.8	302.8	31.9	47.6	14.3
Regional jets	192.5	236.2	351.4	392.7	19.6	81.2	2.1
Narrowbody	217.6	176.7	323.3	526.9	31.6	100.0	4.8
Widebody	315.4	235.1	452.3	773.0	40.8	158.5	7.2
Shorter than 750 km	231.4	201.1	424.5	518.2	38.7	88.0	8.1
750 to 1,500 km	223.6	177.9	311.0	563.3	29.3	96.2	4.8
1,500 to 2,500 km	219.4	179.3	296.4	543.4	29.1	107.5	4.0
2,500 to 4,000 km	219.4	182.3	243.5	556.5	30.0	127.0	4.6
4,000 to 8,000 km	289.6	200.6	404.4	715.3	38.0	156.3	6.3
Longer than 8,000 km	339.5	274.2	574.9	783.4	45.3	150.0	8.2

Table S60: $PM_{2.5}$ concentration change in µg m$^{-3} \cdot (1 \cdot 10^{14}$ kg fuel$)^{-1}$.

Aircraft category	Global	N.A.	EU.	AS.	S.A.	AF. + M.E.	OC.
All aviation	32.92	9.35	43.88	105.48	0.71	2.81	0.12
Piston aircraft	128.18	518.65	216.43	112.28	6.05	19.62	8.80
Business jets	19.63	21.17	32.60	50.06	0.44	2.41	0.04
Turboprop	22.29	9.45	45.03	60.05	1.33	2.15	0.54
Regional jets	25.73	17.71	47.67	68.59	0.77	2.46	0.05
Narrowbody	29.20	8.58	39.72	92.84	0.89	2.50	0.12
Widebody	35.00	8.36	44.04	114.58	0.55	3.05	0.12
Shorter than 750 km	36.09	14.79	64.13	103.51	1.79	2.91	0.30
750 to 1,500 km	33.26	9.50	40.06	109.41	0.76	2.47	0.11
1,500 to 2,500 km	27.25	8.40	32.75	88.82	0.62	2.58	0.07
2,500 to 4,000 km	24.33	8.04	26.35	80.30	0.44	2.80	0.09
4,000 to 8,000 km	30.64	7.24	41.15	98.48	0.51	3.10	0.11
Longer than 8,000 km	35.82	9.18	49.05	114.93	0.62	2.67	0.12

Table S61: BC concentration change in $\mu g\, m^{-3} \cdot (1 \cdot 10^{14}$ kg fuel$)^{-1}$.

Aircraft category	Global	N.A.	EU.	AS.	S.A.	AF. + M.E.	OC.
All aviation	131.0	120.7	219.8	328.0	15.3	26.9	3.6
Piston aircraft	236.9	1,274.0	321.6	93.9	9.2	13.2	28.8
Business jets	221.4	887.3	433.9	164.8	15.6	30.0	2.9
Turboprop	131.0	125.1	315.6	260.8	32.9	22.4	21.2
Regional jets	112.5	392.8	262.1	85.4	13.6	13.5	4.8
Narrowbody	219.9	174.1	376.2	567.3	28.4	38.4	5.0
Widebody	58.0	37.4	82.3	158.0	4.4	18.6	2.0
Shorter than 750 km	294.1	323.7	648.1	615.3	63.1	46.2	12.3
750 to 1,500 km	251.4	174.7	360.9	715.2	21.7	34.8	5.1
1,500 to 2,500 km	153.8	147.2	240.9	395.2	13.6	30.6	2.2
2,500 to 4,000 km	90.6	126.2	117.8	216.8	7.1	28.3	2.2
4,000 to 8,000 km	49.5	42.0	92.8	112.9	4.5	19.7	2.0
Longer than 8,000 km	40.0	31.0	69.5	97.1	4.5	13.8	1.7

SI 6.4.6. Air quality impacts per unit fuel burn within the same region

Table S62: NO_2 concentration change in ppbv $\cdot (1 \cdot 10^{14}$ kg fuel$)^{-1}$.

Aircraft category	Global	N.A.	EU.	AS.	S.A.	AF. + M.E.	OC.
All aviation	-1.74	4.28	-11.65	-19.18	11.76	-9.40	7.75
Piston aircraft	2.48	11.24	38.42	815.19	12.39	-36.00	5.48
Business jets	0.26	15.89	1.77	-149.77	16.54	-31.83	7.91
Turboprop	-0.23	6.15	1.43	-12.20	27.56	-4.58	6.41
Regional jets	-0.43	15.81	6.46	-144.95	11.82	-31.20	2.84
Narrowbody	-0.14	7.98	1.73	-5.78	15.46	-13.48	9.60
Widebody	-2.80	-2.50	-23.24	-25.11	7.14	-6.29	7.16
Shorter than 750 km	2.06	22.38	24.46	1.94	33.52	-1.81	15.36
750 to 1,500 km	1.52	10.01	4.43	11.53	14.26	-5.16	10.21
1,500 to 2,500 km	-0.34	6.29	-4.36	-4.25	11.51	-13.21	6.59
2,500 to 4,000 km	-1.56	6.29	-18.60	-17.26	7.04	-5.37	6.52
4,000 to 8,000 km	-3.16	-2.85	-10.21	-41.96	3.79	-5.52	7.13
Longer than 8,000 km	-4.63	-5.69	-41.97	-52.16	5.24	-17.45	5.24

Table S63: O_3 annual mean concentration change in ppbv $\cdot (1 \cdot 10^{12}$ kg fuel$)^{-1}$.

Aircraft category	Global	N.A.	EU.	AS.	S.A.	AF. + M.E.	OC.
All aviation	2.7	8.0	18.3	21.6	9.4	21.5	2.2
Piston aircraft	3.1	3.6	109.8	1,304.8	32.5	841.4	1.4
Business jets	1.5	2.6	17.9	88.0	10.8	50.6	2.1
Turboprop	1.5	3.2	13.0	15.4	8.9	12.0	1.3
Regional jets	1.9	3.2	15.5	73.8	5.3	45.6	1.4
Narrowbody	2.1	5.6	12.4	15.8	6.7	25.4	2.3
Widebody	3.1	11.6	22.9	23.4	12.8	18.2	2.1
Shorter than 750 km	2.2	6.1	14.8	17.6	7.1	19.7	2.3
750 to 1,500 km	2.1	6.3	13.8	13.2	7.1	20.8	2.7
1,500 to 2,500 km	2.1	5.4	11.9	15.9	7.4	26.5	2.3
2,500 to 4,000 km	2.2	4.8	15.1	17.5	12.9	16.7	1.8
4,000 to 8,000 km	2.8	9.0	16.3	26.7	10.1	16.1	1.8
Longer than 8,000 km	3.3	13.3	30.2	29.5	11.7	26.3	2.2

Table S64: O_3 peak season concentration change in ppbv $\cdot (1 \cdot 10^{12}$ kg fuel$)^{-1}$.

Aircraft category	Global	N.A.	EU.	AS.	S.A.	AF. + M.E.	OC.
All aviation	2.8	8.1	17.1	22.5	10.8	24.5	2.3
Piston aircraft	3.7	4.4	139.8	1,556.3	31.8	1,048.0	1.5
Business jets	1.6	3.2	16.6	90.5	13.1	59.5	2.3
Turboprop	1.5	3.2	14.0	14.4	9.5	12.9	1.5
Regional jets	1.9	3.7	15.0	74.5	6.0	52.8	1.4
Narrowbody	2.2	5.9	11.9	16.8	7.6	29.5	2.5
Widebody	3.2	11.6	21.2	24.6	14.6	20.8	2.2
Shorter than 750 km	2.3	6.7	15.2	18.0	7.8	22.1	2.7
750 to 1,500 km	2.2	6.7	13.1	14.3	8.3	23.9	2.8
1,500 to 2,500 km	2.2	5.7	11.1	17.0	8.7	31.0	2.5
2,500 to 4,000 km	2.2	5.0	12.7	18.3	15.6	19.2	2.0
4,000 to 8,000 km	2.9	8.9	15.3	28.1	11.6	18.4	1.9
Longer than 8,000 km	3.4	13.5	29.4	31.4	13.0	30.3	2.2

Table S65: $PM_{2.5}$ concentration change in μg m$^{-3} \cdot (1 \cdot 10^{12}$ kg fuel$)^{-1}$.

Aircraft category	Global	N.A.	EU.	AS.	S.A.	AF. + M.E.	OC.
All aviation	0.33	0.35	1.84	3.53	0.21	0.51	0.05
Piston aircraft	1.28	6.03	39.66	220.20	6.23	179.65	1.69
Business jets	0.20	0.27	2.29	14.16	0.38	1.85	0.07
Turboprop	0.22	0.27	1.78	2.87	0.40	0.58	0.06
Regional jets	0.26	0.28	2.03	13.01	0.23	1.60	0.03
Narrowbody	0.29	0.29	1.47	2.95	0.22	0.74	0.06
Widebody	0.35	0.41	2.07	3.64	0.20	0.40	0.04
Shorter than 750 km	0.36	0.49	2.30	3.60	0.36	0.73	0.10
750 to 1,500 km	0.33	0.36	1.69	2.78	0.21	0.62	0.06
1,500 to 2,500 km	0.27	0.27	1.23	2.78	0.18	0.74	0.04
2,500 to 4,000 km	0.24	0.22	1.37	2.64	0.23	0.42	0.04
4,000 to 8,000 km	0.31	0.32	1.56	3.87	0.16	0.37	0.03
Longer than 8,000 km	0.36	0.45	2.51	4.61	0.18	0.54	0.03

Table S66: BC concentration change in μg m$^{-3} \cdot (1 \cdot 10^{15}$ kg fuel$)^{-1}$.

Aircraft category	Global	N.A.	EU.	AS.	S.A.	AF. + M.E.	OC.
All aviation	1.3	4.5	9.2	11.0	4.5	4.9	1.3
Piston aircraft	2.4	14.8	58.9	184.1	9.5	121.3	5.5
Business jets	2.2	11.5	30.5	46.6	13.4	23.0	4.4
Turboprop	1.3	3.6	12.5	12.4	9.8	6.0	2.2
Regional jets	1.1	6.2	11.2	16.2	4.1	8.8	3.1
Narrowbody	2.2	5.8	13.9	18.0	6.9	11.3	2.6
Widebody	0.6	1.8	3.9	5.0	1.6	2.4	0.6
Shorter than 750 km	2.9	10.8	23.2	21.4	12.7	11.6	4.1
750 to 1,500 km	2.5	6.6	15.2	18.2	6.1	8.7	2.9
1,500 to 2,500 km	1.5	4.6	9.0	12.4	4.1	8.8	1.3
2,500 to 4,000 km	0.9	3.5	6.1	7.1	3.7	4.3	1.0
4,000 to 8,000 km	0.5	1.9	3.5	4.4	1.4	2.3	0.6
Longer than 8,000 km	0.4	1.5	3.6	3.9	1.3	2.8	0.5

SI 6.4.7. Air quality impacts per unit NO_x emitted within the same region

Table S67: NO_2 concentration change in ppbv · $(1 \cdot 10^{11}$ kg $NO_x)^{-1}$.

Aircraft category	Global	N.A.	EU.	AS.	S.A.	AF. + M.E.	OC.
All aviation	-0.11	0.30	-0.76	-1.18	0.79	-0.52	0.48
Piston aircraft	0.79	4.02	5.74	281.79	3.44	-6.44	1.71
Business jets	0.03	1.59	0.18	-14.96	1.72	-3.16	0.87
Turboprop	-0.02	0.80	0.15	-1.01	2.02	-0.43	0.61
Regional jets	-0.04	1.46	0.54	-12.16	0.99	-2.75	0.32
Narrowbody	-0.01	0.63	0.13	-0.43	1.19	-1.03	0.75
Widebody	-0.15	-0.14	-1.26	-1.34	0.41	-0.32	0.38
Shorter than 750 km	0.15	1.82	1.75	0.13	2.40	-0.11	1.18
750 to 1,500 km	0.11	0.80	0.34	0.78	1.09	-0.34	0.83
1,500 to 2,500 km	-0.02	0.50	-0.33	-0.29	0.87	-0.82	0.47
2,500 to 4,000 km	-0.11	0.48	-1.40	-1.13	0.53	-0.32	0.47
4,000 to 8,000 km	-0.18	-0.18	-0.58	-2.37	0.25	-0.28	0.41
Longer than 8,000 km	-0.24	-0.29	-2.16	-2.65	0.28	-0.91	0.26

Table S68: O_3 annual mean concentration change in ppbv · $(1 \cdot 10^{11}$ kg $NO_x)^{-1}$.

Aircraft category	Global	N.A.	EU.	AS.	S.A.	AF. + M.E.	OC.
All aviation	17.4	56.3	119.1	132.8	63.1	119.5	13.3
Piston aircraft	97.7	129.5	1,639.2	45,103.5	900.9	15,052.3	42.5
Business jets	15.2	26.4	183.9	878.9	111.8	502.6	23.3
Turboprop	15.5	41.1	134.6	127.5	65.2	111.4	12.5
Regional jets	16.8	29.9	128.8	619.3	44.8	402.6	15.7
Narrowbody	16.0	44.5	95.3	118.7	51.3	194.4	18.2
Widebody	16.8	66.5	124.5	124.7	73.0	91.1	11.4
Shorter than 750 km	15.9	49.4	105.9	113.5	50.6	118.4	17.8
750 to 1,500 km	15.5	50.6	104.9	89.2	54.3	135.0	21.9
1,500 to 2,500 km	15.5	43.7	91.0	108.7	56.3	164.1	16.5
2,500 to 4,000 km	15.4	37.2	113.5	114.9	96.7	99.5	13.3
4,000 to 8,000 km	16.4	56.7	92.3	150.6	65.8	81.7	10.5
Longer than 8,000 km	17.0	68.6	155.5	150.1	63.2	137.3	11.0

Table S69: O_3 peak season concentration change in ppbv · $(1 \cdot 10^{11}$ kg $NO_x)^{-1}$.

Aircraft category	Global	N.A.	EU.	AS.	S.A.	AF. + M.E.	OC.
All aviation	17.8	57.1	111.0	138.6	72.3	136.7	13.9
Piston aircraft	118.9	157.3	2,087.2	53,796.9	882.7	18,748.4	45.6
Business jets	15.9	31.6	170.6	904.1	135.8	590.4	25.0
Turboprop	15.5	41.6	144.3	119.9	69.6	119.6	14.2
Regional jets	17.2	34.5	124.6	624.9	49.9	466.0	15.0
Narrowbody	16.7	46.5	91.8	125.8	58.7	225.4	19.4
Widebody	17.2	66.2	115.4	131.1	83.6	104.2	11.9
Shorter than 750 km	16.6	54.3	108.8	116.5	55.7	132.8	20.6
750 to 1,500 km	16.3	53.4	99.7	97.0	63.1	155.5	22.7
1,500 to 2,500 km	16.3	45.4	85.2	116.4	65.9	192.3	17.5
2,500 to 4,000 km	15.6	38.6	95.6	119.9	116.8	114.4	14.2
4,000 to 8,000 km	16.9	56.2	86.7	158.8	75.5	93.6	10.9
Longer than 8,000 km	17.7	69.5	151.6	159.6	70.0	158.2	11.2

Table S70: $PM_{2.5}$ concentration change in $\mu g\,m^{-3} \cdot (1 \cdot 10^{11}\ kg\ NO_x)^{-1}$.

Aircraft category	Global	N.A.	EU.	AS.	S.A.	AF. + M.E.	OC.
All aviation	2.11	2.44	11.99	21.73	1.43	2.86	0.28
Piston aircraft	40.78	215.41	591.97	7,611.95	173.06	3,213.98	52.61
Business jets	1.97	2.73	23.50	141.47	3.90	18.32	0.73
Turboprop	2.29	3.51	18.37	23.78	2.91	5.39	0.54
Regional jets	2.30	2.58	16.90	109.16	1.96	14.12	0.37
Narrowbody	2.25	2.26	11.28	22.16	1.66	5.63	0.47
Widebody	1.91	2.36	11.24	19.44	1.13	2.00	0.19
Shorter than 750 km	2.58	3.99	16.43	23.28	2.58	4.39	0.75
750 to 1,500 km	2.43	2.85	12.84	18.83	1.63	4.00	0.52
1,500 to 2,500 km	2.02	2.13	9.42	19.03	1.40	4.61	0.31
2,500 to 4,000 km	1.73	1.70	10.34	17.30	1.71	2.52	0.26
4,000 to 8,000 km	1.79	2.03	8.83	21.86	1.01	1.86	0.19
Longer than 8,000 km	1.86	2.33	12.94	23.41	0.96	2.81	0.17

Table S71: BC concentration change in $\mu g\,m^{-3} \cdot (1 \cdot 10^{14}\ kg\ NO_x)^{-1}$.

Aircraft category	Global	N.A.	EU.	AS.	S.A.	AF. + M.E.	OC.
All aviation	8.4	31.5	60.1	67.6	30.6	27.3	8.3
Piston aircraft	75.4	529.1	879.6	6,362.9	263.4	2,169.3	172.2
Business jets	22.2	114.3	312.8	465.7	138.6	228.0	48.6
Turboprop	13.4	46.4	128.7	103.3	71.7	56.2	21.2
Regional jets	10.1	57.3	92.9	136.0	34.6	77.3	33.9
Narrowbody	16.9	45.8	106.8	135.4	52.8	86.5	20.0
Widebody	3.2	10.5	21.0	26.8	9.1	12.2	3.3
Shorter than 750 km	21.0	87.3	166.1	138.4	90.7	69.7	31.3
750 to 1,500 km	18.4	52.4	115.7	123.1	46.6	56.3	23.9
1,500 to 2,500 km	11.4	37.3	69.3	84.7	30.7	54.7	9.6
2,500 to 4,000 km	6.5	26.7	46.2	46.7	27.6	25.5	6.9
4,000 to 8,000 km	2.9	11.7	19.9	25.1	9.0	11.8	3.4
Longer than 8,000 km	2.1	7.9	18.3	19.8	7.0	14.5	2.3

SI 6.4.8. Relative air quality impacts per category

This subsection provides the changes in pollutant concentrations for each aircraft category, relative to the total impact of aviation. A negative value indicates the opposite effect of the overall impact by all aviation. Summed effects smaller than 100% indicate that atmospheric non-linearities lead to an underestimation of the total effect when smaller effects are summed. For example, the overall O_3 impact is underestimated by 5% to 7% when the effects of aircraft categories are summed, which is in line with findings of Koffi et al. [34]. Summed values higher than 100% indicate an overestimation.

Table S72: NO_2 concentration change, relative to all aviation [%].

	Global	N.A.	EU.	AS.	S.A.	AF. + M.E.	OC.
All aviation	**100.00%**	**100.00%**	**100.00%**	**100.00%**	**100.00%**	**100.00%**	**100.00%**
Piston aircraft	-0.05%	0.28%	-0.03%	-0.02%	0.01%	0.00%	0.05%
Business jets	-0.16%	11.70%	-0.10%	1.01%	0.54%	0.89%	0.27%
Turboprop	0.14%	1.96%	-0.14%	0.47%	2.47%	0.35%	3.13%
Regional jets	1.04%	37.07%	-2.34%	5.69%	4.20%	3.98%	0.93%
Narrowbody	3.42%	86.77%	-7.11%	13.31%	68.01%	37.26%	38.06%
Widebody	82.81%	-22.69%	92.10%	70.99%	25.92%	48.01%	57.88%
Summed effect	**87.19%**	**115.08%**	**82.39%**	**91.44%**	**101.14%**	**90.49%**	**100.33%**
Shorter than 750 km	-11.96%	59.04%	-24.91%	-0.98%	42.63%	1.41%	22.78%
750 to 1,500 km	-15.52%	41.09%	-6.75%	-14.06%	22.68%	7.17%	15.06%
1,500 to 2,500 km	3.16%	28.31%	6.87%	3.89%	15.91%	14.58%	8.55%
2,500 to 4,000 km	12.20%	26.88%	17.49%	12.46%	4.65%	9.40%	9.97%
4,000 to 8,000 km	41.25%	-12.68%	22.08%	42.31%	7.17%	20.71%	26.17%
Longer than 8,000 km	51.50%	-19.38%	57.21%	43.91%	8.97%	32.43%	18.08%
Summed effect	**80.63%**	**123.25%**	**71.98%**	**87.52%**	**102.01%**	**85.71%**	**100.61%**

Table S73: O_3 annual mean concentration change, relative to all aviation [%].

	Global	N.A.	EU.	AS.	S.A.	AF. + M.E.	OC.
All aviation	**100.00%**	**100.00%**	**100.00%**	**100.00%**	**100.00%**	**100.00%**	**100.00%**
Piston aircraft	0.04%	0.05%	0.05%	0.04%	0.03%	0.03%	0.04%
Business jets	0.61%	1.04%	0.64%	0.53%	0.44%	0.62%	0.26%
Turboprop	0.59%	0.54%	0.80%	0.53%	1.00%	0.40%	2.30%
Regional jets	2.96%	4.06%	3.56%	2.58%	2.37%	2.55%	1.66%
Narrowbody	32.34%	32.87%	32.33%	32.40%	36.71%	30.83%	33.18%
Widebody	58.44%	56.35%	57.65%	58.76%	58.08%	60.80%	61.85%
Summed effect	**94.97%**	**94.90%**	**95.03%**	**94.84%**	**98.63%**	**95.23%**	**99.29%**
Shorter than 750 km	8.31%	8.59%	9.58%	7.92%	11.28%	6.76%	12.35%
750 to 1,500 km	13.88%	13.90%	13.34%	14.30%	14.22%	12.64%	14.33%
1,500 to 2,500 km	12.68%	13.11%	11.91%	12.91%	12.90%	12.82%	10.76%
2,500 to 4,000 km	10.82%	11.06%	9.01%	11.24%	10.69%	12.78%	10.16%
4,000 to 8,000 km	23.53%	21.36%	22.45%	23.92%	23.86%	26.41%	24.35%
Longer than 8,000 km	23.28%	24.27%	26.17%	22.13%	25.10%	21.44%	26.89%
Summed effect	**92.52%**	**92.28%**	**92.46%**	**92.41%**	**98.05%**	**92.85%**	**98.85%**

Table S74: O_3 peak season concentration change, relative to all aviation [%].

	Global	N.A.	EU.	AS.	S.A.	AF. + M.E.	OC.
All aviation	**100.00%**	**100.00%**	**100.00%**	**100.00%**	**100.00%**	**100.00%**	**100.00%**
Piston aircraft	0.05%	0.06%	0.06%	0.04%	0.03%	0.03%	0.04%
Business jets	0.63%	1.23%	0.64%	0.52%	0.46%	0.63%	0.27%
Turboprop	0.57%	0.54%	0.92%	0.47%	0.93%	0.37%	2.49%
Regional jets	2.97%	4.61%	3.70%	2.50%	2.31%	2.58%	1.52%
Narrowbody	32.97%	33.92%	33.41%	32.91%	36.68%	31.27%	33.73%
Widebody	58.61%	55.37%	57.36%	59.22%	58.06%	60.79%	61.41%
Summed effect	**95.80%**	**95.73%**	**96.09%**	**95.66%**	**98.48%**	**95.68%**	**99.46%**
Shorter than 750 km	8.44%	9.29%	10.56%	7.79%	10.82%	6.62%	13.61%
750 to 1,500 km	14.34%	14.46%	13.61%	14.89%	14.42%	12.73%	14.15%
1,500 to 2,500 km	12.98%	13.45%	11.97%	13.26%	13.18%	13.13%	10.93%
2,500 to 4,000 km	10.76%	11.33%	8.15%	11.25%	11.27%	12.85%	10.33%
4,000 to 8,000 km	23.75%	20.84%	22.63%	24.18%	23.89%	26.46%	23.92%
Longer than 8,000 km	23.70%	24.26%	27.38%	22.55%	24.24%	21.61%	26.20%
Summed effect	**93.97%**	**93.62%**	**94.30%**	**93.92%**	**97.82%**	**93.40%**	**99.15%**

Table S75: $PM_{2.5}$ concentration change, relative to all aviation [%].

	Global	N.A.	EU.	AS.	S.A.	AF. + M.E.	OC.
All aviation	**100.00%**	**100.00%**	**100.00%**	**100.00%**	**100.00%**	**100.00%**	**100.00%**
Piston aircraft	0.13%	1.88%	0.17%	0.04%	0.29%	0.24%	2.45%
Business jets	0.65%	2.48%	0.81%	0.52%	0.68%	0.94%	0.39%
Turboprop	0.71%	1.07%	1.08%	0.60%	1.97%	0.81%	4.68%
Regional jets	3.34%	8.10%	4.64%	2.78%	4.60%	3.75%	1.87%
Narrowbody	37.26%	38.55%	38.03%	36.97%	52.55%	37.35%	40.59%
Widebody	54.79%	46.09%	51.73%	55.98%	39.76%	55.93%	49.63%
Summed effect	**96.89%**	**98.17%**	**96.46%**	**96.89%**	**99.84%**	**99.01%**	**99.60%**
Shorter than 750 km	11.09%	15.99%	14.78%	9.92%	25.39%	10.49%	24.56%
750 to 1,500 km	17.97%	18.07%	16.24%	18.45%	18.91%	15.67%	16.11%
1,500 to 2,500 km	13.59%	14.75%	12.25%	13.82%	14.17%	15.08%	9.63%
2,500 to 4,000 km	10.05%	11.69%	8.16%	10.35%	8.36%	13.56%	9.49%
4,000 to 8,000 km	21.17%	17.60%	21.33%	21.23%	16.27%	25.14%	20.57%
Longer than 8,000 km	21.06%	19.01%	21.64%	21.09%	16.78%	18.38%	19.39%
Summed effect	**94.93%**	**97.11%**	**94.40%**	**94.86%**	**99.90%**	**98.32%**	**99.76%**

Table S76: BC concentration change, relative to all aviation [%].

	Global	N.A.	EU.	AS.	S.A.	AF. + M.E.	OC.
All aviation	**100.00%**	**100.00%**	**100.00%**	**100.00%**	**100.00%**	**100.00%**	**100.00%**
Piston aircraft	0.06%	0.36%	0.05%	0.01%	0.02%	0.02%	0.27%
Business jets	1.85%	8.06%	2.17%	0.55%	1.12%	1.22%	0.88%
Turboprop	1.05%	1.09%	1.51%	0.84%	2.26%	0.88%	6.23%
Regional jets	3.67%	13.91%	5.10%	1.11%	3.78%	2.15%	5.77%
Narrowbody	70.54%	60.59%	71.89%	72.65%	77.95%	60.06%	58.46%
Widebody	22.80%	15.97%	19.29%	24.83%	14.90%	35.61%	28.38%
Summed effect	**99.99%**	**99.98%**	**100.00%**	**99.99%**	**100.03%**	**99.94%**	**99.99%**
Shorter than 750 km	22.71%	27.12%	29.81%	18.97%	41.64%	17.39%	34.79%
750 to 1,500 km	34.14%	25.74%	29.20%	38.78%	25.18%	23.07%	25.02%
1,500 to 2,500 km	19.27%	20.01%	17.98%	19.77%	14.54%	18.70%	10.04%
2,500 to 4,000 km	9.41%	14.22%	7.28%	8.99%	6.28%	14.34%	8.42%
4,000 to 8,000 km	8.60%	7.90%	9.60%	7.83%	6.75%	16.65%	12.76%
Longer than 8,000 km	5.91%	4.98%	6.12%	5.73%	5.70%	9.93%	9.01%
Summed effect	**100.04%**	**99.96%**	**99.99%**	**100.06%**	**100.08%**	**100.09%**	**100.04%**

SI 7. Excess mortality

This chapter provides additional details on the number of mortalities associated with each aircraft category and shows estimates for all aviation-attributable mortality for a range of concentration response functions to assess the uncertainty of health impact estimations. However, it first presents a brief discussion on normalised mortality estimates for various aircraft types on short-haul routes in section SI 7.1.

SI 7.1. Normalised mortality estimates for short-haul routes

When regional variations are minimised by comparing aircraft types on shared short-haul routes, turboprop aircraft show the smallest impact on human health. Figure S144 shows that this aircraft type does not exhibit the highest fuel burn efficiency. However, the negative impacts on ground-level NO_x concentrations and subsequent reductions of nitrate aerosol mixing levels in Asia (not shown) yield a limited overall impact. It is expected that this phenomenon is very sensitive to the selected routes, and thus a different route selection may yield larger impacts for this aircraft type.

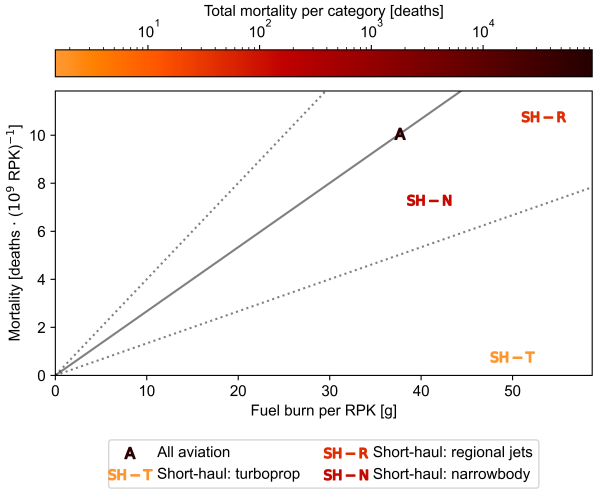

Figure S144: Sensitivity of aviation-attributable mortality rates per RPK to fuel burn per RPK in 2019 per aircraft size on shared short-haul routes. The colour of the markers indicates the total mortality attributed to each aircraft category. The grey line shows the sensitivity for all aviation, with the dashed lines representing a 50% increase or decrease in sensitivity.

In general, the atmospheric sensitivity towards the flights included in figure S144 is smaller than the global average for all aviation, yielding relatively small impacts on human health despite higher fuel burn per RPK. Finally, we note that the majority of impacts are induced in Asia, while most of the fuel burn occurs in Europe and North America. This is in line with the findings of Quadros et al. [15] that a large part of aviation activity in Europe and North America causes air quality degradation outside the respective regions.

SI 7.2. Regional mortality estimates

Tables S77 to S81 provide excess mortality estimates for each aircraft category used in the main study, broken down into individual contributions of species and provided for each of the major six regions used in this study, as well as a global aggregate result. Furthermore, the impact per aircraft category on the total mortality per species in all regions is given for each aircraft size and flight distance in tables S82 and S83.

Table S77: Excess mortalities per region for all flights in 2019.

		Region					
Species	Global	N.A.	EU.	AS.	S.A.	AF. + M.E.	OC.
NO_2	-160	13	-12	-158	4	-4	1
O_3	51,634	5,124	8,445	33,778	760	3,009	44
$PM_{2.5}$	28,197	1,997	7,576	17,993	102	348	10
- of which BC	1,013	136	272	557	11	29	1
All species	**79,671**	**7,134**	**16,009**	**51,614**	**865**	**3,353**	**54**

Table S78: Excess mortalities per region for each aircraft size.

			Region					
Aircraft size	Species	Global	N.A.	EU.	AS.	S.A.	AF. + M.E.	OC.
Piston aircraft	NO_2	0	0	0	0	0	0	0
	O_3	19	3	4	12	0	1	0
	$PM_{2.5}$	61	39	12	7	0	1	0
	- of which BC	1	0	0	0	0	0	0
	All species	**80**	**42**	**16**	**19**	**1**	**1**	**0**
Business jets	NO_2	0	1	0	-1	0	-0	0
	O_3	317	55	55	182	3	18	0
	$PM_{2.5}$	220	57	65	93	1	3	0
	- of which BC	21	11	6	3	0	0	0
	All species	**537**	**114**	**120**	**273**	**4**	**22**	**0**
Turboprops	NO_2	-0	0	0	-1	0	-0	0
	O_3	295	28	69	175	8	12	1
	$PM_{2.5}$	222	22	84	110	2	3	1
	- of which BC	11	1	4	5	0	0	0
	All species	**517**	**50**	**152**	**284**	**9**	**15**	**2**
Regional jets	NO_2	-2	4	1	-8	0	-0	0
	O_3	1,494	214	303	869	18	74	1
	$PM_{2.5}$	1,034	165	354	490	5	13	0
	- of which BC	42	19	14	6	0	1	0
	All species	**2,526**	**383**	**658**	**1,351**	**23**	**87**	**1**
Narrowbody	NO_2	-16	10	6	-33	2	-2	0
	O_3	16,761	1,684	2,720	10,992	275	928	14
	$PM_{2.5}$	10,839	794	2,945	6,841	55	137	4
	- of which BC	712	82	196	403	9	18	1
	All species	**27,584**	**2,488**	**5,672**	**17,800**	**332**	**1,064**	**19**
Widebody	NO_2	-121	-2	-15	-101	1	-2	0
	O_3	30,265	2,898	4,900	19,864	447	1,845	27
	$PM_{2.5}$	14,966	887	3,843	9,912	39	188	5
	- of which BC	227	22	51	140	2	10	0
	All species	**45,109**	**3,784**	**8,728**	**29,675**	**487**	**2,030**	**32**
Summed effect	NO_2	-140	15	-8	-144	4	-4	1
	O_3	49,151	4,882	8,050	32,094	751	2,879	43
	$PM_{2.5}$	27,341	1,965	7,303	17,453	102	345	10
	- of which BC	1,013	136	272	557	11	29	1
	All species	**76,352**	**6,861**	**15,346**	**49,403**	**857**	**3,219**	**54**

Table S79: Excess mortalities per region for each flight distance.

Flight distance [km]	Species	Global	Region N.A.	EU.	AS.	S.A.	AF. + M.E.	OC.
< 750	NO_2	15	7	8	-1	1	-0	0
	O_3	4,246	451	812	2,657	83	199	5
	$PM_{2.5}$	3,420	333	1,150	1,853	25	38	3
	- of which BC	236	37	81	106	5	5	0
	All species	**7,681**	**790**	**1,970**	**4,509**	**109**	**237**	**8**
750 - 1,500	NO_2	17	5	3	8	1	-0	0
	O_3	7,213	718	1,128	4,810	110	381	6
	$PM_{2.5}$	5,179	366	1,258	3,449	21	57	2
	- of which BC	342	35	80	214	3	7	0
	All species	**12,409**	**1,090**	**2,390**	**8,267**	**132**	**437**	**8**
1,500 - 2,500	NO_2	-9	3	-1	-11	1	-1	0
	O_3	6,616	668	995	4,410	96	385	5
	$PM_{2.5}$	3,846	299	931	2,524	15	53	1
	- of which BC	195	27	49	110	2	5	0
	All species	**10,454**	**970**	**1,926**	**6,924**	**111**	**437**	**6**
2,500 - 4,000	NO_2	-20	3	-4	-19	0	-0	0
	O_3	5,738	559	750	3,906	80	392	4
	$PM_{2.5}$	2,769	237	608	1,849	8	47	1
	- of which BC	95	19	19	50	1	4	0
	All species	**8,487**	**799**	**1,355**	**5,736**	**88**	**438**	**5**
4,000 - 8,000	NO_2	-62	-1	-2	-58	0	-1	0
	O_3	12,292	1,094	1,902	8,187	182	801	11
	$PM_{2.5}$	5,795	338	1,592	3,726	16	83	2
	- of which BC	88	11	26	45	1	5	0
	All species	**18,025**	**1,431**	**3,493**	**11,855**	**199**	**884**	**13**
> 8,000	NO_2	-72	-2	-11	-57	0	-1	0
	O_3	11,849	1,266	2,255	7,341	196	658	12
	$PM_{2.5}$	5,806	373	1,606	3,707	17	63	2
	- of which BC	60	7	16	32	1	3	0
	All species	**17,583**	**1,637**	**3,851**	**10,991**	**214**	**720**	**14**
Summed effect	NO_2	-130	16	-6	-137	4	-4	1
	O_3	47,955	4,756	7,843	31,311	747	2,815	43
	$PM_{2.5}$	26,815	1,946	7,146	17,108	102	342	10
	- of which BC	1,014	136	272	558	11	29	1
	All species	**74,639**	**6,718**	**14,983**	**48,281**	**853**	**3,153**	**53**

Table S80: Excess mortalities per region for each aircraft type on short-haul routes.

			Region					
Aircraft size	Species	Global	N.A.	EU.	AS.	S.A.	AF. + M.E.	OC.
Turboprops	NO_2	0	0	0	-0	-0	0	0
	O_3	9	1	2	5	0	0	0
	$PM_{2.5}$	-8	1	3	-12	0	0	0
	- of which BC	0	0	0	0	0	0	0
	All species	**2**	**2**	**6**	**-7**	**0**	**0**	**0**
Regional jets	NO_2	-0	0	0	-0	0	-0	0
	O_3	25	3	6	14	0	1	0
	$PM_{2.5}$	18	2	7	9	0	0	0
	- of which BC	1	0	0	0	0	0	0
	All species	**44**	**4**	**13**	**23**	**0**	**1**	**0**
Narrowbody	NO_2	-0	0	0	-0	-0	0	0
	O_3	87	9	20	50	3	5	1
	$PM_{2.5}$	41	6	22	11	0	1	0
	- of which BC	4	1	2	1	0	0	0
	All species	**128**	**14**	**42**	**61**	**3**	**6**	**1**

Table S81: Excess mortalities per region for intra-European flights shorter than 750 km in 2019.

		Region					
Species	Global	N.A.	EU.	AS.	S.A.	AF. + M.E.	OC.
NO_2	2	-1	10	-8	-0	-0	-0
O_3	1,353	74	481	738	-0	42	-0
$PM_{2.5}$	1,408	22	872	490	0	13	-0
- of which BC	83	0	70	10	0	2	0
All species	**2,762**	**96**	**1,364**	**1,220**	**-0**	**55**	**-0**

Table S82: Excess mortality per region for each aircraft size. Given in percentage of the impact caused by all aviation.

Aircraft size	Species	Global	N.A.	EU.	AS.	S.A.	AF. + M.E.	OC.
Piston aircraft	NO_2	-0.03	0.26	-0.07	-0.00	0.01	-0.01	0.05
	O_3	0.04	0.05	0.05	0.03	0.03	0.03	0.04
	$PM_{2.5}$	0.21	1.98	0.16	0.04	0.28	0.21	1.93
	- of which BC	0.07	0.37	0.05	0.01	0.02	0.02	0.27
	All species	**0.10**	**0.59**	**0.10**	**0.04**	**0.06**	**0.04**	**0.38**
Business jets	NO_2	-0.04	10.81	-1.06	0.91	0.55	0.85	0.27
	O_3	0.61	1.07	0.65	0.54	0.41	0.61	0.26
	$PM_{2.5}$	0.78	2.87	0.86	0.51	0.70	0.95	0.42
	- of which BC	2.06	8.22	2.19	0.56	1.15	1.26	0.88
	All species	**0.67**	**1.59**	**0.75**	**0.53**	**0.45**	**0.65**	**0.29**
Turboprop	NO_2	0.07	1.49	-1.58	0.35	2.04	0.06	3.16
	O_3	0.57	0.55	0.81	0.52	0.99	0.40	2.30
	$PM_{2.5}$	0.79	1.10	1.10	0.61	1.74	0.84	5.58
	- of which BC	1.09	1.03	1.54	0.86	2.11	1.00	6.32
	All species	**0.65**	**0.70**	**0.95**	**0.55**	**1.09**	**0.45**	**2.90**
Regional jets	NO_2	1.53	33.27	-8.46	4.90	5.14	2.82	0.93
	O_3	2.89	4.17	3.59	2.57	2.39	2.46	1.66
	$PM_{2.5}$	3.67	8.25	4.67	2.73	4.96	3.64	2.34
	- of which BC	4.10	14.10	5.28	1.14	4.20	2.34	5.73
	All species	**3.17**	**5.37**	**4.11**	**2.62**	**2.71**	**2.58**	**1.77**
Narrowbody	NO_2	10.13	80.53	-51.28	20.66	65.91	35.47	38.04
	O_3	32.46	32.87	32.21	32.54	36.20	30.86	33.14
	$PM_{2.5}$	38.44	39.75	38.88	38.02	53.73	39.38	41.96
	- of which BC	70.24	60.33	72.05	72.24	77.11	60.43	58.43
	All species	**34.62**	**34.88**	**35.43**	**34.49**	**38.38**	**31.74**	**34.79**
Widebody	NO_2	75.79	-13.63	129.98	64.32	27.38	51.86	57.88
	O_3	58.61	56.57	58.02	58.81	58.84	61.32	61.93
	$PM_{2.5}$	53.08	44.44	50.73	55.09	38.58	53.91	47.41
	- of which BC	22.43	15.93	18.89	25.18	15.43	34.90	28.37
	All species	**56.62**	**53.04**	**54.52**	**57.49**	**56.33**	**60.56**	**59.26**
Summed effect	NO_2	87.45	112.74	67.52	91.13	101.04	91.06	100.33
	O_3	95.19	95.27	95.33	95.01	98.87	95.68	99.34
	$PM_{2.5}$	96.97	98.39	96.41	97.00	100.00	98.93	99.64
	- of which BC	99.99	99.98	100.00	99.99	100.02	99.95	99.99
	Total mortality	**95.83**	**96.18**	**95.86**	**95.72**	**99.01**	**96.02**	**99.40**

Table S83: Excess mortality per region for each flight distance. Given in percentage of the impact caused by all aviation.

Flight distance [km]	Species	Global	N.A.	EU.	AS.	S.A.	AF. + M.E.	OC.
< 750	NO_2	-9.60	52.09	-68.42	0.38	38.77	0.22	22.80
	O_3	8.22	8.80	9.62	7.87	10.92	6.62	12.32
	$PM_{2.5}$	12.13	16.67	15.17	10.30	24.13	10.85	26.07
	- of which BC	23.24	27.09	29.84	19.06	39.66	17.42	34.90
	All species	**9.64**	**11.08**	**12.30**	**8.74**	**12.59**	**7.06**	**14.92**
750 - 1,500	NO_2	-10.71	38.50	-29.62	-5.32	24.78	6.11	15.03
	O_3	13.97	14.02	13.36	14.24	14.43	12.65	14.30
	$PM_{2.5}$	18.37	18.35	16.61	19.17	21.01	16.35	15.96
	- of which BC	33.71	25.89	29.53	38.43	26.50	23.49	24.91
	All species	**15.58**	**15.27**	**14.93**	**16.02**	**15.25**	**13.04**	**14.61**
1,500 - 2,500	NO_2	5.50	26.70	6.57	6.99	16.10	16.69	8.59
	O_3	12.81	13.03	11.79	13.06	12.68	12.78	10.79
	$PM_{2.5}$	13.64	14.99	12.29	14.03	14.24	15.28	10.37
	- of which BC	19.20	19.94	18.01	19.73	14.72	18.45	10.07
	All species	**13.12**	**13.60**	**12.03**	**13.41**	**12.88**	**13.04**	**10.69**
2,500 - 4,000	NO_2	12.58	25.60	31.61	12.19	4.17	10.28	9.98
	O_3	11.11	10.91	8.88	11.56	10.48	13.01	10.19
	$PM_{2.5}$	9.82	11.87	8.03	10.28	8.08	13.58	9.87
	- of which BC	9.34	14.19	7.07	9.05	6.12	14.05	8.42
	All species	**10.65**	**11.21**	**8.46**	**11.11**	**10.18**	**13.08**	**10.13**
4,000 - 8,000	NO_2	38.45	-8.08	13.20	36.48	7.60	23.42	26.11
	O_3	23.81	21.35	22.52	24.24	24.01	26.63	24.36
	$PM_{2.5}$	20.55	16.92	21.02	20.71	15.93	23.96	18.29
	- of which BC	8.64	7.93	9.54	7.99	6.96	15.88	12.69
	All species	**22.62**	**20.06**	**21.82**	**22.97**	**22.99**	**26.36**	**23.28**
> 8,000	NO_2	44.93	-15.13	94.62	36.27	10.39	29.92	18.10
	O_3	22.95	24.71	26.71	21.73	25.86	21.86	26.97
	$PM_{2.5}$	20.59	18.66	21.20	20.60	16.71	18.19	19.03
	- of which BC	5.91	4.92	6.00	5.82	6.10	10.81	9.05
	All species	**22.07**	**22.94**	**24.05**	**21.29**	**24.72**	**21.47**	**25.43**
Summed effect	NO_2	81.16	119.70	47.97	87.00	101.81	86.63	100.61
	O_3	92.87	92.81	92.87	92.70	98.38	93.55	98.92
	$PM_{2.5}$	95.10	97.46	94.32	95.08	100.10	98.21	99.58
	- of which BC	100.03	99.97	100.00	100.07	100.07	100.10	100.04
	Total mortality	**93.69**	**94.16**	**93.59**	**93.54**	**98.59**	**94.04**	**99.06**

SI 7.3. Normalised global mortality estimates

This section provides global mortality estimates for each aircraft category, separated per species, with a 95% confidence interval based on the concentration response functions that were used. Tables S84 to S88 also show the normalised mortality results for various metrics to allow the identification of sensitivity trends. First, however, the sensitivity of aviation-attributable mortality towards NO_x emissions (both normalised per RPK) is presented for each of the aircraft categories in the figures below.

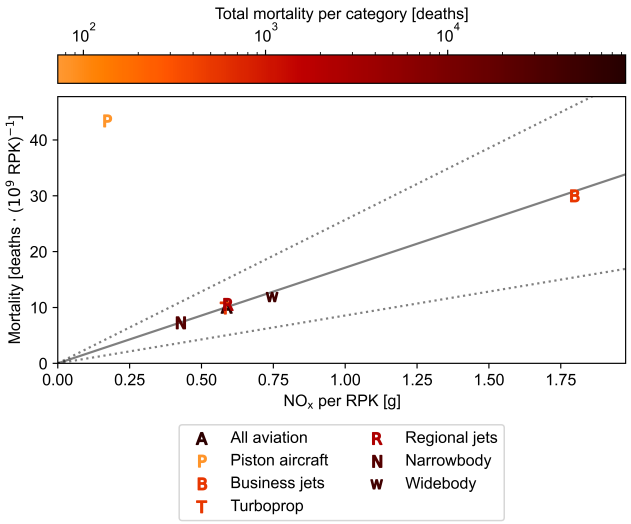

Figure S145: Sensitivity of aviation-attributable mortality rates per RPK to NO_x emissions per RPK in 2019 per aircraft size. The colour of the markers indicates the total mortality attributed to each aircraft category. The grey line shows the sensitivity for all aviation, with the dashed lines representing a 50% increase or decrease in sensitivity.

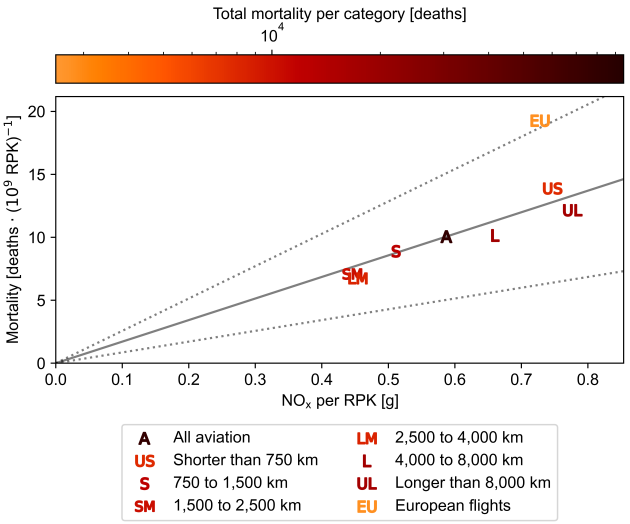

Figure S146: Sensitivity of aviation-attributable mortality rates per RPK to NO_x emissions per RPK in 2019 per flight distance. The colour of the markers indicates the total mortality attributed to each aircraft category. The grey line shows the sensitivity for all aviation, with the dashed lines representing a 50% increase or decrease in sensitivity.

Table S84: Mortality per metric for all flights in 2019.

			Normalised per:			
Species	Estimate	95% CI	$1 \cdot 10^{12}$ RPK	$1 \cdot 10^{9}$ pax	$1 \cdot 10^{6}$ flights	Tg fuel
NO_2	-160	(-114 - -213)	-20	-39	-4	-1
O_3	51,634	(35,127 - 67,507)	6,575	12,617	1,223	174
$PM_{2.5}$	28,197	(19,793 - 37,805)	3,591	6,890	668	95
- of which BC	1,013	(819 - 1,206)	129	248	24	3
All species	**79,671**	**(55,625 - 106,305)**	**10,145**	**19,468**	**1,887**	**269**

Table S85: Mortality per metric for various aircraft sizes.

Aircraft size	Species	Estimate	95% CI	Normalised per: $1 \cdot 10^{12}$ RPK	$1 \cdot 10^{9}$ pax	$1 \cdot 10^{6}$ flights	Tg fuel
Piston aircraft	NO_2	0	(0 - 0)	26	5	0	0
	O_3	19	(13 - 25)	10,437	1,861	10	192
	$PM_{2.5}$	61	(44 - 78)	32,747	5,838	33	604
	- of which BC	1	(1 - 1)	381	68	0	7
	All species	**80**	**(58 - 104)**	**43,210**	**7,703**	**43**	**796**
Business jets	NO_2	0	(0 - 0)	3	4	0	0
	O_3	317	(215 - 415)	17,595	18,790	137	98
	$PM_{2.5}$	220	(158 - 290)	12,225	13,055	95	68
	- of which BC	21	(17 - 25)	1,157	1,236	9	6
	All species	**537**	**(390 - 729)**	**29,823**	**31,849**	**233**	**165**
Turboprop	NO_2	-0	(-0 - -0)	-2	-1	-0	-0
	O_3	295	(200 - 387)	5,665	2,114	67	95
	$PM_{2.5}$	222	(158 - 294)	4,261	1,590	50	71
	- of which BC	11	(9 - 13)	212	79	2	4
	All species	**517**	**(367 - 694)**	**9,924**	**3,704**	**117**	**166**
Regional jets	NO_2	-2	(-3 - -2)	-10	-8	-0	-0
	O_3	1,494	(1,014 - 1,956)	6,246	5,057	267	118
	$PM_{2.5}$	1,034	(733 - 1,374)	4,325	3,502	185	82
	- of which BC	42	(34 - 49)	174	141	7	3
	All species	**2,526**	**(1,779 - 3,376)**	**10,561**	**8,551**	**452**	**200**
Narrowbody	NO_2	-16	(-22 - -12)	-4	-6	-1	-0
	O_3	16,761	(11,389 - 21,939)	4,416	6,007	699	135
	$PM_{2.5}$	10,839	(7,647 - 14,475)	2,856	3,884	452	87
	- of which BC	712	(575 - 847)	188	255	30	6
	All species	**27,584**	**(19,600 - 37,239)**	**7,268**	**9,886**	**1,150**	**222**
Widebody	NO_2	-121	(-161 - -86)	-32	-144	-30	-1
	O_3	30,265	(20,574 - 39,596)	8,078	36,029	7,495	198
	$PM_{2.5}$	14,966	(10,457 - 20,142)	3,994	17,816	3,706	98
	- of which BC	227	(184 - 271)	61	271	56	1
	All species	**45,109**	**(31,128 - 59,847)**	**12,040**	**53,701**	**11,171**	**296**

Table S86: Mortality per metric for various flight distances.

Stage length [km]	Species	Estimate	95% CI	Normalised per: $1 \cdot 10^{12}$ RPK	$1 \cdot 10^{9}$ pax	$1 \cdot 10^{6}$ flights	Tg fuel
< 750	NO_2	15	(11 - 20)	27	13	1	1
	O_3	4,246	(2,884 - 5,560)	7,576	3,562	238	142
	$PM_{2.5}$	3,420	(2,429 - 4,537)	6,101	2,869	192	114
	- of which BC	236	(190 - 280)	420	198	13	8
	All species	**7,681**	**(5,514 - 10,398)**	**13,704**	**6,444**	**430**	**257**
750 - 1,500	NO_2	17	(12 - 23)	12	13	1	0
	O_3	7,213	(4,899 - 9,444)	5,120	5,627	584	137
	$PM_{2.5}$	5,179	(3,650 - 6,925)	3,677	4,041	419	98
	- of which BC	342	(276 - 406)	242	266	28	6
	All species	**12,409**	**(8,837 - 16,799)**	**8,809**	**9,681**	**1,004**	**236**
1,500 - 2,500	NO_2	-9	(-12 - -6)	-6	-11	-1	-0
	O_3	6,616	(4,494 - 8,663)	4,495	8,583	986	136
	$PM_{2.5}$	3,846	(2,704 - 5,152)	2,613	4,990	573	79
	- of which BC	195	(157 - 231)	132	252	29	4
	All species	**10,454**	**(7,349 - 14,035)**	**7,102**	**13,562**	**1,559**	**215**
2,500 - 4,000	NO_2	-20	(-27 - -14)	-16	-50	-7	-1
	O_3	5,738	(3,898 - 7,514)	4,604	14,293	1,865	143
	$PM_{2.5}$	2,769	(1,940 - 3,718)	2,221	6,896	900	69
	- of which BC	95	(76 - 113)	76	236	31	2
	All species	**8,487**	**(5,900 - 11,318)**	**6,809**	**21,139**	**2,759**	**211**
4,000 - 8,000	NO_2	-62	(-82 - -44)	-35	-204	-39	-1
	O_3	12,292	(8,351 - 16,091)	7,032	40,701	7,808	183
	$PM_{2.5}$	5,795	(4,051 - 7,796)	3,315	19,189	3,681	86
	- of which BC	88	(71 - 104)	50	290	56	1
	All species	**18,025**	**(12,429 - 23,909)**	**10,312**	**59,686**	**11,450**	**268**
> 8,000	NO_2	-72	(-96 - -51)	-51	-498	-111	-1
	O_3	11,849	(8,050 - 15,512)	8,359	82,078	18,248	207
	$PM_{2.5}$	5,806	(4,057 - 7,812)	4,095	40,215	8,941	101
	- of which BC	60	(48 - 71)	42	415	92	1
	All species	**17,583**	**(12,104 - 23,300)**	**12,403**	**121,795**	**27,078**	**307**

Table S87: Mortality per metric for various aircraft sizes on short-haul routes.

Aircraft size	Species	Estimate	95% CI	Normalised per: $1 \cdot 10^{12}$ RPK	$1 \cdot 10^{9}$ pax	$1 \cdot 10^{6}$ flights	Tg fuel
Turboprop	NO_2	0	(0 - 0)	2	1	0	0
	O_3	9	(6 - 12)	4,409	2,925	132	88
	$PM_{2.5}$	-8	(-11 - -5)	-3,673	-2,436	-110	-74
	- of which BC	0	(0 - 0)	150	100	5	3
	All species	**2**	**(1 - 2)**	**738**	**489**	**22**	**15**
Regional jets	NO_2	-0	(-0 - -0)	-19	-12	-1	-0
	O_3	25	(17 - 33)	6,270	4,184	266	117
	$PM_{2.5}$	18	(13 - 25)	4,575	3,052	194	86
	- of which BC	1	(1 - 1)	202	135	9	4
	All species	**44**	**(31 - 58)**	**10,826**	**7,224**	**459**	**203**
Narrowbody	NO_2	-0	(-0 - -0)	-1	-1	-0	-0
	O_3	87	(59 - 114)	4,930	3,388	384	121
	$PM_{2.5}$	41	(30 - 54)	2,346	1,612	182	57
	- of which BC	4	(3 - 5)	220	151	17	5
	All species	**128**	**(92 - 172)**	**7,275**	**4,999**	**566**	**178**

Table S88: Mortality per metric for inter-European flights shorter than 750 km.

Species	Estimate	95% CI	Normalised per: $1 \cdot 10^{12}$ RPK	$1 \cdot 10^{9}$ pax	$1 \cdot 10^{6}$ flights	Tg fuel
NO_2	2	(1 - 2)	11	5	0	0
O_3	1,353	(919 - 1,771)	9,338	4,372	385	181
$PM_{2.5}$	1,408	(1,005 - 1,857)	9,718	4,550	401	188
- of which BC	83	(67 - 99)	575	269	24	11
All species	**2,762**	**(1,992 - 3,730)**	**19,066**	**8,927**	**786**	**370**

SI 7.4. Global mortality estimates using alternative CRFs

In this section, the alternative concentration response functions from section SI 4.3 are used to estimate the global mortality for each species. This provides insights into the uncertainty associated with the selection of a specific CRF.

Table S89: Global aviation-attributable mortality estimates for NO_2 using alternative concentration response functions. The CRF in bold indicates the one used in the main study.

CRF	End-point	Estimate	95% CI
Faustini	**Respiratory**	**-160**	**(-213 - -114)**
Hoek	All cause	-2,288	(-3,290 - -1,304)
Huangfu	All cause	-846	(-1,675 - -425)
Huangfu	Respiratory	-200	(-329 - -67)
Beelen (multi-pollutant)	All cause	-425	(-2,085 - 1,299)
Beelen (single-pollutant)	All cause	-425	(-1,675 - 429)
Faustini	All cause	-1,716	(-2,651 - -804)
Faustini	Cardiovascular	-2,329	(-3,090 - -1,572)
Turner	All cause	-891	(-1,324 - -671)
Turner	Circulatory	-791	(-886 - -599)

Table S90: Global aviation-attributable mortality estimates for O_3 using alternative concentration response functions. The CRF in bold indicates the one used in the main study.

CRF	End-point	Estimate	95% CI
Turner	**Respiratory**	**51,634**	**(35,127 - 67,507)**
Huangfu	All cause	69,518	(0 - 138,213)
Huangfu	Respiratory	18,263	(-9,297 - 44,866)
Jerrett (multi-pollutant)	Respiratory	19,226	(6,340 - 31,747)
Jerrett (single-pollutant)	Respiratory	13,069	(3,425 - 22,039)
Turner	All cause	69,610	(34,995 - 137,736)
Turner (threshold)	Respiratory	60,823	(40,536 - 76,872)
Di (multi-pollutant)	All cause	36,098	(32,834 - 39,359)
DI (single-pollutant)	All cause	74,991	(71,769 - 78,209)

Table S91: Global aviation-attributable mortality estimates for $PM_{2.5}$ using alternative concentration response functions. The CRF in bold indicates the one used in the main study.

CRF	End-point	Estimate	95% CI
Burnett	**NCD + LRI**	**27,309**	**(19,064 - 36,766)**
Hoek	All cause	25,306	(16,907 - 33,925)
Hoek	Cardiovascular	17,016	(8,886 - 25,056)
Jannsen	All cause	29,343	(16,797 - 37,682)
Di (multi-pollutant)	All cause	29,638	(28,854 - 30,421)
Di (single-pollutant)	All cause	33,925	(32,761 - 34,700)
Krewski	All cause	12,438	(4,188 - 20,527)
Krewski	Cardiopulmonary	19,565	(13,232 - 25,722)
Jerrett (single-pollutant)	Cardiovascular	23,596	(17,777 - 29,501)
Jerrett (multi-pollutant)	Cardiovascular	31,610	(23,596 - 39,520)
Chen	All cause	32,372	(24,513 - 36,245)
Vodonos	All cause	43,093	(40,597 - 46,418)
Beelen	All cause	56,888	(16,665 - 102,660)

Table S92: Global aviation-attributable mortality estimates for BC using alternative concentration response functions. The CRF in bold indicates the one used in the main study.

CRF	End-point	Estimate	95% CI
Hoek	**All cause**	**1,013**	**(819 - 1,206)**
Janssen	All cause	997	(671 - 1,475)

SI 7.5. Effects of BC versus general $PM_{2.5}$

In tables S93 to S97, the difference in impacts between two approaches for $PM_{2.5}$ is shown. The separated impacts show the contribution of BC and other $PM_{2.5}$ separately, with a more sensitive CRF applied to the BC. When no distinction is used between the $PM_{2.5}$ constituents and BC is treated with the same toxicity as other $PM_{2.5}$, a smaller overall impact is observed.

Table S93: Impact of non-uniform toxicity for $PM_{2.5}$ on global premature mortality estimates for all aviation. A comparison between a uniform approach and increased toxicity for BC.

Separated $PM_{2.5}$ impacts			Uniform $PM_{2.5}$
BC	Other $PM_{2.5}$	Combined	
1,013	27,183	28,197	27,309

Table S94: Impact of non-uniform toxicity for $PM_{2.5}$ on global premature mortality estimates per aircraft size. A comparison between a uniform approach and increased toxicity for BC.

Aircraft size	Separated $PM_{2.5}$ impacts			Uniform $PM_{2.5}$
	BC	Other $PM_{2.5}$	Combined	
Piston	1	60	61	60
Business jets	21	199	220	203
Turboprop	11	211	222	212
Regional jets	42	993	1,034	999
Narrowbody	712	10,127	10,839	10,214
Widebody	227	14,739	14,966	14,766

Table S95: Impact of non-uniform toxicity for $PM_{2.5}$ on global premature mortality estimates per flight distance. A comparison between a uniform approach and increased toxicity for BC.

Flight distance [km]	Separated $PM_{2.5}$ impacts			Uniform $PM_{2.5}$
	BC	Other $PM_{2.5}$	Combined	
< 750	236	3,184	3,420	3,215
750 - 1,500	342	4,838	5,179	4,879
1,500 - 2,500	195	3,652	3,846	3,676
2,500 - 4,000	95	2,674	2,769	2,686
4,000 - 8,000	88	5,707	5,795	5,718
> 8,000	60	5,746	5,806	5,753

Table S96: Impact of non-uniform toxicity for $PM_{2.5}$ on global premature mortality estimates per aircraft size on shared short-haul routes. A comparison between a uniform approach and increased toxicity for BC.

Aircraft size	Separated $PM_{2.5}$ impacts			Uniform $PM_{2.5}$
	BC	Other $PM_{2.5}$	Combined	
Turboprop	0	-8	-8	-8
Regional jets	1	18	18	18
Narrowbody	4	37	41	38

Table S97: Impact of non-uniform toxicity for $PM_{2.5}$ on global premature mortality estimates for intra-European flights shorter than 750 km. A comparison between a uniform approach and increased toxicity for BC.

Separated $PM_{2.5}$ impacts			Uniform $PM_{2.5}$
BC	Other $PM_{2.5}$	Combined	
83	1,324	1,408	1,335

References

[1] B. Graver, K. Zhang, and D. Rutherford. CO_2 emissions from commercial aviation, 2018. Technical report, International Council on Clean Transportation, September 2019.

[2] B. Graver, D. Rutherford, and S. Zheng. CO_2 emissions from commercial aviation: 2013, 2018, and 2019. Technical report, International Council on Clean Transportation, October 2020.

[3] B. Graver and D. Rutherford. Low-Cost Carriers and U.S. Aviation Emissions Growth, 2005-2009. White paper, March 2018. URL https://theicct.org/publication/low-cost-carriers-and-u-s-aviation-emissions-growth-2005-to-2019/.

[4] F. D. A. Quadros, M. Snellen, J. Sun, and I. C. Dedoussi. Global Civil Aviation Emissions Estimates for 2017–2020 Using ADS-B Data. *Journal of Aircraft*, pages 1–11, May 2022. ISSN 1533-3868. DOI: 10.2514/1.C036763.

[5] W. Hoermann. Introduction to the ICAO Engine Emissions Databank. Technical report, European Union Aviation Safety Agency, 2021.

[6] D. S. Lee, G. Pitari, V. Grewe, K. Gierens, J. E. Penner, A. Petzold, M. J. Prather, U. Schumann, A. Bais, T. Berntsen, D. Iachetti, L. L. Lim, and R. Sausen. Transport impacts on atmosphere and climate: Aviation. *Atmospheric Environment*, 44:4678–4734, December 2010. ISSN 13522310. DOI: 10.1016/j.atmosenv.2009.06.005.

[7] M. E. Stettler, A. M. Boies, A. Petzold, and S. R. Barrett. Global Civil Aviation Black Carbon Emissions. *Environmental Science and Technology*, 47:10397–10404, September 2013. ISSN 0013936X. DOI: 10.1021/es401356v.

[8] X. Liu, K. Chance, C. E. Sioris, T. P. Kurosu, R. J. Spurr, R. V. Martin, T. M. Fu, J. A. Logan, D. J. Jacob, P. I. Palmer, M. J. Newchurch, I. A. Megretskaia, and R. B. Chatfield. First directly retrieved global distribution of tropospheric column ozone from GOME: Comparison with the GEOS-CHEM model. *Journal of Geophysical Research Atmospheres*, 111, January 2006. ISSN 01480227. DOI: 10.1029/2005JD006564.

[9] A. P. Protonotariou, M. Tombrou, C. Giannakopoulos, E. Kostopoulou, and P. L. Sager. Study of CO surface pollution in Europe based on observations and nested-grid applications of GEOS-CHEM global chemical transport model. *Tellus, Series B: Chemical and Physical Meteorology*, 62:209–227, September 2010. ISSN 02806509. DOI: 10.1111/j.1600-0889.2010.00462.x.

[10] S. D. Eastham, D. K. Weisenstein, and S. R. Barrett. Development and evaluation of the unified tropospheric-stratospheric chemistry extension (UCX) for the global chemistry-transport model GEOS-Chem. *Atmospheric Environment*, 89:52–63, June 2014. ISSN 13522310. DOI: 10.1016/j.atmosenv.2014.02.001.

[11] Y. Y. Yan, J. T. Lin, Y. Kuang, D. Yang, and L. Zhang. Tropospheric carbon monoxide over the Pacific during HIPPO: two-way coupled simulation of GEOS-Chem and its multiple nested models. *Atmospheric Chemistry and Physics*, 14:12649–12663, December 2014. ISSN 16807324. DOI: 10.5194/acp-14-12649-2014.

[12] S. D. Eastham and S. R. Barrett. Aviation-attributable ozone as a driver for changes in mortality related to air quality and skin cancer. *Atmospheric Environment*, 144:17–23, November 2016. ISSN 1352-2310. DOI: 10.1016/J.ATMOSENV.2016.08.040.

[13] S. D. Eastham, M. S. Long, C. A. Keller, E. Lundgren, R. M. Yantosca, J. Zhuang, C. Li, C. J. Lee, M. Yannetti, B. M. Auer, T. L. Clune, J. Kouatchou, W. M. Putman, M. A. Thompson, A. L. Trayanov, A. M. Molod, R. V. Martin, and D. J. Jacob. GEOS-Chem High Performance (GCHP v11-02c): A next-generation implementation of the GEOS-Chem chemical transport model for massively parallel applications. *Geoscientific Model Development*, 11:2941–2953, July 2018. ISSN 19919603. DOI: 10.5194/gmd-11-2941-2018.

[14] L. Hu, C. A. Keller, M. S. Long, T. Sherwen, B. Auer, A. D. Silva, J. E. Nielsen, S. Pawson, M. A. Thompson, A. L. Trayanov, K. R. Travis, S. K. Grange, M. J. Evans, and D. J. Jacob. Global simulation of tropospheric chemistry at 12.5 km resolution: performance and evaluation of the GEOS-Chem chemical module (v10-1) within the NASA GEOS Earth system model (GEOS-5 ESM). *Geoscientific Model Development*, 11:4603–4620, November 2018. ISSN 19919603. DOI: 10.5194/gmd-11-4603-2018.

[15] F. D. Quadros, M. Snellen, and I. C. Dedoussi. Regional sensitivities of air quality and human health impacts to aviation emissions. *Environmental Research Letters*, 15, October 2020. ISSN 17489326. DOI: 10.1088/1748-9326/abb2c5.

[16] Global Health Estimates 2019: Deaths by Cause, Age, Sex, by Country and by Region, 2000-2019. Technical report, World Health Organization, Geneva, 2020.

[17] R. Burnett, H. Chen, M. Szyszkowicz, N. Fann, B. Hubbell, C. A. Pope, J. S. Apte, M. Brauer, A. Cohen, S. Weichenthal, J. Coggins, Q. Di, B. Brunekreef, J. Frostad, S. S. Lim, H. Kan, K. D. Walker, G. D. Thurston, R. B. Hayes, C. C. Lim, M. C. Turner, M. Jerrett, D. Krewski, S. M. Gapstur, W. R. Diver, B. Ostro, D. Goldberg, D. L. Crouse, R. V. Martin, P. Peters, L. Pinault, M. Tjepkema, A. V. Donkelaar, P. J. Villeneuve, A. B. Miller, P. Yin, M. Zhou, L. Wang, N. A. Janssen, M. Marra, R. W. Atkinson, H. Tsang, T. Q. Thach, J. B. Cannon, R. T. Allen, J. E. Hart, F. Laden, G. Cesaroni, F. Forastiere, G. Weinmayr, A. Jaensch, G. Nagel, H. Concin, and J. V. Spadaro. Global estimates of mortality associated with long-term exposure to outdoor fine particulate matter. In *Proceedings of the National Academy of Sciences of the United States of America*, volume 115, pages 9592–9597. National Academy of Sciences, September 2018. DOI: 10.1073/pnas.1803222115.

[18] A. L. Goodkind, J. S. Coggins, and J. D. Marshall. A Spatial Model of Air Pollution: The Impact of the Concentration-Response Function. *Journal of the Association of Environmental and Resource Economists*, 1:451–479, December 2014. ISSN 2333-5955. DOI: 10.1086/678985.

[19] A. Faustini, R. Rapp, and F. Forastiere. Nitrogen dioxide and mortality: Review and meta-analysis of long-term studies. *European Respiratory Journal*, 44:744–753, September 2014. ISSN 13993003. DOI: 10.1183/09031936.00114713.

[20] G. Hoek, R. M. Krishnan, R. Beelen, A. Peters, B. Ostro, B. Brunekreef, and J. D. Kaufman. Long-term air pollution exposure and cardio-respiratory mortality: A review. *Environmental Health: A Global Access Science Source*, 12, 2013. ISSN 1476069X. DOI: 10.1186/1476-069X-12-43.

[21] M. C. Turner, M. Jerrett, C. A. Pope, D. Krewski, S. M. Gapstur, W. R. Diver, B. S. Beckerman, J. D. Marshall, J. Su, D. L. Crouse, and R. T. Burnett. Long-Term Ozone Exposure and Mortality in a Large Prospective Study. *American journal of respiratory and critical care medicine*, 193:1134–1142, May 2016. ISSN 15354970. DOI: 10.1164/rccm.201508-1633OC.

[22] P. Huangfu and R. Atkinson. Long-term exposure to NO_2 and O_3 and all-cause and respiratory mortality: A systematic review and meta-analysis. *Environment International*, 144, November 2020. ISSN 18736750. DOI: 10.1016/j.envint.2020.105998.

[23] R. Beelen, O. Raaschou-Nielsen, M. Stafoggia, Z. J. Andersen, G. Weinmayr, B. Hoffmann, K. Wolf, E. Samoli, P. Fischer, M. Nieuwenhuijsen, P. Vineis, W. W. Xun, K. Katsouyanni, K. Dimakopoulou, A. Oudin, B. Forsberg, L. Modig, A. S. Havulinna, T. Lanki, A. Turunen, B. Oftedal, W. Nystad, P. Nafstad, U. D. Faire, N. L. Pedersen, C. G. Östenson, L. Fratiglioni, J. Penell, M. Korek, G. Pershagen, K. T. Eriksen, K. Overvad, T. Ellermann, M. Eeftens, P. H. Peeters, K. Meliefste, M. Wang, B. Bueno-De-Mesquita, D. Sugiri, U. Krämer, J. Heinrich, K. D. Hoogh, T. Key, A. Peters, R. Hampel, H. Concin, G. Nagel, A. Ineichen, E. Schaffner, N. Probst-Hensch, N. Künzli, C. Schindler, T. Schikowski, M. Adam, H. Phuleria, A. Vilier, F. Clavel-Chapelon, C. Declercq, S. Grioni, V. Krogh, M. Y. Tsai, F. Ricceri, C. Sacerdote, C. Galassi, E. Migliore, A. Ranzi, G. Cesaroni, C. Badaloni, F. Forastiere, I. Tamayo, P. Amiano, M. Dorronsoro, M. Katsoulis, A. Trichopoulou, B. Brunekreef, and G. Hoek. Effects of long-term exposure to air pollution on natural-cause mortality: An analysis of 22 European cohorts within the multicentre ESCAPE project. *The Lancet*, 383:785–795, 2014. ISSN 1474547X. DOI: 10.1016/S0140-6736(13)62158-3.

[24] M. Jerrett, R. T. Burnett, C. A. Pope, K. Ito, G. Thurston, D. Krewski, Y. Shi, E. Calle, and M. Thun. Long-Term Ozone Exposure and Mortality. *The New England Journal of Medicine*, 360:1085–1095, March 2009.

[25] Q. Di, Y. Wang, A. Zanobetti, Y. Wang, P. Koutrakis, C. Choirat, F. Dominici, and J. D. Schwartz. Air pollution and mortality in the medicare population. *New England Journal of Medicine*, 376:2513–2522, June 2017. ISSN 0028-4793. DOI: 10.1056/nejmoa1702747.

[26] J. Chen and G. Hoek. Long-term exposure to PM and all-cause and cause-specific mortality: A systematic review and meta-analysis. *Environment International*, 143, October 2020. ISSN 18736750. DOI: 10.1016/j.envint.2020.105974.

[27] D. Krewski, M. Jerrett, R. T. Burnett, R. Ma, E. Hughes, Y. Shi, M. C. Turner, C. A. P. III, G. Thurston, E. E. Calle, and M. J. Thun. Extended follow-up and spatial analysis of the american cancer society study linking particulate air pollution and mortality, May 2009. URL https://www.researchgate.net/publication/26690365.

[28] N. A. Janssen, G. Hoek, M. Simic-Lawson, P. Fischer, L. van Bree, H. T. Brink, M. Keuken, R. W. Atkinson, H. R. Anderson, B. Brunekreef, and F. R. Cassee. Black carbon as an additional indicator of the adverse health effects of airborne particles compared with PM_{10} and $PM_{2.5}$. *Environmental Health Perspectives*, 119:1691–1699, 2011. ISSN 15529924. DOI: 10.1289/ehp.1003369.

[29] A. Vodonos, Y. A. Awad, and J. Schwartz. The concentration-response between long-term $PM_{2\cdot5}$ exposure and mortality; A meta-regression approach. *Environmental Research*, 166:677–689, October 2018. ISSN 10960953. DOI: 10.1016/j.envres.2018.06.021.

[30] L. Jaegleh, D. J. Jacob, W. H. Brune, and P. O. Wennberg. Chemistry of HO_x radicals in the upper troposphere. *Atmospheric Environment*, 35:469–489, 2001. DOI: 10.1016/S1352-2310(00)00376-9.

[31] H. Lee, S. C. Olsen, D. J. Wuebbles, and D. Youn. Impacts of aircraft emissions on the air quality near the ground. *Atmospheric Chemistry and Physics*, 13:5505–5522, 2013. ISSN 16807316. DOI: 10.5194/acp-13-5505-2013.

[32] O. A. Søvde, S. Matthes, A. Skowron, D. Iachetti, L. Lim, B. Owen, Øivind Hodnebrog, G. D. Genova, G. Pitari, D. S. Lee, G. Myhre, and I. S. Isaksen. Aircraft emission mitigation by changing route altitude: A multi-model estimate of aircraft NO_x emission impact on O_3 photochemistry. *Atmospheric Environment*, 95:468–479, 2014. ISSN 18732844. DOI: 10.1016/j.atmosenv.2014.06.049.

[33] J. Maruhashi, V. Grewe, C. Frömming, P. Jöckel, and I. C. Dedoussi. Transport patterns of global aviation NO_x and their short-term O_3 radiative forcing - a machine learning approach. *Atmospheric Chemistry and Physics*, 22:14253–14282, November 2022. ISSN 16807324. DOI: 10.5194/acp-22-14253-2022.

[34] B. Koffi, S. Szopa, A. Cozic, D. Hauglustaine, and P. V. Velthoven. Present and future impact of aircraft, road traffic and shipping emissions on global tropospheric ozone. *Atmospheric Chemistry and Physics*, 10:11681–11705, 2010. ISSN 16807316. DOI: 10.5194/acp-10-11681-2010.